

# **Sensitive Isotope Analysis of Micropollutants in Complex Sample Matrices**

## **Dissertation**

der Mathematisch-Naturwissenschaftlichen Fakultät  
der Eberhard Karls Universität Tübingen  
zur Erlangung des Grades eines  
Doktors der Naturwissenschaften  
(Dr. rer. nat.)

vorgelegt von  
M.Sc. Aileen Melsbach  
aus Plauen

Tübingen 2019

Gedruckt mit Genehmigung der Mathematisch-Naturwissenschaftlichen Fakultät der Eberhard Karls Universität Tübingen.

Tag der mündlichen Qualifikation:

14. November 2019

Dekan:

Prof. Dr. Wolfgang Rosenstiel

1. Berichterstatter:

Prof. Dr. Martin Elsner

2. Berichterstatter:

Prof. Dr. Christian Zwiener



## **Danksagung – Acknowledgement**

Der größte Dank gebührt meinem Doktorvater Prof. Dr. Martin Elsner. Insbesondere für die hervorragende Betreuung, die zahlreichen Diskussionen und sein Engagement. Außerdem möchte ich mich für die unzähligen Möglichkeiten bedanken, Einblicke über mein Kernthema hinaus zu erlangen. Das Forschungsumfeld und die Laborausstattung ließen dabei keine Wünsche offen.

Zudem möchte ich mich herzlich bei Prof. Dr. Christian Zwiener für die Zweitbetreuung dieser Arbeit, sowie die hilfreichen Kommentare innerhalb der Thesis Komitee Meetings bedanken.

Additionally, I would like to thank Prof Dr Robert Kalin for his great support, comments and ideas within my thesis committee meetings.

Desweiteren möchte ich mich bei PD Dr. Thomas Gröger, insbesondere für seine Geduld, Beratung und seine Hilfsbereitschaft beim Erlernen der comprehensiven GC×GC bedanken.

Ich bedanke mich außerdem bei Julien Farlin und Denis Pittois für ihre Unterstützung bei den Probennahmen und -extraktionen, sowie für die Gastfreundschaft während meiner Zeit in Luxembourg.

Weiterer Dank gilt:

Dr. Armin Meyer, Martina Daubmeier und Ramona Brejcha, mit denen die Identifizierung und Behebung der technischen Probleme, gleich doppelt so viel Spaß gemacht hat.

Meinen Kollegen aus der Isotopenchemie Gruppe, sowie meinen (ehemaligen) Bürokollegen Dr. Heide Schürner, Judith Feichtmeyer und Dr. Sviatlana Marozava, die immer für eine heitere Arbeitsatmosphäre gesorgt haben.

Ein ganz großes Danke möchte ich auch meinen Eltern Conny & Michael, sowie meiner „Omma“ Anne und meinem Opa Günter sagen. Ihr habt mein Interesse an der Wissenschaft erst geweckt, stets an mich geglaubt und mir alles ermöglicht, damit ich diesen Weg gehen konnte. Manuel, auch Dir bin ich unendlich dankbar. Besonders für Deine Liebe, Unterstützung und Deinen Rückhalt in all den Jahren.



# Table of Contents

<b>ZUSAMMENFASSUNG.....</b>	<b>1</b>
<b>SUMMARY.....</b>	<b>V</b>
<b>1. GENERAL INTRODUCTION .....</b>	<b>1</b>
1.1. GROUNDWATER CONTAMINATION WITH MICROPOLLUTANTS .....	2
1.2. APPROACHES TO IDENTIFY THE ENVIRONMENTAL FATE OF MICROPOLLUTANTS .....	2
1.3. CHALLENGES IN COMPOUND-SPECIFIC STABLE ISOTOPE ANALYSIS IN COMPLEX SAMPLE MATRICES .....	5
1.3.1. INSTRUMENTAL CHALLENGES IN THE ANALYSIS OF POLAR MICROPOLLUTANTS .....	6
1.3.2. ANALYTICAL CHALLENGES OF POLAR MICROPOLLUTANTS IN COMPLEX SAMPLE MATRICES.....	7
1.4. AIMS AND OBJECTIVES .....	10
<b>2. <sup>13</sup>C- AND <sup>15</sup>N-ISOTOPE ANALYSIS OF DESPHENYLCHLORIDAZON BY LIQUID CHROMATOGRAPHY– ISOTOPE-RATIO MASS SPECTROMETRY AND DERIVATIZATION GAS CHROMATOGRAPHY–ISOTOPE- RATIO MASS SPECTROMETRY .....</b>	<b>13</b>
2.1. ABSTRACT .....	14
2.2. INTRODUCTION .....	15
2.3. EXPERIMENTAL / METHODS .....	17
2.3.1. CHEMICALS .....	17
2.3.2. EA-IRMS MEASUREMENT FOR DETERMINATION OF REFERENCE VALUES .....	17
2.3.3. ISOTOPE ANALYSIS BY LC-IRMS .....	18
2.3.4. DERIVATIZATION PROCEDURE WITH (TRIMETHYLSILYL) DIAZOMETHANE (TMSD) .....	19
2.3.5. GC-IRMS CONDITIONS FOR NITROGEN ISOTOPE ANALYSIS.....	20
2.3.6. CORRECTION PROCEDURE OF ISOTOPE VALUES .....	21
2.3.7. PEAK IDENTIFICATION AND QUANTIFICATION WITH GC-QMS.....	21
2.3.8. ISOTOPE RATIOS OF COMMERCIALY AVAILABLE CHLORIDAZON PRODUCTS - SOURCE FINGERPRINTING .....	22
2.3.9. EVOLUTION OF ISOTOPE RATIOS DERIVING FROM DIFFERENT CHLORIDAZON SOURCES .....	22
<b>2.4. RESULTS AND DISCUSSION.....</b>	<b>23</b>
2.4.1. DPC-CARBON ISOTOPE ANALYSIS .....	23
2.4.2. DERIVATIZATION OF DPC – NITROGEN ISOTOPE ANALYSIS.....	25
2.4.3. ISOTOPE RATIOS OF COMMERCIALY AVAILABLE CHLORIDAZON PRODUCTS - SOURCE FINGERPRINTING .....	27
2.4.4. EVOLUTION OF ISOTOPE RATIOS OF DPC FROM DIFFERENT CHLORIDAZON SOURCES.....	28

<b>2.5. CONCLUSION AND OUTLOOK.</b> .....	<b>30</b>
---	-----------

<b><u>3. DUAL-ELEMENT ISOTOPE ANALYSIS OF DESPHENYLCHLORIDAZON TO INVESTIGATE ITS ENVIRONMENTAL FATE IN A SYSTEMATIC FIELD STUDY - A LONG-TERM LYSIMETER EXPERIMENT</u></b> .....	<b>33</b>
---	-----------

<b>3.1. ABSTRACT</b> .....	<b>34</b>
<b>3.2. INTRODUCTION</b> .....	<b>35</b>
<b>3.3. EXPERIMENTAL / METHODS</b> .....	<b>38</b>
3.3.1. EXPERIMENTAL SET-UP OF LYSIMETER EXPERIMENTS.....	38
3.3.2. CONCENTRATION MEASUREMENTS OF CLZ, DPC AND MDPC.....	39
3.3.3. LARGE VOLUME SOLID-PHASE EXTRACTION .....	39
3.3.4. ELEMENTAL ANALYZER-ISOTOPE RATIO MASS SPECTROMETRY MEASUREMENT FOR DETERMINATION OF REFERENCE VALUES .....	40
3.3.5. CARBON ISOTOPE ANALYSIS OF DPC BY LC- IRMS .....	40
3.3.6. DERIVATIZATION OF DPC FOR NITROGEN ISOTOPE ANALYSIS.....	41
3.3.7. SEPARATION OF DRAINAGE SAMPLE FRACTIONS FOR ANALYSIS OF DPC AND MDPC.....	41
3.3.8. NITROGEN ISOTOPE ANALYSIS OF DPC AND MDPC .....	41
3.3.9. CORRECTION PROCEDURE FOR ISOTOPE ANALYSIS .....	42
3.3.10. CONCENTRATION MEASUREMENT OF CLZ AND DPC FROM SOIL SAMPLES.....	42
3.3.11. STATISTICAL ANALYSES.....	43
<b>3.4. RESULTS AND DISCUSSION</b> .....	<b>43</b>
3.4.1. WATER DYNAMICS .....	43
3.4.2. TRENDS IN COMPOUND CONCENTRATIONS AFTER DPC SURFACE APPLICATION .....	44
3.4.3. INSIGHTS INTO DPC TRANSFORMATION BY ISOTOPE ANALYSIS OF DPC SURFACE APPLICATION .....	46
3.4.4. CLZ SURFACE APPLICATION MIMICKING A REALISTIC FIELD SCENARIO .....	48
3.4.5. TRANSFORMATION-POTENTIAL AFTER HERBICIDE INJECTION BELOW THE VADOSE ZONE .....	52
3.4.6. DUAL-ELEMENT ISOTOPE PLOT TO IDENTIFY DPC FORMATION AND TRANSFORMATION.....	54
<b>3.5. ENVIRONMENTAL SIGNIFICANCE AND OUTLOOK</b> .....	<b>55</b>

<b><u>4. ISOTOPE FRACTIONATION OF MICROPOLLUTANTS DURING LARGE-VOLUME EXTRACTION: A CRITICAL METHOD EVALUATION FOR ATRAZINE AT LOW NG/L CONCENTRATIONS IN GROUNDWATER</u></b> .....	<b>57</b>
---	-----------

<b>4.1. ABSTRACT</b> .....	<b>58</b>
----------------------------	-----------

<b>4.2. INTRODUCTION</b> .....	<b>59</b>
<b>4.3. MATERIALS AND METHODS</b> .....	<b>61</b>
4.3.1. CHEMICALS .....	61
4.3.2. ENVIRONMENTAL SAMPLES .....	61
4.3.3. GENERAL ANALYSIS OF THE ENVIRONMENTAL SAMPLES – TOTAL ORGANIC CARBON.....	61
4.3.4. SAMPLE PRE-TREATMENT AND SPIKING WITH THE TARGET ANALYTES.....	62
4.3.5. ANALYTE ENRICHMENT WITH SOLID-PHASE EXTRACTION .....	62
4.3.6. SAMPLE CLEAN-UP WITH PREPARATIVE HPLC.....	63
4.3.7. QUANTIFICATION WITH GC-QMS .....	63
4.3.8. EA-IRMS MEASUREMENT FOR DETERMINATION OF REFERENCE VALUES .....	64
4.3.9. GC-IRMS CONDITIONS FOR CARBON ISOTOPE ANALYSIS.....	64
4.3.10. CORRECTION PROCEDURE APPLIED FOR ISOTOPE ANALYSIS .....	65
<b>4.4. RESULTS AND DISCUSSION</b> .....	<b>66</b>
4.4.1. RECOVERY OF ATZ, DEA AND BAM FROM GROUNDWATER .....	66
4.4.2. ISOTOPE FRACTIONATION AFTER LARGE VOLUME EXTRACTION .....	69
4.4.3. SUGGESTIONS FOR IMPROVEMENT .....	72
<b>4.5. ENVIRONMENTAL SIGNIFICANCE AND OUTLOOK</b> .....	<b>72</b>
4.5.1. POSSIBLE BIAS IN THE INTERPRETATION OF ENVIRONMENTAL DATA.....	73
4.5.2. OPPORTUNITIES FOR FURTHER ANALYTICAL DEVELOPMENTS .....	75
<b><u>5. GENERAL CONCLUSION AND OUTLOOK</u></b> .....	<b><u>77</u></b>

**6. OUTLOOK: DEVELOPMENT OF A COMPREHENSIVE GC×GC-IRMS TOWARDS A MORE SENSITIVE ISOTOPE ANALYSIS OF MICROPOLLUTANTS - PART I** .....

<b><u>6.1. INTRODUCTION</u></b> .....	<b><u>82</u></b>
<b><u>6.2. MATERIALS AND METHODS</u></b> .....	<b><u>85</u></b>
6.2.1. CHEMICALS .....	85
6.2.2. EA-IRMS MEASUREMENT FOR DETERMINATION OF REFERENCE VALUES .....	85
6.2.3. GC-IRMS – INITIAL STATE OF THE INSTRUMENTATION.....	85
6.2.4. GC-IRMS METHOD FOR CARBON ISOTOPE ANALYSIS AFTER MODIFICATIONS .....	86
6.2.5. EVALUATION OF THE INSTRUMENT PERFORMANCE .....	86
6.2.6. OPTIMIZATION OF GC EQUIPMENT BY REDUCTION OF DEAD VOLUME .....	87
6.2.7. TRANSFORMATION OF IRMS .....	89
<b><u>6.3. PRELIMINARY RESULTS AND DISCUSSION</u></b> .....	<b><u>89</u></b>

6.3.1. CHALLENGES IN MODIFYING THE INSTRUMENTAL SET-UP .....	89
<b>6.4. CONCLUSION AND OUTLOOK .....</b>	<b>93</b>
<b><u>APPENDIX .....</u></b>	<b><u>95</u></b>
<b>A. SUPPORTING INFORMATION OF CHAPTER 2 .....</b>	<b>96</b>
A.1. GENERAL INFORMATION .....	96
A.2. EXPERIMENTAL / METHODS.....	97
<b>A.2.1. PEAK IDENTIFICATION AND QUANTIFICATION WITH GC-QMS .....</b>	<b>97</b>
<b>A.2.3. SEEPAGE WATER EXTRACTION METHOD VALIDATION WITH SPIKED SAMPLES.....</b>	<b>98</b>
<b>A.2.4. FRACTIONATIVE HPLC –SAMPLE CLEAN-UP METHOD FOR THE EXPERIMENT:.....</b>	<b>99</b>
<b>A.2.5. FRACTIONATIVE HPLC –SEPARATION OF DPC FROM MDPC IN ENVIRONMENTAL SAMPLES PRIOR DERIVATIZATION. ....</b>	<b>100</b>
A.3. RESULTS AND DISCUSSION .....	102
<b>B. SOLID-PHASE EXTRACTION METHOD FOR STABLE ISOTOPE ANALYSIS OF PESTICIDES FROM LARGE VOLUME ENVIRONMENTAL WATER SAMPLES.....</b>	<b>106</b>
<b>C. SUPPORTING INFORMATION OF CHAPTER 3 .....</b>	<b>117</b>
C.1. FORMATION AND TRANSFORMATION OF DESPHENYLCHLORIDAZON .....	117
C.2. MATERIALS AND METHODS .....	117
C.3. RESULTS .....	126
<b>D. ADSORBING VS. NONADSORBING TRACERS FOR ASSESSING PESTICIDE TRANSPORT IN ARABLE SOILS .....</b>	<b>140</b>
<b>E. SUPPORTING INFORMATION OF CHAPTER 4 .....</b>	<b>158</b>
E.1. VOLUMES AND CONCENTRATIONS OF GROUNDWATER USED FOR THIS STUDY.....	158
E.2. HYPOTHESIZED ATZ-HUMIC SUBSTANCE-COMPLEX .....	159
E.3. GENERAL ANALYSIS – TOTAL ORGANIC CARBON .....	160
<b><u>ABBREVIATIONS .....</u></b>	<b><u>162</u></b>
<b><u>REFERENCES .....</u></b>	<b><u>167</u></b>
<b><u>CURRICULUM VITAE .....</u></b>	<b><u>179</u></b>

## Zusammenfassung

In den letzten Jahrzehnten wurden zunehmend Berichte über die Kontamination von Gewässern durch Spurenschadstoffe veröffentlicht. Dabei stellen persistente und polare Spurenschadstoffe ein besonders großes Risiko dar, da sie in das Grundwasser sickern können und somit die Haupt-Trinkwasserquelle vieler europäischer Länder verunreinigen können. Aus diesem Grund ist es im Interesse der Umweltbehörden und der Forschung das Verhalten dieser Spurenschadstoffe in der Umwelt zu untersuchen. Herkömmliche Methoden zur Einschätzung des Umweltverhaltens basieren auf Konzentrationsmessungen eines Schadstoffes, sowie dessen Abbauprodukt. Wird ein Abbauprodukt allerdings nicht nur gebildet, sondern dieses ebenfalls weiter transformiert, können die Resultate über das Abbauverhalten der Muttersubstanz mehrdeutig sein. Neben dem weiteren Abbau des Metaboliten kann es durch unterschiedliche Mobilitäten des Metaboliten und des Ausgangsstoffes, sowie durch wiederholte Remobilisierungen aus dem Boden zu Fehleinschätzungen bezüglich des Abbaus kommen, was eine Risikobeurteilung erschwert.

Eine alternative Herangehensweise zur Identifikation von Abbauprozessen ist die substanzspezifische Stabil-Isotopen-Analytik (compound-specific stable isotope analysis, CSIA). Bei dieser Methode wird die natürliche Verteilung der Isotopenhäufigkeit eines Elements (z.B. Kohlenstoff, Stickstoff) analysiert. Bisher war die substanzspezifische Stabil-Isotopen-Analytik allerdings auf die Analyse von Schadstoffen im unteren  $\mu\text{g/l}$  Konzentrationsbereich beschränkt. Daher war ein Ziel dieser Arbeit den Anwendungsbereich der substanzspezifischen Stabil-Isotopen-Analytik zu erweitern, um robuste Analysen für umweltrelevante Konzentrationen zu bewerkstelligen. Realisiert wurde dies durch die Entwicklung analytischer Methoden für polare Spurenschadstoffe in Umweltproben, sowie deren Anwendung auf systematische Feldstudien. Zudem wurden die Limitierungen der substanzspezifischen Stabil-Isotopen-Analytik im untern  $\text{ng/l}$  Konzentrationsbereich untersucht. Dafür wurden indikativ die häufig detektierten Spurenschadstoffe Desphenylchloridazon (DPC), 2,6-Dichlorbenzamid (BAM), Atrazin (ATZ) und Desethylatrazin (DEA) als Modellsubstanzen verwendet.

Im zweiten Kapitel dieser Arbeit wurden Methoden zur Kohlen- und Stickstoffisotopenanalyse ( $\delta^{13}\text{C}$  und  $\delta^{15}\text{N}$ ) polarer Spurenschadstoffe am Beispiel von DPC entwickelt. Zur Bestimmung der Kohlenstoffisotopenverhältnisse wurde

Flüssigchromatographie mit einem Isotopenmassenspektrometer (LC-IRMS) gekoppelt, während für die Bestimmung der Stickstoffisotopenverhältnisse eine Methode mittels Derivatisierung und Gaschromatographie-Isotopenmassenspektrometrie entwickelt wurde. Beide Methoden zeigten reproduzierbare und akkurate  $\delta^{13}\text{C}$  und  $\delta^{15}\text{N}$  Isotopenwerte mit einer Präzisionsgrenze im  $\mu\text{g/l}$  Konzentrationsbereich. Dabei waren 996 ng an DPC auf der GC-Säule (on-column) ausreichend für die Kohlenstoffisotopenanalyse. Für die Stickstoffisotopenanalyse musste das DPC zunächst mit einem 160-fachen Überschuss an Trimethylsilyldiazomethan (TMSD) derivatisiert werden. Dabei wurde eine Präzisionsgrenze von 1200 ng DPC auf der GC-Säule bestimmt. Da Spurenschadstoffe in der Umwelt allerdings in einem geringeren Konzentrationsbereich vorkommen (ng/l bis  $\mu\text{g/l}$ ), war eine Optimierung dieser Methode hinsichtlich ihrer Sensitivität notwendig. Durch die Probeninjektion direkt auf die GC-Säule (on-column Injektion) statt der bisherigen Splitless-Injektionstechnik, konnte für die Bestimmung der Stickstoffisotopenverhältnisse eine Präzisionsgrenze von 100 ng DPC auf der GC-Säule erreicht werden. Danach wurde die Eignung beider Methoden für die Messung von niedrig konzentrierten Umweltproben geprüft. Dafür wurden die Stickstoffisotopenverhältnisse von DPC in mit DPC kontaminiertem Sickerwasser analysiert. Zusätzlich wurde das Sickerwasser mit Chloridazon (CLZ) versetzt, welches sich nach und nach zu DPC abgebaut hat. Die Analyse der Stickstoffisotopenverhältnisse von DPC zeigte Unterschiede in den Isotopensignaturen, was die Differenzierung zwischen unterschiedlichen Eintragungsquellen des DPCs ermöglicht.

Nachdem die Methoden zur CSIA polarer Spurenschadstoffe am Beispiel des DPCs in Kapitel 2 entwickelt worden war, wurde eine systematische Feldstudie zum Umweltverhalten des DPC und seiner Ausgangsverbindung CLZ in Lysimetern durchgeführt. Die in Kapitel 3 beschriebene Studie lieferte neue Erkenntnisse über den Abbau von DPC. Dabei wurde der Aspekt der zeitgleichen Bildung und Transformation des Metaboliten betrachtet. Die Erkenntnisse wurden mithilfe zweier analytischer Ansätze ermittelt: der bereits etablierten Methode basierend auf den Konzentrationsverhältnissen von Metabolit zu Ausgangsstoff, und der seit kurzem verfügbaren Kohlenstoff- und Stickstoffisotopenanalytik. Es zeigte sich, dass: (i) DPC in allen Lysimetern mit einer signifikanten  $^{13}\text{C}$  und  $^{15}\text{N}$  Anreicherung von bis zu +4 ‰ bzw. +3 ‰ transformiert wurde und (ii) das gebildete DPC, welches noch nicht transformiert worden war, den gleichen Stickstoffisotopenwert wie sein Ausgangsstoff CLZ hatte. Nachdem es allerdings weiter abgebaut wurde, konnte eine signifikante Kohlenstoff- und Stickstoffisotopenfraktionierung beobachtet werden. Das Ausmaß der Isotopenfraktionierung wurde teilweise durch die Remobilisierung von nicht-transformiertem DPC abgeschwächt.



Zudem zeigte sich, dass das Ausmaß der Isotopenfraktionierung in Abhängigkeit von der Art der Anwendung des Herbizides und des Metaboliten variierte. Dies impliziert den Einfluss von Pflanzen und der präferentiellen Flüsse auf die Bildung und den Abbau von DPC. Zusätzlich konnte gezeigt werden, dass (iii) bei einer Transformation von DPC die Isotopensignatur als Indikator für den Abbau zuverlässiger war, als das Verhältnis von Metabolit zu Ausgangsverbindung. Daher diente CSIA als Indikator für die DPC-Transformation, vorausgesetzt, es findet keine gleichzeitige Bildung und Transformation von DPC statt. Sobald jedoch die DPC-Bildung dominierte, war der Nachweis des DPC-Abbaus durch CSIA nicht mehr eindeutig, da die Änderungen der Isotopenwerte durch den erneuten Eintrag von DPC verringert wurden. Dabei erreichten die Metabolit-zu-Ausgangsstoff-Verhältnisse ein Maximum und konnten somit den Nachweis für die DPC-Bildung erbringen. Das bedeutet, dass sich beide Methoden ergänzen, insbesondere, wenn nur ein teilweiser Abbau des Herbizids stattfindet, denn während das Metabolit-zu-Ausgangsstoff-Verhältnis Informationen über die Remobilisierung eines Analyten liefert, zeigt CSIA die Entwicklung des Abbaus einer Verbindung.

Das vierte Kapitel dieser Arbeit befasst sich mit den Herausforderungen der CSIA polarer und persistenter Spurenschadstoffe im natürlichen System Grundwasser. Zur Identifikation und Bewertung der Herausforderungen wurde Grundwasser mit ATZ, DEA und BAM versetzt und die Modellsubstanzen aus großen Volumina extrahiert. Im Gegensatz zu den vorangegangenen Laborversuchen, bei denen die Analyten in Leitungswasser gelöst waren, führte die Extraktion der Substanzen aus dem Grundwasser zu kleinen und nicht reproduzierbaren Wiederfindungsraten. Als Grund für die unvollständige Wiederfindung der Analyten wird der Einfluss der Grundwassermatrix bei der Extraktion angenommen. So können organische Bestandteile des Grundwassers wie z.B. Humin- und Fulvinsäuren mit den Modellsubstanzen ATZ und DEA sogenannte Analyt-Fulvinsäure-Komplexe bilden. Diese Komplexe werden vor allem unter sauren pH-Bedingungen gebildet und das Einstellen eines niedrigen pH-Wertes war Teil dieser Methode. Neben den unvollständigen Wiederfindungsraten wurde bei der großvolumigen Probenanreicherung (Extraktion von bis zu 100 L pro Probe) eine starke Isotopenfraktionierung beobachtet. Die Fraktionierung entsteht durch den Einfluss der Matrix, welche ebenfalls bei der Festphasenextraktion angereichert wurde. Dabei beeinträchtigt die Isotopensignatur der organischen Bestandteile des Grundwassers die Isotopensignatur des Analyten und kann, falls nicht identifiziert, zu einer Fehleinschätzung in der Quantifizierung des Schadstoffabbaus führen. Die Prüfung der in diesem Kapitel vorgestellten Methode zeigt die Notwendigkeit einer kritischen Begutachtung und Identifikation von Fehlerquellen im

Vorfeld von künftigen Methodenentwicklungen mit besonderem Augenmerk auch auf Matrixeffekte. Ziel zukünftiger Studien wird es sein, die in diesem Kapitel identifizierten Limitierungen der substanzspezifischen Stabil-Isotopen-Analytik durch die Weiterentwicklung und Optimierung von Methoden und Analysegeräten zu eliminieren.

## Summary

Reports of the contamination of natural water bodies with micropollutants have increased in the last decades. Most importantly, persistent and polar micropollutants are of major concern as they may leach into groundwater, the main source of drinking water in many countries within the European Union. Consequently, for environmental authorities and researchers, it is important to investigate the environmental fate of such micropollutants. Conventional assessment approaches rely on changes in concentrations of the contaminant and its metabolite. This, however, is often inconclusive as the simultaneous formation and transformation of the metabolite, differences in the mobility between parent compound and metabolite, or repeated mobilization may lead to erroneous interpretations. Compound-specific stable isotope analysis (CSIA) is a complementary approach to identify transformation processes based on the analysis of natural isotope abundances of an element (e.g. carbon, nitrogen). As CSIA has so far been limited to the analysis of pollutants in the sub- $\mu\text{g/L}$  range, this thesis aims to broaden the application of CSIA by developing analytical methods for polar micropollutants in environmental samples, applying these for systematic field studies and testing the limits of CSIA in concentrations in the low  $\text{ng/L}$  range. To this end, the frequently detected micropollutants desphenylchloridazon (DPC), 2,6-dichlorobenzamide (BAM), atrazine (ATZ) and desethylatrazine (DEA) were used as model compounds.

In the second chapter of this thesis, methods for carbon- and nitrogen-isotope analysis ( $\delta^{13}\text{C}$  and  $\delta^{15}\text{N}$ ) of polar micropollutants were developed using liquid chromatography-isotope-ratio mass spectrometry (LC-IRMS) and derivatization gas chromatography-IRMS (GC-IRMS). DPC was used as a representative compound for polar contaminants during method development. Both methods resulted in reproducible and accurate  $\delta^{13}\text{C}$  and  $\delta^{15}\text{N}$  analysis of DPC with a limit of precise isotope analysis in the  $\mu\text{g/L}$  concentration range. For carbon isotope analysis 996 ng of DPC on-column were sufficient. Nitrogen isotope analysis was achieved by derivatization of DPC with a 160-fold excess of (trimethylsilyl)diazomethane. To enable the application of CSIA to environmental samples, where micropollutants are present in a concentration range of  $\text{ng/L}$  to sub- $\mu\text{g/L}$ , more sensitive methods were required. Thus, the nitrogen isotope analysis was optimized using on-column injection, which resulted in accurate  $\delta^{15}\text{N}$  analysis for amounts greater than 100 ng DPC on-column. The feasibility of both methods was proven by measuring the isotopic composition of DPC in DPC-containing

environmental-seepage water spiked with chloridazon (CLZ). The analysis indicated that it is possible to distinguish DPC containing different isotopic signatures.

After the feasibility of CSIA for polar micropollutants such as DPC was shown, a systematic field study of the DPC and its parent compound CLZ was carried out as detailed in Chapter 3. This study gave new insights into DPC degradation pinpointing the influence of simultaneous formation and transformation of the metabolite using two analytical approaches—the well-established metabolite-to-parent compound ratio and the recently available carbon and nitrogen CSIA. We found that (i) DPC was transformed in all lysimeters, showing a significant enrichment in  $^{13}\text{C}$  and  $^{15}\text{N}$  by approximately +4 ‰ and +3 ‰, respectively. (ii) Formed DPC, which had not been subject to further transformation yet, showed the same nitrogen isotope value as its precursor CLZ. As further transformation took place, significant carbon and nitrogen isotope fractionation was observed that was partially attenuated when mixing with freshly mobilized DPC from the vadose zone took place. The extent of isotope fractionation varied depending on the method of application of the parent herbicide and metabolite, implying the influence of plants, and the preferential flow on the formation and degradation of DPC. Additionally, we demonstrated that (iii) when DPC was further transformed, the isotopic signature, as an integrated signal of DPC degradation, was more reliable as an indicator of degradation than the metabolite-to-parent-compound ratio. Hence, this study enables the application of CSIA as an indication of DPC transformation, provided that there is no simultaneous formation and transformation of DPC. On the other hand, when DPC formation dominated and evidence from CSIA was not conclusive because changes in isotope values were reduced by the fresh input, metabolite-to-parent-ratios reached a maximum and could provide evidence of DPC formation. This leads to the conclusion that both methods are complementary, in particular when only partial degradation of the herbicide is occurring. While the metabolite-to-parent ratio provides information about the re-mobilization of a compound, CSIA shows the evolution of a compound's degradation.

In Chapter 4 of this thesis, challenges in CSIA of polar and persistent micropollutants in groundwater were identified and critically discussed by evaluating a large volume extraction method of up to 100 L groundwater using ATZ, DEA and BAM as model compounds in low ng/L concentration ranges. It was found that, in contrast to previous laboratory experiments, where tap water was used, extracts from environmental groundwater resulted in low and non-reproducible recoveries. Since groundwater contains organic matter such as humic and fulvic acids, and as acidification was part of the extraction procedure, it is assumed that the change

in pH prior to solid-phase extraction (SPE) may favor the formation of analyte-fulvic acid complexes leading to the low recoveries observed. In addition to unsatisfactory recoveries, the extensive sample enrichment also resulted in an extensive isotope fractionation as the isotopic signature of the organic matter interfered with the carbon isotope ratio of the target analytes. Such an interference would lead to an overestimation in the quantification of degradation, if unidentified. Thus, it is essential for future analytical method developments to critically evaluate each method and to include the investigation about a possible influence of sample matrix on the analysis already in the pre-tests. As this study has shown the limitations of CSIA of polar micropollutants in complex sample matrices, future studies may use this as a starting point towards more sensitive isotope analysis by methodological and instrumental advances.



# **1. General Introduction**

### 1.1. Groundwater Contamination with Micropollutants

Worldwide, groundwater is one of the most important resources for drinking water abstraction<sup>1-3</sup>. To ensure its quality, groundwater is constantly screened for contaminants. In the last decades, however, reports about the detection of micropollutants in natural water bodies have increased<sup>4-8</sup>. Micropollutants are typically detected in water in concentration ranges of pg/L to the low µg/L range, and their toxicity may have an impact on human and ecosystem health even at these low concentrations<sup>9</sup>. Frequently identified micropollutants are agrochemicals and their degradation products<sup>10</sup>, due to their widespread application. Because of their persistency, some of these contaminants still emerge in groundwater screenings even though their application was forbidden decades ago. An example of such a micropollutant is atrazine (ATZ), which is frequently detected in natural water bodies exceeding the limit permissible in drinking water (0.1 µg/L)<sup>11-13</sup>, even though its application has been forbidden by the European Union since 2004<sup>14</sup>. Consequently, the presence of such persistent mobile organic contaminants (PMOCs) is of major concern<sup>15</sup>.

For some micropollutants, such as chloridazon (CLZ) and dichlobenil (DCB), the risk of groundwater contamination is even increased when more polar transformation products are formed. Both desphenylchloridazon (DPC, from chloridazon) and 2,6-dichlorobenzamide (BAM, from dichlobenil) are more persistent and more polar than their respective parent compounds, resulting in a higher leaching potential<sup>5, 16-18</sup>. It is therefore important to assess the environmental fate of such polar micropollutants.

### 1.2. Approaches to Identify the Environmental Fate of Micropollutants

The detection and conclusive demonstration of a contaminant's degradation or transformation in the field is often difficult. Analytical techniques which are commonly used to identify the environmental fate of a compound usually rely on concentration measurements and the resulting metabolite-to-parent compound molar ratio as well as further dating tools<sup>19-22</sup>. Assessing a compound's fate in the field based on these tools, however, may be biased, as the metabolite-to-parent ratio can be influenced by i) further transformation of the metabolite, ii) changes of the ratio due to a recharge of the parent compound, or iii) a non-closed mass balance caused by processes such as sorption or the presence of additional transformation pathways<sup>23, 24</sup>. Thus, in addition to these conventional methods, a complementary approach has been developed within the last decades: compound-specific stable isotope analysis (CSIA). CSIA



## 1. General Introduction

---

uses the natural isotopic abundance of the target analyte<sup>25</sup>. Isotope values, such as carbon ( $\delta^{13}\text{C}$ ) and nitrogen ( $\delta^{15}\text{N}$ ) isotope values are usually expressed using the delta notation in per mille (‰) as described in equation 1.1 and 1.2. The isotope ratios ( $^{13}\text{C}/^{12}\text{C}_{\text{sample}}$  and  $^{15}\text{N}/^{14}\text{N}_{\text{sample}}$ ) are stated relative to the international references Vienna PeeDee Belemnite (V-PDB) for carbon and air for nitrogen<sup>26, 27</sup>.

$$\delta^{13}\text{C} = \frac{{}^{13}\text{C}/{}^{12}\text{C}_{\text{Sample}} - {}^{13}\text{C}/{}^{12}\text{C}_{\text{Reference}}}{{}^{13}\text{C}/{}^{12}\text{C}_{\text{Reference}}} \quad \text{eq. 1.1}$$

$$\delta^{15}\text{N} = \frac{{}^{15}\text{N}/{}^{14}\text{N}_{\text{Sample}} - {}^{15}\text{N}/{}^{14}\text{N}_{\text{Reference}}}{{}^{15}\text{N}/{}^{14}\text{N}_{\text{Reference}}} \quad \text{eq. 1.2}$$

The isotopic ratio of a compound can give evidence on the origin of the analyte and serves as a compound's isotopic "fingerprint". These ratios change during (bio)degradation or transformation due to kinetic isotope effects, as molecules with lighter isotopes (e.g.  $^{12}\text{C}$  or  $^{14}\text{N}$ ) are usually transformed faster than their heavier counterparts (e.g.  $^{13}\text{C}$  or  $^{15}\text{N}$ ). Consequently, an enrichment of heavy isotopes is observed in the remaining substrate, resulting in an isotopic "footprint" of degradation<sup>24, 28</sup>. Different scenarios of the evolution of the isotope ratio of a contaminant during a reaction are shown in Figure 1.1.

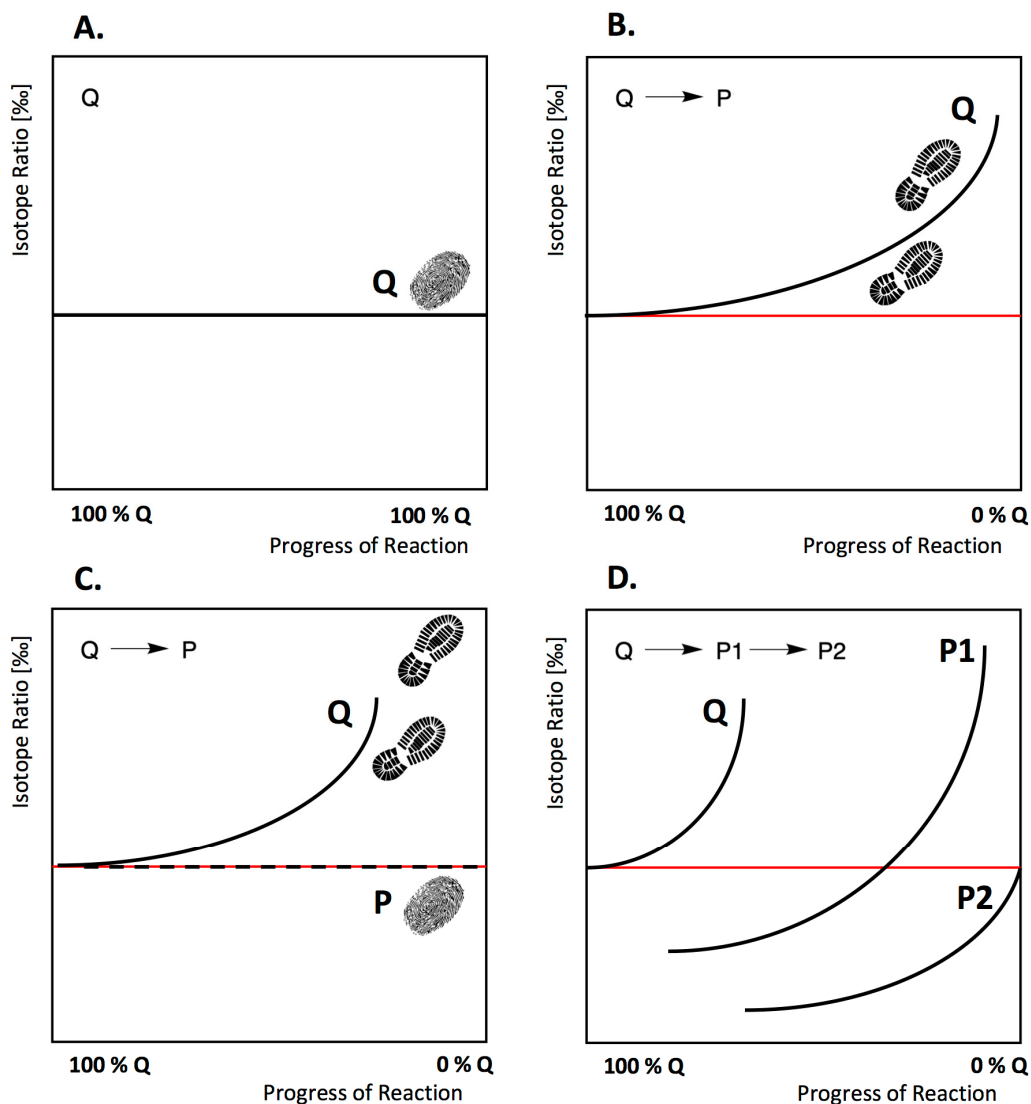


**Figure 1.1: Evolution of isotope ratios of a reactant Q during a reaction, when A. Q is not involved in any process and does show the source isotopic signature, B. the reactant Q is transformed or (bio)degraded into a product P and shows a change in its isotopic signature, C. Q is degraded to metabolite P – Q is reacting, for example at a carbon atom, while its nitrogen group is unaffected. This leads to a change in the  $^{13}\text{C}/^{12}\text{C}$  isotope ratio in Q, while P shows the source signature in its  $^{15}\text{N}/^{14}\text{N}$  isotope ratio, D. Q is biodegraded and its products P1 and P2 are formed in sequence; the source signature (“Fingerprint”) of the parent compound is shown as a red line.**

While the analysis of only one element (e.g.  $^{12}\text{C}/^{13}\text{C}$ ) can detect significant differences in isotope values, in the field it is often difficult to pinpoint the reason for these changes (mixing of sources vs. degradation, etc.). Thus, the isotope analysis of an additional element (e.g.  $^{15}\text{N}/^{14}\text{N}$ ) can be essential to provide complementary insights into such processes, which are often crucial to distinguish between different transformation pathways<sup>24</sup>.

In environmental science, CSIA has been successfully applied to study the origin and degradation of pollutants and micropollutants such as industrial products (e.g., chlorinated

solvents and petroleum hydrocarbons), pharmaceuticals and pesticides in soil and water<sup>28-33</sup>. In particular, CISA was used to identify different sources of micropollutants<sup>33, 34</sup> as well to investigate whether transformation of a pollutants occurs<sup>30, 35</sup>. Once transformation of a contaminant had been identified, CSIA was used to distinguish different degradation pathways<sup>23, 36-39</sup> and estimate the corresponding transformation rates<sup>40, 41</sup>.

So far, this has only been accomplished for a small group of pollutants such as chlorinated ethanes. In that case, recent method developments<sup>42-44</sup> enabled the investigation of how different transformation pathways<sup>43, 45-47</sup> are linked to transformation pathways observed in the field<sup>44</sup>. For micropollutants such as ATZ and BAM, however, development of analytical methods<sup>48, 49</sup> and their application towards the investigation of transformation pathways<sup>23, 50</sup> have just started in recent years. The link towards their investigation in the field has only partly been accomplished, and such approaches are still limited due to several challenges faced in CSIA<sup>29, 48</sup>, as described in the following section.

### **1.3. Challenges in Compound-Specific Stable Isotope Analysis in Complex Sample Matrices**

There are several challenges that need to be solved in order to enable the full application of CSIA and thus the increased knowledge of the environmental fate of polar micropollutants. Here, the challenges can be attributed to two main reasons: (i) limitations due to the instrumental set-up, (ii) analytical challenges caused by the concentration at which polar micropollutants are present in the environment as well as their complex chemical properties (e.g., presence of heteroatoms)<sup>51</sup>.

Compound-specific stable isotope analysis is accomplished by coupling either a gas chromatograph (GC) or a liquid chromatograph (LC) to an isotope ratio mass spectrometer (IRMS). Both GC-IRMS and LC-IRMS are based on the principle of chromatographic separation hyphenated with the ability of detecting isotope ratios by combustion or pyrolysis of the separated analytes into a suitable measurement gas such as CO<sub>2</sub> or N<sub>2</sub><sup>51, 52</sup>. The system commonly used for CSIA is shown in Figure 1.2.

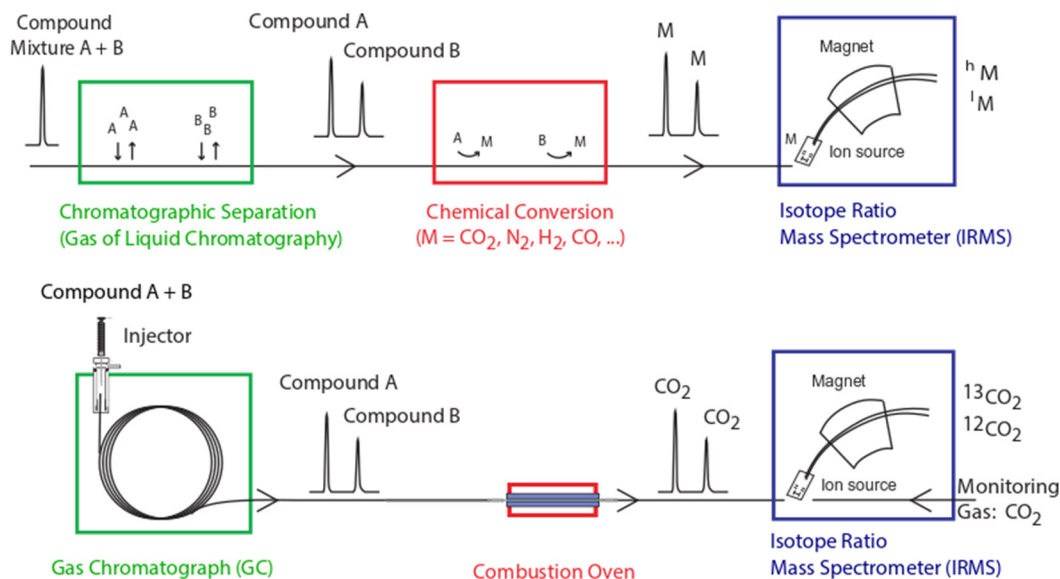


Figure 1.2: A. Schematic principle of CSIA and B. instrumental set-up of a gas chromatograph coupled to an isotope ratio mass spectrometer used for carbon isotope analysis of volatile and semi-volatile compounds, adapted from Elsner et al.<sup>51</sup>.

### 1.3.1. Instrumental Challenges in the Analysis of Polar Micropollutants

Pesticides and their metabolites often contain functional groups and heteroatoms that reduce their volatility. Consequently, as in the case of DPC, they tend to decompose after injection into the GC and are thus not amenable for GC-IRMS analysis. There are two approaches for the analysis of polar micropollutants: (i) to enhance their volatility by derivatization prior to GC-IRMS analysis, (ii) determination of the isotope ratio by LC-IRMS. For carbon isotope analysis, derivatization GC-IRMS analysis is challenging as the derivatization agent may introduce extraneous carbon atoms into the analyte molecule, which changes the isotopic signature of the target analyte. To guarantee that the derivatization used is non-isotope-discriminating, all derivatization procedures need extensive validation. Thus, LC-IRMS is often used for the determination of carbon isotope values of polar micropollutants, as analytes can be analyzed without derivatization<sup>53</sup>. As shown in Figure 1.3, LC-IRMS oxidation of the analyte into a suitable measurement gas is realized by its reaction with the chemical oxidation agent peroxodisulfate at an elevated temperature and in aqueous phase<sup>54</sup>. This application is particularly challenging for method development of analytes in complex sample matrices, as full peak separation has to be achieved, while the mobile phase must not consist of organic solvents. (If organic solvents were added to the mobile phase, they would be transformed to

## 1. General Introduction

CO<sub>2</sub> like the analyte and thus interfere with its carbon isotope ratio as they become indistinguishable<sup>55, 56</sup>.)

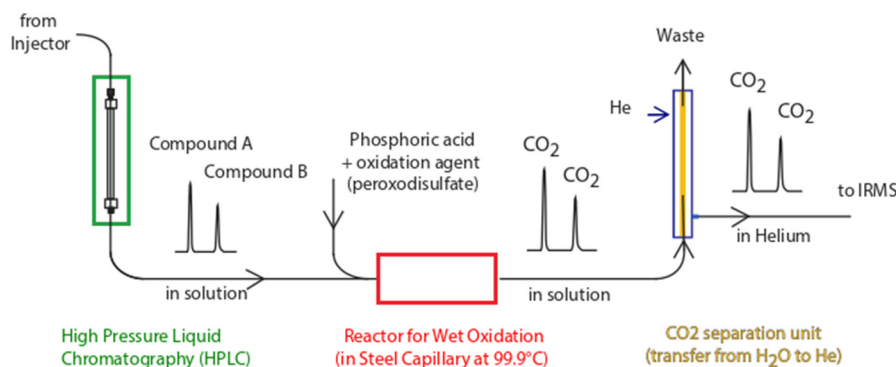


Figure 1.3: Schematic set-up of a liquid chromatograph coupled to an isotope ratio mass spectrometer<sup>51</sup>.

An additional challenge is that this approach is limited to the detection of carbon isotope ratios as there is no method to quantitatively generate N<sub>2</sub> from a nitrogen-containing analyte by wet oxidation. Further, it is challenging to measure the isotope ratio of the generated N<sub>2</sub> against the high background of N<sub>2</sub> present in the atmosphere<sup>56, 57</sup>. Consequently, derivatization GC-IRMS is used for nitrogen isotope analysis of polar micropollutants, as nitrogen isotopes are less affected by derivatization. As no extraneous nitrogen atom is introduced, the nitrogen isotope ratio of the derivatized compound is expected to be equivalent to the nitrogen isotope ratio of the non-derivatized analyte. (See Elsner et al.<sup>51</sup> and Reinnicke et al.<sup>58</sup> for a detailed summary of derivatization reagents frequently used for derivatization GC-IRMS.)

As each method has its advantages and disadvantages, derivatization GC-IRMS and LC-IRMS are complementary methods and are used in combination to measure the isotope ratios of carbon and nitrogen of a polar micropollutant<sup>51</sup>.

### 1.3.2. Analytical Challenges of Polar Micropollutants in Complex Sample Matrices

#### 1.3.2.1. Challenges in GC-IRMS Analysis Attributed to the Complex Chemical Structure of Polar Micropollutants

Polar compounds potentially lead to analytical challenges because of their complex chemical properties. In particular the presence of heteroatoms can cause difficulties to combust the analyte completely into the measurement gas. In the case of incomplete conversion systematic isotope fractionation may occur. Additionally, for GC-IRMS applications it can be demanding

to convert polar substances into the gas phase and to separate them chromatographically as their polarity has an effect the peak shape<sup>51, 58</sup>.

### 1.3.2.2. Small Concentrations of Micropollutants in Complex Sample Matrices

In contrast to conventional analytical methods like GC-MS, CSIA requires higher amounts of sample for precise and true isotope analysis. This can be attributed to differences in the natural isotope abundance of the elements as the heavier isotopes are rarer than their lighter counterparts (Table 1.1). Consequently, instruments must be highly sensitive in order to detect small differences within the small amount of the heavy isotope<sup>51</sup>.

**Table 1.1: CSIA isotope parameters for elements occurring in micropollutants; adapted from <sup>34, 51, 59, 60</sup>, n.a. = not applicable.**

Element	Minor Isotope	Natural Abundance [%]	Interface	Analyzed Gas	Mass needed on column	Precision [‰]
Hydrogen	<sup>2</sup> H	0.01557	Pyrolysis	H <sub>2</sub>	30 ng H	6
Carbon	<sup>13</sup> C	1.1056	Combustion	CO <sub>2</sub>	10 ng C	0.5
Nitrogen	<sup>15</sup> N	0.3663	Combustion	N <sub>2</sub>	42 ng N	1
Chlorine	<sup>37</sup> Cl	24.211	n.a.	C <sub>x</sub> H <sub>y</sub> Cl <sub>z</sub> or HCl	5 or 10-30 ng TCE	0.2 or 0.5-1

Comparing the mass of an element needed for accurate isotope analysis with the concentrations of micropollutants that are typically present in groundwater (pg/L to low µg/L), methodological and instrumental advances are essential<sup>61</sup>.

One methodological approach is the application of large volume solid-phase extraction (SPE) in combination with on-column injection. As shown by Schreglmann et al.<sup>48</sup> and Torrentó et al.<sup>62</sup>, this approach enables the concentration of target analytes in the low µg/L range without any isotope discrimination. Nevertheless, extensive sample clean-up is required as SPE does not only concentrate the target analyte, but also matrix components causing co-elution with the target analyte and interferences in the determination of the isotopic signature. Thus, further approaches such as (semi-)preparative HPLC and/or molecularly imprinted solid-phase extraction (MISPE) are often necessary for sample preparation in addition to concentration techniques<sup>63</sup>.

Beside methodological advances to realize the trace analysis of compounds, recent instrumental modifications were developed focusing on the improvement of sensitivity by the optimization of peak width, reduction in the system's dead volume, in sample loss, and increase in resolution<sup>64</sup>. Thus, to increase the instrument's sensitivity, different devices have been suggested for optimization. These include modification of the injection technique<sup>65</sup>, thinner diameters of capillaries used for GC and transferline<sup>66</sup> as well as different designs of the combustion furnace<sup>66, 67</sup> and interfaces<sup>65</sup>. In all studies, a gain in sensitivity was reported. The lowest limit of precise isotope analysis was published by Baczynski et al.<sup>66</sup>, where carbon isotope ratios of *n*-alkanes were analyzed accurately at a concentration of 100 pmol carbon on column.

For the identification and quantification of analytes in complex sample matrices, multidimensional separation techniques such as comprehensive GC×GC-TOFMS have been widely applied<sup>68-71</sup>. In contrast, its application in isotope analysis is only slowly emerging<sup>72-75</sup> and even though it has been shown that these instrumental modifications do not introduce an isotope fractionation and decrease the limit of precise isotope analysis, they have not yet been applied to environmental samples with complex matrices.

Consequently, appropriate analytical approaches to investigate the environmental fate of polar micropollutants by CSIA are not available. Even though first methods for pesticides have been developed<sup>76</sup> and optimized<sup>48</sup> for the analysis of contaminants in a µg/L range, micropollutants occur in the environment in even lower concentrations (low µg/L to ng/L). Thus, the development of isotope fractionation-free enrichment methods for environmental samples is as crucial as the development of highly sensitive LC-IRMS methods for carbon isotope analysis and suitable GC-IRMS methods for nitrogen isotope analysis in combination with the minimization of sample preparation.

### 1.4. Aims and Objectives

This thesis aims to enable sensitive isotope analysis of micropollutants in complex sample matrices in order to understand the environmental fate of polar, persistent, and mobile organic contaminants using ATZ, its metabolite DEA, BAM and DPC as model compounds. In order to achieve this aim, analytical methods for carbon and nitrogen isotope analysis of commonly detected micropollutants had to be developed, optimized and validated. I focused in particular on the improvement of the sensitivity and accuracy to enable a broad application of these methods from laboratory experiments, where analytes are usually measured in concentrations of mg/L, to controlled field experiments, where target analytes were present in only low  $\mu\text{g/L}$  concentration ranges. Finally, this thesis aims to apply CSIA in order to measure analytes in groundwater samples (low ng/L concentration range).

The first part of this thesis (Chapter 2) investigates the feasibility of dual-element compound-specific stable isotope analysis (CSIA) to identify the origin of polar and fairly ubiquitous compounds as well as their transformation in relevant concentration. DPC was used as a model compound for these polar micropollutants. To analyze DPC, an LC-IRMS and a derivatization GC-IRMS method for carbon and nitrogen isotope analysis is developed and validated.

The methods are then applied in Chapter 3 to investigate the fate of polar and persistent micropollutants under controlled environmental conditions using, as in Chapter 2, DPC as model compound. To pinpoint the environmental fate of DPC, CLZ and DPC were applied separately in three scenarios. Firstly, to investigate DPC transformation in the absence of interferences caused by the parent compound, DPC was applied to the soil surface without the presence of its parent compound CLZ. In the second scenario, CLZ was applied to the soil surface to study the concurrent formation of DPC from CLZ and its potential degradation and thus mimic a realistic field scenario. Finally, CLZ was injected into the soil below the vadose zone to investigate the processes of sorption versus formation versus transformation. The environmental fate of DPC was investigated by combining “traditional” approaches of concentration measurements (metabolite-to-parent compound ratio) and by measuring its change in carbon and nitrogen isotope value in a systematic lysimeter field study.

Chapter 2 and 3 addressed the analysis of micropollutants in low  $\mu\text{g/L}$  concentration range. Their concentrations in groundwater, however, are often in the low ng/L range. Thus, in Chapter 4, sample preparation for CSIA was assessed to pinpoint the impact of large volume extraction of groundwater on the isotope fractionation of contaminants. Furthermore, the aim



## 1. General Introduction

---

of this chapter was to critically evaluate the necessity of careful method assessments. In particular, the goal was to demonstrate how the interpretation of field samples may be biased in the absence of careful method validation.



## 2. <sup>13</sup>C- and <sup>15</sup>N-Isotope Analysis of Desphenylchloridazon by Liquid Chromatography–Isotope-Ratio Mass Spectrometry and Derivatization Gas Chromatography–Isotope-Ratio Mass Spectrometry

Author	Author position	Scientific ideas (%)	Data generation (%)	Analysis and Interpretation (%)	Paper writing done (%)
A. Melsbach	1	60	70	70	60
V. Ponsin	1	5	25	5	5
C. Torrentó	3	0	5	10	5
C. Lihl	4	0	0	0	5
T. Hofstetter	6	10	0	5	5
D. Hunkeler	7	10	0	5	10
M. Elsner	8	15	0	5	10
Title of paper:	<sup>13</sup> C- and <sup>15</sup> N-Isotope Analysis of Desphenylchloridazon by Liquid Chromatography–Isotope-Ratio Mass Spectrometry and Derivatization Gas Chromatography–Isotope-Ratio Mass Spectrometry				
Status in publication process:	Accepted; Melsbach, A.; Ponsin, V.; Torrentó, C.; Lihl, C.; Hofstetter, T. B.; Hunkeler, D.; Elsner, M., <sup>13</sup> C and <sup>15</sup> N isotope analysis of desphenylchloridazon by liquid chromatography isotope ratio mass spectrometry (LC-IRMS) and derivatization-gas chromatography isotope ratio mass spectrometry (GC-IRMS). <i>Anal. Chem.</i> <b>2019</b> , <i>91</i> (5), 3412-3420. DOI: <a href="https://doi.org/10.1021/acs.analchem.8b04906">10.1021/acs.analchem.8b04906</a>				

I confirm that the above-stated is correct.

---

Date, Signature of the candidate

I/We certify that the above-stated is correct.

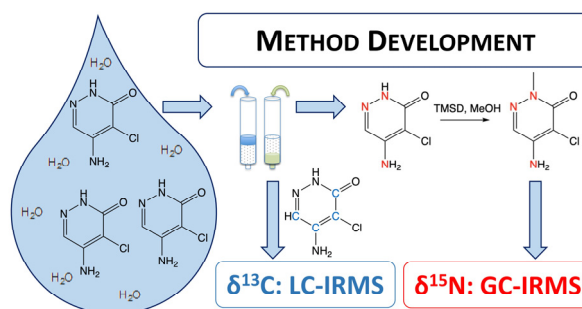
---

Date, Signature of the doctoral committee or at least of one of the supervisors

## 2.1. Abstract

Widespread application of herbicides impacts surface water and groundwater. Their metabolites (e.g., desphenylchloridazon from chloridazon) may be persistent and even more polar than the parent herbicide, which increases the risk of groundwater contamination. When

parent herbicides are still applied, metabolites are constantly formed and may in addition be degraded. Evaluating their degradation based on concentration measurements is, therefore, difficult. This study presents compound-specific stable isotope analysis (CSIA) of nitrogen and carbon isotope ratios at natural abundances as alternative analytical approach to track origin, formation and degradation of desphenylchloridazon (DPC), the major degradation product of the herbicide chloridazon. Methods were developed and validated for carbon and nitrogen isotope analysis ( $\delta^{13}\text{C}$  and  $\delta^{15}\text{N}$ ) of DPC by liquid chromatography-isotope ratio mass spectrometry (LC-IRMS) and derivatization-gas chromatography-IRMS (GC-IRMS), respectively. Injecting standards directly onto an Atlantis LC-column resulted in reproducible  $\delta^{13}\text{C}$  isotope analysis (standard deviation  $< 0.5\text{‰}$ ) by LC-IRMS with a limit of precise analysis of 996 ng DPC on-column. Accurate and reproducible  $\delta^{15}\text{N}$  analysis with a standard deviation  $< 0.4\text{‰}$  was achieved by GC-IRMS after derivatization of  $> 100$  ng DPC with 160-fold excess of (trimethylsilyl)diazomethane. Application of the method to environmental seepage water indicated that newly formed DPC could be distinguished from “old” DPC by different isotopic signatures of the two DPC sources.



### 2.2. Introduction

In many regions of the European Union, groundwater is our most important drinking water resource and is therefore constantly screened for contaminants<sup>1, 5</sup>. In recent years, there is growing concern about pollution by persistent and mobile organic contaminants such as polar compounds and their metabolites<sup>10, 15, 77, 78</sup>. Metabolites are often more persistent and polar than the parent compounds resulting in a high leaching potential with an increased risk to contaminate groundwater<sup>16</sup>. For some of them, however, methods are lacking to demonstrate their origin, formation and degradation. To evaluate their environmental fate, conventional models rely on parent-compound-to-metabolite-ratios. However, as pesticides are still applied on the field, there is a constant formation of persistent metabolites. Thus, the evaluation of metabolite degradation with conventional models based on concentration measurements may lead to bias. Further bias is introduced, when one contaminant is formed from at least two different sources (parent compound)<sup>23</sup>.

A representative compound for polar contaminants is desphenylchloridazon (DPC). It is among the most frequently detected micropollutants related to crop production, exceeding concentrations of 10 µg/L in natural water<sup>4, 5, 79-85</sup>. DPC is formed by microbial degradation of the selective systemic herbicide chloridazon (CLZ)<sup>85-88</sup>. CLZ is being applied in the agricultural production of mangold, beetroot and sugar beet<sup>89</sup>. Consequently, there is a constant formation of DPC deriving from newly applied CLZ. DPC can be transformed to methyl-desphenylchloridazon (MDPC)<sup>19, 79</sup>. Its transformation pathway and environmental fate, however, are still mostly unknown.

This study presents compound-specific stable isotope analysis (CSIA) as an alternative approach to identify a compound's origin and transformation by analyzing stable isotope ratios at natural abundance<sup>34</sup>. As herbicides deriving from different manufacturers may differ in their <sup>13</sup>C/<sup>12</sup>C and/or <sup>15</sup>N/<sup>14</sup>N isotopic signatures, isotope analysis enables a distinction between different sources. In particular, DPC contains the same nitrogen atoms as its parent compound CLZ so that it is expected to show also the same nitrogen isotope signature - provided that the isotope ratio is not changed by isotope effects during degradation. In contrast, only part of the carbon atoms of CLZ are transferred to DPC, because it is formed by cleavage of the phenyl-ring from the heterocyclic pyridazine-ring (see structures in Table A1) so that DPC may show a different carbon isotope signature compared to CLZ. Carbon isotope analysis, however, may still be particularly insightful, because changes in isotope ratios of DPC may be detected by CSIA to deliver evidence about formation and (bio)degradation of this persistent metabolite.

Since molecules with light isotopes are usually degraded more rapidly than those with heavy isotopes, transformation leads to an enrichment of heavy isotopes in the fraction of remaining pesticide<sup>23</sup>. This increase in the isotope ratio (e.g.,  $^{13}\text{C}/^{12}\text{C}$ ) can therefore give evidence of the degradation of the compound<sup>23</sup>. By combining both elements in the form of a dual-element isotope plot, further information about the reaction mechanism of a compound's degradation or its origin can be gained<sup>61</sup>.

Even though methods for carbon- and nitrogen-isotope analysis exist for several pesticides and their metabolites<sup>23, 29, 32, 33, 49, 90-92</sup>, most CSIA methods of environmental compounds have focused so far on GC-amenable compounds. CSIA is typically accomplished by coupling gas chromatography (GC) to isotope ratio mass spectrometry (IRMS). Like most polar organic compounds, however, DPC is not amenable to GC as it decomposes before reaching a boiling point (see Table A1). To analyze the isotopic composition of such polar organic compounds, derivatization-GC-IRMS has been brought forward as alternative strategy<sup>32, 33, 58, 93</sup>. This approach is chosen as the methylation of DPC enhances its GC suitability. Methylation of a compound using "mild" derivatization reagents (e.g., trimethyl sulfonium hydroxide (TMSH), methanol/ $\text{BF}_3$ ) allows control over the isotope ratio of the methyl group that is introduced. Hence, the change in the  $^{13}\text{C}/^{12}\text{C}$  composition of the target analyte caused by the introduction of an additional carbon atom can be corrected by equations stated in the literature<sup>58, 94, 95</sup>. However, these mild reagents fail to derivatize groups of low reactivity such as amino-, amide-, or hydroxyl-groups.

Consequently, for compounds containing less reactive groups an alternative strategy must be followed. For  $^{13}\text{C}/^{12}\text{C}$  isotope analysis, liquid chromatography is the method of choice<sup>51, 96-98</sup>. LC-IRMS has the advantage that compounds can be analyzed directly without derivatization, but the liquid chromatography presents the challenge that carbon isotope measurements must be conducted without organic eluents, which otherwise would be converted to  $\text{CO}_2$  and would interfere with  $^{13}\text{C}/^{12}\text{C}$  analysis of the analyte<sup>56, 57</sup>. For nitrogen isotope analysis such sensitive LC-IRMS is not possible, but here GC-IRMS after derivatization by more reactive reagents is an option, because for  $^{15}\text{N}/^{14}\text{N}$  analysis control over carbon isotope ratios is not required. To this end, the idea of Kuhlmann<sup>99</sup> is followed, where the methylation of DPC with diazomethane is described. Further adaptations described by Mogusu et al.<sup>33</sup> use (trimethylsilyl)diazomethane (TMSD), a less explosive substitute compared to diazomethane, to methylate polar organic compounds<sup>100, 101</sup>. For diazomethane and TMSD the control over

the isotope value of the additional carbon atom is lost since no reproducible isotope effects are expected<sup>58</sup>. As the methylation leaves the <sup>15</sup>N/<sup>14</sup>N ratio unaffected, however, this approach is well suitable for nitrogen isotope analysis.

Following these two approaches, this study demonstrates the feasibility of dual-element isotope analysis of a very polar and fairly ubiquitous environmental contaminant using complementary methods for LC-IRMS and GC-IRMS. The development of a precise and true method<sup>102</sup> for LC-IRMS and GC-IRMS to measure <sup>13</sup>C/<sup>12</sup>C and <sup>15</sup>N/<sup>14</sup>N isotope ratios of DPC is presented. The developed methods were optimized and a feasibility study tested the applicability to environmental seepage water to probe for formation of DPC from different sources simulating a typical field situation.

### 2.3. Experimental / Methods

#### 2.3.1. Chemicals

Desphenylchloridazon (5-Amino-4-chloro-3-pyridazinone, CAS no.: 6339-19-1) was obtained from BASF (99.8%, Limburgerhof, Germany). Methyl-desphenylchloridazon (5-amino-4-chloro-2-methyl-3(2H)-pyridazine, CAS no.: 17254-80-7) was purchased from LGC Standards GmbH (Wesel, Germany). Chloridazon ( $\geq 98\%$ , CAS no.: 1698-60-8) and Acetochlor (96.3%, CAS no.: 34256-82-1) were sourced from Chemos GmbH & Co. KG (Regenstauf, Germany). Desethylatrazine (purity not available, CAS no.: 6190-65-4) was produced by Synchem (Felsberg, Germany). (Trimethylsilyl)diazomethane, 2.0 M dissolved in diethyl ether (CAS no.: 18107-18-1, acute toxicity and health hazardous), sodium persulfate ( $\geq 99.9\%$ , CAS no.: 7775-27-1) and phosphoric acid ( $\geq 85\%$ , CAS no.: 7664-38-2) were supplied by Sigma Aldrich (Merck KGaA, Darmstadt, Germany), while methanol ( $\geq 99.9\%$ , CAS no.: 67-56-1) and acetone ( $\geq 99.9\%$ , CAS no.: 67-64-1) were received from Roth (Karlsruhe, Germany). Ultrapure water was derived from a Millipore DirectQ apparatus (Millipore, Bedford, MA, USA).

#### 2.3.2. EA-IRMS Measurement for Determination of Reference Values

Carbon and nitrogen isotope composition of our in-house standards of CLZ, DPC and MDPC were characterized by an elemental analyzer-isotope ratio mass spectrometer (EA-IRMS) as described in Meyer et al.<sup>76</sup>. A system consisting of an EuroEA (Euro Vector, Milano, Italy)

was hyphenated to a Finnigan MAT 253 IRMS via a Finnigan™ ConFlow III interface (Thermo Fisher Scientific, Bremen, Germany). The standards were calibrated against the organic referencing materials USG 40 (L-glutamic acid), USG 41 (L-glutamic acid) and IAEA 600 (caffeine) provided by the International Atomic Agency (Vienna, Austria).

The carbon ( $\delta^{13}\text{C}$ ) and nitrogen ( $\delta^{15}\text{N}$ ) isotope values are reported in per mil relative to PeeDee Belemnite (V-PDB) and air, respectively, according to the equations 2.1 and 2.2:

$$\delta^{13}\text{C} = \frac{{}^{13}\text{C}/{}^{12}\text{C}_{\text{Sample}} - {}^{13}\text{C}/{}^{12}\text{C}_{\text{Reference}}}{{}^{13}\text{C}/{}^{12}\text{C}_{\text{Reference}}} \quad \text{eq. 2.1}$$

$$\delta^{15}\text{N} = \frac{{}^{15}\text{N}/{}^{14}\text{N}_{\text{Sample}} - {}^{15}\text{N}/{}^{14}\text{N}_{\text{Reference}}}{{}^{15}\text{N}/{}^{14}\text{N}_{\text{Reference}}} \quad \text{eq. 2.2}$$

For carbon analysis by LC-IRMS,  $\delta^{13}\text{C}$  values were determined relative to our laboratory  $\text{CO}_2$  monitoring gas, which was introduced at the beginning and the end of each analysis run.  $\delta^{15}\text{N}$  values were determined analogously relative to our laboratory  $\text{N}_2$  monitoring gas. Both gases were previously calibrated against RM8563 ( $\text{CO}_2$ ) and NSVEC ( $\text{N}_2$ ), supplied by the International Atomic Energy Agency (IAEA).

### 2.3.3. Isotope Analysis by LC-IRMS

High-performance liquid chromatography (HPLC) was carried out on a Dionex system consisting of an Ultimate 3000 HPLC pump and an Ultimate 3000 autosampler (Thermo Fisher Scientific). Chromatography was performed with an Atlantis T3 Sentry guard column (3  $\mu\text{m}$ , 3.9 mm  $\times$  20 mm, 100 Å, Waters) and an Atlantis T3 column (3  $\mu\text{m}$ , 3 mm  $\times$  100 mm, 100 Å, Waters) operated at 500  $\mu\text{L}/\text{min}$  isocratically with a pH 2 phosphoric acid solution at room temperature. Isotopic ratio measurements were carried out on a Delta V Advantage IRMS coupled to the LC system by an Isolink interface (Thermo Fisher Scientific). The eluting compounds were quantitatively oxidized using oxidant (90 g/L  $\text{Na}_2\text{S}_2\text{O}_8$ ) and phosphoric acid (1.5 M  $\text{H}_3\text{PO}_4$ ), each introduced at a flow rate of 30  $\mu\text{L}/\text{min}$  in the oxidation reactor held at 99.9 °C. Before use, the reagent solutions were degassed in an ultrasonic bath under vacuum

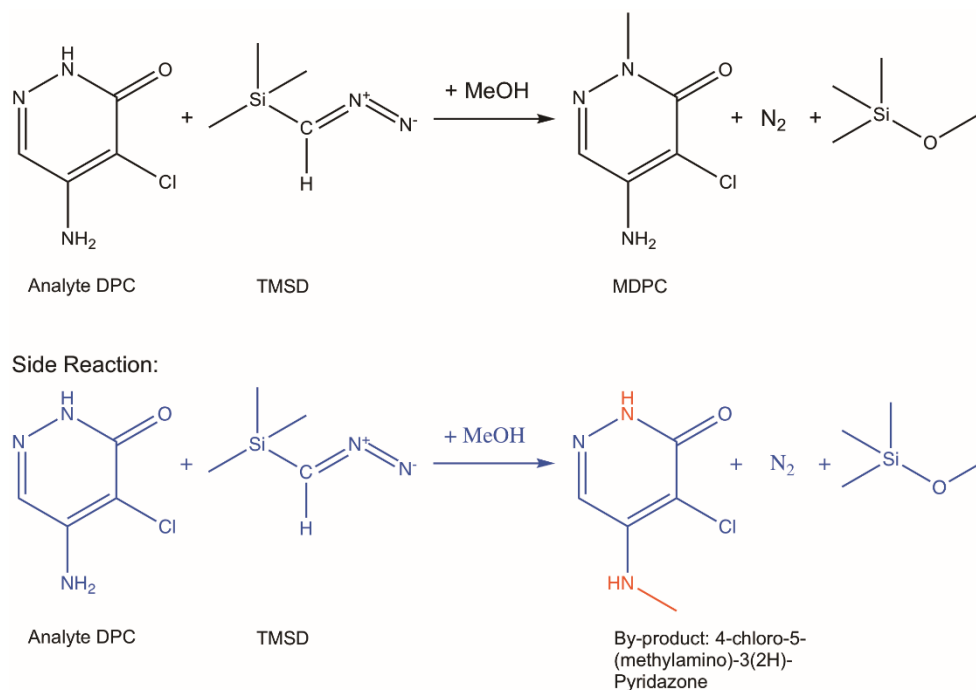


for 30 min. To avoid re-uptake of CO<sub>2</sub>, all solutions were continuously sparged with helium during use. In order to avoid clogging in the system, an in-line filter with a pore size of 5 μm (Vici, Schenkon, Switzerland) was placed in front of the oxidation reactor of the LC-IsoLink interface. The ion source was held at  $2 \times 10^{-6}$  mbar, the accelerating voltage was 3 kV, and ions were generated by electron ionization at 124 eV. The injection volume ranged between 10 and 100 μL. Peak identification was based on retention times in comparison with external standards. The LC-IRMS system and data collection were controlled using Isodat 3.0 software (Thermo Fisher Scientific).

### 2.3.4. Derivatization Procedure with (Trimethylsilyl)diazomethane (TMSD)

Derivatization of DPC was accomplished based on the method of Kuhlmann<sup>99</sup> using diazomethane, as previous attempts with TMSH and methanol / BF<sub>3</sub> had been unsuccessful (data not shown). However, due to the classification of diazomethane as toxic and explosive, here the more stable (trimethylsilyl)diazomethane (TMSD) was tested as a less explosive substitute. Reaction of the target analyte with TMSD forms diazomethane *in situ*, which subsequently methylates the analyte (see Scheme 2.1) to form MDPC. The derivatization of DPC with TMSD was carried out offline in 20 mL headspace vials. A 250 mg/L standard of DPC, dissolved in methanol, was used for method development. Derivatization of the target analyte was evaluated at different temperatures (50°C and 70°C, Figure A5), by varying reaction times (data not shown), and with different TMSD-to-analyte ratios. TMSD-to-analyte ratios varied between 90 and 230, which corresponds to 80 μL to 200 μL of a 2 M TMSD solution in diethyl ether added to 1 mL of a 250 mg/L DPC solution. After adding the TMSD, the vial was tightly crimped and placed for 2 h into a heated water bath. Afterwards, the methanol was evaporated until complete dryness using a gentle stream of nitrogen. As tested with standards, no nitrogen isotope fractionation was introduced during evaporation. The residue was reconstituted 3 times with acetone and transferred into a GC vial with a 200 μL insert. The final reconstitution volume for isotope measurements was 200 μL. The limit of precise isotope analysis and the method's trueness was determined using varying concentrations of the DPC standard (5 mg/L to 1000 mg/L).

## 2. <sup>13</sup>C- and <sup>15</sup>N-Isotope Analysis of Desphenylchloridazon



**Scheme 2.1:** Derivatization reaction of DPC with TMSD with methanol as a catalytic converter, the formation of the by-product during derivatization is shown in blue; the difference between the methylation of the amino-group is highlighted in red.

### 2.3.5. GC-IRMS Conditions for Nitrogen Isotope Analysis

For the analysis of  $\delta^{15}\text{N}$  isotope ratios, a GC-IRMS system consisting of a TRACE GC Ultra gas chromatograph (Thermo Fisher Scientific, Milan, Italy) coupled with a Finnigan MAT 253 isotope ratio mass spectrometer (IRMS) (Thermo Fisher Scientific, Bremen, Germany) was used. Both instruments were linked via a Finnigan Combustion III interface (Thermo Fisher Scientific). The IRMS was operated at a vacuum of  $2.1 \times 10^{-6}$  mbar, an accelerating potential of 9 kV and an emission energy of 2 mA. For combustion of the target analyte, a NiO tube/CuO-NiO reactor (Thermo Fisher Scientific) was used at a temperature of 1030 °C. The gas chromatograph was equipped with a DB-1701 column (J&W Scientific, Santa Clara, CA) with a length of 30 m, an inner diameter of 0.25 mm and a film thickness of 1  $\mu\text{m}$ . The instrument was operated with helium carrier gas (grade 5.0) at a flow rate of 1.4 mL/min. Splitless injection was performed into a splitless liner at 250 °C (Thermo Fischer Scientific, Australia). The GC temperature program started at 100 °C and was held for 1 min, followed by a temperature ramp of 25 °C/min to 240 °C, followed by another temperature ramp of 10 °C/min until the final temperature of 280 °C was held for 5 min. In contrast, for on-column injection, the flow and injector temperature were controlled by an Optic 3 device (ATAS, GL Science, Eindhoven, Netherlands) equipped with a custom-made glass on-column liner.

Samples were injected using a PAL autosampler (CTC Analytics AG, Zwingen, Switzerland). The ATAS injector had an initial temperature of 50 °C, held for 300 s and was then ramped with 4 °C/s to 250 °C. The split flow started at 14 mL/min. After injection, the split flow was set to 0 mL/min for 120 s and finally set to its initial value of 14 mL/min. Simultaneously, the flow rate started at 0.3 mL/min (held for 120 s) and was increased to 1.4 mL/min within 120 s. Meanwhile, the initial temperature of the GC oven was set to 40 °C, held for 1 min, ramped by 25 °C/min to 240 °C, held for 0 min, ramped with 10 °C and held for 5 min. The injection volume ranged between 1 and 3 µL for splitless injection and 1 and 4 µL for on-column injection. To control the system and to verify the method, retention times and isotope values were constantly monitored by bracketing samples with in-house standards of desethylatrazine (DEA), acetochlor (ACETO) and MDPC.

### 2.3.6. Correction Procedure of Isotope Values

All reported isotope ratios are expressed as arithmetic means of three replicate measurements with their respective standard deviations ( $\pm \sigma$ ). For LC-IRMS, calibration was performed using in-house standards and monitoring gas peaks allocated throughout the chromatograms. Trueness of the LC-IRMS system was achieved by correction with a bracketing method using a DPC standard (Table A2), whose signature had previously been determined by EA-IRMS.

For correction of  $\delta^{15}\text{N}$  isotope values, two approaches were applied. In the first measurement campaign, as there was no MDPC standard within the required concentration range commercially available, a correction based on the comparison with DEA and ACETO was used to test for the trueness of isotope values after conversion to  $\text{N}_2$  in the combustion furnace. The EA-IRMS values (Table A2) of these standards were plotted against the measured GC-IRMS values. The differences were used to correct values of the derivatized DPC analyte. DPC was measured by three laboratories (Table A3) to increase the accuracy and thus reduce measurement errors deriving from other analytical methods. In the second measurement campaign, authentic MDPC synthesized by LGC Standards GmbH was used so that the principle of identical treatment by Werner and Brand<sup>26</sup> could be applied, and drifts during measurements as well as differences within the combustion efficiency were corrected directly.

### 2.3.7. Peak Identification and Quantification with GC-qMS

Gas chromatography – quadrupole mass spectrometry (GC-qMS) measurements were carried out to identify MDPC and any co-products generated during derivatization. The instrumental

set-up is described within the Supporting Information A.2.1. One microliter of a derivatized 250 mg/L solution was injected and measured in scan mode. MDPC was identified using the presence of mass-to-charge ratios 159 and 145 as qualifier ions. Additionally, the retention time and spectra were confirmed by measuring the non-derivatized authentic standard of MDPC.

### **2.3.8. Isotope Ratios of Commercially Available Chloridazon Products - Source Fingerprinting**

Carbon and nitrogen isotope ratios of CLZ standards from different suppliers (see Table A4) were analyzed to check whether CLZ standards deriving from different suppliers show different isotopic signatures as a result of industrial production. All samples were measured with the EA-IRMS method already described.

### **2.3.9. Evolution of Isotope Ratios Deriving from Different Chloridazon Sources**

The developed method was applied to investigate whether it is possible to track DPC deriving from different CLZ sources in seepage water (collected from a lysimeter site, described in detail by Torrentó et al.<sup>103</sup>). Thereto, 30 µg/L CLZ ( $\delta^{15}\text{N} = -31.5 \pm 1.0 \text{ ‰}$ ) were spiked into 10 L seepage water that contained 10 µg/L DPC ( $\delta^{15}\text{N} = -15.1 \pm 1.0 \text{ ‰}$ ) originating from another CLZ source from previous experiments. The samples were then stored at 13 °C in the dark over various periods of time (0 to 11 months). Subsequently, the concentration of CLZ, DPC and MDPC was measured with ultrahigh performance liquid chromatography (UHPLC) (see the Supporting Information A.2.2.). The nitrogen isotope values of DPC were determined with derivatization-GC-IRMS. To this end, samples were concentrated using the solid-phase extraction procedure by Torrentó et al.<sup>62</sup> (see the Supporting Information A.2.3. and Figure A1). Prior to GC-IRMS analysis, preparative HPLC was required as an additional clean-up step. Method details are described in the Supporting Information A.2.4. and Figure A2.

## 2.4. Results and Discussion

### 2.4.1. DPC-Carbon Isotope Analysis

To determine the limit of precise isotope analysis of the LC-IRMS method, a DPC standard was injected at concentrations between 2.8 and 133 nmol C on column (Figure 2.1). A chromatogram is shown in Figure A4. The limit of precise isotope analysis was determined with the moving mean procedure described by Jochmann et al.<sup>104</sup> using an uncertainty interval of  $\pm 0.5$  ‰. This limit obtained for carbon isotope analysis of DPC measured by LC-IRMS was 27.5 nmol C on column (996 ng DPC on column), which corresponds to an injection of 50  $\mu$ L of a 0.14 mM (20 mg/L) solution of DPC. This value is within the range of detection limits previously determined for other compounds analyzed by LC-IRMS<sup>32, 105</sup>.

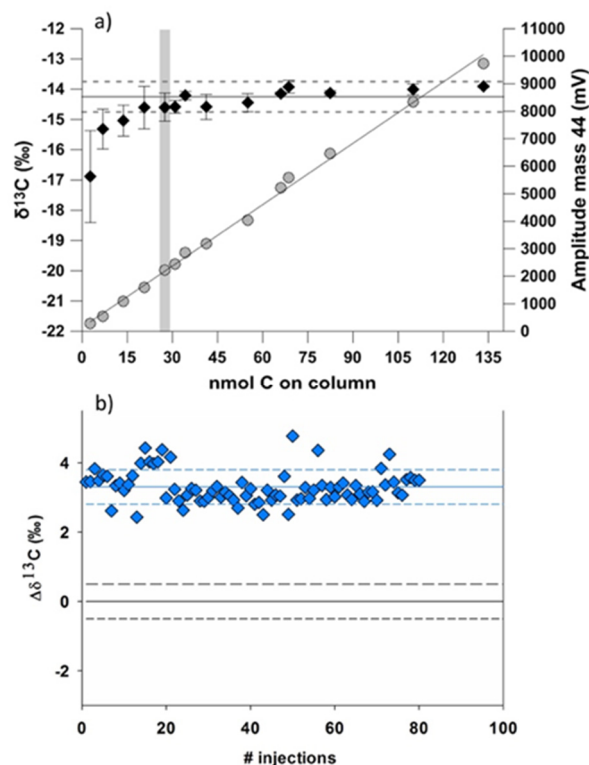


**Figure 2.1:** a) Correlation of amount-dependency tests for carbon isotope values as well as the amplitude by LC-IRMS. Grey circles represent the average intensity for each amount on column, while black diamonds represent the average corresponding delta value of replicate measurements; The limit of precise isotope analysis was determined following the procedure described by Jochmann et al.<sup>104</sup> and is shown by the grey rectangle. The grey horizontal line stands for the mean of all values with intensities above the gray rectangle, b) Reproducibility of carbon isotope values (blue diamonds) of DPC with LC-IRMS, the results are stated as the deviation of the measured value from the value determined by EA-IRMS ( $\Delta\delta^{13}\text{C}$ ); the blue line shows the average carbon isotope values  $\pm 0.5$  ‰ (dashed lines), the black line represents the EA  $\delta^{13}\text{C}$  value of DPC  $\pm 0.5$  ‰ (dashed lines).

The method showed good reproducibility of  $\delta^{13}\text{C}$  values, with a mean value of  $-14.6 \pm 0.5$  ‰ for 80 individual injections of 27.5 nmol C of DPC on column comprising different measurement sequences over a time of 3.5 months (Figure 2.1b). A mean absolute offset of +3.3 ‰ between the average value determined by LC-IRMS and the EA value was measured. Such a difference between LC-IRMS values and EA-IRMS values has been previously observed for amino acids<sup>105, 106</sup>, caffeine and ethanol<sup>107</sup>, pharmaceuticals<sup>108</sup>, and bentazone<sup>58</sup>. Several analyses in Flow Injection Analysis (FIA) mode (i.e. bypassing the LC column) resulted in the same offset between EA values and FIA-IRMS values (data not shown). This observation suggests incomplete wet oxidation of DPC rather than a chromatography-related issue as a reason for this offset. Attempts to optimize oxidation conditions neither led to a reduced offset, nor to a higher intensity of the DPC peak. As the  $\delta^{13}\text{C}$  values obtained by LC-IRMS were reproducible, the resulting offset was constant and could be corrected accordingly.

### 2.4.2. Derivatization of DPC – Nitrogen Isotope Analysis

As shown in Figure 2.2, DPC derivatization resulted in MDPC and its isomer 4-chloro-5-(methylamino)-3(2H)-pyridazone as a major by-product, as well as a minor by-product deriving from the reaction of TMSD with itself. Both products were identified by GC-qMS. Additionally, MDPC was verified using an authentic standard. For method development and optimization purposes, the yield of derivatized DPC was tested by GC-qMS for two temperatures, 50 °C and 70 °C, maintaining the same TMSD-to-analyte-ratio (expressed as molar ratio (n(TMSD):n(analyte) ratio). Temperature dependence was minor, indicating robustness of the method. A slightly higher yield of the target analyte (derivatized DPC) was achieved at a temperature of 70 °C (Supporting Information A.3.2, Figure A5), thus, method validation at the GC-IRMS was continued using this temperature for derivatization. The ratio of the isomer to the target analyte remained at approximately 1/10, unaffected by the temperature. The recovery of derivatized DPC at 70°C was approximately 65 %, which was quantified using an authentic standard at different concentrations ( $R^2 > 0.99$ , data not shown).

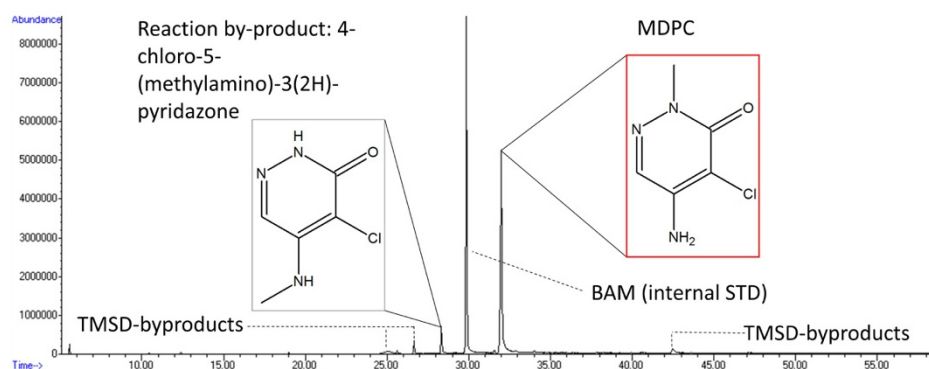


**Figure 2.2:** Chromatogram of DPC derivatized with TMSD showing the derivatization products MDPC (red box) and the reaction by-product 4-chloro-5-(methylamino)-3(2H)-pyridazon (grey box). 2,6-dichlorobenzamide (BAM) was used as an internal standard. An authentic standard of MDPC was applied for peak identification.

Figure 2.3a shows the measured  $\delta^{15}\text{N}$  isotope values of 250 mg/L DPC derivatized with increasing excess of the derivatization reagent TMSD. A plateau of the  $\delta^{15}\text{N}$  isotope value is reached at an excess of TMSD of greater than 150 n(TMSD):n(analyte) indicating optimum transformation of DPC to MDPC at this proportion. Following the approaches of Reinnicke et al.<sup>58</sup> and Mogusu et al.<sup>33</sup>, further method validation was carried out with an excess of 160 n(TMSD):n(analyte) as a conservative approach. The  $\delta^{15}\text{N}$  isotope values show a deviation from the EA-IRMS value ( $\Delta\delta^{15}\text{N}$ ) of  $-1.6 \pm 0.4$  ‰ (black markers in Figure 2.3b)

that can be corrected for. Since the pure non-derivatized standard of MDPC shows a similar off-set (red markers in Figure 2.3b), we conclude that this deviation results from incomplete combustion of the target analyte rather than from isotopically sensitive branching due to formation of the major by-product during derivatization.

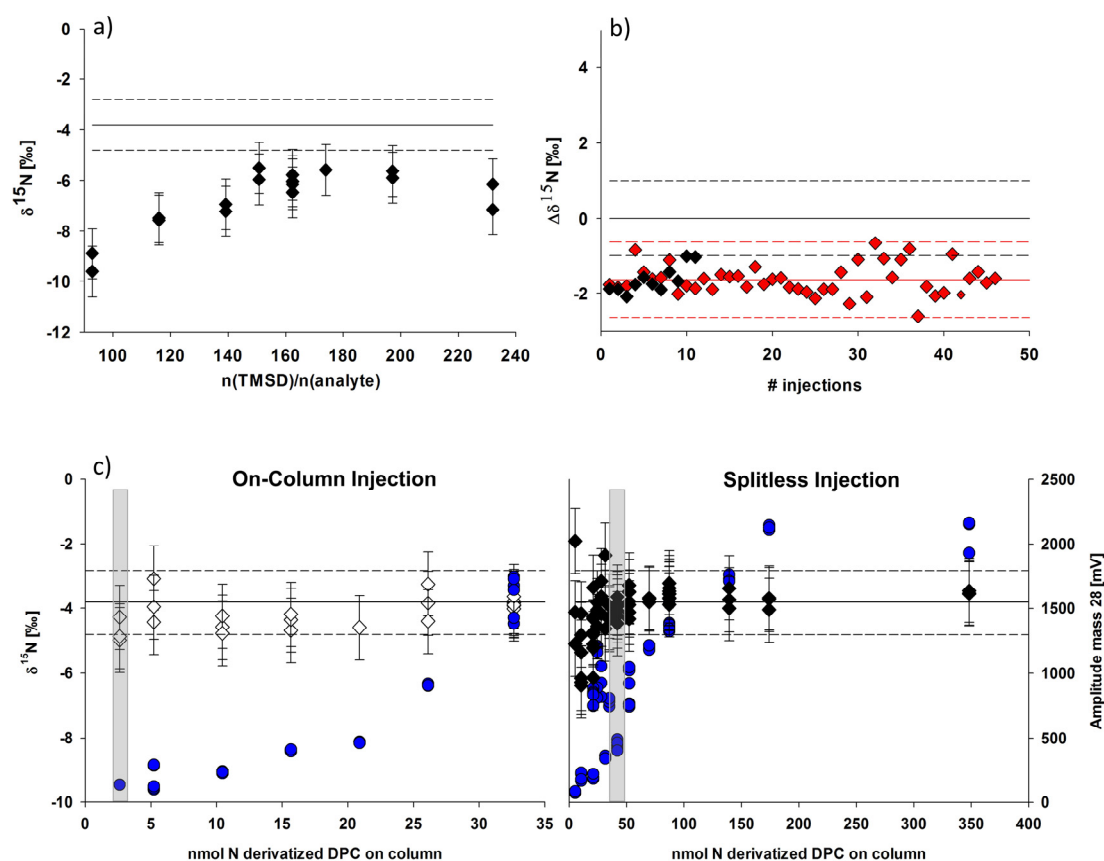


**Figure 2.3:**  $\delta^{15}\text{N}$  values of DPC in a) dependence on the excess of TMSD used for the derivatization procedure, b) the reproducibility of  $\delta^{15}\text{N}$  values of derivatized DPC (black diamonds) and MDPC (red diamonds) measured with GC-IRMS; and c)  $\delta^{15}\text{N}$  values of DPC and the amplitude (blue circles) in dependence on the amount of nitrogen of derivatized DPC injected onto the column to determine the limit of precision – the amount of derivatized DPC equals the initial amount of DPC used for derivatization; black diamonds show the  $\delta^{15}\text{N}$  isotope values using splitless injection, while the white diamonds show the precision gained with on-column injections; data was corrected for the off-set caused by combustion efficiency; the grey rectangle marks the limit of precise nitrogen isotope analysis. Results in panel (b) are stated as the deviation of the measured value from the value determined by EA-IRMS ( $\Delta\delta^{15}\text{N}$ ); the red line shows the average  $\delta^{15}\text{N}$  isotope value and its tolerated standard deviation of  $\pm 1\%$  (red dashed line); the black line shows the target isotope value determined with the EA, while the dashed lines indicate the tolerated standard deviation of  $\pm 1\%$ .

Figure 2.3c shows the nitrogen isotope values of DPC derivatized with an excess of TMSD greater than  $n(\text{TMSD}):n(\text{analyte}) = 150$  (140  $\mu\text{L}$  of a 2 M TMSD solution on 1 mL of a 5 mg/L



to 1000 mg/L analyte solution) injected with two different injection techniques. All values were corrected for the offset due to incomplete combustion. For comparison, the EA-IRMS reference value is shown as black line. The limit of precise nitrogen isotope analysis of DPC is, as expected, amplitude-dependent. For splitless injection, this limit is equal to 31 nmol N derivatized DPC injected, corresponding to an injection of 1.2 µg non-derivatized DPC. Additionally, on-column injection was tested as a more sensitive method. In accordance with the findings of Schreglmann et al. for sensitive isotope analysis of atrazine<sup>48</sup>, on-column injections of the derivatized DPC resulted in a decrease of the limit of precise isotope analysis by a factor of 10 as shown in Figure 2.3b. Thus, 2.06 nmol N of derivatized DPC on-column (100 ng DPC on-column) were sufficient for accurate results, which corresponds to an injection of 1 µL of a 0.69 mM DPC-solution.

### **2.4.3. Isotope Ratios of Commercially Available Chloridazon Products - Source Fingerprinting**

$\delta^{13}\text{C}$  and  $\delta^{15}\text{N}$  EA-IRMS measurements of commercially available CLZ products were used to investigate the possibility to distinguish between different sources. The results are shown as a dual-element isotope plot in Figure 2.4. There is a significant variability for both elements.  $\delta^{15}\text{N}$  isotope values ranging from -5.7 ‰ to -32.0 ‰ were measured (Table A4). As both, CLZ and DPC, contain the identical N-atoms, the metabolite can be related to the parent based on their nitrogen isotope compositions. This highlights the potential of  $\delta^{15}\text{N}$  values of DPC to serve as a fingerprint to retrace the parent compound CLZ.

In contrast to nitrogen isotope values of CLZ, the detected variability of its  $\delta^{13}\text{C}$  values cannot directly be used to conclude on the carbon isotope signature of DPC because cleavage of the phenyl-ring may cause differences in the isotopic signature between parent compound and metabolite.

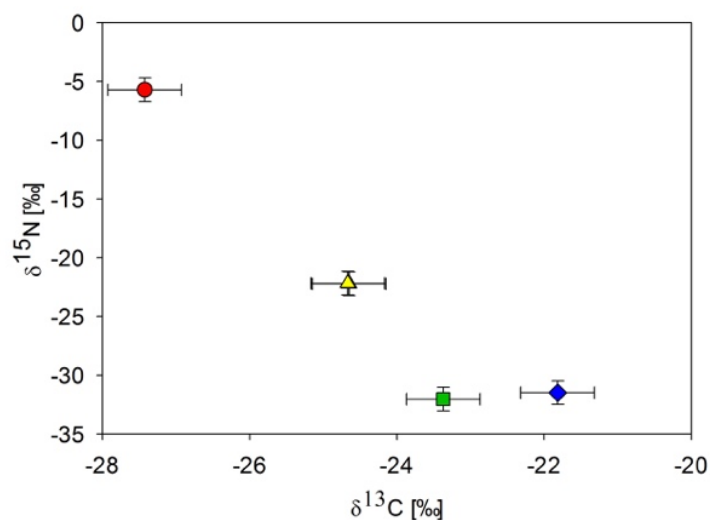


Figure 2.4: Dual-Isotope plot of Chloridazon standards derived from different suppliers.

#### 2.4.4. Evolution of Isotope Ratios of DPC from Different Chloridazon Sources

The developed method was applied to DPC-containing environmental seepage water spiked with CLZ. Its original composition is listed in the Supporting Information (Table A5). The spiked seepage water was used to test whether a mixture of the nitrogen isotope value of DPC deriving from the spiked CLZ and the DPC already present in the water could be observed over a defined time period, simulating a typical field situation.

Concentration measurements of CLZ, DPC and MDPC in the seepage water (Figure 2.5, upper panel and Table A6 in the Supporting Information) showed a significant decrease in CLZ concentration (white) after 7 months ( $t_1$ ) and concentrations below the limit of detection after 11 months ( $t_2$ ). Simultaneously, the DPC concentration increased over time consisting of the initial DPC (shaded grey) and newly formed DPC from degraded CLZ (white). After 8 months, the concentration of DPC remained constant (data not shown). The formation of DPC from CLZ agrees with the findings of Buttiglieri et al.<sup>85</sup> and Schuhmann et al.<sup>19</sup> in environmental samples, where CLZ was degraded within the first 8 to 12 weeks after application on an agricultural field.

The corresponding nitrogen isotope values are shown in the panel below (Figure 2.5). Concomitant with the disappearance of CLZ by reaction a shift in  $\delta^{15}\text{N}$  of DPC towards the isotopic composition of the added CLZ ( $-31.5 \pm 1.0$  ‰) was observed. Formation of MDPC was small (the ratio of MDPC to DPC was always smaller than 10 %) so that its influence on

the DPC nitrogen isotope and its contribution to the mass balance in the samples can be neglected. Also, the interference of MDPC with derivatized DPC on the nitrogen isotope value remains within the uncertainty of the presented isotope analysis. In the case that this ratio is greater in environmental samples, fractionative HPLC can be used to separate the two analytes prior to derivatization-GC-IRMS (Supporting Information A.2.5).

As the initial nitrogen isotopic composition as well as the concentrations of both DPC and CLZ are known, a two sources-mixing model, based on the weighted arithmetic mean of the isotope ratio, was applied to investigate whether DPC nitrogen isotope values accurately reflect the relative contribution of either source. To this end, it is assumed that all additional DPC is formed from CLZ and calculations were based on the EA-IRMS values of the CLZ that was applied. The differences between the measured points and the calculated isotope values (dashed lines) of Figure 2.5 (lower panel) were less than 1 ‰ and thus within the measurement uncertainty of the instrument. This indicates that nitrogen isotope values of DPC did indeed reflect the relative contribution of the DPC from different origin and, therefore, the approach holds promise for future source elucidation of the CLZ metabolite in field samples.

We note that the mass balance does not close for DPC formation from CLZ (Figure 2.5). Possible explanations are either (a) that part of the CLZ was degraded without forming DPC (potentially producing biomass) or (b) that DPC was degraded via a so far unknown transformation pathway that did not entail nitrogen isotope fractionation. Evidence against the second hypothesis, however, is given by our observation that after complete CLZ degradation the concentration of DPC remained constant (data not shown). While further investigations into this matter are beyond the scope of this feasibility test, the possibility to add also carbon isotope analysis to the picture – as newly established in this contribution – clearly provides an added value to probe not only for formation of metabolites from different sources, but also for their further degradation.

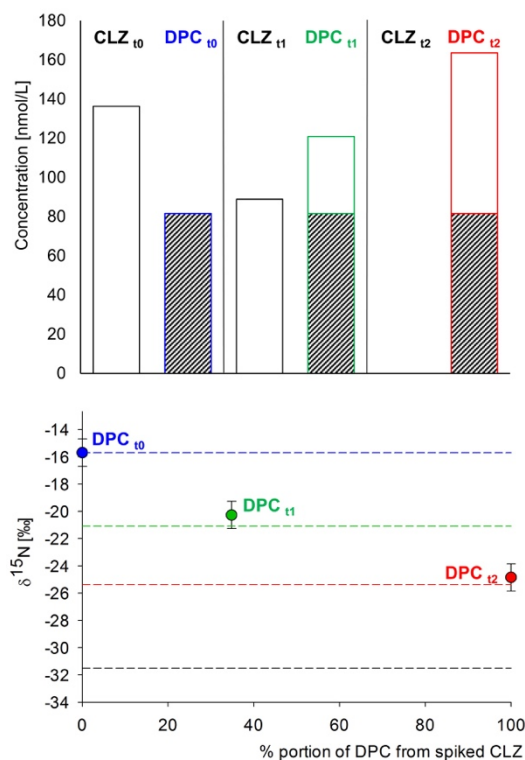


**Figure 2.5: Degradation of CLZ to DPC over time and the resulting change of the  $\delta^{15}\text{N}$  value of DPC due to two different sources of CLZ. Measured  $\delta^{15}\text{N}$  values are shown as circles, while the dashed lines are the corresponding calculated  $\delta^{15}\text{N}$  value based on the mixing of the two CLZ sources originating from the initial  $\delta^{15}\text{N}$  of DPC  $t_0$  and the spiked CLZ (initial  $\delta^{15}\text{N}$  shown as black dashed line). It is assumed that the CLZ is degraded completely to DPC. Samples were taken directly after spiking with CLZ ( $t_0$ ) and after storage for 7 months ( $t_1$ ) and 11 months ( $t_2$ ).**

## 2.5. Conclusion and Outlook.

With LC-IRMS and GC-IRMS, this study brings forward two complementary approaches to accomplish reproducible, precise and true carbon and nitrogen compound-specific stable isotope analysis of DPC in the  $\mu\text{g/L}$ –concentration range (996 ng and 100 ng DPC on column for carbon and nitrogen isotope analysis, respectively). Taking reported DPC concentration of 0.72  $\mu\text{g/L}$  to 7.4  $\mu\text{g/L}$  in surface and ground water into account<sup>85</sup>, the combination of the presented methods with large-volume extraction as presented by Torrentó et al.<sup>62</sup> enables the isotopic analysis of DPC in environmental water samples. Thus, the application of the developed methods brings forward a basis for analysis of environmental water samples from field surveys, and the combination of the developed methods gives access to dual-element isotope plots. Our study highlights the potential of such plots to distinguish different sources. Future DPC degradation studies may use such dual element isotope information to obtain additional information about transformation pathways of DPC and underlying mechanisms<sup>39</sup>.

## 2. <sup>13</sup>C- and <sup>15</sup>N-Isotope Analysis of Desphenylchloridazon

---

Until now, only transformation to MDPC is known, which was, however, observed to occur on longer time scales than in our experiment<sup>19</sup>. Additionally, as shown in the degradation experiment of chloridazon, these methods can be used to distinguish the source of DPC by measuring the nitrogen isotope signature and to identify the mixing of DPC deriving from different CLZ sources.



### 3. Dual-Element Isotope Analysis of Desphenylchloridazon to Investigate its Environmental Fate in a Systematic Field Study - A Long-Term Lysimeter Experiment

Author	Author position	Scientific ideas (%)	Data generation (%)	Analysis and Interpretation (%)	Paper writing done (%)
A. Melsbach	1	40	40	40	60
C. Torrentó	1	20	35	30	10
V. Ponsin	3	0	5	0	5
J. Bolotin	4	0	10	0	0
L. Lachat	5	0	5	0	0
V. Prasuhn	6	5	5	0	0
T. Hofstetter	7	10	0	10	10
D. Hunkeler	8	10	0	5	5
M. Elsner	9	15	0	15	10
Title of paper:	Dual-Element Isotope Analysis of Desphenylchloridazon to Investigate its Environmental Fate in a Systematic Field Study - A Long-Term Lysimeter Experiment				
Status in publication process:	Accepted, <i>Environ. Sci. Technol.</i> 2020, XXXX, XXX, XXX-XXX, <a href="https://doi.org/10.1021/acs.est.9b04606">https://doi.org/10.1021/acs.est.9b04606</a>				

I confirm that the above-stated is correct.

---

Date, Signature of the candidate

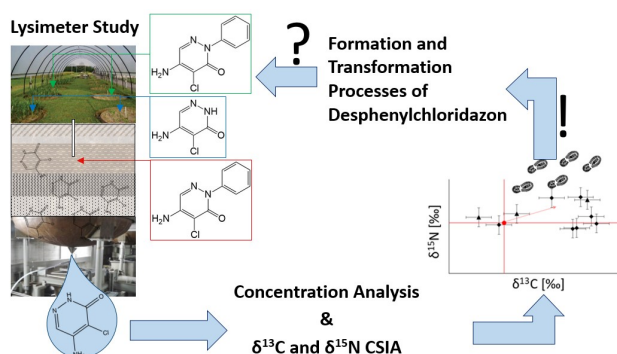
I/We certify that the above-stated is correct.

---

Date, Signature of the doctoral committee or at least of one of the supervisors

### 3.1. Abstract

Desphenylchloridazon (DPC), the main metabolite of the herbicide chloridazon (CLZ), is more water soluble and persistent than CLZ and frequently detected in water bodies. When assessing DPC transformation in the environment, results can be non-conclusive if based on



concentration analysis alone, because estimates may be confounded by simultaneous DPC formation from CLZ. This study investigated the fate of DPC by combining concentration-based methods with compound-specific C and N stable isotope analysis (CSIA). Additionally, DPC formation and transformation processes were experimentally deconvolved in a dedicated lysimeter study considering three scenarios. First, surface application of DPC enabled studying its degradation in the absence of CLZ. Here, CSIA provided evidence of two distinct DPC transformation processes: one shows significant changes only in  $^{13}\text{C}/^{12}\text{C}$ , whereas the other involves changes in both  $^{13}\text{C}/^{12}\text{C}$  and  $^{15}\text{N}/^{14}\text{N}$  isotope ratios. Second, surface application of CLZ mimicked a realistic field scenario showing that during DPC formation,  $^{13}\text{C}/^{12}\text{C}$  ratios of DPC were depleted in  $^{13}\text{C}$  relative to CLZ, while  $^{15}\text{N}/^{14}\text{N}$  ratios remained constant. Finally, CLZ depth injection simulated preferential flow and demonstrated the importance of the topsoil for retaining DPC. The combination of the lysimeter study with CSIA enabled insights into DPC transformation in the field that are superior to studies of concentration trends.



#### 3.2. Introduction

Groundwater is one of the most important drinking water resources<sup>1</sup> and, therefore, constantly screened for contaminants<sup>5, 84, 97, 109</sup>. Due to their extensive application in agriculture, pesticides and their metabolites<sup>78</sup> are commonly detected in ground and surface water. A prominent example is desphenylchloridazon (DPC), the main metabolite of the herbicide chloridazon (CLZ). CLZ is a selective systemic herbicide that is used to control broad-leaved weeds in the agricultural production of Swiss chard, red beet and sugar beet<sup>4, 78, 85, 87, 110, 111</sup>. The metabolite DPC is a compound of concern as it is continuously formed from CLZ. The continuous input of newly formed DPC makes it challenging to evaluate its environmental transformation from concentration data over time. Detection of DPC has increasingly been reported exceeding concentrations of 10 µg/L in natural water bodies<sup>4, 78-81</sup>. DPC can be transported into ground and surface water by precipitation events as it is water-soluble (490 mg/L), and has a lower tendency to bind to the soil (Freundlich constant  $K_{foc}$  of 50 mL/g) than CLZ ( $K_{foc}$  of 199 mL/g). Additionally, DPC has a high leaching potential, which is indicated by the groundwater ubiquity score (GUS) of 5.5, a parameter used to evaluate pesticides for their potential to seep into the groundwater<sup>111-113</sup>. Thus, there is great interest in the question whether DPC can be subject to further transformation. The fate of DPC, however, is not well understood yet<sup>82-84</sup>. It is known that DPC is a persistent and polar compound. In soil, it can be further transformed into methyl-desphenylchloridazon (MDPC, Figure C1)<sup>79, 85, 86, 88</sup>. Whether there is a wider range of degradation pathways, remains unclear.

Current attempts to quantify degradation of organic micropollutants are often based on metabolite-to-parent-compound ratios. This is an analytical approach based on concentration measurements. It is advantageous to quantify degradation even at low concentration ranges, and is simple to use<sup>114</sup>. However, in case of DPC, which may be simultaneously formed while undergoing further transformation (Figure C1), metabolite-to-parent ratios can lead to erroneous interpretations<sup>23</sup>. An additional confounding factor is a different drainage-dependent re-mobilization of the parent compound and the metabolite due to differences in their mobility. Thus, concentrations may fluctuate in a non-trivial manner making it difficult, if not impossible, to inform about how much of the DPC has been transformed. Consequently, a complementary method is needed to detect transformation if metabolite analysis alone is not conclusive.

Compound-specific stable isotope analysis (CSIA) allows to identify degradation processes by analyzing variations of natural stable isotope abundances of different isotopic elements

during (bio)degradation and transformation of organic contaminants<sup>29, 115-117</sup>. While CSIA of polar micropollutants has rarely been performed at field scales<sup>29</sup>, analytical methods for the analysis of carbon ( $^{13}\text{C}/^{12}\text{C}$ ) and nitrogen ( $^{15}\text{N}/^{14}\text{N}$ ) isotope ratios of DPC have recently become available<sup>118</sup>. So far, isotope studies of DPC have been carried out neither in laboratory experiments nor in field applications, however. As illustrated in Figure C1, unique insight on the formation and subsequent transformation of DPC can be expected. On the one hand,  $^{13}\text{C}/^{12}\text{C}$  and  $^{15}\text{N}/^{14}\text{N}$  ratios of DPC are expected to show the isotopic signature of the pyridazinone ring in the precursor CLZ. When CLZ is transformed, its phenyl-ring is first oxidized and then cleaved off. Thus, any isotope effect-induced changes in  $^{13}\text{C}/^{12}\text{C}$  and  $^{15}\text{N}/^{14}\text{N}$  ratios will be manifested in the molecular average of CLZ and in the oxidized phenyl-part that is cleaved off. In contrast, none of the molecular positions of the pyridazinone-ring are involved in the reaction, meaning that only secondary kinetic isotope effects occur so that the isotope ratios within the pyridazinone-ring remain mainly unaffected when they end up in DPC (Figure C1). If, however, further transformation of DPC takes place, this process is expected to result in pronounced changes in isotope ratios in DPC, because now, carbon and nitrogen atoms are directly involved (primary isotope effect). This would lead to carbon and nitrogen isotope fractionation in DPC giving a strong indication of further DPC transformation<sup>24</sup>. CSIA of DPC, therefore, holds promise to identify both processes, formation of DPC from CLZ, as well as independent further transformation of DPC. According to the current mechanistic picture, DPC is only formed from CLZ and transformed through N-methylation<sup>86, 88, 119</sup>. Thus, the combined analysis of carbon and nitrogen isotope ratios of DPC may offer new insights into its fate in soil leachate.

Evidence from CSIA may be inconclusive, however, if physical processes (e.g., multiple sorption-desorption steps, dissolution from non-aqueous phase, volatilization/diffusion, dispersion) or the heterogeneity of the system, the soil in this case, affect degradation-induced changes in isotope ratios. For example, a freshly dissolved compound, which has not been transformed yet, can mix with water containing the contaminant that has already undergone varying degrees of degradation and thus isotope fractionation<sup>120-122</sup>. Consequently, the transformation-induced isotope ratios in the degraded fraction might not be discernible any longer<sup>123, 124</sup>. When applying CSIA to a field site either for the interpretation of a compound's environmental fate or to monitor the success of remediation processes, it is therefore suggested to combine it with complementary approaches in order to obtain as many lines of evidence as possible<sup>120, 125, 126</sup>.

### 3. Dual-Element Isotope Analysis of DPC to Investigate its Environmental Fate

---

Thus, the aim of this study was to explore different complementary and innovative approaches for assessing the environmental long-term fate of DPC in drainage water after agricultural application over a period of 3 years. To that end, we combined concentration measurements with the analysis of carbon and nitrogen isotope ratios in a comprehensive and systematic study in a well-characterized model lysimeter system. This lysimeter system mimics pesticides fate in natural soil environment under high control over environmental and hydrological factors (i.e. soil type and humidity, precipitation levels, temperature, evapotranspiration, etc.). In order to separate the relevant transport and transformation processes, these complementary approaches were integrated into a dedicated experimental design where CLZ and DPC were applied in three different scenarios (Figure C2): (i) DPC was applied to the lysimeter directly, without the presence of CLZ, to investigate whether further DPC transformation is observable in drainage water and whether this transformation is detectable from analyzing carbon and nitrogen isotope signatures of DPC when interfering simultaneous formation of DPC can be excluded. (ii) The concurrent formation of DPC from CLZ and potential DPC transformation were evaluated through surface application of CLZ to the lysimeters. (iii) To simulate the preferential flow and to study whether DPC formation and transformation is also occurring below the top soil, CLZ was injected below the root zone. For each scenario, these complementary approaches were tested with two different soil types through a replication of the lysimeter studies with moraine and gravel soil, respectively.

## 3.3. Experimental / Methods

### 3.3.1. Experimental Set-up of Lysimeter Experiments

For this study, the lysimeter facility from Agroscope was used, located in Zurich-Reckenholz, Switzerland. The facility itself and the characteristics of the lysimeters are described in detail by Torrentó et al.<sup>103</sup>. Briefly, the site consisted of 12 gravitation lysimeters (L) (3.14 m<sup>2</sup> surface area, 2.5 m depth, approximately 14 000 kg of soil in each) filled with two soil types (gravel/moraine). Both soil types consisted of repacked Cambisol. Cambisols, widely and intensively used as agricultural land, are among the most extensive soil types on earth, extending over about 11 % of the global land surface<sup>127</sup>. The soils used in this study differed in the B horizon and the draining properties of the parent material, and thus they were expected to show a different extent of preferential flow<sup>103</sup>. Gravel soil was represented by well-drained sandy loamy Cambisol (L1-L6), while moraine soil consisted of a poorly drained loamy Cambisol (L7-L12) (Table C1). Six of these lysimeters were used for this study (three of each soil type). The lysimeters were planted in 2014 with corn (*Zea mays* L.) followed by sugar beet (*Beta vulgaris* ssp. *vulgaris* var. *altissima* Doel) in 2015, with corn (*Zea mays* L.) again in 2016 and finally with broccoli, Chinese cabbage, lettuce and leek in 2017. 3.0 kg/ha (0.96 g/lysimeter) of CLZ were applied on the surface of two lysimeters (L4 and L8) simulating the scenario of pesticide application at the three- to four-leaf stage in the field<sup>85</sup>. To simulate preferential transport through topsoil, two additional lysimeters were used (L6 and L7), where 2.0 g of CLZ were injected in each lysimeter at a depth of 40 cm at eleven injection points uniformly distributed over the area of each lysimeter by using a metal rod connected to a gear pump through a Teflon tube. Additionally, 3.2 kg/ha (1.0 g/lysimeter) DPC was applied on the surface of two lysimeters (L1 and L12). In addition to CLZ or DPC, the following tracers were applied at the same time as the pesticides: uranine (1.3 kg/ha) and NaBr (500 kg/ha) to lysimeters L1 and L12, uranine (1.3 kg/ha) to lysimeters L4 and L8, and uranine (0.4 g injected in each lysimeter) to lysimeters L6 and L7. Bromide was used as conservative tracer and uranine ( $K_{foc}$  of 120 mL/g) as a marker for preferential leaching shortly after pesticide application<sup>103</sup>. A detailed set-up is shown in the Supporting Information (sections C.2.2 and C.2.3). Details about application methods can be found in Torrentó et al.<sup>103</sup>. All lysimeters were irrigated artificially and the seepage water was collected for analysis over a time period of 3 years (Table C2).

#### 3.3.2. Concentration Measurements of CLZ, DPC and MDPC

For concentration measurements of CLZ, DPC and MDPC, an Ultimate® 3000 RS high-pressure liquid chromatography (HPLC) (Dionex, Thermo Fisher Scientific, Waltham, MA, USA) coupled to a 4000-hybrid triple quadrupole-linear ion trap mass spectrometer (QTRAP®, ABSciex, Framingham, MA, USA) was used. Five microliters were injected on an Acquity UPLC BEH Shield RP18 column (100 × 2.1 mm, 1.7 μm, Waters, Milford, MA, USA) maintained at 25 °C. The separation was performed at a flow rate of 0.4 mL/min using a binary mobile phase system consisting of 0.05% formic acid in water (mobile phase A) and 0.05 % formic acid in acetonitrile (mobile phase B) according to the following gradient program: 5-15 % phase B in 2 min, 15-100 % phase B in 4 min, holding at 100 % phase B for 2 min, and re-equilibration at 2 % phase B for 6 min. Detection was performed in electrospray positive ionization (ESI+) using the multiple reaction monitoring (MRM) mode by monitoring both a quantifier (Q) and a qualifier (q) transition ion for each compound. Precursor and fragment ions (m/z) were 222.1 and 104.0 (Q) or 77.0 (q) for CLZ, 146.0 and 117.0 (Q) or 66.0 (q) for DPC, 160.0 and 117.0 (Q) or 88.0 (q) for MDPC, and 227.0 and 108.0 (Q) or 81.0 (q) for CLZ-d<sub>5</sub>, respectively (Table S3). Quantification was performed using standard curves calculated from standard solutions of CLZ, DPC and MDPC at 0.25, 0.5, 1, 3, 5 and 10 ng/mL, each containing deuterated CLZ-d<sub>5</sub> as internal standard at a constant concentration of 2 ng/mL. The limits of quantification were 0.05 μg/L for CLZ, 0.4 μg/L for DPC and 0.1 μg/L for MDPC. For those drainage water samples with CLZ, DPC and MDPC concentrations lower than 0.2 μg/L, solid-phase extraction (SPE) of 20-mL samples was performed using 6 mL cartridges packed with 0.2 g of Bakerbond SDB-1 sorbent and 0.2 g of Septra ZT sorbent, as described by Torrentó et al.<sup>62</sup>. After SPE, the extracts were analyzed by UHPLC-QTOF-MS. The method is briefly described in the Supporting Information (C.2.5.).

#### 3.3.3. Large Volume Solid-Phase Extraction

For isotope analysis, all lysimeter samples were filtered through 0.7 μm glass fiber filters and were concentrated by SPE using the method described in Torrentó et al.<sup>62</sup>, as detailed in the Supporting Information (C.2.6.).

#### 3.3.4. Elemental Analyzer-Isotope Ratio Mass Spectrometry Measurement for Determination of Reference Values

Carbon and nitrogen isotope reference values of our in-house standards of CLZ, DPC and MDPC were determined by elemental analysis – isotope ratio mass spectrometry (EA-IRMS) according to the method of Meyer et al.<sup>76</sup>. The system consisted of an EuroEA (Euro Vector, Milano, Italy) coupled with a Finnigan MAT 253 IRMS via a Finnigan™ ConFlow III interface (Thermo Fisher Scientific, Bremen, Germany). For calibration, USG 40, USG 41 (L-glutamic acid) and IAEA 600 (caffeine), supplied by the International Atomic Agency (IAEA), were used as organic reference materials.

Carbon ( $\delta^{13}\text{C}$ ) and nitrogen ( $\delta^{15}\text{N}$ ) isotope values are usually expressed using the Delta notation in per mille as described in equation 3.1 and 3.2. There, the isotope ratios ( $^{13}\text{C}/^{12}\text{C}_{\text{sample}}$  and  $^{15}\text{N}/^{14}\text{N}_{\text{sample}}$ ) are stated relative to the international references PeeDee Belemnite (V-PDB) for carbon and air for nitrogen.

$$\delta^{13}\text{C} = \frac{{}^{13}\text{C}/{}^{12}\text{C}_{\text{Sample}} - {}^{13}\text{C}/{}^{12}\text{C}_{\text{Reference}}}{{}^{13}\text{C}/{}^{12}\text{C}_{\text{Reference}}} \quad \text{eq. 3.1}$$

$$\delta^{15}\text{N} = \frac{{}^{15}\text{N}/{}^{14}\text{N}_{\text{Sample}} - {}^{15}\text{N}/{}^{14}\text{N}_{\text{Reference}}}{{}^{15}\text{N}/{}^{14}\text{N}_{\text{Reference}}} \quad \text{eq. 3.2}$$

#### 3.3.5. Carbon Isotope Analysis of DPC by LC- IRMS

For carbon isotope analysis of DPC we applied the method of Melsbach et al.<sup>118</sup>. Briefly, 10 to 100  $\mu\text{L}$  of SPE extracts reconstituted in ultrapure water were injected into an LC-IRMS Dionex system consisting of an Ultimate 3000 HPLC pump and an Ultimate 3000 autosampler (Thermo Fisher Scientific) coupled via an LC-Isolink interface with a Delta V Advantage IRMS (Thermo Fisher Scientific). Chromatography was accomplished using a Sentry guard column (3  $\mu\text{m}$ , 20 mm) and an Atlantis T3 column (3  $\mu\text{m}$ , 100 mm, Waters) at a flow rate of 500  $\mu\text{L}/\text{min}$ . Phosphoric acid at pH 2 was chosen as mobile phase. The method was run isocratically at room temperature. The analytes were converted by wet oxidation at a temperature of 99.9  $^{\circ}\text{C}$  after the separation unit. There to, 90 g/L  $\text{Na}_2\text{S}_2\text{O}_8$  and phosphoric acid (1.5 M  $\text{H}_3\text{PO}_4$ ) were introduced at a flow rate of 30  $\mu\text{L}/\text{min}$ . The vacuum inside the IRMS was

### 3. Dual-Element Isotope Analysis of DPC to Investigate its Environmental Fate

---

$2 \times 10^{-6}$  mbar. Its ion source was set to an accelerating voltage of 3 kV and an electron ionization energy of 124 eV. The isotope ratios were calibrated using our laboratory monitoring gas ( $\text{CO}_2$ ), which had previously been calibrated against the international standard RM8563 ( $\text{CO}_2$ ), supplied by the IAEA.

#### 3.3.6. Derivatization of DPC for Nitrogen Isotope Analysis

Nitrogen isotope analysis was conducted using the derivatization procedure proposed by Melsbach et al.<sup>118</sup>. Briefly, DPC was methylated to MDPC by adding an excess of greater than  $160 \text{ n}_{\text{analyte}}/\text{n}_{\text{TMSD}}$  ( $140 \mu\text{L}$  of a 2 M TMSD solution) into a vial containing a standard or a SPE extract reconstituted in 1 mL methanol. The vial was crimped tightly before putting it into a  $70^\circ\text{C}$  water bath for 2 h. For samples from lysimeters with CLZ depth injection, the volume of the 2 M TMSD solution added to the reconstituted SPE extracts was increased to  $200 \mu\text{L}$  to ensure complete derivatization, as concentrations of DPC were up to an order of a magnitude higher compared to the other lysimeter samples. Afterwards, the solvent was evaporated to dryness. The sample was then reconstituted in  $50 \mu\text{L}$  acetone.

#### 3.3.7. Separation of Drainage Sample Fractions for Analysis of DPC and MDPC

For drainage water samples from the lysimeters where CLZ was applied on the surface and for which the ratio of DPC to naturally formed MDPC was greater than 10 %, preparative HPLC was used prior to derivatization to isolate this naturally formed MDPC and thus to avoid interferences in the isotopic signature of DPC when subjected to methylation in the derivatization procedure. The method is briefly summarized in the Supporting Information (C.2.7.)<sup>118</sup>. Additionally, both DPC and MDPC fractions were used for  $\delta^{15}\text{N}$  isotope analysis when possible. For samples with an MDPC to DPC ratio  $<10 \%$ , no preparative HPLC method was applied prior to derivatization, as the influence of the isotope ratio of MDPC on the isotope ratio of derivatized DPC is negligible and lies within the measurement error for nitrogen CSIA ( $\pm 1 \%$ ) of the developed  $^{15}\text{N}$  GC-IRMS method<sup>118</sup>.

#### 3.3.8. Nitrogen Isotope Analysis of DPC and MDPC

The method is described by Melsbach et al.<sup>118</sup> Briefly, a TRACE GC Ultra gas chromatograph (Thermo Fisher Scientific, Milan, Italy) coupled with a Finnigan MAT 253 IRMS (Thermo

Fisher Scientific, Bremen, Germany) was used. A Finnigan Combustion III interface (Thermo Fisher Scientific) connected both instruments. The analytes were combusted at a temperature of 1030 °C with a NiO tube/CuO-NiO reactor (Thermo Fisher Scientific). The gas chromatograph contained a DB-1701 column (30 m × 0.25 mm × 1 μm, J&W Scientific, Santa Clara, CA). Helium (grade 5.0) at a flow rate of 1.4 mL/min was used as carrier gas. Injection was carried out with a GC Pal autosampler (CTC, Zwingen, Switzerland). A sample volume ranging between 1 and 3 μL was injected into a splitless liner (Thermo Fischer Scientific, Australia) at a temperature of 250 °C. The GC oven was programmed to start at a temperature of 100 °C (held for 1 min), ramped with 25 °C/min to 240 °C, and with 10 °C/min to 280 °C (held for 5 min). The isotope ratios were calibrated using our laboratory monitoring gas (N<sub>2</sub>), which had previously been calibrated against the international standard NSVEC (N<sub>2</sub>), supplied by the IAEA.

#### 3.3.9. Correction Procedure for Isotope Analysis

Analogous to the correction procedure described by Melsbach et al.<sup>118</sup>, all samples and standards were measured in triplicate and their isotope ratios are reported as the arithmetic means with their respective estimated standard deviations ( $\pm \sigma$ ). In addition to the calibration of the measurement gas, samples are bracketed within the sequences by in-house standards of DPC and MDPC, whose isotopic signature had been determined with EA-IRMS (Table C4). Here, the principle of identical treatment by Werner and Brand<sup>26</sup> was applied to correct for trueness by identifying drifts and off-sets, caused by different combustion efficiency.  $\delta^{15}\text{N}$  correction was performed using MDPC synthesized by LGC Standards GmbH, while an authentic DPC standard was used for  $\delta^{13}\text{C}$  correction of the LC-IRMS method.

#### 3.3.10. Concentration Measurement of CLZ and DPC from Soil Samples

CLZ and DPC residues were measured within the first soil layers (0 to 10 cm) approximately one year after herbicide/metabolite application. To obtain a representative and homogenous sample, subsamples for soil analysis were collected in quadruplets and combined afterwards. The total amount was at least 100 g soil per sample. Sample extraction and analysis were carried out by Eurofins Sofia GmbH using LC-MS/MS.



#### 3.3.11. Statistical Analyses.

Pearson correlation analysis and one-way analyses of variance (ANOVA) tests were performed to identify patterns and to measure the statistical significance of the relationship between variables. ANOVA tests were performed to assess the differences between soil types and pesticide application methods regarding total accumulated drainage, total DPC mass leached, maximum change of carbon and nitrogen isotope signatures 900 days after pesticide application/injection. Separate Pearson linear correlations were performed to evaluate the relationship between irrigation and drainage, between soil humidity and drainage, between drainage and DPC mass leached, and between evapotranspiration and DPC mass leached. All tests were performed using the statistical package Minitab 13.31 (Minitab Inc., State College, PA). All statistical differences were set to the  $\alpha = 0.05$  significance level ( $p \leq 0.05$ ).

### 3.4. Results and Discussion

#### 3.4.1. Water Dynamics

Total accumulated drainage 900 days after CLZ or DPC application/injection was between 488 to 656 mm for gravel soil and between 337 and 502 mm for moraine soil. In relation to the water input, drainage represented 25-39 % and 18-27 % of the total irrigation, respectively. Increased drainage coincided with periods of high irrigation intensity and high soil water content. A significant positive correlation (Pearson's correlation coefficient –  $r$  – from 0.30 to 0.49,  $p < 0.0001$ ) between intensity of daily irrigation and daily drainage was observed for the six lysimeters. As detailed by Torrentó et al.<sup>103</sup>, who used the same lysimeters to assess the fate of the herbicide atrazine and its metabolites, soil humidity data revealed that large irrigation events resulted in a greater contribution of preferential flow to drainage, and that this effect was more significant for the moraine than for the gravel soil. A statistically significant ( $p < 0.05$ ) correlation was observed between soil humidity and drainage for both gravel and moraine soil at all depths where capacitance sensors were installed (at 16, 36, 56, 76, and 96 cm for moraine soil and at 11, 51, and 71 cm for gravel soil)<sup>103</sup>. This correlation was stronger for moraine ( $r$  between 0.15 and 0.22, except for one depth with  $r = 0.08$ ) than for gravel soil ( $r$  between 0.06 and 0.16), and is in accordance with the fact that fluctuations in the soil water content were smaller for the latter, especially at greater depths<sup>103</sup>. The total accumulated drainage after 900 days was influenced by the application method (higher drainage for depth injection,  $p = 0.331$ ) and by the soil type (higher for gravel soil,  $p = 0.426$ ).

Large amounts of drainage from the gravel soil are probably a consequence of the higher water permeability and low water content at field capacity of this soil<sup>103</sup>.

The average monthly and annual irrigation, drainage, and evapotranspiration values for the lysimeters used in this study are shown in Table S5. Annual evapotranspiration, estimated by the water balance computation as explained by Torrentó et al.<sup>103</sup>, was for the four years of study (2014 to 2017) higher for moraine (315 to 633 mm) than for gravel soil (266 to 585 mm), although the effect was not statistically significant ( $p = 0.718$ ). A significant effect ( $p = 0.002$ ) on annual evapotranspiration was however observed for crop type: evapotranspiration was higher for sugar beet and corn than for broccoli, Chinese cabbage, lettuce and leek. The effects of soil type and pesticide application method on evapotranspiration 900 days after pesticide application were not statistically significant ( $p = 0.093$  and  $p = 0.579$ , respectively). The influence of the cover vegetation on drainage and pesticides fate was not assessed, since no significant differences in the plants development were observed between lysimeters. For details, see Supporting Information Section C.3.2.

#### 3.4.2. Trends in Compound Concentrations after DPC Surface Application

Neither CLZ, nor DPC had ever been applied to any of the lysimeters prior that study so that trends for CLZ and DPC concentrations could be uniquely attributed to our experimental design. Through application of the metabolite DPC to the surface of the lysimeters, it was possible to investigate the fate of DPC separately, in the absence of CLZ and without interference of constantly formed DPC. The breakthrough of DPC in the seepage water differed between the soil types (Figure 3.1b). In the lysimeter with moraine soil (L12), concentrations changed more rapidly in relation with drainage events than for gravel soil (L1). For gravel soil (L1), DPC was detected in the drainage water for the first time after 137 days, while it broke through only 15 days after application in moraine soil (L12). In these lysimeters, a positive correlation was observed between drainage and DPC mass leached, being more significant for gravel ( $r = 0.36$ ,  $p = 0.029$ ) than for moraine soil ( $r = 0.31$ ,  $p = 0.113$ ). The observed dependency of the drainage response, and the analytes' concentration therein, on the irrigation agrees with Torrentó et al.<sup>103</sup> for the fate of the herbicide atrazine and its metabolites in these lysimeters. Table C6 summarizes the observed breakthrough parameters for each lysimeter. Two main DPC concentration peaks were detected in the drainage water of these two lysimeters after approximately 550 and 850 days (Figure 3.1e). They coincided with two

### 3. Dual-Element Isotope Analysis of DPC to Investigate its Environmental Fate

---

intense irrigation events (November 2016 and September 2017, Table C2). In moraine soil (L12, 303 and 441 mm), less accumulated drainage had occurred at peak concentration of DPC than in the gravel soil (L1, 458 and 852 mm). Concentrations in the gravel soil were approximately one order of magnitude higher than in moraine soil. In contrast to our previous study<sup>103</sup>, no rapid breakthrough peak was observed shortly after application, neither for DPC nor for uranine (Figure C4). Bromide mass recovery curves (Figure C5) showed an asymmetric sigmoidal shape, which is characteristic for transport through a porous matrix with some retardation. Smoother trends for DPC compared to the tracers indicate retardation by sorption and/or attenuation by degradation. DPC leaching was therefore mainly driven by porous matrix flow, although intense irrigation events resulted in a greater contribution of preferential flow. This was observed mainly in moraine soil. For example, after 425 and 670 days, sharp increases in DPC concentrations were measured (Figure C4). This might be a consequence of transport by preferential flow induced by intense irrigation events (July 2016 and March 2018, respectively, Table C2).

The transformation product of DPC, MDPC, was first detected after 256 days and 425 days for gravel and moraine soil, respectively. At the end of the monitoring period (950 days after DPC application), 6.0 % of the DPC mass was recovered in the drainage water of the gravel soil and only 0.3 % in the moraine soil (details about the calculation of analyte recovery can be found in the Supporting Information Section C.2.9). MDPC accounted for 0.55 % and 0.06 % of the applied DPC, respectively. One year after application, a DPC residue of approximately 3 % and 7 % of the applied DPC was quantified within the first soil layers (0 to 10 cm) of gravel and moraine soil, respectively (Table C7). Thus, an incomplete mass balance was observed. Here, possible explanations might be: (i) sorption of DPC to lower soil layers within the root zone, where further sampling was not possible without disturbing the lysimeter, (ii) the uptake and metabolism of DPC by plants<sup>19,128</sup>, and (iii) the presence of DPC-fulvic acid complexes, as their functional groups can bind DPC. This has been demonstrated by Gatzweiler<sup>129</sup>, who conducted lysimeter experiments with <sup>14</sup>C-labelled CLZ. Using thin-layer chromatography and analyzing the radioactivity, Gatzweiler<sup>129</sup> detected DPC in fulvic acid fractions verifying the existence of these DPC-fulvic acid complexes. Nevertheless, the MDPC/DPC concentration ratio suggests that further DPC degradation to MDPC occurred in both soils, mainly after 425 days. (As both DPC and MDPC have a similar GUS leaching potential and show only minor differences in their mobility, no major retardation effect on the transport of either compound is expected so that the use of metabolite-to-parent compound ratios appears justified in this case)<sup>111</sup>. This further degradation agrees

with the findings of Schuhmann et al.<sup>19</sup> and the environmental degradation pathway predicted by Roberts et al.<sup>88</sup>. This demonstrates that transformation of DPC is occurring only slowly. For the moraine soil, a local maximum for the MDPC/DPC concentration ratio was reached after 750 days (Figure 3.1, L12e). To obtain additional insight into DPC transformation, we, therefore, evaluated the results from CSIA of the lysimeter experiment.

#### 3.4.3. Insights into DPC Transformation by Isotope Analysis of DPC Surface Application

Initially, the  $\delta^{13}\text{C}$  and  $\delta^{15}\text{N}$  values of the leached DPC were close to the original isotope signature of the applied DPC (Figures 3.1, L1d and L12d). Over the course of the observation period carbon isotope signatures of DPC showed significant enrichment in  $^{13}\text{C}$  ( $\Delta\delta^{13}\text{C}_{\text{DPC}}$ ) of approximately +4 ‰ in both soil types. The heavy irrigation event 672 days after DPC surface application (March 2017, Table C2) caused a new small DPC breakthrough peak, in which DPC isotope values returned to the original isotopic composition, most likely because new DPC was mobilized, which had not yet been subject to transformation. This effect was more significant in moraine soil, where a greater contribution of preferential flow in response to this heavy irrigation event was observed, resulting in a recovery of up to 20 % of the total mass of DPC leached in the drainage water after the monitoring period. Additionally, significant changes of nitrogen isotope signatures ( $\Delta\delta^{15}\text{N}_{\text{DPC}}$ ) of +2 ‰ to +3 ‰ were observed – however, mainly in the gravel soil (L1). Furthermore, these shifts were observed at a later time point than the enrichment in  $^{13}\text{C}$ , approximately 450 days after application. The fact that during the first 450 days DPC was only becoming enriched in  $^{13}\text{C}$ , and then in both  $^{13}\text{C}$  and  $^{15}\text{N}$ , suggests that DPC was transformed by two distinct processes and that only the latter one starting after 450 days involved a reaction of a nitrogen atom. The transition between the two trends coincides with an increase in the MDPC/DPC concentration ratio (Figure 3.1, L1e). As there had never been any application of CLZ or DPC to these lysimeters, the carbon and nitrogen isotope values of DPC can be uniquely attributed to the substance applied in this study, and changes in these isotope signatures are attributable to its further degradation. Interestingly, due to the high concentrations of MDPC in the drainage water, it was possible to measure the  $\delta^{15}\text{N}$  of formed MDPC after purification by preparative HPLC (Tables C9 and C10). In both lysimeters, the  $\delta^{15}\text{N}$  of MDPC was significantly more negative (approximately by 4‰) compared to the  $\delta^{15}\text{N}$  value of the DPC at that time (Figure 1d). Since DPC contains three nitrogen atoms out of which only one is methylated, it can be estimated that the methylation

### 3. Dual-Element Isotope Analysis of DPC to Investigate its Environmental Fate

---

of DPC causes a nitrogen isotope effect of approximately  $3 \times 4 \text{ ‰} = +12 \text{ ‰}$  at the reactive atom. Our data for the DPC surface application show an enrichment in  $^{13}\text{C}$  and, to a lesser extent, in  $^{15}\text{N}$  for DPC in both soils, which was significantly masked in the moraine soil due to the leaching of fresh DPC after heavy irrigation events. Transformation extent can thus be underestimated. Here, transformation of DPC may be easier to detect using the metabolite-to-parent concentration ratio, at least for the pathway involving MDPC formation. On the other hand, using the metabolite-to-parent concentration ratio only to investigate the transformation of DPC, the evidence of an additional transformation mechanism would have remained undetected. Additionally, CSIA appears to be more robust as the integrated isotope signal, which indicates degradation remains measurable, even if the metabolite might be subject to sorption or further transformation.

### 3. Dual-Element Isotope Analysis of DPC to Investigate its Environmental Fate

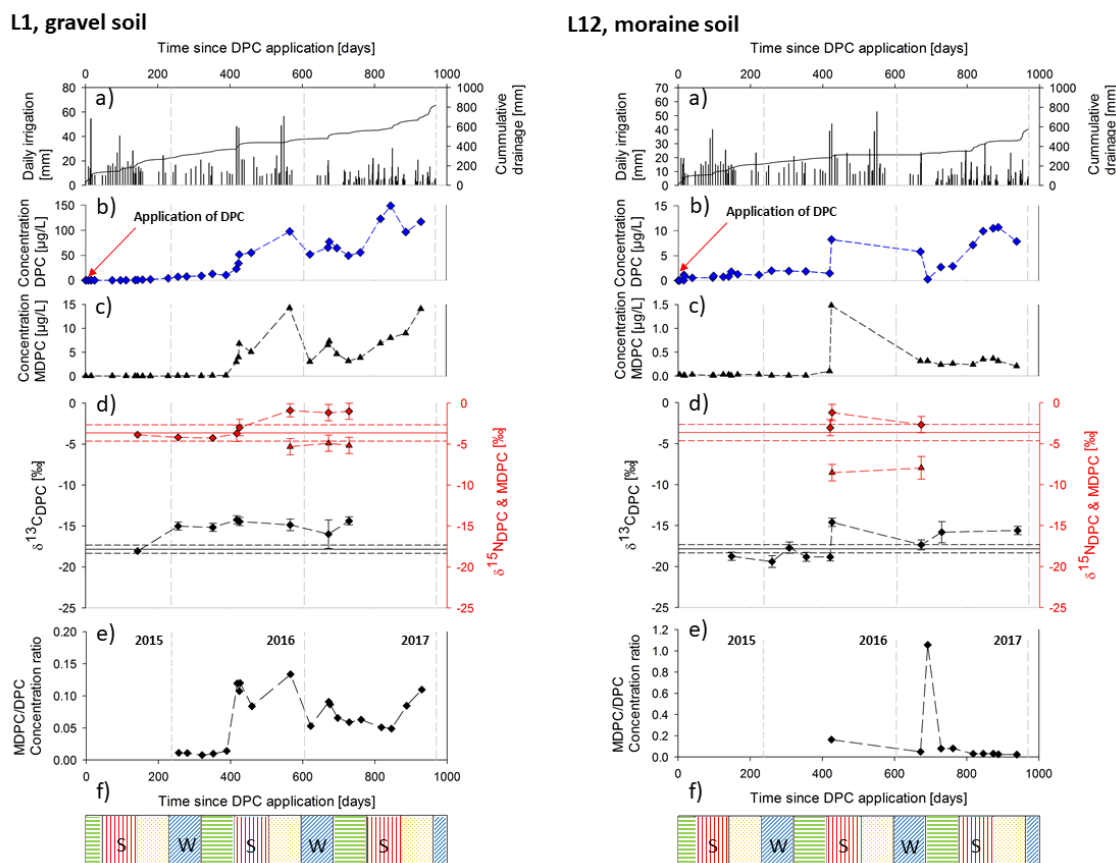


**Figure 3.1.** Lysimeters with DPC application on surface (a single application in May 2015): L1 in gravel soil (left panels) and L12 in moraine soil (right panels). a) Daily irrigation (black bars) and cumulative drainage (grey line); b)-c) Concentration of DPC (blue diamonds) and MDPC (black triangles), note that different scales are used for both soil types; d) Carbon (black diamonds) and nitrogen (red diamonds) isotope ratios of DPC and nitrogen isotope values of MDPC (red triangles), error bars show the associated uncertainties ( $\pm 0.5\text{‰}$  for carbon,  $\pm 1.0\text{‰}$  for nitrogen isotope analysis); or when exceeding this uncertainty, standard deviations of triplicate measurements are given, EA isotope values of the applied DPC are shown as lines, whereas associated uncertainties ( $\pm 0.5\text{‰}$  for carbon,  $\pm 1.0\text{‰}$  for nitrogen isotope analysis) are shown as dashed lines in the corresponding color, respectively; e) metabolite-to-parent compound molar ratio of MDPC/DPC (black diamonds); f) season corresponding to the time since application – spring (green horizontal lines), summer (red vertical lines), autumn (yellow dots), winter (blue diagonal lines); the grey dashed lines repeated in each sub-figure represent the start of a new year.

#### 3.4.4. CLZ Surface Application Mimicking A Realistic Field Scenario

For the surface application of CLZ (Figure 3.2, L4 and L8), the metabolites DPC and MDPC were detected in the seepage water 425 days after CLZ application, coinciding with a heavy irrigation event (July 2016, Table C2), while the applied parent compound remained below or close to the limit of detection of  $0.05\text{ }\mu\text{g/L}$  during the time of monitoring (970 days). Analytes breakthrough curves and concentrations differed between the soil types. For uranine, a rapid

breakthrough shortly after application was detected in moraine soil (Figure C4). During the monitoring period, the maximum uranine concentration was measured within the first day, after only 4 mm of accumulated drainage (Table C6), suggesting that it was mainly transported through preferential flow, bypassing large fractions of the soil matrix. Furthermore, a pronounced uranine peak tailing was observed, which is typical for preferential flow (Figure C4). Furthermore, the DPC mass recovery curves were significantly different for the two soils (Figure C5), giving further evidence of a greater contribution of transport through preferential flow for moraine soil. This difference in soil type agrees with the results of the lysimeters with surface application of DPC as well as well as with the findings for other compounds described in Torrentó et al.<sup>103</sup>.

Approximately 0.5 % and 0.13 % of the applied CLZ was leached as DPC after 950 days in gravel and moraine soil, respectively. When analyzing the CLZ and DPC content in the upper soil, for none of the lysimeters a closed mass balance was obtained. While no CLZ was detected in the first soil layer (0 to 10 cm) approximately 1 year after CLZ application to the lysimeter surface (consistent with Pestemer & Malkomes<sup>130</sup>), DPC amounts corresponding to 5 to 9 % of the applied CLZ were found (Table C7). CLZ and DPC are expected to be incorporated into maize plants based on the findings of Schuhmann et al.<sup>19</sup> and Stephenson & Ries<sup>128</sup>. In addition, Barra et al.<sup>131</sup> showed that during the first 90 days after CLZ application, CLZ dissipation was mainly due to volatilization and degradation, whereas later on, when CLZ was already in the subsurface, its disappearance from soil occurred mainly due to degradation. Higher DPC/CLZ concentration values were measured in the drainage water of the gravel soil compared to moraine soil. These results suggest that either DPC leached more rapidly through the soil matrix in the gravel soil because of higher permeability. Or, alternatively, the extent of CLZ degradation was higher for the gravel soil compared to moraine soil, as there is a greater contribution of preferential flow in moraine soil, which bypasses the top layer where degradation is mostly expected to take place. When preferential flow occurs, pesticides bypass large fractions of the soil matrix, reducing the degradation and sorption potential, as the topsoil is microbiologically more active and with higher organic matter content. CSIA results provide additional insights about these two hypotheses (see below). Concentration ratios and isotope results point to a higher extent of CLZ degradation in gravel than in moraine soil. Nevertheless, some metabolite-to-parent ratio values may be underestimated, because CLZ was below the limit of detection and, therefore, CLZ concentrations corresponding to the detection limit were chosen for calculation, resulting in a minimum estimated ratio in that case.

### 3. Dual-Element Isotope Analysis of DPC to Investigate its Environmental Fate

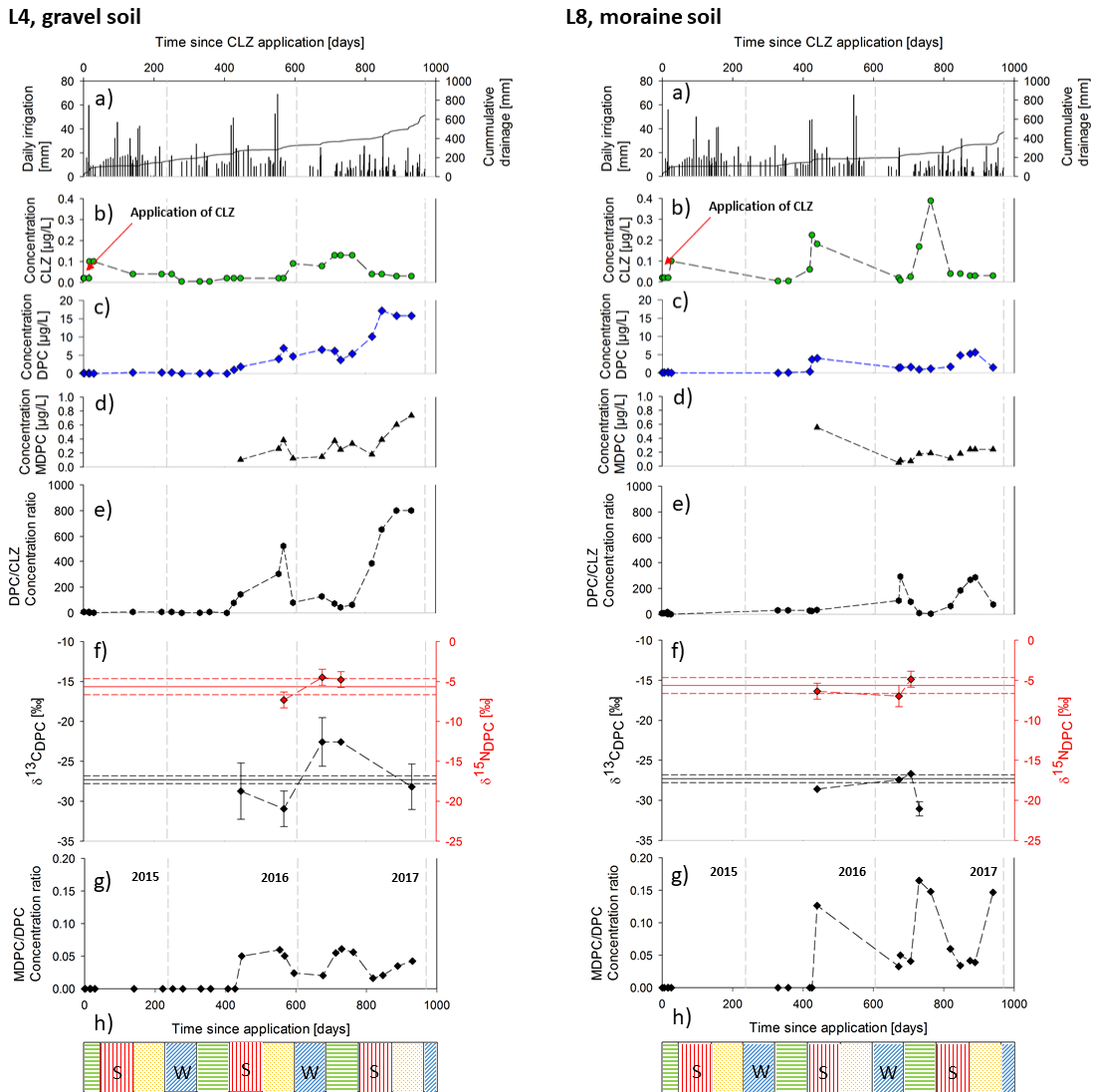


**Figure 3.2.** Lysimeters with CLZ application on surface (a single application in May 2015), L4 (left panels) and L8 (right panels). a) Daily irrigation (black bars) and cumulative drainage (grey line), b)-d) Concentration of CLZ (green circles), DPC (blue diamonds) and MDPC (black triangles) over time, e) metabolite-to-parent compound molar ratio of DPC/CLZ (black hexagon), f) carbon (black diamonds) and nitrogen (red diamonds) isotope ratios of DPC, error bars show the associated uncertainties ( $\pm 0.5\text{‰}$  for carbon,  $\pm 1.0\text{‰}$  for nitrogen isotope analysis; or when exceeding this uncertainty, standard deviations of triplicate measurements are given, EA isotope values of the applied CLZ are shown as lines, whereas associated uncertainties ( $\pm 0.5\text{‰}$  for carbon,  $\pm 1.0\text{‰}$  for nitrogen isotope analysis) are shown as dashed lines in the corresponding color, respectively; g) metabolite-to-parent compound molar ratio of MDPC/DPC (black diamonds), h) season corresponding to the time since application – spring (green horizontal lines), summer (red vertical lines), autumn (yellow dots), winter (blue diagonal lines); the grey dashed lines repeated in each sub-figure represent the start of a new year.

In lysimeters with CLZ surface application (Figure 3.2, L4f and L8f), some carbon isotope values of DPC show a shift to more negative  $\delta^{13}\text{C}$  values compared to the carbon isotope



signature of the applied CLZ (Table C4). This behavior is observable in both lysimeters, especially after heavy rain events such as that one performed 550 days after CLZ application (November 2016, Table C2), which resulted in a depletion in  $^{13}\text{C}$  by 3.4 ‰ for gravel soil (L4). This shift may be attributed to the mobilization of freshly formed DPC, which is formed from CLZ by loss of the aromatic moiety through C–N bond cleavage. Presuming that the phenyl-ring contains more  $^{13}\text{C}$  atoms than the average molecule (Figure C1), which may have been introduced by the synthesis process, this would result on a  $^{13}\text{C}$ -depletion. Alternatively, the shift may be due to secondary normal carbon isotope effects. Once transformation of DPC starts – as evidenced by the detection of MDPC – this  $^{13}\text{C}$ -depletion may be masked compared to the carbon isotope composition of the applied CLZ, as an enrichment in  $^{13}\text{C}$  in DPC is expected. Consistently, observed  $\delta^{13}\text{C}_{\text{DPC}}$  values are close to or higher than the EA-IRMS value of the applied CLZ.

In moraine soil (L8), no evidence of DPC degradation was obtained based on carbon isotope values, as changes of  $\delta^{13}\text{C}$  values were within the uncertainty of the method (Figure 3.2, L8f). In contrast, carbon isotope values of DPC in gravel soil (L4) showed an enrichment in  $^{13}\text{C}$  by up to +8.4 ‰ (Figure 3.2, L4f) indicating that DPC was further transformed. At a subsequent time point (930 days after application), however, the  $\delta^{13}\text{C}_{\text{DPC}}$  value changed back close to the original isotopic signature detected at the beginning of monitoring. This indicates that the change in  $\delta^{13}\text{C}$  DPC values was “diluted” by the input of newly mobilized DPC, as supported by a concomitant increase of the DPC/CLZ concentration ratio (Figure 3.2, L4e). Hence, the two lines of evidence (isotope and DPC/CLZ concentration ratios) were found to complement each other in the assessment of DPC degradation – when one line of evidence was about to fail, the other was able to provide conclusive evidence.

The more substantial changes in both  $\delta^{13}\text{C}_{\text{DPC}}$  values and DPC/CLZ concentration ratios indicate that DPC degradation was higher in L4 (gravel soil) than in L8 (moraine soil) leading to the hypothesis that differences in the transformation rate of CLZ to DPC existed. This is supported by the findings of Capri et al.<sup>132</sup>, who reported that the extent of CLZ degradation is influenced by the moisture content of the soil. As described by Torrentó et al.<sup>103</sup>, there is a higher soil water content and less fluctuation of the water content in the gravel soil than in moraine soil. On the other hand, for both moraine and gravel soil,  $\delta^{15}\text{N}$  values of the DPC formed are, as hypothesized in Figure C1, close to the nitrogen isotope signature of the applied CLZ. Based on the findings of Lingens et al.<sup>86</sup>, the pyridazinone-ring of the CLZ molecule is not involved in the first transformation steps (dioxygenation of the phenyl-ring, Figure C1) so

that no significant nitrogen isotope fractionation is expected during CLZ transformation to DPC<sup>51, 118, 119, 133</sup>. As the isotope effect during multi-step reactions is reflected by the rate-limiting steps, our results indicate that the amidase-driven cleavage of the moiety (2-hydroxymuconate) at the C–N bond, may be not rate-limiting. As a result, changes in nitrogen isotope values of DPC can be uniquely attributed to its further degradation.

#### 3.4.5. Transformation-Potential after Herbicide Injection Below the Vadose Zone

Finally, two lysimeters (L6 and L7) were chosen to simulate the preferential flow after a heavy irrigation event by injecting CLZ into a depth of 40 cm, following the approach described by Torrentó et al.<sup>103</sup>. In contrast to surface application observations, CLZ and DPC broke through a few days after CLZ was injected (Figure C6). The second metabolite MDPC was detected in the drainage water after 130 days. The detection of the metabolites indicated that CLZ degradation occurred, even when it was injected below the root zone. Additionally, significantly greater concentrations of CLZ, DPC and MDPC (1 to 2 orders of magnitude higher) were measured in the drainage water of the lysimeter with CLZ depth injection compared to the CLZ surface applications. In contrast to surface application observations, early breakthrough of injected uranine and CLZ occurred for the two soil types within a few days (< 11 days for gravel and 6 hours for moraine soil) and after a small amount of accumulated drainage (< 55 mm and 8 mm, respectively). This rapid response and the peak tailing for both solutes are typical for preferential flow. More than 80 % of the total uranine recovered mass was received during this early breakthrough. These results confirm that preferential flow was enhanced by depth injection. In agreement with Torrentó et al.<sup>103</sup>, the response to intense irrigation events was more significant than for surface applications. It results in several fluctuations of CLZ and DPC concentrations in the drainage water during the first 370 days for both soils (Figure C4). A great increase in CLZ and DPC concentrations occurred in both lysimeters after 330-345 days (at 225-320 mm of accumulated drainage), coinciding with the heavy irrigation events in May 2015 (Table C2). After this pulse, no CLZ was recovered, while a steady increment in accumulated mass recovery was observed for DPC for both soils (Figure C5).

At the end of the monitoring period (1250 days after CLZ injection), total leached analytes accounted for 24 and 22 % of the injected CLZ mass, respectively. Even though comparison between the two application methods may be limited (eleven uniformly distributed CLZ

injections versus broad surface application), higher recoveries were obtained for CLZ injection after the same time of monitoring (950 days): from 2.0 to 3.4 % of CLZ, between 16.4 and 17.2 % of DPC and from 0.2 to 0.4 % of MDPC compared to no CLZ leaching, 0.13 to 0.15 % of DCP and below 0.02 % of MDPC with surface application. As the mass balance remains incomplete for CLZ injection, there is evidence that additional processes occurred. With surface application, processes such as volatilization<sup>131</sup>, additional transformation pathways<sup>88</sup> and uptake by plants<sup>19</sup> likely accounted for the mass losses. Additional influences on the low recovery, which might also occur after CLZ depth injection, might be the low mobility for CLZ<sup>134</sup> and the formation of putative fulvic acid complexes of DPC<sup>129</sup>. The DPC/CLZ concentration ratio in these lysimeters with CLZ depth injection shows that the main fraction of DPC seems not to be involved in sorption as this concentration ratio has a single global maximum starting approximately 600 days after CLZ injection (Figure C6). This global concentration maximum is two orders of magnitude greater than DPC/CLZ concentration ratios observed for CLZ surface application. It shows the importance of the topsoil to retain DPC. As indicated by the MDPC/DPC concentration ratio, further transformation of DPC occurred, although its extent and nature is unknown.

ANOVA tests were performed to assess the differences between the two soil types and the CLZ application method (i.e. surface application vs. depth injection) regarding DPC leaching and its carbon and nitrogen isotope fractionation. The results showed that the DPC mass leached after 900 days was significantly influenced by the CLZ application method ( $p < 0.0001$ ). A 90- to 260-fold increase in DPC leaching was observed for depth injection compared to surface application. Although the effect of soil type was not statistically significant ( $p = 0.998$ ), CLZ surface application resulted in higher DPC mass leached for gravel than for moraine soil.

Similar to observations in lysimeters with CLZ surface application, carbon isotope data of DPC show an enrichment in  $\delta^{13}\text{C}$  of 3.8 ‰ after 648 days of herbicide injection below the root zone in the gravel soil, while no significant change is observed in moraine soil (Figure C6). There, up to 648 days, no significant changes in  $^{13}\text{C}/^{12}\text{C}$  and  $^{15}\text{N}/^{14}\text{N}$  ratios were measured. The  $\delta^{15}\text{N}$  value of DPC shows the initial isotope composition of the CLZ applied to the lysimeter. In very few cases, it was possible to measure  $\delta^{15}\text{N}$  values of MDPC formed from DPC (Figure C6 and Table C11). Nitrogen isotope values of MDPC were by approximately 6 ‰ more negative than  $\delta^{15}\text{N}$  signature of its parent compound DPC. This shift agrees with the findings in DPC transformation experiments (Figure 3.1, L1 and L12) and, thus, supports

the nitrogen isotope effect of DPC methylation of approximately +12 ‰ as estimated above (Table C9 and C10). According to the ANOVA results, isotope fractionation was mainly influenced by the soil type (higher  $^{13}\text{C}$  and  $^{15}\text{N}$  enrichment for gravel soil) rather than by the CLZ application method.

#### 3.4.6. Dual-Element Isotope Plot to Identify DPC Formation and Transformation

A dual-element plot was used for an overview of observed trends in carbon and nitrogen isotope signatures of DPC (i) either from formation from CLZ, or (ii) when DPC was further transformed. In Figure 3.3a, isotope data of all lysimeters with DPC surface application are combined, whereas in Figure 3.3b, data of all lysimeters with CLZ application/injection are shown. In Figure 3.3a, where DPC represents the original applied compound, a general trend towards more positive  $\delta^{15}\text{N}$  and  $\delta^{13}\text{C}$  values is observable. This observation is consistent with the well-established phenomenon that, in most cases, heavy isotopes become enriched in the remaining substrate during (bio)degradation. As detailed above, DPC in first drainage samples (first 450 days) of the gravel soil showed a significant enrichment in  $^{13}\text{C}$  but not in  $^{15}\text{N}$ , indicating that two distinct processes for DPC transformation occurred. In contrast, Figure 3b shows two opposing trends pointing to the occurrence of both DPC formation and transformation. On the one hand, similar to the lysimeters with DPC application, a trend is observed towards more positive  $\delta^{13}\text{C}$  and  $\delta^{15}\text{N}$  values during the transformation of DPC. On the other hand, numerous data points show more negative  $\delta^{13}\text{C}$  and  $\delta^{15}\text{N}$  isotope values. As this trend is only observable for lysimeters with CLZ application and injection, we attribute it to the formation of DPC. As discussed above, possible explanations for the observed depletion in  $^{13}\text{C}$  (more negative  $\delta^{13}\text{C}$  values) is (i) an artefact of an uneven  $^{13}\text{C}$  isotope distribution in the cleaved phenyl-ring during DPC formation; or (ii) that the formation of DPC from CLZ (Figure C1) may be accompanied by a small and normal secondary carbon isotope effect.

### 3. Dual-Element Isotope Analysis of DPC to Investigate its Environmental Fate

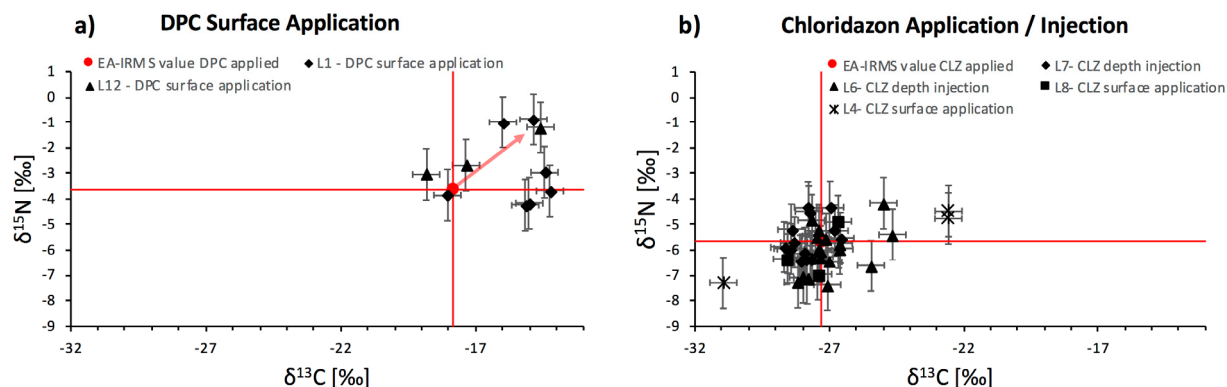


Figure 3.3. Dual-element isotope plot of a) DPC degradation in lysimeters L1 and L12, where DPC was applied on the surface, and b) formation and degradation of DPC in the lysimeters where CLZ was either applied (L4 and L8) or injected in a depth of 40 cm (L6 and L7); the red circles represent the isotopic signature of the applied/injected a) DPC and b) CLZ – position of CLZ and DPC differ within the dual-element isotope plots due to their different isotopic source signatures (Table C4).

#### 3.5. Environmental Significance and Outlook

The isotope fractionation in DPC observed for the three tested scenarios is particularly important because (i) the change in carbon and nitrogen isotopic signature of DPC evidenced transformation of an apparently persistent metabolite, and (ii) these changes provide evidence that likely more than one transformation pathway is involved in DPC transformation. In soil, only methylation of DPC to MDPC is known and thus our data suggest the need for further laboratory experiments and mechanistic studies on DPC (bio)degradation to gain further insight into possible additional transformation pathways. (iii) Formed DPC, which had not been subject to further transformation yet, showed the same nitrogen isotope signature as its precursor CLZ. Hence,  $\delta^{15}\text{N}$  values may serve as isotopic fingerprints to identify the origin of such compounds in groundwater.

When applying CSIA, the combination with conventional methods was found to be complementary and advantageous, especially when formation and transformation of the metabolite was occurring simultaneously. Once introduction of newly formed metabolite dominated, evidence from CSIA was not necessarily conclusive because transformation-related changes in isotope ratios were masked by the continuous input of DPC. Here, additional information was gained by metabolite-to-parent concentration ratios, which became greatest and could provide evidence of DPC formation. Vice versa, when metabolite-to-parent-ratios were small because DPC was further transformed, it was the changes in isotope ratios of DPC which still carried the isotopic imprint of the reaction and, hence, made transformation

visible. For further understanding of the environmental fate of DPC, reference experiments focusing on the determination of stable isotope fractionation factors as well as microbial processes during DPC transformation are required in order to identify transformation mechanisms and quantify them.

For the future, our approach with CSIA in combination with concentration measurements and systematic long-term lysimeter experiments holds promise to answer questions about transformation pathways and the extent of soil / vadose zone (bio)transformation not only for DPC – one of the most widely detected substances – in groundwater, but also for other micropollutants of concern and their metabolites. Additionally, this study confirmed that the application of CSIA in combination with solid-phase extraction<sup>62, 118</sup> is feasible for the analysis of polar micropollutants in drainage water at environmentally relevant concentrations. Thus, it can be also applied to studies in agricultural soil and groundwater from common unconsolidated sand and/or gravel aquifers with catchment areas within agricultural production.

## 4. Isotope Fractionation of Micropollutants during Large-Volume Extraction: A Critical Method Evaluation for Atrazine at Low ng/L Concentrations in Groundwater

Author	Author position	Scientific ideas (%)	Data generation (%)	Analysis and Interpretation (%)	Paper done writing (%)
A. Melsbach	1	65	50	90	85
J. Farlin	2	5	10	0	0
D. Pittois	3	0	10	0	0
A. Meyer	4	0	10	0	0
K. Hölzer	5	0	10	0	0
T. Daubmeier	6	0	10	0	0
T. Gallé	7	15	0	0	0
M. Elsner	8	15	0	10	15
Title of paper:		Isotope Fractionation of Micropollutants during Large-Volume Extraction: A Critical Method Evaluation for Atrazine at Low ng/L Concentrations in Groundwater			
Status in publication process:		Submitted to <i>Isot. Environ. Health Stud.</i>			

I confirm that the above-stated is correct.

---

Date, Signature of the candidate

I/We certify that the above-stated is correct.

---

Date, Signature of the doctoral committee or at least of one of the supervisors

### **4.1. Abstract**

Micropollutants are frequently detected in groundwater, including even some pesticides that were prohibited decades ago. Thus, the question arises whether they may be slowly eliminated by natural attenuation, and whether such natural degradation over long time scales in groundwater can be observed by adequate analytical methods. Conventional approaches rely on parent compound/metabolite ratios, but they are difficult to interpret if metabolites are subject to sorption or further transformation. In this case, compound-specific stable isotope analysis (CSIA) presents an alternative approach to identify transformations processes. The method is based on the analysis of natural isotope abundances in pesticides and their changes when these micropollutants are degraded. However, the underlying analysis by gas chromatography-isotope ratio mass spectrometry (GC-IRMS) is challenged by the low concentrations of micropollutants in groundwater, which are in the range of tens of ng/L. Consequently, large amounts of water need to be extracted. Due to interfering matrix effects, however, the development of non-isotope discriminating enrichment and clean-up steps is necessary to ensure reliable CSIA by GC-IRMS. Hence, the aim of this study was to evaluate the accuracy of isotope ratio measurements of the frequently detected micropollutants atrazine, desethylatrazine and 2,6-dichlorobenzamid after enrichment from large volumes of water (up to 100 L) with solid-phase extraction and subsequent sample clean-up by preparative high-pressure liquid chromatography. Associated isotope discrimination was found to depend on numerous factors including organic matter content and extraction volume. This emphasizes the importance of careful method evaluation of sample preparation and sample pre-treatment prior to reliable CSIA.



### **4.2. Introduction**

Pesticides from agricultural applications and their metabolites are frequently detected in surface and groundwater. Since groundwater is the main source of drinking water in many countries of the European Union, the presence of these compounds is of fundamental societal concern<sup>10, 78</sup>. Intriguingly, contaminants such as atrazine (ATZ), its metabolite desethylatrazine (DEA) and 2,6-dichlorobenzamid (BAM) are detected in groundwater in concentrations of tens to hundreds of nanograms per liter<sup>11, 18, 135, 136</sup> even though their application has been legally banned decades ago. ATZ is a herbicide, which was applied for broad-leaf and grassy weed control in the production of crops, sugar cane and corn. Its application was forbidden by the European Union in 2004<sup>14</sup>. ATZ is known to be either dealkylated to DEA and desisopropylatrazine (DIA)<sup>137</sup>, or hydrolyzed to hydroxyatrazine (HAT)<sup>138</sup>. Its degradation pathway depends on the hydraulic and chemical characteristics of the environmental department as well as on the pH-value and sorption to organic matter<sup>139</sup>. In the environment, the extent of degradation in the topsoil is much greater than in aquifers<sup>140-142</sup>, as microbial activity is highest in the topsoil. In an aquifer, however, the transit time of pesticides can be orders of magnitude greater compared to their transit time in unsaturated soil. Thus, it is of great interest whether the attenuation of ATZ within the aquifer is significant, and whether such slow transformation can be observed in groundwater over the time scale of decades. Recent studies based on concentration analysis and modelling show that a comprehensive investigation of such long time scales in the environment is challenging<sup>21, 22, 143</sup>.

In a similar case as for ATZ, the application of dichlobenil (DCB, 2,6-dichlorobenzonitrile) was forbidden in 2008, since its main metabolite BAM appeared in groundwater in concentrations of up to 5400 ng/L<sup>144-148</sup>. DCB had been used mainly in non-agricultural areas such as court yards, private gardens, industrial sites and railway lines to control grasses, broad leaved weeds and to eliminate tree roots<sup>18</sup>. Due to the sorption of DCB to soil, its concentration in groundwater is negligible. Its main metabolite BAM, in contrast, shows a much lower tendency to sorption and a much higher mobility so that it can leach through the vadose zone into groundwater<sup>49</sup>. In the environment, further degradation of BAM does not seem to be prevalent<sup>18</sup> and long-term studies on degradation of BAM in the field are missing.

Conventional approaches to assess degradation of pesticides rely on the measurement of parent compound concentrations or molar ratios of metabolite-to-parent compounds. Such concentration ratios, however, can be biased if the parent compound or the metabolite are

subject to sorption. Thus, they may show inconsistent trends if parent compounds are repeatedly introduced by fresh mobilization from soil. Additionally, such concentration based assessments can give inaccurate estimates if the metabolite is further transformed and are even not applicable if the pesticide's metabolite is not known. In these cases, compound-specific stable isotope analysis (CSIA) is a complementary and alternative approach to detect the occurrence of pesticide degradation. Analysis of naturally occurring stable isotopes (e.g.,  $^{13}\text{C}$ ,  $^{12}\text{C}$ ) and changes in their relative abundance ( $^{13}\text{C}/^{12}\text{C}$ ) in pesticide target compounds can be used to quantify the extent of pesticide degradation<sup>23</sup>. These changes in isotope ratios are a result of kinetic isotope effects occurring during biodegradation of organic compounds. Reactive bonds containing the heavy isotope (e.g.,  $^{13}\text{C}$ ) react more slowly in comparison to bonds containing the lighter isotope (e.g.,  $^{12}\text{C}$ ), leading to an enrichment of heavy isotopes in the remaining compound fraction. In contrast to conventional analytical methods, however, detection limits are not imposed by the analysis of total concentrations, but CSIA by GC-IRMS needs to analyze also the abundance of more seldom isotopes with high precision. For example, to measure the carbon isotopic composition precisely by GC-IRMS, 1 nmol C on column is needed as the  $^{13}\text{C}$  isotope is rare (about 1.11 % of total carbon) compared to the more abundant  $^{12}\text{C}$  isotope. Micropollutants, however, are often detected in groundwater in the nanograms-per-liter concentration range<sup>51</sup>. As a consequence, large amounts of water have to be extracted to achieve a robust isotope analysis. Recent method development enabled CSIA of ATZ and BAM within the sub- $\mu\text{g}$  per liter range. Schreglmann et al.<sup>48</sup> presented a non-isotope discriminating enrichment method for accurate CSIA of ATZ and DEA extracted from up to 10 L of water. Besides the method for large-volume water extraction of ATZ and DEA, Torrentó et al.<sup>62</sup> described a method including the extraction of BAM from up to 30 L. However, to assess the long-term environmental fate of a herbicide, methods are needed enabling its detection in groundwater bodies in even lower concentration ranges (low ng per liter range)<sup>11, 48, 149</sup>. Thus, to obtain the amount of target analyte required for accurate CSIA, a large-volume extraction of up to 300 L and therefore an up-scale of methods published so far would be necessary. Large-scale SPE, however, does not only enrich the target analyte, but also interferences from the sample matrix and other pollutants. Consequently, an additional sample clean-up using for example preparative high pressure liquid chromatography (HPLC) is necessary to eliminate interferences. Therefore, method validation is required to ensure that no method-related isotope fractionation is introduced. The aim of this study was to assess whether the extraction of target compounds from large water sample volumes may

## 4. A Critical Method Evaluation for Atrazine at Low ng/L Concentrations in Groundwater

compromise accurate CSIA. Thereto, large volumes of spiked and natural groundwater were used to test for the recovery of ATZ, DEA and BAM and to measure the carbon isotopic signature of each target analyte.

### **4.3. Materials and Methods**

#### **4.3.1. Chemicals**

Atrazine (2-Chloro-4-ethylamino-6-isopropylamino-1,3,5-triazine, CAS no.: 1912-24-9), Desethylatrazine (2-Amino-4-chloro-6-isopropylamino-1,3,5-triazine, CAS no.: 6190-65-4) and 2,6-dichlorobenzamide (98.5 %, CAS no.: 2008-58-4) were purchased from Dr. Ehrendorfer GmbH (Augsburg, Germany). Ametryn (2-Ethylamino-4-isopropylamino-6-methylthio-1,3,5-triazine, 98.5 %, CAS no.: 834-12-8) was produced by Fluka, supplied by Sigma Aldrich (Steinheim, Germany). Formic acid ( $\geq 98$  %, CAS no.: 64-18-6), methanol ( $\geq 99.9$  %, CAS no.: 67-56-1), acetonitrile ( $\geq 99.9$  %, CAS no.: 75-05-8) and ethyl acetate ( $\geq 99.9$  %, CAS no.: 141-78-6) were supplied by Carl Roth (Karlsruhe, Germany). Potassium dihydrogen phosphate was purchased from Alfa Aesar GmbH & Co. KG (Karlsruhe, Germany). Ultrapure water was received from a Millipore DirectQ apparatus (Millipore, Bedford, MA, USA).

#### **4.3.2. Environmental Samples**

Water samples from the groundwater spring Haertgen 1 (national code: SCC-125-03) in the Luxembourg Sandstone Formation were collected within three different sampling campaigns. The water was collected in 15 L and 2 L Schott bottles (Schott AG, Mainz, Germany). A volume of 185 L per campaign was sampled and pre-treated immediately.

#### **4.3.3. General Analysis of the environmental samples – Total Organic Carbon**

The total organic carbon (TOC) was measured with a Torch Combustion Analyzer TOC/TN from TELEDYNE TEKMAR. One milliliter of sample was acidified using 1 mL of phosphoric acid (21 %). The inorganic carbon was then removed by purging with synthetic air. The organic carbon in the sample was subsequently converted to carbon dioxide (CO<sub>2</sub>) by

catalytic combustion using a platinum-based catalyzer. Afterwards, the formed CO<sub>2</sub> was transferred into an infrared detector.

#### **4.3.4. Sample Pre-Treatment and Spiking with the Target Analytes**

Prior to spiking the groundwater with the target analyte, the groundwater was acidified, as pre-tests with spiked tap water had shown an increase of analyte recovery after acidification. To this end, 30 mL of formic acid ( $\geq 98\%$ ) were added to 2 L of groundwater. Afterwards, the acidified water was transferred into 2 L custom-made Schott-bottles (Schott AG, Mainz, Germany) with a cylindrical rounded bottom. The non-contaminated groundwater was then spiked with different concentrations of ATZ, DEA and BAM (Table E1).

#### **4.3.5. Analyte Enrichment with Solid-Phase Extraction**

For solid-phase extraction (SPE), 6 mL CHROMABOND EASY cartridges (Machery-Nagel GmbH & Co. KG, Düren, Germany) with 200 mg modified polystyrene-divinylbenzene copolymer sorbent were used. As the sorbent mass was designed to work up to a maximum sample volume of 4 L, the total sample was split into aliquots of 4 L, the aliquots were extracted on separate cartridges and the extracts were reunited after the extraction method. Each cartridge was pre-conditioned with 5 mL methanol at a flow rate of 1 mL/min and an equilibration time of 0.1 min using a Gilson GX-274 ASPEC (Gilson Incorporated, Middleton, WI). Subsequently, the samples were loaded by pumping the spiked water from the 2 L Schott-bottles onto the cartridges using a vacuum manifold. After the sample had passed the cartridge, they were kept on the vacuum manifold until the sorbent was dried completely. Then, in contrast to conventional SPE, a subsequent washing step was skipped and the cartridges were transferred directly into the Gilson GX-274 ASPEC instrument, where the elution of the samples was carried out automatically into 10 mL tubes with 2 mL methanol at a flow rate of 0.5 mL/min and an equilibration time of 0.5 min. After elution with methanol, the samples were transferred into 7 mL clear vials with solid caps (PTFE liner) (Supelco, Bellefonte, PA). Finally, the corresponding volumes of each sample were combined and evaporated until dryness.

#### 4.3.6. Sample Clean-up with preparative HPLC

Prior to GC analysis, samples were subjected to a clean-up step adapting the fractionated HPLC method described by Schreglmann et al.<sup>48</sup>. To this end, the sample extracts were dissolved in 800  $\mu$ L ultrapure water/acetonitrile (70/30). To avoid a blockage of the HPLC column, samples were filtered prior to injection using a 4 mm single use filter device with a 0.2  $\mu$ m PTFE Membrane (Whatman, Buckinghamshire, United Kingdom). The samples were injected onto a Synergi 4  $\mu$ m Hydro-RP 80 Å (100 mm  $\times$  4.6  $\mu$ m; Phenomenex, Aschaffenburg, Deutschland) operated in a Shimadzu UHPLC-DAD (Nexera XR, LC-20AD XR). Separation of the analytes was achieved using a gradient of 1 mM phosphate buffer at a pH of 7 and acetonitrile (ACN) at a flow rate of 1.0 mL/min. The method started at 30 % ACN, which was held for 5 min. The proportion of ACN was then increased linearly to 65 % within 7 min. Subsequently, the gradient was increased to 80 % within 0.5 min and held for 1.5 min. At the end of the run, the proportion of ACN was reduced to 30 % again (held for 3 min). The detector was operated at an absorbance of 220 nm. BAM, DEA and ATZ eluted at retention times of 3.5 min, 4.8 min, and 10.5 min, respectively. Thus, the fraction for BAM and DEA was collected from 2.1 to 6.7 min. For ATZ, the fraction from 9.5 to 13.0 min was taken for further analysis. Finally, the samples were freeze-dried and reconstituted in 50  $\mu$ L ethyl acetate.

#### 4.3.7. Quantification with GC-qMS

The recovery of the target analytes from the groundwater samples was determined with gas chromatography – quadrupole mass spectrometry (GC-qMS). Thereto, a 7890A GC was hyphenated with a 5975C qMS (Agilent, Santa Clara, CA, US). For peak separation, a DB-5 column (60 m  $\times$  0.25 mm  $\times$  1  $\mu$ m) (J&W Scientific, Santa Clara, CA) was used. The helium carrier gas (grade 5.0) was set to a flow of 1.4 mL/min. Using a CombiPAL autosampler (CTC Analytics AG, Zwingen, Switzerland), three microliters of each sample were injected in splitless mode at a temperature of 250 °C. The GC program started at a temperature of 70 °C, which was held for 1 min. Afterwards, the temperature was ramped with 18 °C/min to 155 °C. Then, the temperature was increased with 2 °C/min to 240 °C and finally with 30 °C/min to 260 °C (held for 5 min) before the column was baked for 11 min at a temperature of 280 °C. The target analytes were introduced into the MS via a heated transfer line (250 °C). Subsequently, the ions were created with electron impact ionization at an electron-accelerating voltage of 70 V. The MS was run in scan mode (from mass-to-charge ratio (m/z) 40 to 550).

ChemStation E.02.02.1431 was used as software to control the instrument and to evaluate the data. To determine the recovery, the target analytes were quantified with Ametryn (20 mg/L) dissolved in ethyl acetate as an internal standard using its  $m/z$  227 as a quantifier ion. Data evaluation for DEA and BAM was carried out using  $m/z$  172 and 173, respectively, as quantifier ions. ATZ was quantified using the mass-to-charge ratio 200. All analytes were identified by their mass spectrum and by comparison of their retention times with those of an authentic standard.

#### **4.3.8. EA-IRMS Measurement for Determination of Reference Values**

The carbon isotope composition of the reference standards of ATZ, DEA and BAM were determined by elemental analyzer-isotope ratio mass spectrometry (EA-IRMS)<sup>76</sup>. Thereto, an EuroEA (Euro Vector, Milano, Italy) was coupled to a Finnigan MAT 253 IRMS via a FinniganTM ConFlow III interface (Thermo Fisher Scientific, Bremen, Germany). The reference standards were calibrated against the organic referencing materials L-glutamic acid (USG 40 and USG 41) and caffeine (IAEA 600) supplied by the International Atomic Agency (Vienna, Austria). The carbon isotope ratios are reported as isotope values ( $\delta^{13}\text{C}$ ) in per mil relative to the international reference PeeDee Belemnite (V-PDB) according to equation 4.1:

$$\delta^{13}\text{C} = \frac{{}^{13}\text{C}/{}^{12}\text{C}_{\text{Sample}} - {}^{13}\text{C}/{}^{12}\text{C}_{\text{Reference}}}{{}^{13}\text{C}/{}^{12}\text{C}_{\text{Reference}}} \quad \text{eq. 4.1}$$

The isotope values were measured relative to our laboratory  $\text{CO}_2$  monitoring gas. The gas had been previously calibrated against RM8563 ( $\text{CO}_2$ ) purchased from the International Atomic Energy Agency (IAEA). The reference gas was introduced into the system three times at the beginning and at the end of each analysis run.

#### **4.3.9. GC-IRMS Conditions for Carbon Isotope Analysis**

Carbon isotope analysis was conducted with a TRACE GC Ultra gas chromatograph (Thermo Fisher Scientific, Milan, Italy) hyphenated via a Finnigan Combustion III interface (Thermo Fisher Scientific) with a Finnigan MAT 253 isotope ratio mass spectrometer (IRMS) (Thermo Fisher Scientific, Bremen, Germany). For the analysis, the IRMS parameters were kept at a

#### 4. A Critical Method Evaluation for Atrazine at Low ng/L Concentrations in Groundwater

vacuum of  $2.1 \times 10^{-6}$  mbar, an accelerating potential of 9 kV and an emission energy of 2 mA. Target analytes were transformed to CO<sub>2</sub> at a temperature of 1030 °C using a NiO tube/CuO-NiO reactor (Thermo Fisher Scientific). The GC was equipped with a 60 m Rxi-5ms column (Restek GmbH, Bad Homburg, Germany) with an inner diameter of 0.25 mm and a film thickness of 1 µm. At the beginning of the GC temperature program, the oven was set to a temperature of 50 °C, which was held for 1 min. Afterwards, the oven temperature was increased linearly with 18 °C/min to 155 °C, followed by 5 °C/min to 240 °C (held for 0 min). Subsequently, the temperature was increased with 30 °C/min to 260 °C, held for 5 min. Finally, a ramp of 15 °C/min heated the column to a temperature of 280 °C, which was held for 9 min. A volume of between 1 µL and 3 µL of sample extract was injected on-column using a PAL autosampler (CTC Analytics AG, Zwingen, Switzerland). The helium (grade 5.0) carrier gas flow and injector temperature program were controlled by an Optic 3 device (ATAS, GL Science, Eindhoven, Netherlands). The ATAS injector was equipped with a custom-made glass on-column liner. It had an initial temperature of 50 °C (held for 300 s). Subsequently, the injector temperature was increased with 4°C/s to 250 °C. Meanwhile, the split flow, which started at 14 mL/min, was set to 0 ml/min for 120 s and then back to its initial flow of 14 mL/min. At the beginning of each run, the flow rate was set to 0.3 mL/min, held for 2 min and then increased linearly to 1.4 mL/min within 120 s. To control and verify the instrument performance, reference standards of ATZ, DEA and BAM were used to monitor retention time and shifts in  $\delta^{13}\text{C}$  values during the sequence.

##### **4.3.10. Correction Procedure applied for Isotope Analysis**

For each sample we aimed to measure the isotope value three times. All reported isotope ratios are expressed as arithmetic means of samples collected in different sampling campaigns with the respective estimates of their standard deviations ( $\pm \sigma$ ). The calibration was performed by bracketing the samples with authentic reference standards to apply the principle of identical treatment by Werner and Brand<sup>26</sup>. With this method, drifts that occurred within a sequence as well as differences in the combustion efficiency were corrected directly.

#### **4.4. Results and Discussion**

##### **4.4.1. Recovery of ATZ, DEA and BAM from Groundwater**

The extraction of different water volumes resulted in unsatisfactory and non-reproducible recoveries for all three target analytes (Figure 4.1). Considering the differences between the mass spiked and the mass recovered, the applied method seems to be non-quantitative when extracting the large volumes of groundwater targeted in this study.



#### 4. A Critical Method Evaluation for Atrazine at Low ng/L Concentrations in Groundwater

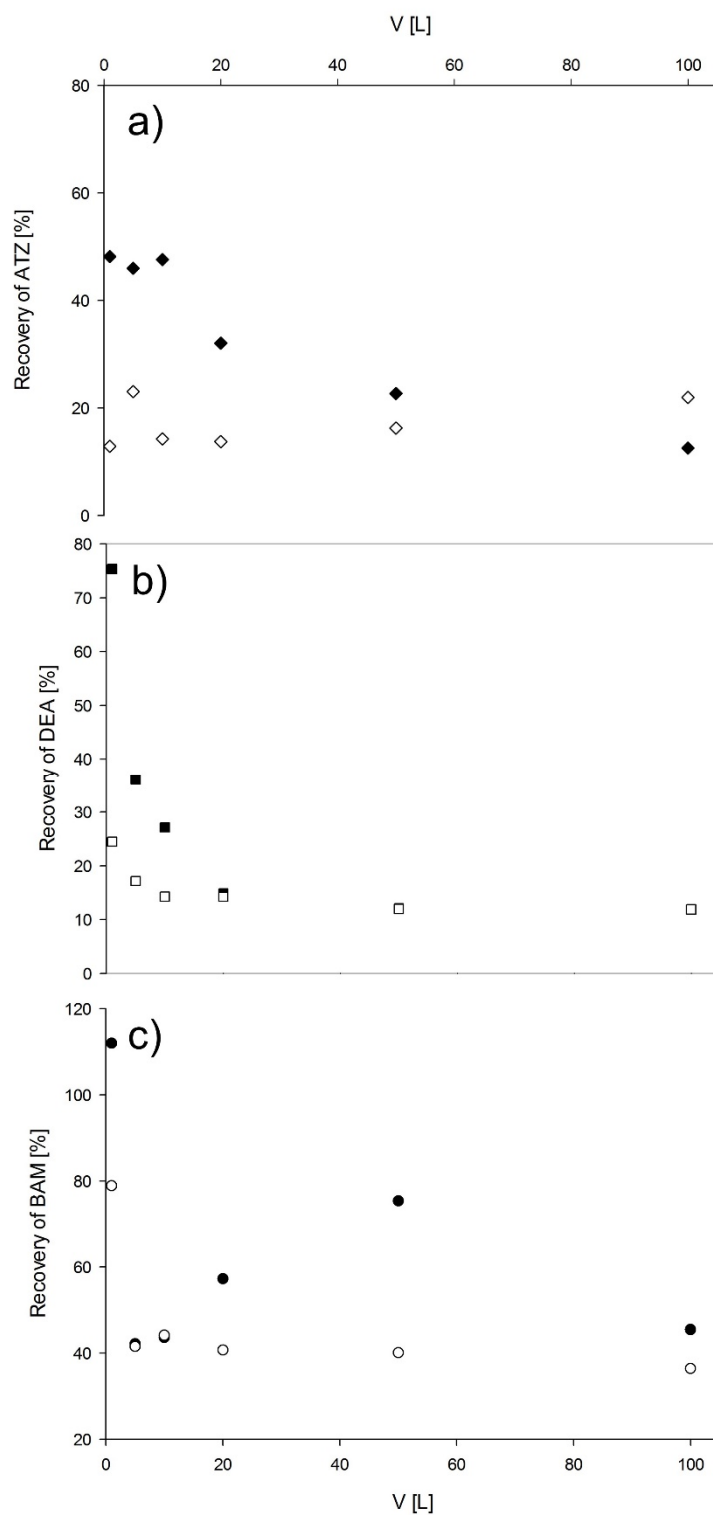


Figure 4.1: Recovery in percent of a) ATZ (diamonds) b) DEA (squares) and c) BAM (circles) in relation to water volumes extracted; Extracts from spiked samples for which the original groundwater was collected on 15<sup>th</sup> October 2015 are represented as black symbols, while those for which the groundwater was collected on 21<sup>st</sup> October 2015 are represented as white shapes.

#### 4. A Critical Method Evaluation for Atrazine at Low ng/L Concentrations in Groundwater

Non-quantitative SPE may potentially be caused by a breakthrough of the target analyte. This can occur due to high mass loadings or due to high sample volumes, where the target analyte already sorbed to the cartridge material is washed off. For the method presented in this study, the latter reason is unlikely, as a maximum volume of 4 L groundwater was loaded onto the SPE column. Alternatively, minor losses might occur during transformation steps. Another reason for low recoveries may be the interaction of analytes with components present in water matrix. Indeed, pre-tests with tap water, where matrix components are minimized, gave much greater ATZ recoveries of  $105 \pm 17\%$  ( $V = 4\text{ L}$ ;  $n = 3$ ) applying the same extraction method at a pH of 2. Similar discrepancies in analyte recoveries between tap and environmental water were observed in our recent study for other polar micropollutants such as desphenylchloridazon (DPC), where recoveries of DPC in tap water were measured at approximately 100 %, while DPC from environmental water showed a recovery of 30 %<sup>62</sup>. Comparably low recoveries have been measured for ATZ in soil<sup>150</sup>. Commonly detected matrix components, which are present in soil and groundwater but not in tap water, are humic substances (HS) like fluvic and humic acids. Even though previously published studies of ATZ extraction methods from groundwater showed higher recoveries of up to 100 %<sup>151, 152</sup>, there are only few studies validating the extraction of atrazine from large volumes of water rich in humic substances, and at trace concentrations of micropollutants<sup>153</sup>. On the other hand, the interaction of ATZ with HS, in particular with humic acids and fulvic acids has been studied before<sup>154-156</sup>. It has been observed that, depending on the pH-value of the water and the amount of HS present, ATZ-HS complexes may be formed. For a pH smaller than 5, complexes between ATZ and the HS are formed by either a proton-transfer bonding or a hydrogen bonding between N in the secondary amino groups or the triazine ring of ATZ with the oxygen containing functional groups within the humic acids<sup>157</sup> (Scheme E1). The water in the Luxembourg Sandstone Formation is reported to have a pH of approximately 7<sup>158, 159</sup>. Consequently, due to the acidification of the water prior SPE, the pH of the water was decreased to approximately 4, which is expected to facilitate the ionic interaction between ATZ and HS. Unfortunately, data about the TOC content of the extracted groundwater are not available. However, Figure E1 shows the total organic carbon of the spring from where the groundwater for spiked samples was taken and where the TOC was analyzed over a period of 16 months. Here, significant variations over time (between 0.6 mg/L and 2 mg/L) are observable. Hence, diurnal differences in the TOC content of the water are a likely hypothesis

to explain the low recoveries and the inter-day differences in the recovery observed in our study.

#### 4.4.2. Isotope Fractionation After Large Volume Extraction

Figure 4.2 shows the differences in isotope values of extracts from spiked groundwater samples compared to the reference value of the standard with which they were spiked.

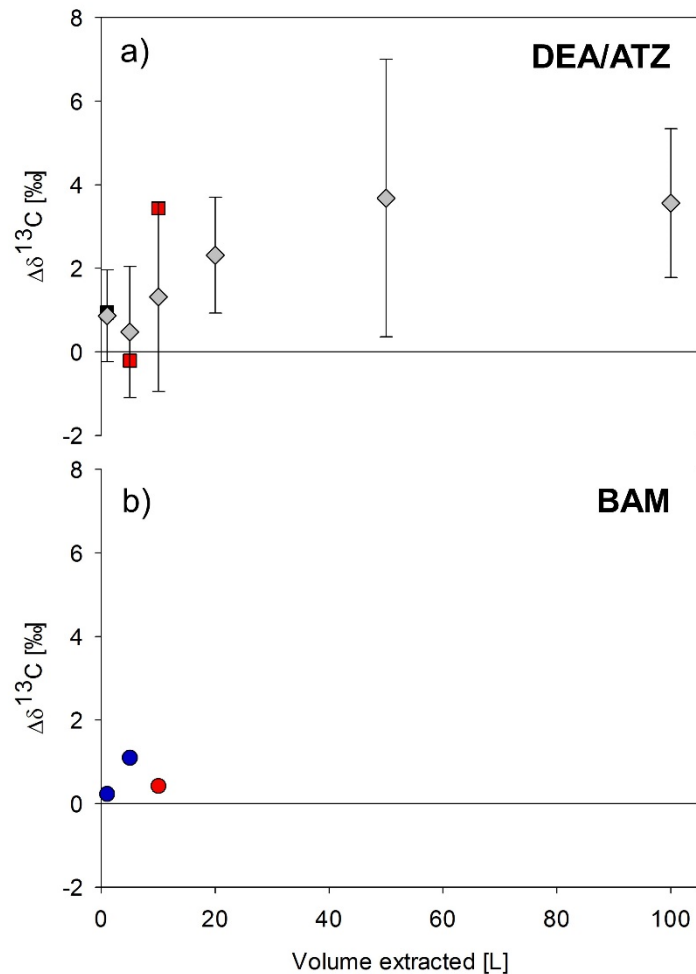


**Figure 4.2: Deviation of carbon isotope values of standard measurements induced by large volume water extraction of a) ATZ (grey diamonds), DEA (black diamonds) and b) BAM (blue circles); the y-axis represents the deviation from the true value, where the black line indicates the absence of isotope fractionation; red symbols correspond to samples for which only a single measurement was achieved**

For ATZ, no isotopic discrimination was observed for extraction volumes smaller than 10 L (Figure 4.2a). Contrary to expectations, however - and contrary to the results of an alternative method where much greater recoveries were observed<sup>62</sup> - the method introduced a significant isotope fractionation of up to 6 ‰ for extraction volumes greater than 10 L. As described by

Bakkour et al.<sup>63</sup> solid phase extraction of a target analyte from large samples volumes implies that concomitantly also matrix constituents become enriched including TOC of groundwater and even oligomers of the SPE material (Figure 4.3). In the SPE extraction protocol described here, the high background may be a particular result of the missing washing step within the SPE. This step is not mandatory but results in cleaner samples, as it is usually applied to remove interfering undesirable compounds without eluting the target analyte<sup>160</sup>. It is accomplished by choosing a washing solvent similar or slightly stronger than the solvent used within the sample load step. Thus, matrix compounds, which are not as retained by the sorbent as the target analyte, will be washed out, while the compound of interest remains within the sorbent<sup>160</sup>. Therefore, by omitting this step within the procedure, not only the target analytes were eluted after sample loading but also the groundwater matrix. DEA showed no isotope fractionation for extraction volumes lower than 10 L. As shown in Figure 4.2b, isotope fractionation was also not observed for BAM. However, neither DEA, nor BAM could be measured for extraction volumes greater than 10 L, as background interferences were too high compared to the low signals for peak detection (Figure E2).

If in the case of a high background the  $\delta^{13}\text{C}$  value of GC-IRMS measurements does not represent the isotopic ratio of the target analyte, this may have several reasons. (1) *Difficulty of background correction.* After peak separation target compounds are combusted to  $\text{CO}_2$  prior to IRMS analysis. Thus, peak separation and background correction are critical since otherwise it would not be possible to distinguish whether  $\text{CO}_2$  origins from the target analyte or from interfering matrix components. If the TOC is so high that an adequate background correction is no longer feasible, peaks would represent a mean of the  $\delta^{13}\text{C}$  of the background and the target analyte. As the background has an isotopic signature different from the target analyte, determination of analyte-specific isotope ratios and, hence, identification of shifts in  $\delta^{13}\text{C}$  values of ATZ that would demonstrate natural degradation in the field would be biased. (2) *Compromised oxidation efficiency.* Such an elevated background may in addition compromise the oxidation efficiency of the oxidation reactor which is positioned after the GC column to convert target compounds to  $\text{CO}_2$  prior to isotope analysis. This combustion of target analytes to  $\text{CO}_2$  is achieved by oxygen stored in form of  $\text{CuO}$  and  $\text{NiO}$  in the reactor. By loading too much carbon onto the reactor, the combustion capacity of the reactor may be exhausted. As a result, target analytes are only partially combusted and measured  $\delta^{13}\text{C}$  are more negative (“lighter”) than their true isotope signature. High variations in the standard

#### 4. A Critical Method Evaluation for Atrazine at Low ng/L Concentrations in Groundwater

deviations (SD) of different sampling dates suggest that the observed deviations from true values are not reproducible so that the bias introduced by the method cannot be corrected.

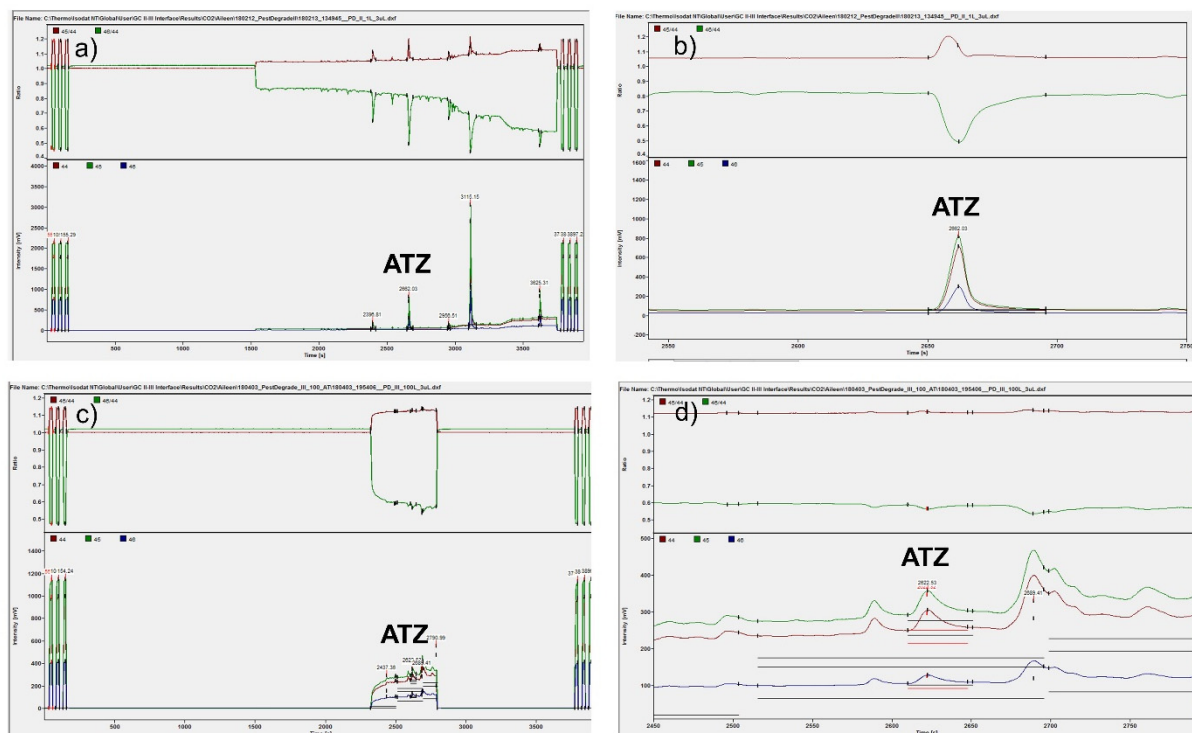
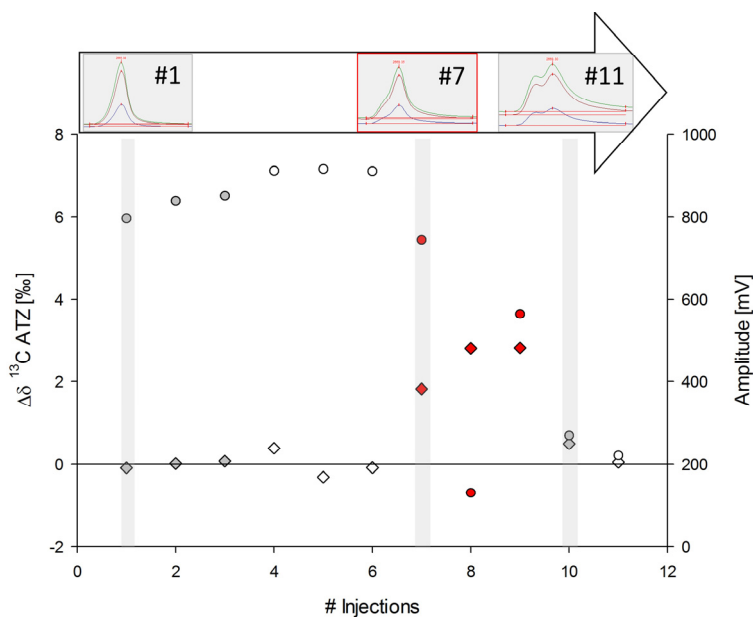


Figure 4.3: Chromatograms of ATZ after HPLC-cleanup and on-column injection of a and b) 1 L of water extraction and c and d) 100 L of water extraction

(3) *Compromised chromatographic performance.* Additionally, the high content of dissolved organic carbon caused chromatographic challenges, as the matrix and the target analyte were sorbed to the pre-column of the on-column injection creating active spots, which resulted in reduced amplitudes of the target analyte in samples, and even in standards measured after a sample. Such matrix residues sorbed to the pre-column could not be removed by heating of the GC oven and caused either partial or complete blockages of the system, which needed to be removed by shortening the corresponding parts of the pre-column. Thus, the high matrix background did not only affect the sample itself, but there was carry-over of the matrix affecting also isotope analysis of atrazine standards introduced after samples of large volume water extraction. An additional effect observed were isotope effects during chromatography leading to double peaks (Figure 4.4). Its influence on the isotope value of the target analyte needed to be eliminated by either automatic or by manual integration of both peaks.



**Figure 4.4:** Deviation of atrazine carbon isotope values of standard measurements and spiked groundwater samples used for method validation observed within a sequence; circles represent the amplitude and diamonds the deviation from target carbon isotope values of standard 1 (grey), standard 2 (white) and spiked groundwater samples (10 L sample extraction, red).

#### 4.4.3. Suggestions for Improvement

The results of our evaluation present the case of an extraction method which needs to be further optimized in order to achieve sensitive, accurate and robust isotope analysis. Here, it appears advisable to omit the acidification as a sample preparation step for SPE and rather add a buffer to in order to reduce possible interactions of the target analytes with humic substances. We further hypothesize that the method tested may be significantly improved for robust and accurate carbon isotope analysis if measures are taken to eliminate interferences from DOC of groundwater and, potentially, from soluble SPE cartridge material. Further sample clean-up could be achieved by different approaches. To start with, interfering matrix components may be eliminated by including a washing step within the SPE, after the sample has been loaded and prior to its elution.

#### 4.5. Environmental Significance and Outlook

Hence, the results of this study highlight a case which necessitates further optimization in order to emphasize the necessity of a careful method validation of large volume extraction. They show that the hyphenation of many analytical procedures may not only have an influence on the recovery, but also on the integrity and reproducibility of isotope values and thus on the

interpretation of field data. Consequently, prior to the extraction and measurement of environmental samples, methods need to be carefully validated, such as in Torrentó et al.<sup>62</sup>. The following case of an environmental study illustrates that otherwise inaccurate conclusions may be drawn.

##### **4.5.1. Possible Bias in the Interpretation of Environmental Data**

Figure 4.5a shows isotope values of ATZ from different natural atrazine-containing groundwater samples that were analyzed in parallel to the method evaluation presented in this manuscript. This comparison includes samples deriving from an aquifer of the Luxemburg Sandstone Formation, which have all been prepared for CSIA according to the protocol described in this chapter. In contrast, for the other samples (Franconia and Austria), sample pre-treatment and extraction was carried out according to the methods of Schreglmann et al.<sup>48</sup>.

Groundwater samples analyzed from Franconian and Austrian aquifers according to Schreglmann et al.<sup>48</sup> showed isotope values of atrazine close to commercially available products, which usually fall within a range of  $\delta^{13}\text{C}$  values between -26 ‰ to -33 ‰<sup>76, 161-163</sup>. In contrast, there is a correlation between  $\delta^{13}\text{C}$  and the ATZ concentration detected in the Luxembourg Sandstone Formation (Figure 4.5b and c).

Carbon isotope values of samples collected in the Luxembourg Sandstone Formation (Figure 4.5b), show a significant enrichment in  $^{13}\text{C}$  of up to -16 ‰ within the low ng/L concentration range. Comparing the measured  $\delta^{13}\text{C}$  values from Luxembourg to the carbon isotope values of ATZ measured in other field samples and to the isotope signatures of commercially available products, the detected  $^{13}\text{C}$  enrichment would be interpreted as an indication of extensive degradation. According to laboratory degradation experiments of Meyer et al.<sup>23</sup> and Lihl et al.<sup>50</sup>, where degradation of ATZ by *Arthrobacter aurencens* TC1 and *Rhodococcus* sp. NI 86/21 was quantified, a  $\delta^{13}\text{C}$  (ATZ) of -16 ‰ would indicate that 80 to 90 % of the ATZ has already been degraded presuming an ATZ source signature of -26 ‰.

When relating the measured carbon isotope value of ATZ to the extracted water volume, however (Figure 4.5c) a correlation of  $^{13}\text{C}$  enrichment with the extraction volume becomes apparent, in a similar manner as observed in Figure 4.2. This trend is not observed for the samples collected in Austria and Franconia. Hence, based on our observations in the present study, isotopic shifts induced by extensive sample extraction would be a likely explanation of these results.

#### 4. A Critical Method Evaluation for Atrazine at Low ng/L Concentrations in Groundwater

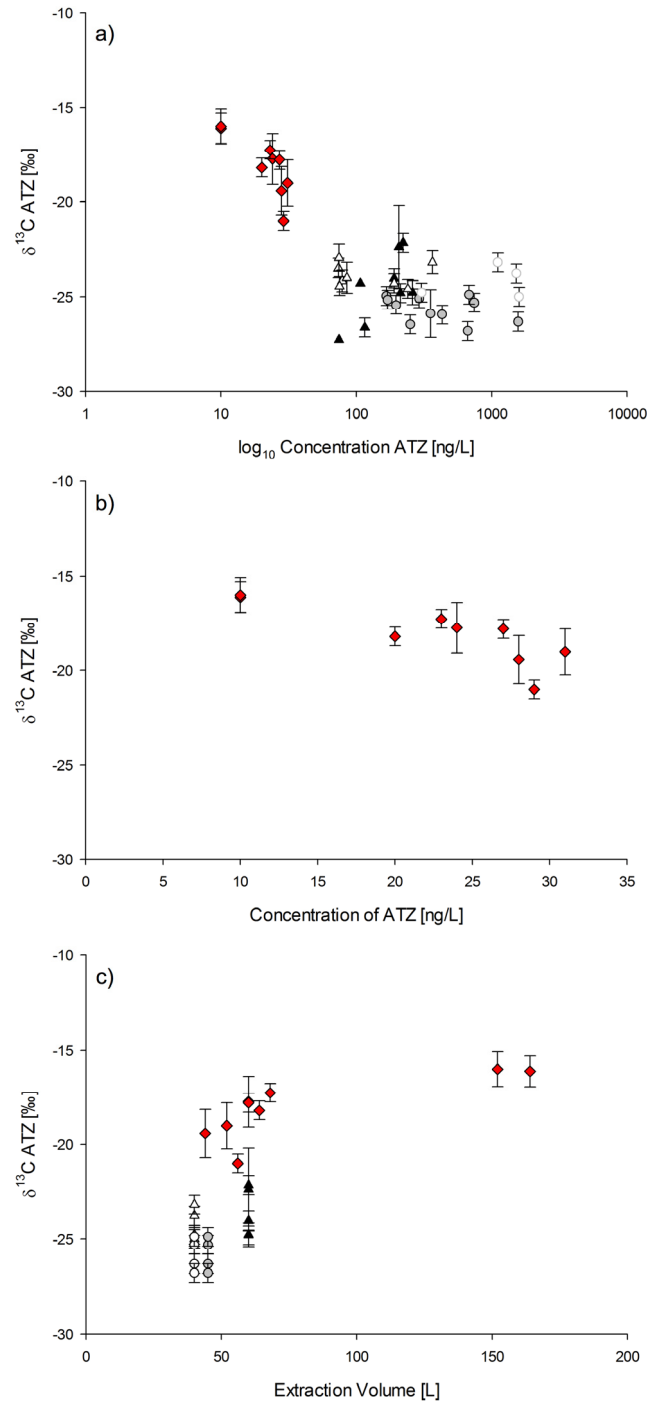


**Figure 4.5:** a) and b) Carbon isotope values of ATZ versus analyte concentration in natural groundwater samples.; c) carbon isotope values of ATZ in relation to the volume of water extracted for CSIA; red diamonds represent samples collected in the aquifer of the Luxembourg Sandstone Formation and extracted according to the method evaluated here. In contrast, circles (ATZ samples from two different collection sites in Austria) and triangles (ATZ samples from two different collection sites in Franconia) were extracted according to the method of Schreglmann et al.<sup>48</sup>.

Consequently, the application of the SPE protocol described may lead to potentially inaccurate conclusions about degradation in natural samples if it is not accompanied by a method evaluation as presented here. This emphasizes the general need of careful method validation.



#### **4.5.2. Opportunities for Further Analytical Developments**

To further decrease limits of sensitive CSIA, different opportunities exist. First, fractionative HPLC clean-up can be repeated using a different gradient method in order to separate target analytes from additional remaining interferences. Second, Molecularly Imprinted Solid Phase Extraction (MISPE), a selective enrichment method to remove matrix in organic solvents by specific intramolecular interactions, can be applied after fractionative HPLC. Here, materials have been developed for organic micropollutants such as triazines<sup>164, 165</sup> but not yet for BAM. Both approaches, however - fractionative HPLC and MISPE - are highly labor intensive. Hence, the application of comprehensive GC×GC-IRMS represents a further attractive option to enable carbon isotope analysis of analytes in complex matrices. Here, resolution and separation capacity are increased by adding a second dimension to the system and thus separate the background from the target analyte<sup>72</sup>. Hence, dedicated analytical efforts are necessary, and bear potential, to further push the limits for analysis of organic trace compounds in groundwater.

#### 4. A Critical Method Evaluation for Atrazine at Low ng/L Concentrations in Groundwater

## **5. General Conclusion and Outlook**

The emerging contamination of natural water bodies and drinking water recourses with persistent and polar micropollutants, such as the frequently detected desphenylchloridazon (DPC), 2,6-dichlorobenzamide (BAM), atrazine (ATZ) and desethylatrazine (DEA), emphasizes the need to investigate the environmental fate of these micropollutants. To tackle these questions, compound-specific stable isotope analysis (CSIA) has been established as an important method to evaluate the formation and transformation of micropollutants in complex sample matrices.

In the first part of this thesis (Chapter 2), sensitive methods for the carbon and nitrogen isotope analysis were developed using DPC as a model compound. Both methods enabled CSIA of polar micropollutants in a sub  $\mu\text{g/L}$  concentration range. A step towards more sensitive isotope analysis was realized by using a different injection technique for nitrogen isotope analysis. The method was optimized by factor 10, resulting in limits of precise isotope analysis of approximately 100 ng DPC on-column per method. It was shown that the combination of both developed methods gives access to dual-element isotope plots. Nitrogen isotope values, in particular, can be used to distinguish different sources of DPC and to identify if they derive from different parent compounds. The combination of the presented methods, especially with the large-volume extraction presented by Torrentó et al.<sup>62</sup> (Appendix B) enables the isotopic analysis of DPC in environmental water, as shown in Chapter 3.

Chapter 3 proves the feasibility of the application of the developed nitrogen and carbon isotope analysis for the investigation of the environmental fate of polar micropollutants such as DPC in a controlled lysimeter site, as described by Torrentó et al.<sup>166</sup> (Appendix D). It emphasizes the importance of the combination of analytical methods such as the metabolite-to-parent ratio, especially when pollutants are partially degraded. Due to the simultaneous formation and transformation of the metabolite and its re-mobilization, the isotope ratios could have been masked by the new input. Consequently, the metabolite-to-parent ratio provided evidence of DPC formation. On the other hand, when further transformation of the metabolite occurred, the concentration ratios were inconclusive. In this case, changes in isotope ratios provided evidence about degradation of the metabolite. Within this chapter, the application of the persistent metabolite was investigated for the first time without interference caused by the simultaneous formation and transformation of DPC. We found that DPC is formed from its parent compound chloridazon (CLZ) independent of its form of application and soil type. Furthermore, during the long-term investigation, DPC was transformed to

methyl-desphenylchloridazon (MDPC) in all lysimeters. Plants, sorption and the preferential flow had an influence on the formation and degradation of DPC. However, quantification showed that only a minor fraction was transformed, indicating the persistency of this micropollutant. A significant enrichment in  $^{13}\text{C}$  and  $^{15}\text{N}$  by approximately +4 ‰ and +3 ‰ was observed, which was, however, influenced by dilution effects with freshly mobilized DPC from the vadose zone. DPC which had not been further transformed showed the same  $\delta^{15}\text{N}$  as its parent compound. Thus, the fingerprint of DPC may be used to track its original source and identify whether more than one source is responsible for the contamination.

In Chapter 4, this thesis pinpoints the challenges observed in CSIA of polar micropollutants in groundwater matrices using ATZ, DEA, and BAM as model compounds. Extensive sample enrichment resulted in an incomplete recovery and caused isotope fractionation leading to an overestimation of a micropollutant's degradation. This study, therefore, emphasizes the need for a careful method evaluation and validation as a part of method development. It was shown that not every method developed in the laboratory is suitable for environmental sample matrices, in particular if changes in pH are part of the method. In the case of ATZ and DEA we retrospectively hypothesized that a change of pH prior to SPE may favor the formation of analyte-fulvic acid complexes leading to very low recoveries. Consequently, even more extensive sample enrichment and clean-up would be required for accurate CSIA as matrix compounds have a significant influence on the chromatography and the isotope ratio. Due to these limitations, there is an urgent need for more sensitive isotope analysis by methodological and instrumental advances.

The knowledge gained within the scope of this thesis might be the basis for future degradation studies of polar micropollutants like DPC, as the analytical method development enables dual-element isotope analysis, which is used to receive information about the transformation pathways of DPC and the underlying mechanism.

Furthermore, besides methodological advances as discussed in Chapter 4, instrumental developments towards a more sensitive comprehensive GC×GC-IRMS are crucial steps for future isotope analysis of trace compounds in complex matrices. GC×GC-IRMS could probably enable carbon isotope analysis of micropollutants in complex sample matrices in the low ng/L range and would therefore minimize sample pre-treatment and preparation efforts. These advances would open a broad field of application in environmental science. For example, GC×GC-IRMS might be an attractive option to enable the detection of

micropollutants in groundwater and thus to investigate their long-term environmental fate in the field. Additionally, sensitive comprehensive GC×GC-IRMS might prove mass transfer limitations of micropollutants in bacteria at low  $\mu\text{g/L}$  ranges not only in Chemostats<sup>167</sup> but also in the field.

Pushing limits of precise isotope analysis even further towards the  $\text{pg/L}$  ranges, as shown by Baczynski et al.<sup>66</sup> and adding a second dimension, GC×GC-IRMS may be combined with non-target analysis to trace contaminants in waste water and surface water to their source.

As a result of the urgent need for further instrumental developments, first approaches are shown in the following section.

**6. Outlook: Development of a Comprehensive GC×GC-IRMS  
Towards a More Sensitive Isotope Analysis of Micropollutants -  
Part I**

### 6.1. Introduction

In recent years, reports about the detection of micropollutants (pesticides, pharmaceuticals) in surface- and groundwater accumulated and the assessment of a compound's environmental fate using compound-specific stable isotope analysis (CSIA) by gas chromatography-isotope ratio mass spectrometry (GC-IRMS) has been raising increasing interest. The method is based on the analysis of isotope ratios at natural isotope abundances and isotopic shifts therein. So far, however, the analysis of micropollutants has been limited to the low  $\mu\text{g/L}$  or higher  $\text{ng/L}$  concentration range<sup>48</sup>. This contrasts with frequent detection of micropollutants in the low  $\text{ng/L}$  range. To target these concentrations, high sensitivity, robustness and accuracy are crucial parameters for CSIA. Chromatographic developments for peak separation and the improvement of pre-concentration techniques (e.g., solid-phase or liquid-liquid extraction) have been improved, and have thus widened the field of applications of CSIA. The specific application of CSIA for polar micropollutants remains, however, limited and challenging, as these techniques do not only enrich the analyte, but also interfering matrix components so that the measurement of isotope ratios may be biased<sup>48, 51, 63, 168-170</sup>. Thus, new approaches are required to enhance (i) the sensitivity of CSIA and (ii) the resolution in order to enable the analysis of micropollutants in environmental samples. Latest approaches address the optimization of these parameters by modifying the analytical instrumentation of GC-IRMS systems rather than just focusing on sample pre-treatment (extraction, pre-concentration, etc.)<sup>65-67, 73, 76, 171, 172</sup>. To increase the sensitivity and to optimize the resolution of a GC-IRMS, it is crucial to obtain narrow peak widths ( $w$ ) in relation to the peak's retention time ( $RT$ ) and thus to increase the efficiency of the system, which is usually measured in the number of theoretical plates ( $N$ ) of a GC column (equation 6.1).

$$N = 5.45 \times \left( \frac{RT}{w_{1/2}} \right) \quad \text{eq. 6.1}$$

In current GC-IRMS systems, the carrier gas is currently channeled through components with relatively large internal diameters (ID) such as 0.25 mm - 0.32 mm GC capillary columns, as well as through components with dead volumes e.g., a T-valve, a reactor for analyte combustion (inner diameter 0.5 mm) and a reduction oven, which affect the resolution negatively. It is therefore necessary to avoid dead volumes and minimize the internal diameters of the components (capillaries and reactors) as this will reduce the half-peak width  $w_{1/2}$  and thus improve the system's resolution<sup>173</sup>.



This approach was first applied by Sacks et al.<sup>64</sup> for the analysis of fatty acid methyl esters. A fast GC with narrow columns was hyphenated to an IRMS, which resulted in reduced average peak widths of 720 ms compared to previously reported peak widths of 4.7 s and a precision of  $\pm 1.4$  ‰ for 100 pmol carbon on column.

Baczynski et al.<sup>66</sup> improved the precision of the approach from Sacks et al.<sup>64</sup> by reducing the diameter of capillaries (0.1 mm instead of 0.15 mm), using a PTV inlet instead of a microfluidic switch and by optimizing the combustion method. This enabled an accurate analysis of *n*-alkanes (*n*-C<sub>16</sub> – *n*-C<sub>30</sub>) for 100 pmol carbon on column with a precision of  $\pm 0.9$  ‰. An additional critical device effecting the instrument's sensitivity is the open-split, as more than two thirds of a sample are lost at this part<sup>174</sup>. It is used to control the helium flow from the GC to the IRMS in order to protect the vacuum and to transfer the analyte into the IRMS. In this case, Baczynski et al.<sup>66</sup> described the optimization of the open-split by aligning the capillary of the transfer line to the IRMS sniffing capillary to increase the instrument's sensitivity.

Besides these initiatives to improve the sensitivity and resolution by modification of commercially available unidimensional GC-IRMS systems, attempts have been made to enhance these parameters by the combination of multidimensional GC application with IRMS<sup>72, 73, 75, 175</sup>. Multidimensional GC (MDGC) is achieved by adding a second column to the system via an interface such as a dean switch. In this case, it is called heart-cut 2D-GC and is considered to be one of the first approaches of MDGC<sup>176</sup>. To achieve multidimensional separation, the interface 'samples' a fraction of the eluent, mostly one peak within a selected time frame, and transfers it from the first column onto the second column. The second column has similar dimensions but a different polarity compared to the first column which improves the resolution of closely eluting compounds. This technique is, however, only of interest if information of a target analyte within a defined retention time range and thus no information about the entire sample is necessary. In this case comprehensive GC×GC is used, a technique where the complete eluent is transferred via a modulator interface from the first column onto the second column without destroying the separation achieved in the first dimension<sup>72, 177</sup>. To preserve the separation from the first dimension, the second column is shorter (e.g., 1 m - 2 m), has a smaller internal diameter (e.g., 0.1 mm - 0.18 mm) and a different selectivity compared to the first column. Thus, instrumental modifications as described by Baczynski et al.<sup>66</sup> are technical requirements for qualitative GC×GC separation. Depending on the target analyte, different types of modulators, either a valved-based or a thermal modulator are possible<sup>178, 179</sup>.

An overview of different modulator systems and their operating mode is published by Edwards et al.<sup>178</sup>.

For trace analysis of micropollutants in complex sample matrices, comprehensive GC×GC-IRMS is potentially more powerful compared to heart-cut GC for two reasons. First, the influence of matrix components may lead to shifts in retention times so that peaks may be lost if they happen to move out of the heart-cut window for transfer to the second dimension. Consequently, this would lead to biased isotope results in heart-cut 2D-GC-IRMS<sup>175</sup>. An additional promising advantage of comprehensive GC×GC is the possibility of cryofocusing by using a cryogenic modulator. In this case, the target analyte is frozen in the first dimension and released by heat on the second dimension. This procedure results in sharpened peaks (reduced peak width and increased amplitudes) and thus an improved sensitivity and higher resolution<sup>180</sup>.

The first instrumental set-up and application of comprehensive GC×GC coupled to an IRMS has been published by Tobias et al.<sup>72</sup> for the analysis of steroids in urine. Before application of GC×GC-IRMS for steroid analysis in complex sample matrices such as urine, extensive sample pre-treatment<sup>72-74</sup> such as the combination of SPE, liquid-liquid extraction and preparative HPLC were involved for carbon isotope analysis in order to reduce the complexity of the sample matrix. Thus, by applying comprehensive GC×GC sample preparation requirements were reduced<sup>72, 73</sup>.

The aim of this study is to increase the sensitivity and resolution without introducing an isotopic discrimination to detect polar micropollutants in complex sample matrices at low ng/L concentration ranges. This preliminary study targeted the following instrumental modifications based on the studies of Baczynski et al.<sup>66</sup> and Tobias et al.<sup>74</sup> to achieve improvements on the GC-IRMS system for enhanced sensitivity and peak separation: In the first part, instrumental modifications focused on the improvement of the existing one-dimensional GC-IRMS system. In order to achieve this, the dead volume of the system as well as the peak width were targeted by reducing the inner diameter of all capillaries and the GC-column. In addition, a new combustion reactor based on a nickel tube with a platinum-wire inside and a modified open-split were developed. Furthermore, the data acquisition of the isotope ratio mass spectrometer and its corresponding software were improved. The second part of this work aims to improve the resolution by adding a second chromatographic dimension using a thermal modulator. To validate the system and monitor its improvement,

frequently detected herbicides such as the triazine atrazine as well as the chloroacetanilides metolachlor and acetochlor were used as model compounds.

### 6.2. Materials and Methods

#### 6.2.1. Chemicals

Atrazine (ATZ, purity not available, CAS no. 1912-24-9) was purchased from Cfm Oskar Tropitzsch GmbH (Markredwitz, Germany). Both, acetochlor (ACETO, 96.3 %, CAS no. 34256-82-1) and metolachlor (METO, 96.2 %, CAS no. 51218-45-2) were supplied by Chemos GmbH (Regenstauf, Germany). Ethyl acetate ( $\geq 99.9$  %, CAS no.: 141-78-6) and acetone ( $\geq 99.9$  %, CAS no.: 67-64-1) were produced by Roth (Karlsruhe, Germany).

#### 6.2.2. EA-IRMS Measurement for Determination of Reference Values

The isotopic compositions of the ATZ, METO and ACETO standards used for the instrument evaluation were determined using an elemental analyzer-isotope ratio mass spectrometer (EA-IRMS)<sup>76</sup>. Thereto, an EuroEA (Euro Vector, Milano, Italy) was coupled to a Finnigan MAT 253 IRMS via a Finnigan™ ConFlow III interface (Thermo Fisher Scientific, Bremen, Germany). All standards were calibrated against the organic referencing materials USG 40 (L-glutamic acid), USG 41 (L-glutamic acid) and IAEA 600 (caffeine). The referencing materials were provided by the International Atomic Energy Agency (IAEA, Vienna, Austria).

Carbon isotope values ( $\delta^{13}\text{C}$ ) are reported in per mil relative to PeeDee Belemnite (V-PDB). They are expressed according to equation 6.2:

$$\delta^{13}\text{C} = \frac{{}^{13}\text{C}/{}^{12}\text{C}_{\text{Sample}} - {}^{13}\text{C}/{}^{12}\text{C}_{\text{Reference}}}{{}^{13}\text{C}/{}^{12}\text{C}_{\text{Reference}}} \quad \text{eq. 6.2}$$

$\delta^{13}\text{C}$  values were determined relative to our laboratory  $\text{CO}_2$  monitoring gas, which was previously calibrated against RM8563 ( $\text{CO}_2$ ), supplied by the IAEA.

#### 6.2.3. GC-IRMS – Initial State of the Instrumentation

Isotope analysis was originally carried out with a TRACE GC Ultra gas chromatograph (Thermo Fisher Scientific, Milan, Italy) coupled to a Finnigan MAT 253 isotope ratio mass

spectrometer (IRMS) (Thermo Fisher Scientific, Bremen, Germany) as shown in Figure 6.1A. As interface between the two instruments, a Finnigan Combustion III interface (Thermo Fisher Scientific) was used. The IRMS was operated at an accelerating potential of 9 kV and an emission energy of 2 mA. The vacuum was held at  $2.1 \times 10^{-6}$  mbar. At a temperature of 1030 °C, target analytes were combusted to the measurement gas CO<sub>2</sub> using a GC IsoLink reactor consisting of NiO tube/CuO-NiO (Thermo Fisher Scientific). A volume of 1 µL standard was injected splitless into the Thermo injector (250 °C) using a PAL autosampler (CTC Analytics AG, Zwingen, Switzerland). Helium (grade 5.0) with a flow of 1.4 mL/min was used as a carrier gas. The GC oven was equipped with an Rxi-5ms column (60 m × 0.25 mm × 1 µm, Restek GmbH, Bad Homburg, Germany). For peak separation the method described by Meyer et al.<sup>23</sup> was applied. Briefly, the GC temperature program started at 70 °C, which was held for 1 min. Afterwards, the temperature was ramped with 18 °C/min to 155 °C, and then with 2 °C/min to 240 °C (held for 0 min). With a ramp of 30 °C/min, the temperature was then increased to 260 °C, and held for 5 min. Finally, the temperature was ramped with 15 °C/min to 280 °C, which was held for 11 min.

### 6.2.4. GC-IRMS method for Carbon Isotope Analysis after Modifications

A volume of 1 µL standard was injected with a split flow of 30 mL/min using a PAL autosampler (CTC Analytics AG, Zwingen, Switzerland). The GC oven was equipped with an Rxi-5ms column (20 m × 0.18 mm × 0.36 µm, Restek GmbH, Bad Homburg, Germany). The temperature program started at 65 °C. After 1 min, the temperature was increased with 25 °C/min to 175 °C, which was held for 5 min. Finally, the temperature was ramped with 15 °C/min to 280 °C, which was held for 13 min. The carrier gas flow (helium, grade 5.0), injector temperature (250 °C) and split flow were controlled by an Optic 3 device (ATAS, GL Science, Eindhoven, Netherlands).

### 6.2.5. Evaluation of the Instrument Performance

To validate the instrument's performance, ATZ, ACETO and METO (5 mg/L, 10 mg/L, 50 mg/L, 100 mg/L, 200 mg/L, 300 mg/L) reference standards were measured prior to and after instrumental changes focusing on parameters such as  $\delta^{13}\text{C}$  values, peak width and amplitude.

### 6.2.6. Optimization of GC equipment by Reduction of Dead Volume

As shown in Figure 6.1B, different modifications were carried out in order to eliminate potential dead volumes in the system and to improve the instrument's sensitivity. Pre-column, post-column and transfer line were exchanged to reduce the internal diameter capillaries from 0.32 mm and 0.25 mm towards the smaller 0.15 mm fused silica columns.

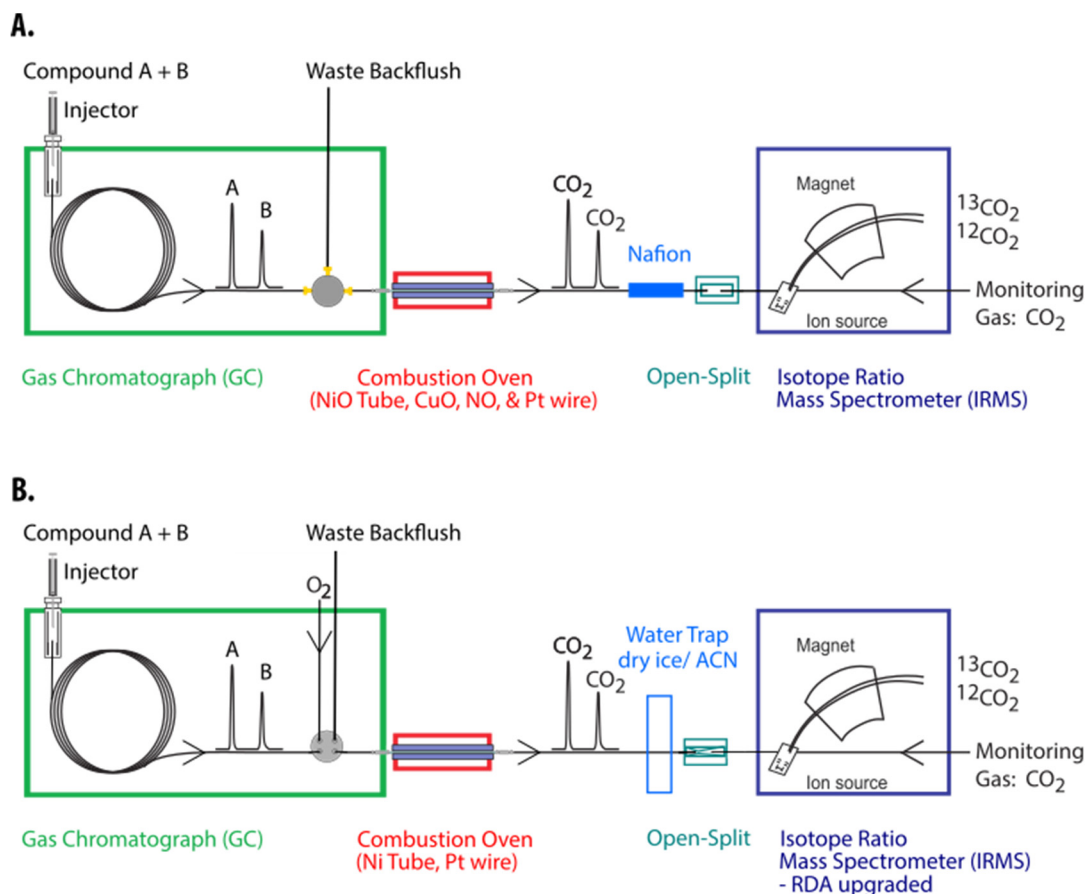


Figure 6.1: Schematic of a GC-IRMS system A. prior to the instrumental modification and B. after the optimization of the unidimensional GC-IRMS system, adapted from Elsner et al.<sup>51</sup>.

#### 6.2.6.1. Replacement of T-Valve by 4-Port Splitter

The previously installed T-valve was replaced by a new 4-port Splitter (SGE by Trajan Scientific, Crownhill, UK) in order to enable the oxygen addition required for the new combustion reactor set-up (Figure 6.2). To this end, the fused silica capillary (post-column, 10 cm × 0.15 mm) from the GC column was attached to CAP A, while the outflow was connected to the reactor via CAP B (10 cm × 0.15 mm fused silica capillary). The oxygen was introduced into the system via an external regulator, which was connected to CAP D via a

60 cm fused silica capillary (ID = 0.15 cm). The waste was connected to CAP C. In this case, to avoid blockages, a fused silica column with an internal diameter of 0.32 mm was used.

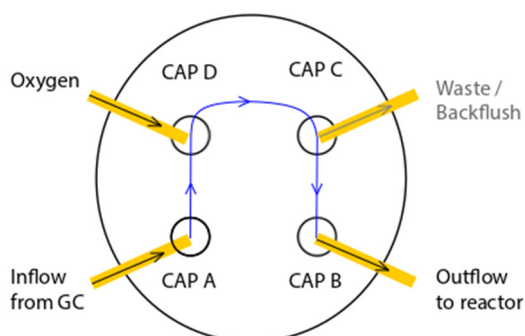


Figure 6.2: Schematic set-up of the 4-port splitter.

### 6.2.6.2. *New Combustion Reactor*

As there is no reactor with internal diameters smaller than 0.5 mm commercially available, electroformed Ni-tubing reactors (VICI, Schenk, Switzerland) with different internal diameters (0.1 mm and 0.25 mm) were tested for their efficiency to transform the target analytes ATZ, METO and ACETO to CO<sub>2</sub>. The reactor was placed in a ceramic tube (Firalit Degussit AL23, ID 1 mm) to protect the furnace. Additionally, the combination of the Ni-tube with platinum-wire (0.01 mm, 99.9 %, goodfellow, Hamburg, Deutschland) was investigated. All reactors were operated at a temperature of 1030 °C. To provide oxygen for the transformation of the target analytes to CO<sub>2</sub>, different amounts of O<sub>2</sub> (2 % to 42 % O<sub>2</sub> in He) were added to the reactor via the 4-port splitter. The pressure was controlled with an external regulator (Thermo Fischer Scientific, Bremen, Germany).

### 6.2.6.3. *Bypass of the Nafion Membrane and Reduction Oven*

In order to reduce the dead volume, the transfer line was connected directly to the open-split of the GC-III interface, so that the nafion membrane unit (normally used for water removal) and the reduction oven were bypassed. Instead, a mixture of dry ice and acetone (approximately -70 °C) was used as water trap, and reduction was targeted in the Ni reactor.

#### **6.2.6.4. Open-Split**

The open-split was built by fixing a custom-made pressfit (glassblower) in a (i) 20  $\mu\text{L}$  and (ii) 50  $\mu\text{L}$  glass capillary using epoxy adhesive. Afterwards, the transfer line from the GC was connected to the lower end of the pressfit and fixed with glue (2-K epoxy adhesive, Uhu Plus Schnellfest). To avoid clogging of the open-split the transfer line was therefore seeped through by helium. To adjust the position of the sniffing capillary that dipped into the upper end of the pressfit, and to optimize helium backflush flow and helium carrier gas flow, 5  $\mu\text{L}$  volumes of air were injected and parameters were adjusted / optimized to reach maximum amplitudes.

#### **6.2.7. Transformation of IRMS**

A rapid data acquisition upgrade of the electronics and the software was carried out by Thermo Fisher Scientific (Bremen, Germany) including modifications in the resistor and capacitors in the faraday cup electronics.

### **6.3. Preliminary Results and Discussion**

#### **6.3.1. Challenges in Modifying the Instrumental Set-Up**

##### **6.3.1.1. Open-Split**

The assembling of the open-split showed that the approach using (i) 20  $\mu\text{L}$  glass capillaries does lead to small peak widths and high intensities of air injection - an air injection of 5  $\mu\text{L}$  resulted in a peak width of 8 s and an amplitude of 30 V. However, this open-split set-up also showed an increased risk of breaking of the sniffing capillary. Thus, a second set-up with a larger glass capillary (ii) 50  $\mu\text{L}$  was used for further instrument developments.

##### **6.3.1.2. Nickel Reactor**

The nickel reactor was not as fragile and more flexible than the ceramic IsoLink reactor purchased from Thermo Fisher Scientific. Thus, the application of nickel reactor tubes with 0.1 mm ID proved to be unsuitable as this internal diameter has a tendency for blockages either due to deformations or due to precipitation of NiO. Consequently, a reactor with an ID of 0.25 mm was used for further instrument development. For the analyte transformation to  $\text{CO}_2$ , each reactor was oxidized for 12 h with 40 %  $\text{O}_2$  in helium prior to analysis. To protect the

filament, the needle valve was closed during the pre-oxidation. Nevertheless, even after pre-oxidation a constant flow of oxygen needed to be mixed into the carrier gas flow passing through the reactor, since the storage capacity of oxygen in nickel seemed to be small (Figure 6.3).

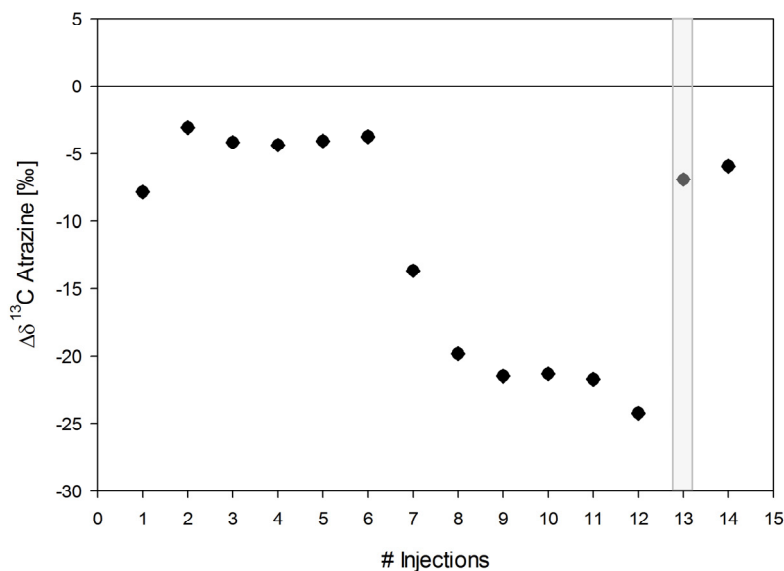


**Figure 6.3:** Deviation of carbon isotope values of a 300 mg/L atrazine standard measurements (black diamonds) measured with a Ni-reactor (ID 0.25 mm) at a temperature of 1030 °C. The reactor was oxidized prior to the measurement for 12 h overnight. The grey bar shows the influence of continuous oxygen addition to the system. Isotope values are shown as the deviations of the measured value from the Elemental-Analyzer reference isotope value.

Increasing the operating temperatures of the nickel reactor did not improve the trueness and precision of the analysis. It was improved by decreasing the oxygen addition from 40 % to 2 % oxygen in helium (Figure 6.4). Based on this observation and the fact that the reduction oven was bypassed in the modified set-up, it is assumed that the missing accuracy is either caused by incomplete combustion or, more probably, by the excess of oxygen. As the tested analytes contain nitrogen, it is likely that the excess of oxygen and the nitrogen atom formed  $\text{NO}_2$ , which was detected as  $m/z$  46. This interfered with the ion currents measured for carbon isotope analysis:  $m/z$  44 ( $^{12}\text{C}^{16}\text{O}^{16}\text{O}^+$ ),  $m/z$  45 ( $^{13}\text{C}^{16}\text{O}^{16}\text{O}^+$ ,  $^{12}\text{C}^{17}\text{O}^{16}\text{O}^+$ ) and  $m/z$  46 ( $^{12}\text{C}^{16}\text{O}^{18}\text{O}^+$ ,  $^{12}\text{C}^{17}\text{O}^{17}\text{O}^+$ ,  $^{13}\text{C}^{17}\text{O}^{16}\text{O}^+$ ). The ion current  $m/z$  46 is used to correct for the contribution of  $^{17}\text{O}$  isotope in the  $m/z$  45 signal and thus to calculate the abundance of  $^{13}\text{C}$  <sup>173</sup>, <sup>181</sup>. As the abundance of this  $m/z$  46 is however biased by the detection of  $\text{NO}_2$ , the  $^{18}\text{O}$  and thus also the  $^{17}\text{O}$  isotope is overestimated. Due to the automatic  $^{17}\text{O}$  correction done by the software, the calculated abundance of  $^{13}\text{C}$  is underestimated and thus carbon isotope ratios are



## 6. Development of a GC×GC-IRMS Towards a More Sensitive Isotope Analysis

biased. Precise results close to true isotope values for all three model compounds, with standard deviations smaller than  $\pm 0.5$ , were achieved by inserting a platinum wire into the reactor and a continuous addition of 7 % oxygen in helium prior to the combustion reactor. This might be explained by the combination of the high temperature with the catalytic properties of the platinum wire<sup>182</sup> which broke down the interfering  $^{14}\text{NO}_2$ . Consequently, the 46/44 mV ratios and thus the  $^{17}\text{O}$ -correction employed within the commercial software were less biased. This agrees as well with the observation that trueness improved after the continuous addition of oxygen was decreased to 7 % oxygen in helium after pre-oxidation.

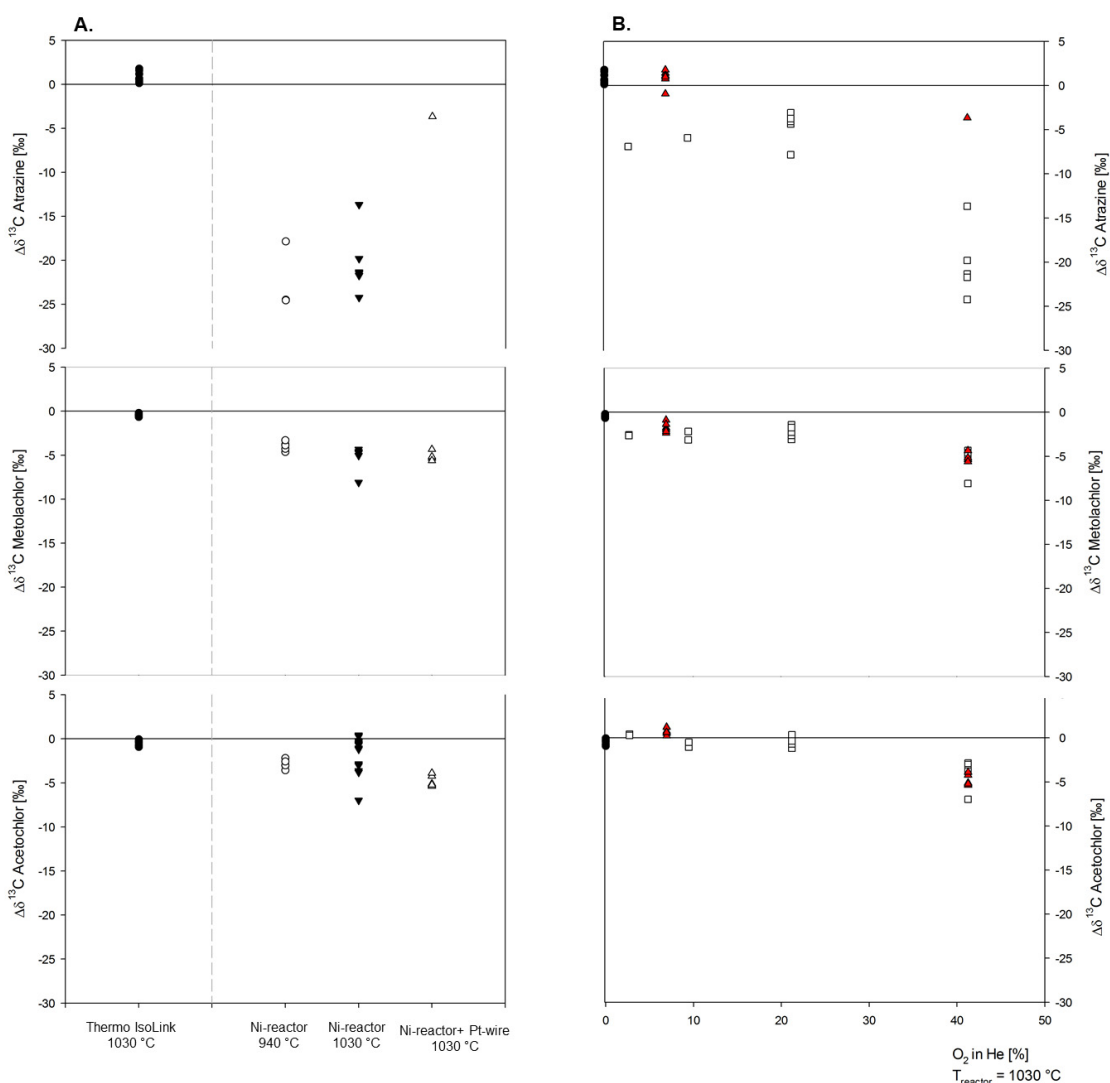


**Figure 6.4:** Deviation of carbon isotope values of standard measurements (300 mg/L) of atrazine, metolachlor and acetochlor using A. different reactors and temperatures applying 2.0 bar  $\text{O}_2$  to a Ni-tube reactor in each set-up; black circles show the results from analyte combustion with Thermo IsoLink reactor (original set-up), white circles show analyte combustion at 940 °C using a Ni-tube, black triangles show analyte combustion at 1030 °C. Analyte combustion at 1030 °C using Ni-tube with platinum wire is shown with white triangles. B. adding different concentrations of oxygen to the helium mobile phase, black circles show the results from analyte combustion with Thermo IsoLink reactor, combustion with a Ni-tube is shown as white squares, while red triangles represent combustion of the analytes with a Ni-tube containing a platinum wire.

### 6.3.1.3. Reduction of the Dead Volume

Smaller internal diameters of the capillaries, the reactor and the open-split and thus the reduction in dead volumes resulted in a decrease in peak widths. The peak width of the air injection could be reduced by the factor of 3 (Figure 6.5) and the peak width of the model compounds used for evaluation was decreased 1.5 times. For example, prior to the modifications ATZ was measured with a peak width of 30 s at a peak area of 0.6 Vs, while a similar peak area of 0.7 Vs resulted in a peak width of 20 s in the modified set-up. Even though the peak width was decreased, this result can still be compared to peak widths reported by Schreglmann et al.<sup>48</sup>, who reported for comparable peak area peak widths of 10 s to 20 s for cold on-column injection of ATZ into a non-modified instrumental set-up. Thus, there might be further potential in reducing the peak width by either optimizing or changing the injection technique from split to cold on-column injection. The potential for further optimization is emphasized by Baczynski et al.<sup>66</sup>, who reported a reduction of the peak width for the analysis of n-alkanes by the factor of 2 (from 6 s to 3 s, peak area = n.a.). In this case, a direct comparison of the reported peak widths to our results, as done with the results of Schreglmann et al.<sup>48</sup>, is not possible due to the differences in chemical properties of the measured substances (n-alkanes vs. triazine derivative and chloroacetanilides). Polar compounds show different sorption and combustion behaviors compared to non-polar analytes due to their functional groups leading to an effect on the peak shape<sup>51, 172</sup>.

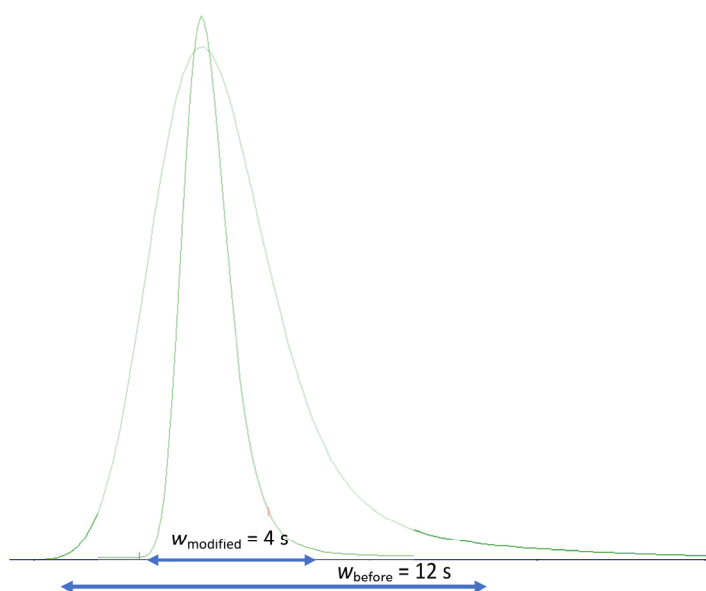


Figure 6.5: Argon peaks ( $m/z = 40$ ) of similar amplitude from air injection into the old system and into the modified GC-IRMS system with smaller diameters, new reactor and custom made open-split.

### **6.3.1.4. Loss in Sensitivity**

After the modifications a loss in sensitivity by the factor of 10 was observed. The decrease may be explained by two broken lenses ( $x$ -symmetry and EL2) of the IRMS electronics. Additionally, as suggested by Blumberg et al.<sup>183</sup>, a loss in sensitivity can be caused by a deficient installation of a modified part, e.g. a faulty adjusted helium protection stream in the open-split. Thus, for improvement, the instrumental set-up needs to be further controlled and optimized<sup>184</sup>.

### **6.4. Conclusion and Outlook**

The system modification towards a more sensitive CSIA has started successfully. First results indicate that the new reactor design can provide accurate results with standard deviations smaller than 0.5 ‰. Due to the modified set-up, however, a decrease in sensitivity by a factor of 10 was observed. Thus, future approaches aim to gain back the sensitivity by adjusting the open split and to investigate the influence of the 4-port splitter. As soon as the loss in sensitivity is eliminated, it is aimed to determine the limit of precision and reproducibility of the micropollutants ATZ, ACETO and METO. Additionally, in order to identify the cause of the observed peak width, e.g. by dead volume or sorption to column or reactor, and thus to enable further optimization of that parameter, it is aimed to measure further substances with different volatility and polarity (e.g. with different functional groups). Such substances may be methane, *n*-alkanes, toluene, chlorinated substances like chlorobenzene and chlorophenol, benzotriazole and its derivatives. Additionally, the analysis of these substances enables further characterization of the new reactor compared to existing reactors in regards to its suitability for different substances, the limit of precise isotope analysis and the trueness of isotope values.

In a second part of the project, the GC-IRMS will be converted to a GC×GC-IRMS by adding a thermal modulator (ZX1, Zoex, Houston, TX) in order to enable the analysis of micropollutants in complex sample matrices. In particular, this project aims to re-analyze the environmental samples from Chapter 3 and Chapter 4, whose analysis had been previously limited by the missing sensitivity of the instrumentation. Therefore, new methods must be developed and validated, including analytical methods as well as the test of the sample evaluation.

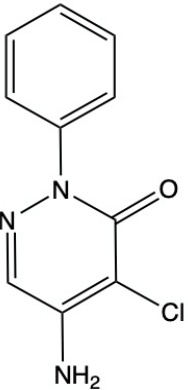
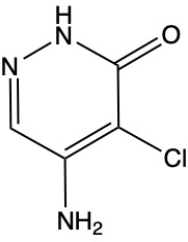
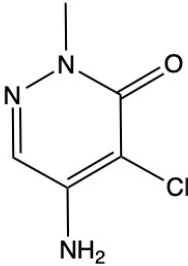


# Appendix

## A. Supporting Information of Chapter 2

## A.1. General Information

Table A1: Properties of chloridazon and its metabolites desphenylchloridazon and methyl-desphenylchloridazon <sup>19, 99, 111, 185</sup>. n.a. = not available

	Chloridazon	Desphenylchloridazon	Methyl-desphenylchloridazon
IUPAC Name	5-amino-4-chloro-2-phenylpyridazin-3(2H)-one	5-amino-4-chloro-3(2H)-pyridazine	5-amino-4-chloro-2-methyl-3(2H)-pyridazine
Chemical Structure			
Empirical formula	C <sub>10</sub> H <sub>8</sub> ClN <sub>3</sub> O	C <sub>4</sub> H <sub>4</sub> ClN <sub>3</sub> O	C <sub>5</sub> H <sub>7</sub> ClN <sub>3</sub> O
Molecular Weight (g/mol)	221.6	145.55	159.58
Melting Point	205-206 °C	315 °C sublimation	with n.a.
Boiling Point	n.a.	n.a.	n.a.
Solubility in water (mg/L)	422	490	n.a.
pK <sub>a</sub>	3.38	9.05	n.a.
GC suitability	Yes	After derivatization	Yes

## A.2. Experimental / Methods

### A.2.1. Peak Identification and Quantification with GC-qMS

The retention time of the target analyte was confirmed with a gas chromatography – quadrupole mass spectrometry (GC-qMS). A 7890A GC was coupled with a 5975C qMS (Agilent, Santa Clara, CA, US). The gas chromatograph was equipped with a DB-1701 column (J&W Scientific, Santa Clara, CA) with a length of 30 m, an inner diameter of 0.25 mm and a film thickness of 1  $\mu$ m. The instrument was operated with helium carrier gas (grade 5.0) at a flow of 1.4 mL/min. A volume of 1  $\mu$ L was injected with a CombiPAL autosampler (CTC Analytics AG, Zwingen, Switzerland) in splitless mode (injection temperature 250 °C). The GC temperature program, adapted from Kuhlmann<sup>99</sup>, started at 100 °C and was held for 1 min. Subsequently, the temperature was ramped with 5 °C/min to its final temperature of 240 °C and held for 30 min. Via a heated transfer line of 250 °C, the analyte was transferred into the MS. Ions were generated using an electron impact ionization with an electron-accelerating voltage of 70 V. The MS was operated in scan mode (from m/z 40 to 550). For instrument control and data evaluation, the software ChemStation E.02.02.1431 was used. The data evaluation was carried out using m/z 145 and 159 as qualifier ions for MDPC. The m/z 159 was also used as a quantifier ion.

### A.2.2. Concentration Measurements with UHPLC

Concentrations of CLZ and DPC were determined by ultra-high pressure liquid chromatography quadrupole time of flight mass spectrometry (UHPLC-QTOF-MS). A Synapt G2 Q-TOF mass spectrometer (Waters, Milford, MA, USA) equipped with an electrospray (ESI) probe and coupled to an Acquity UPLC™ system (Waters) was used. A detailed description of the method can be found in Torrentó et al.<sup>62</sup>. Briefly, the mass spectrometer was operated in positive ionization mode using the MS full scan mode. An Acquity UPLC BEH C18 column (50 mm  $\times$  2.1 mm, 1.7  $\mu$ m, Waters) was used, at a flow rate of 0.4 mL/min in gradient mode. A guard column (5 mm  $\times$  2.1 mm, 1.7  $\mu$ m) with an identical phase was placed before the column. Water and formic acid 0.05% (solvent A) and acetonitrile and formic acid 0.05% (solvent B) were used as mobile phase, according to the following gradient: 2-65% B in 4.5 min, 65-100% B in 1 min, holding at 100% B for 1.5 min and re-equilibration at 2% B for 1.5 min.

Quantification was performed by the internal standard method, based on peak areas, using terbuthylazine as internal standard. The quantifier ions for CLZ, DPC and MDPC were

222.039, 146.012 and 160.028, respectively. With this method, the limit of quantification was 28.1  $\mu\text{g/L}$  for DPC, 9.0  $\mu\text{g/L}$  for MDPC and 4.3  $\mu\text{g/L}$  for CLZ.

### A.2.3. Seepage Water Extraction Method Validation with Spiked Samples.

The extraction method developed by Torrentó et al.<sup>62</sup> was used. Briefly, 4 to 10 L water samples were extracted by solid phase extraction (SPE) using cartridges packed with 8 g of the hydrophobic Bakerbond SDB-1 (J.T. Baker) sorbent and 8 g of the hydrophilic Septra ZT (Phenomenex) sorbent. Cartridges were conditioned four times with 15 mL of ethyl acetate (EtAc) followed by four times 15 mL of ultrapure water. Samples were extracted at a flow rate of 5 mL/min. Afterwards, the cartridges were washed four times with 15 mL of ultrapure water and dried under vacuum overnight to remove the excess of water. The eluates were eluted eight times with 15 mL EtAc. The eluates were evaporated until dryness followed by reconstitution with the required volume of ultrapure water for LC-IRMS injections and methanol for derivatization prior to GC-IRMS injection.

Before extracting DPC-containing environmental seepage water samples, the SPE method was validated with 10 L seepage water samples spiked with 1 to 50  $\mu\text{g/L}$  DPC<sup>62</sup>. As shown in Figure A1, an offset of carbon and nitrogen isotope values of the spiked samples from the EA-value is observed. As this offset is constant and also reflected in the standards, it can be corrected accordingly.

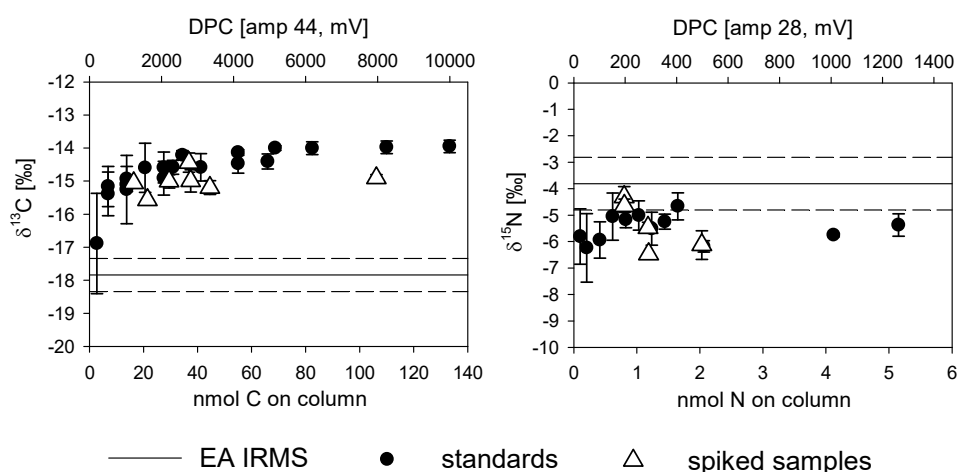


**Figure A1:** Validation of the SPE method for the determination of carbon (left panel) and nitrogen (right panel) isotope ratios of DPC in 10-L drainage water samples (black circles) spiked with 1 to 50  $\mu\text{g/L}$  DPC. Results of analyzed standards (empty triangles) and the EA/IRMS values (black lines) are also shown. The error bars indicate the standard deviations of quadruplicate (carbon) or triplicate (nitrogen) measurements. The dashed lines represent the interval of the ratios measured by EA/IRMS  $\pm 0.5\text{‰}$  for carbon and  $\pm 1\text{‰}$  for nitrogen.



#### A.2.4. Fractionative HPLC –Sample Clean-Up Method for the Experiment: Evolution of Isotope Ratios of DPC from Different Chloridazon Sources.

In contrast to the spiked samples for SPE method validation, the DPC-containing environmental seepage water samples that were spiked with CLZ showed co-eluting interferences in the derivatization GC-IRMS, so that an additional clean-up step was required. Thus, a fractionated HPLC was used after derivatization. Samples were reconstituted in 800  $\mu\text{L}$  MilliQ water/acetonitrile (90/10) and injected into a Shimadzu UHPLC-DAD (Nexera XR, LC-20AD XR) equipped with a Synergi 4  $\mu\text{m}$  Hydro-RP 80  $\text{\AA}$  (100 mm x 4.6  $\mu\text{m}$ ; Phenomenex, Aschaffenburg, Deutschland). Thereto, a gradient of 0.1 mM  $\text{KH}_2\text{PO}_4$  buffer at a pH of 7 and acetonitrile (ACN) was pumped at a flow rate of 1.0 mL/min. The method started at a percentage of 10 % ACN, held for 2 min and increased linearly to 20 % within 4 min. Subsequently, the gradient was increased to 50 % within 3 min and to 75 % within 9 min, held for 2 min, before the proportion of ACN was decreased to 10 % again (held for 5 min). The detector was operated at an absorbance of 210 nm. The derivatized DPC eluted at a retention time of 3 min. Thus, the fraction with the target analyte was collected from 1.75 to 4.10 min. Subsequently, the solvents of both standards and samples were evaporated by freeze-drying and reconstituted in 30  $\mu\text{L}$  acetone. As shown in Figure A2, no isotope fractionation was induced.

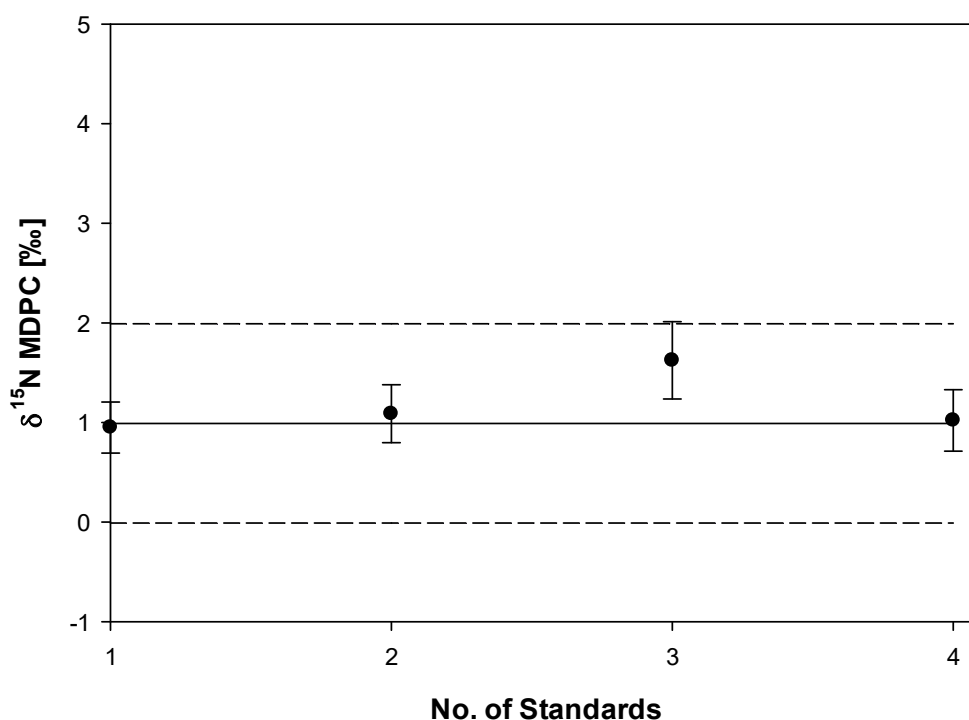


Figure A2: MDPC standards, which were enriched with fractionative HPLC prior GC-IRMS. The black line indicates the referencing value of the standard determined with EA-IRMS, the dashed line shows the limits within the acceptable standard deviation ( $\pm 1\%$ ).

***A.2.5. Fractionative HPLC –Separation of DPC from MDPC in Environmental Samples prior Derivatization.***

Within the presented feasibility study, the influence of MDPC was negligible. Thus, the following method has not been applied. However, for samples in which the ratio of DPC to MDPC is greater 10%, fractionative HPLC needs to be used prior to derivatization to separate the two analytes. As the method described previously in A.2.4. does not separate DPC and MDPC, a new method had to be developed. Therefore, both standards and samples were reconstituted in 800  $\mu$ L MiliQ water/ACN (99/1) and injected into a Shimadzu UHPLC-DAD (Nexera XR, LC-20AD XR). For peak separation, a Synergi 4  $\mu$ m Hydro-RP 80 Å (100 mm x 4.6  $\mu$ m; Phenomenex, Aschaffenburg, Deutschland) was used at a temperature of 35 °C. The mobile phase consisted of a 0.5 mM KH<sub>2</sub>PO<sub>4</sub> buffer at a pH of 7 and ACN and pumped at a flow rate of 1.0 mL/min. A gradient method was used starting at a percentage of 1 % ACN, held for 2 min. Then, the ACN was increased linearly to 10 % within 4 min. The gradient was then increased to 50 % within 3 min. Finally, the ACN was increased linearly to 75 % within 9 min, held for 2 min. Before the next run, the proportion of ACN was decreased to 1 % again (held for 5 min). The absorbance of the detector was set to 210 nm. DPC eluted at a retention time of 4.2 min, so its fraction was collected from 1.8 min to 7.0 min. MDPC was retarded for 7.7 min. Thus, the fraction containing MDPC was collected from 7.0 min to 11.0 min. Afterwards, the ACN/water mixture of these fractions were evaporated by freeze-drying. Both, standards and samples were reconstituted in 50  $\mu$ L acetone. The standard measurements of DPC and MDPC (Figure A3) show that no isotope fractionation was induced.

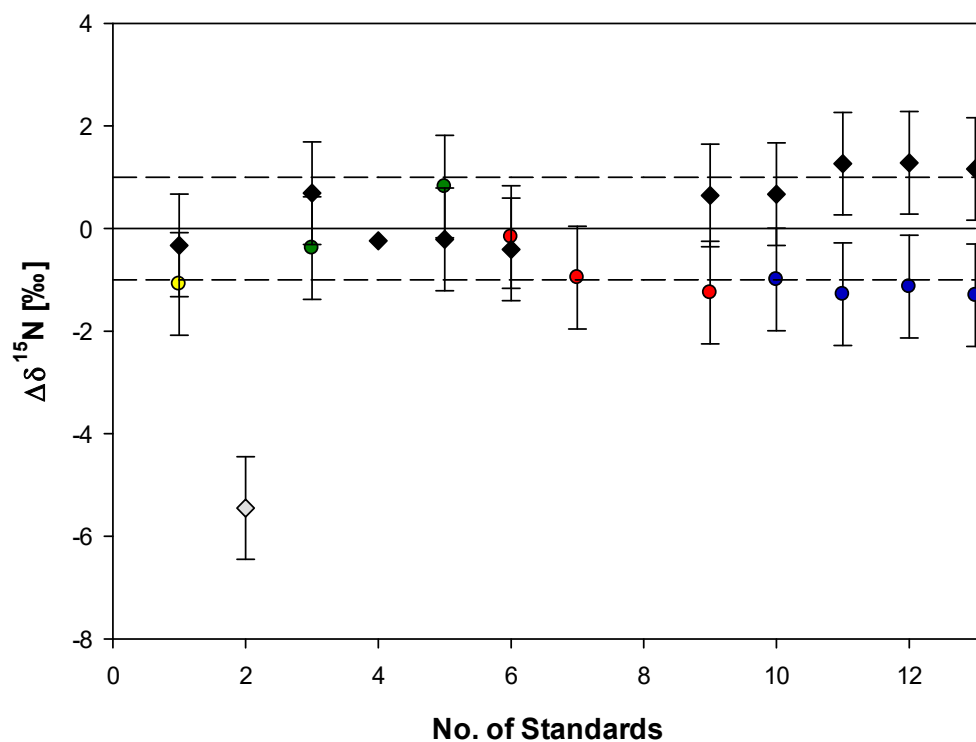


Figure A3: Derivatized DPC standards (circles) and MDPC standards (black diamonds), which were enriched with fractionative HPLC prior derivatization GC-IRMS. The different colors of circles represent different derivatization and measurement days. The black line indicates the referencing value of the standard determined with EA-IRMS, the dashed line shows the limits within the acceptable standard deviation ( $\pm 1\%$ )

## A.3. Results and Discussion

Table A2: Isotope Ratios of  $^{13}\text{C}$  and  $^{15}\text{N}$  of selected compounds used for isotope correction determined by EA-IRMS

Standard	$\delta^{13}\text{C} \pm \text{SD} [\text{‰}]$	$\delta^{15}\text{N} \pm \text{SD} [\text{‰}]$
	n = 5	n = 5
Desphenylchloridazon	$-17.84 \pm 0.05$	$-3.81 \pm 0.04$
Methyldesphenylchloridazon	$-21.17 \pm 0.06$	$+0.99 \pm 0.12$
Desethylatrazine	$-32.08 \pm 0.09$	$-9.42 \pm 0.08$
Acetochlor	$-25.00 \pm 0.06$	$+0.46 \pm 0.09$

Table A3: Round Robin Test of Isotope Ratios of DPC determined by EA-IRMS

Standard	$\delta^{13}\text{C} \pm \text{SD} [\text{‰}]$	$\delta^{15}\text{N} \pm \text{SD} [\text{‰}]$
	n = 5	n = 5
HMGU Laboratory 1	$-17.84 \pm 0.05$	$-3.81 \pm 0.04$
HMGU Laboratory 2	$-17.93 \pm 0.09$	$-3.78 \pm 0.12$
ETH Zurich	n.a.	$-3.64 \pm 0.27$

### A.3.1. LC-IRMS Chromatogram of DPC

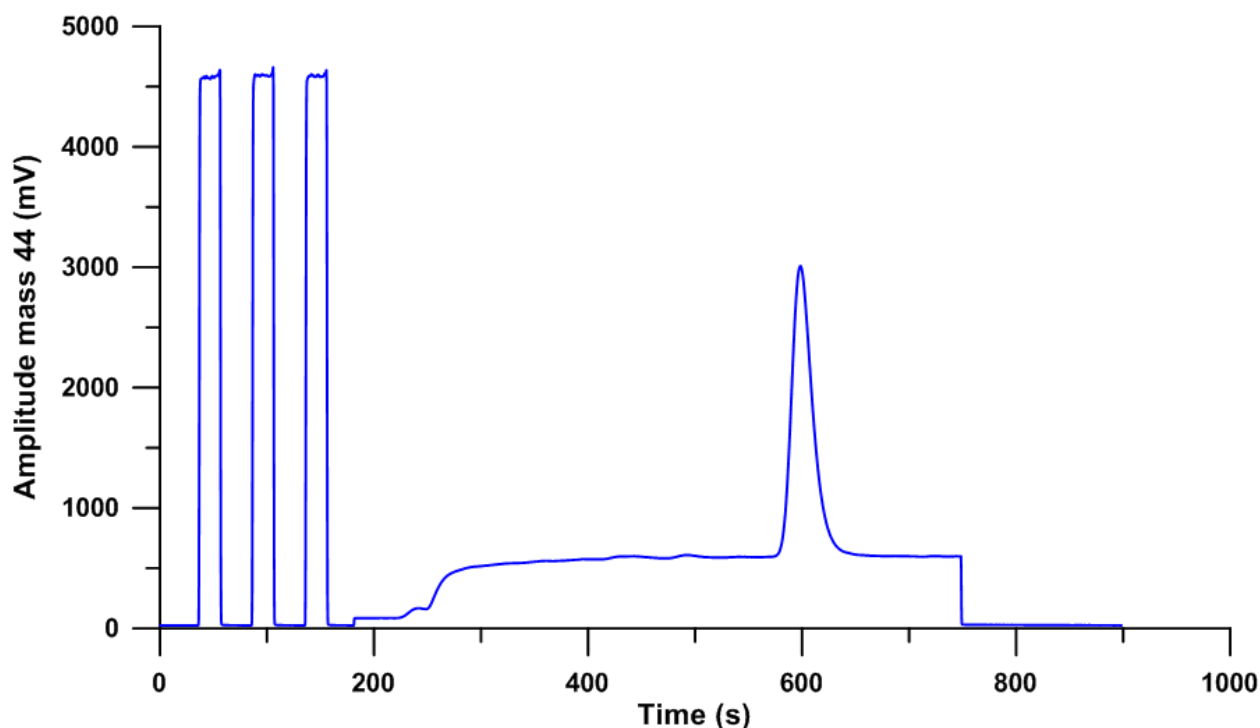


Figure A4: LC-IRMS chromatogram of a DPC standard (27.5 nmol C on column) showing the trace for mass 44.

### A.3.2. Temperature optimization during DPC derivatization.

Figure A5 shows the application of TMSD excess applied to 250 mg/L DPC solved in methanol in relation to the resulting peak area ratio (PAR) at a temperature of 50 °C and 70 °C. BAM (250 mg/L) dissolved in methanol was used as an internal standard. The PAR is calculated by applying the following equation A1:

$$\text{PAR} = \frac{\text{Peak Area (Target Analyte)}}{\text{Peak Area (Internal Standard)}} \quad \text{eq. A1}$$

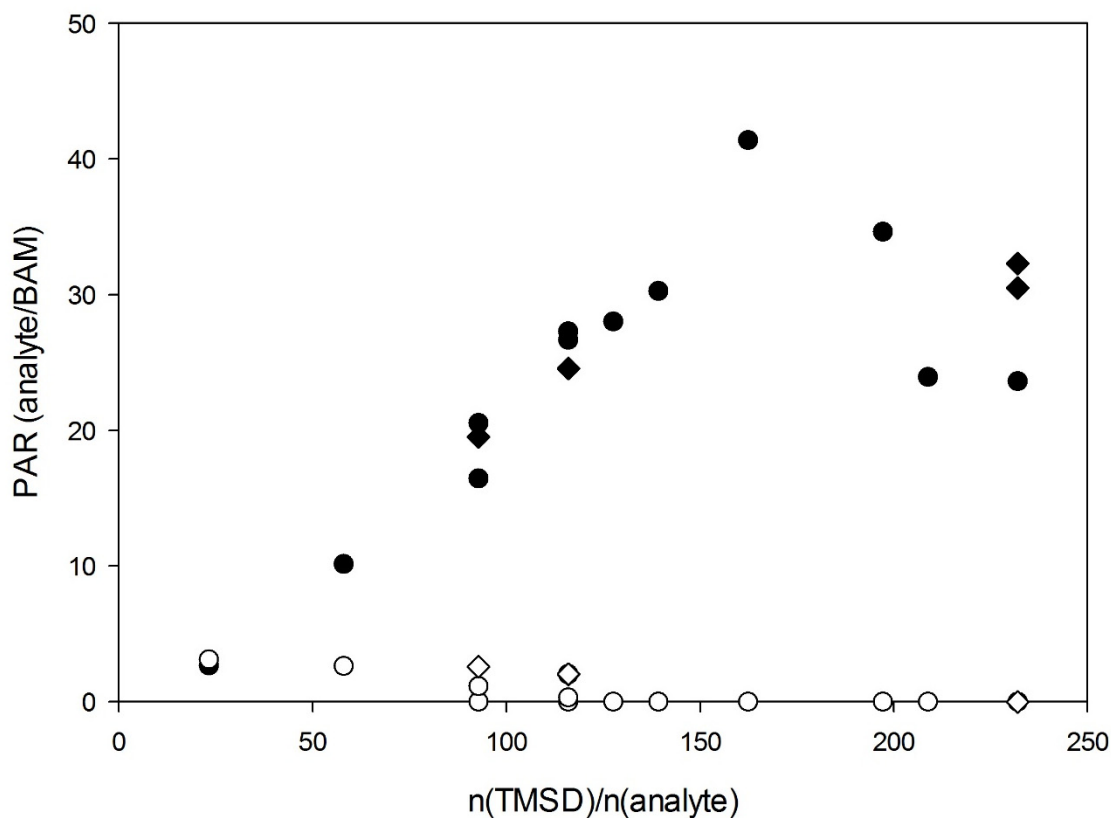


Figure A5: Derivatization of 250 mg/L DPC with varying excess of TMSD at 50 °C (diamonds) and 70 °C (circles). The black symbols show the PAR of derivatized DPC in relation to BAM (internal standard), while the white symbols represent the PAR of the remaining fraction of DPC in relation to BAM

Table A4: Isotope Ratios of <sup>13</sup>C and <sup>15</sup>N of commercially available chloridazon products determined by EA-IRMS

Producer	$\delta^{13}\text{C} \pm \text{SD} [\text{‰}]$ n = 5	$\delta^{15}\text{N} \pm \text{SD} [\text{‰}]$ n = 5
Dr. Ehrenstorfer	-24.65 ± 0.04	-22.22 ± 0.03
Sigma Aldrich	-23.37 ± 0.03	-32.04 ± 0.05
Neochema	-24.67 ± 0.04	-22.17 ± 0.05
Oskar Tropitzsch	-27.43 ± 0.02	-5.70 ± 0.03
Chemos	-21.82 ± 0.03	-31.49 ± 0.99

## A. Supporting Information of Chapter 2

---

**Table A5: Initial composition of seepage water used for the experiment: Evolution of Isotope Ratios of DPC from Different Chloridazon sources**

<b>Compound</b>	<b>Concentration [<math>\mu\text{g/L}</math>]</b>
CLZ (source A)	< 0.02
DPC (from degraded CLZ A)	10.5
MDPC	< 0.05
Atrazine	10
Desethylatrazine	10
Acetochlor	10
Metolachlor	10
2,6 Dichlorobenzamid	10

**Table A6: Concentration analytes in the seepage water used for the two-source mixing model**

<b>Time CLZ application</b>	<b>after</b>	<b>Sample ID</b>	<b>Concentration CLZ [nmol/L]</b>	<b>Concentration DPC [nmol/L]</b>	<b>Concentration MDPC [nmol/L]</b>
0 months		t <sub>0</sub>	136.0	81.7	<0.3
7 months		t <sub>1</sub>	88.7	120.9	0.5
11 months		t <sub>2</sub>	0.0	163.5	0.5

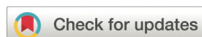
# B. Solid-Phase Extraction Method for Stable Isotope Analysis of Pesticides from Large Volume Environmental Water Samples



## Analyst

PAPER

View Article Online  
View Journal | View Issue



Cite this: *Analyst*, 2019, **144**, 2898

## Solid-phase extraction method for stable isotope analysis of pesticides from large volume environmental water samples†

Clara Torrentó,<sup>1</sup> Rani Bakkour,<sup>1</sup> Gaétan Glauser,<sup>2</sup> Aileen Melsbach,<sup>3</sup> Violaine Ponsin,<sup>4</sup> Thomas B. Hofstetter,<sup>5</sup> Martin Elsner<sup>6</sup> and Daniel Hunkeler<sup>1</sup>

Compound-specific isotope analysis (CSIA) is a valuable tool for assessing the fate of organic pollutants in the environment. However, the requirement of sufficient analyte mass for precise isotope ratio mass spectrometry combined with prevailing low environmental concentrations currently limits comprehensive applications to many micropollutants. Here, we evaluate the upscaling of solid-phase extraction (SPE) approaches for routine CSIA of herbicides. To cover a wide range of polarity, a SPE method with two sorbents (a hydrophobic hypercrosslinked sorbent and a hydrophilic sorbent) was developed. Extraction conditions, including the nature and volume of the elution solvent, the amount of sorbent and the solution pH, were optimized. Extractions of up to 10 L of agricultural drainage water (corresponding to up to 200 000-fold pre-concentration) were successfully performed for precise and sensitive carbon and nitrogen CSIA of the target herbicides atrazine, acetochlor, metolachlor and chloridazon, and metabolites desethylatrazine, desphenylchloridazon and 2,6-dichlorobenzamide in the sub- $\mu\text{g L}^{-1}$ -range.  $^{13}\text{C}/^{12}\text{C}$  and  $^{15}\text{N}/^{14}\text{N}$  ratios were measured by gas chromatography-isotope ratio mass spectrometry (GC/IRMS), except for desphenylchloridazon, for which liquid chromatography (LC/IRMS) and derivatization-GC/IRMS were used, respectively. The method validated in this study is an important step towards analyzing isotope ratios of pesticide mixtures in aquatic systems and holds great potential for multi-element CSIA applications to trace pesticide degradation in complex environments.

Received 23rd January 2019,  
Accepted 13th March 2019  
DOI: 10.1039/c9an00160c  
rsc.li/analyst

## Introduction

Due to abundant agricultural use, pesticides are frequently found in soil and groundwater.<sup>1–5</sup> Pesticide leaching is a problem for groundwater quality and a threat to human health if contaminated groundwater is used as drinking water. To mitigate existing pollution, it is critical to identify sources and to assess the fate of the numerous pesticides present in the environment. Existing methods for elucidating pesticide degradation include, for example, monitoring of parent compound disappearance, detection of transformation products, and evidence of intrinsic transformation potential by molecular biology tools.<sup>6</sup> Nevertheless, measuring the concentration of the parent compounds does not allow distinguishing transformation from other processes such as dilution or sorption, especially in the vadose zone, where concentrations tend to fluctuate strongly under transient and varying hydrological conditions. Furthermore, for the metabolites of many pesticides, transformation reactions are not well known. Degradation processes may therefore not become evident from analysis of the concentration dynamics.

<sup>1</sup>Centre for Hydrogeology and Geothermics (CHYN), University of Neuchâtel, 2000 Neuchâtel, Switzerland. E-mail: clara.torrento@gmail.com;  
Tel: +34 934 033 773

<sup>2</sup>Eawag, Swiss Federal Institute of Aquatic Science and Technology, 8600 Dübendorf, Switzerland

<sup>3</sup>Neuchâtel Platform of Analytical Chemistry (NPAC), University of Neuchâtel, 2000 Neuchâtel, Switzerland

<sup>4</sup>Helmholtz Zentrum München, Institute of Groundwater Ecology, 85764 Neuherberg, Germany

<sup>5</sup>Technical University of Munich, Chair of Analytical Chemistry and Water Chemistry, 81377 Munich, Germany

† Electronic supplementary information (ESI) available: Further details on chemicals and reagents, analytical methods, optimization of the extraction methods, CSIA methods and validation of the SPE-CSIA procedure. See DOI: 10.1039/c9an00160c

‡ Present address: Grup MAiMA, Departament de Mineralogia, Petrologia i Geologia Aplicada, Facultat de Ciències de la Terra, Universitat de Barcelona (UB), C/Martí i Franquès s/n, 08028, Barcelona, Spain.

§ Present address: Technical University of Munich, Chair of Analytical Chemistry and Water Chemistry, 81377 Munich, Germany.

¶ Present address: University of Guelph, G360 Institute for Groundwater Research, N1G 2W1 Guelph, Canada.



Compound-specific isotope analysis (CSIA) is a powerful tool to track and quantify pollutant degradation in environmental systems.<sup>7–10</sup> Molecules with light isotopes in the reactive position are degraded at different rates than molecules containing heavy isotopes. Consequently, temporal and spatial shifts in isotope ratios are indicative of degradation and enable tracking degradation processes. In addition, monitoring the changes of isotope signatures of two (or more) elements is recommended to obtain a more reliable assessment of degradation and to derive the extent and relative contribution of different reaction mechanisms.<sup>9,11,12</sup>

Although CSIA is in widespread use to study the fate of many contaminants,<sup>11,13–15</sup> applications are still emerging for pesticides.<sup>16</sup> Various analytical methods have been recently developed.<sup>17–29</sup> Nonetheless, application of CSIA of pesticides to field studies remain scarce<sup>24,30–34</sup> because of two major challenges. First, isotope effect-free extraction and pre-concentration methods are required to allow CSIA at low environmentally relevant concentrations by gas chromatography-isotope ratio mass spectrometry (GC/IRMS) or – in the case of compounds like desphenylchloridazon for which GC/IRMS-based carbon isotope analysis does not work – by liquid chromatography-IRMS (LC/IRMS).<sup>35</sup> To accomplish accurate (*i.e.* true and precise)<sup>36</sup> CSIA in specific compounds, the required analyte amount is much higher than for concentration analysis (up to 5 nmol of C and 10 nmol of N on-column may be necessary).<sup>37</sup> In environmental water samples, most pesticides and their metabolites are present in trace concentrations (ng L<sup>-1</sup> to µg L<sup>-1</sup> range), which are relevant for regulatory purposes; the EU Directive 98/83/EC establishes maximum permissible concentrations of 0.1 µg L<sup>-1</sup> for individual pesticides and relevant degradation products and 0.5 µg L<sup>-1</sup> for total pesticides. A more than 100 000-fold pre-concentration (*i.e.* 10–100 mg L<sup>-1</sup>) may therefore be required for CSIA. Hence, there is a need for an efficient preparative procedure from large volumes of environmental water samples that can provide the required large amounts of analyte without compromising accurate CSIA. Second, GC/IRMS and LC/IRMS analyses require baseline separation of the target compounds from interfering substances and complex mixtures.<sup>9,16,38</sup> Indeed, during sample pre-concentration, matrix components are enriched together with the target compounds, potentially compromising the chromatographic resolution of the latter. Furthermore, environmental samples usually contain mixtures of pollutants and thus, to minimize workload, pre-concentration methods should be suitable for extracting various compounds at the same time, covering a broad polarity range but ensuring good chromatographic resolution.

A method of choice for the extraction and pre-concentration of pesticides from large volumes of aqueous solution is solid-phase extraction (SPE). The sorbent is selected depending on the characteristics of the analytes to be retained and on the complexity of the sample matrix. A great variety of sorbents with a broad range of properties are commercially available. Excellent reviews regarding sorbents mostly used for micropollutants,<sup>39–42</sup> as well as several examples of pesticide

extractions from large-volume water samples<sup>43,44</sup> have been published. Schreglmann *et al.*<sup>30</sup> validated a SPE-CSIA method for atrazine and desethylatrazine extraction from up to 10 L of tap water spiked at concentrations from 0.5 to 50 µg L<sup>-1</sup> by using a hydrophilic divinylbenzene sorbent. However, no extraction and pre-concentration methods applied to large-volume samples for accurate CSIA of mixtures of herbicides covering a broad polarity range at nanomolar concentrations in environmental waters are currently available.

The main objective of the present study is therefore to develop and validate a SPE-CSIA method for determining carbon and nitrogen isotope ratios of pesticides and metabolites covering a wide range of polarities that commonly occur together in groundwater at nanomolar concentrations. The mixture selected for this work (atrazine -ATR-, desethylatrazine -DEA-, desisopropylatrazine -DIA-, acetochlor -ACETO-, metolachlor -METO-, chloridazon -CLZ-, desphenylchloridazon -DPC-, methyl-desphenylchloridazon -M-DPC-, and 2,6-dichlorobenzamide -BAM-) displays a broad range of polarity (octanol–water partition coefficient, log *K*<sub>ow</sub>, ranging from -0.4 to 3.1) (Table 1). To this end, we (i) optimized SPE conditions for the mixture of the target compounds; (ii) scaled the selected SPE method to large-volume samples; (iii) validated instrumental methods for carbon and nitrogen CSIA of the selected compounds; and (iv) validated the entire SPE-CSIA procedure for C and N CSIA of the target compounds in agricultural drainage water samples.

## Experimental section

### Optimization of the SPE method at small scale

We first compared the performance of different SPE sorbents for extracting the target compounds from small-volume samples of distilled water. The sorbents were selected based on previously published studies as follows. For ATR, DEA and DIA extraction from environmental water samples, polystyrene-divinylbenzene (PS-DVB)-based sorbents with hydrophilic character such as Oasis HLB and Strata-X have been mainly used,<sup>45–47,48</sup> but also silica-based,<sup>49</sup> graphitized carbon-based<sup>49</sup> and hypercrosslinked polystyrene-divinylbenzene (HC-PS-DVB) sorbents.<sup>51</sup> CLZ has been successfully extracted with Oasis HLB<sup>49,50</sup> and HC-PS-DVB sorbents.<sup>51,52</sup> Schatz (2012)<sup>53</sup> found that only the HC-PS-DVB sorbents Bakerbond SDB-1 and LiChrolut EN were able to retain DPC. Nevertheless, other authors have used Oasis HLB for extracting DPC and M-DPC, although recoveries have not been reported.<sup>5,54</sup> Successful extraction of the chloroacetanilides ACETO and METO has been reported using the PS-DVB sorbents Oasis HLB and Strata X,<sup>45,47,49,51</sup> as well as C18 bonded silica.<sup>55</sup> The reported approaches for extracting BAM have mainly used Oasis HLB<sup>56,57</sup> and other DVB phases.<sup>58</sup> Based on this body of literature, and considering the wide range of polarity of the selected pesticides, the following sorbents were tested in this study: one graphitized carbon-based sorbent (Supelclean ENVI-Carb), one styrene-divinylbenzene (ST-DVB) sorbent (Strata-SDB-L), two PS-DVB sorbents with hydrophilic character

**Table 1**  $\log K_{OW}$  values of the target compounds, sorbent characteristics and average extraction recoveries (%) for sorbent screening using the six selected sorbents. Sorbent specific surface area increases from left column to right column. The average extraction recoveries were obtained from replicated experiments ( $n = 6$  or  $11$ , except for SDB-L, with  $n = 2$ ). 20 mL of distilled water spiked to  $12.5 \mu\text{g L}^{-1}$  of each pesticide ( $25 \mu\text{g L}^{-1}$  for DPC) were extracted. The relative standard deviations (RSD %) are shown in parenthesis. na = for some of the tests, the metabolites M-DPC, DIA and DEA were not added because the standards were not available when the tests were performed

Type of sorbent phase	ENVI-Carb		Strata SDB-L		Septra ZT		Oasis HLB		Bakerbond SDB-1		LiChrolut EN	
	Graphitized carbon-based		Styrene-divinylbenzene (ST-DVB)		Polystyrene-divinylbenzene (PS-DVB), hydrophilic		Polystyrene-divinylbenzene (PS-DVB), hydrophilic		Hypercrosslinked polystyrene-divinylbenzene (HC-PS-DVB)			
Sorbent area (i.e. amount $\times$ specific surface area)	60 m <sup>2</sup> (0.5 g, 120 m <sup>2</sup> g <sup>-1</sup> )		250 m <sup>2</sup> (0.5 g, 500 m <sup>2</sup> g <sup>-1</sup> )		152–166 m <sup>2</sup> (0.2 g, 760–830 m <sup>2</sup> g <sup>-1</sup> )		152–166 m <sup>2</sup> (0.2 g, 760–830 m <sup>2</sup> g <sup>-1</sup> )		183–240 m <sup>2</sup> (0.2 g, 915–1200 m <sup>2</sup> g <sup>-1</sup> )			
$\log K_{OW}$	$n = 6$		$n = 2$		$n = 6$		$n = 6$		$n = 11$		$n = 11$	
DPC	-0.40	0	0	0	9 (43)	5 (26)	99 (16)	90 (26)	99 (16)	90 (26)	99 (16)	90 (26)
M-DPC	-0.30	0	54 (18)	54 (18)	90 (6)	57 (3)	77 (14)	na	77 (14)	na	77 (14)	na
DIA	1.15	na	na	na	106 (7)	na	103 (10)	103 (8)	103 (10)	103 (8)	103 (10)	103 (8)
DEA	1.51	na	na	na	103 (11)	na	99 (9)	98 (15)	99 (9)	98 (15)	99 (9)	98 (15)
BAM	0.77	67 (11)	52 (28)	52 (28)	90 (13)	73 (5)	85 (16)	93 (8)	85 (16)	93 (8)	85 (16)	93 (8)
CLZ	1.14	0	0	0	89 (5)	76 (3)	84 (9)	83 (6)	84 (9)	83 (6)	84 (9)	83 (6)
ATR	2.61	47 (55)	16 (28)	16 (28)	95 (17)	18 (7)	95 (7)	94 (10)	95 (7)	94 (10)	95 (7)	94 (10)
ACETO	3.03	84 (6)	42 (33)	42 (33)	95 (12)	69 (6)	100 (8)	98 (14)	95 (12)	100 (8)	98 (14)	98 (14)
METO	3.13	94 (9)	57 (18)	57 (18)	102 (14)	73 (5)	105 (7)	85 (16)	102 (14)	73 (5)	105 (7)	85 (16)

(Oasis HLB and Septra ZT, which is the bulk phase of Strata X) and two hydrophobic HC-PS-DVB sorbents with ultra-high surface area (Bakerbond SDB-1 and LiChrolut EN). Details about the properties of the tested SPE sorbents can be found in Table S1 (ESI†).

The performance of the method was evaluated in terms of extraction efficiency from a mixture of the target compounds under different conditions, based on previous studies: concentration levels (from 1 to  $25 \mu\text{g L}^{-1}$ ), water volumes (from 20 to 500 mL), pH values (3 and unmodified pH), sorbent mass (0.2 to 1 g), and elution solvents (ethyl acetate and methanol). Atrazine- $d_5$ , alachlor- $d_{13}$  and chloridazon- $d_5$  were added to the samples at 1.25, 5.0 and  $5.0 \mu\text{g L}^{-1}$ , respectively, as surrogate standards. The internal standard terbuthylazine was added to the final extracts at  $50 \mu\text{g L}^{-1}$ . Samples were then analyzed by ultra-high pressure liquid chromatography quadrupole time of flight mass spectrometry, as explained below. Recoveries were determined by comparing the peak areas obtained in the spiked samples with those obtained in standard solutions at equivalent concentrations. The overall recovery of each pesticide was calculated as the mean recovery of the spiked samples extracted on different days using the same method and the same equipment. Repeatability was expressed as relative standard deviation (RSD).

#### Optimization of the large-volume water extraction procedure

The SPE approach was further evaluated to rule out SPE-induced isotope fractionation from large-volume samples. First, efficiency of the SPE approach was tested with 5 L and 10 L tap water spiked with  $0.1 \mu\text{g L}^{-1}$  of the target compounds. Second, the method performance was evaluated with spiked environmental aqueous samples to identify potential interferences from matrix compounds during chromatographic separ-

ation. Samples from the drainage water of lysimeters filled with arable soils were used.<sup>59</sup> Sorbent performance was evaluated in 10 L filtered (0.7  $\mu\text{m}$  glass fibre filters) drainage water samples spiked with 0.1 to  $50 \mu\text{g L}^{-1}$  of the target compounds. Finally, the integrity of the isotope values after large-volume SPE was assessed. Validation tests consisted of ten liter samples spiked with standards of the target compounds with known isotope signatures (at 0.5 to  $50 \mu\text{g L}^{-1}$ ), for which SPE was performed following the optimized method.

#### Analytical methods

A detailed description of the analytical methods is available in the ESI†. Briefly, concentrations of the target compounds in the SPE eluates were determined by ultra-high pressure liquid chromatography quadrupole time of flight mass spectrometry (UIPLC-QTOF-MS), using the qualifier and quantifier ions listed in Table S2 (ESI†). Among the target compounds, DPC is the most polar one and is therefore not directly amenable to gas chromatographic separation. For CSIA, for that reason, the following strategy was chosen. Whereas the other compounds were analyzed by GC/IRMS without prior modification, LC/IRMS was used for carbon isotope analysis of DPC, and GC/IRMS after derivatization was used for nitrogen isotope analysis of DPC, respectively.<sup>35</sup> Carbon and nitrogen CSIA of ATR, ACETO, METO, DEA and BAM in ethyl acetate (EtAc) was performed by GC/IRMS according to modified methods.<sup>19,23,30,60</sup> Carbon CSIA of DPC in water was performed by LC/IRMS as explained elsewhere.<sup>35</sup> For measuring N isotope signatures of DPC, derivatization with trimethylsilyldiazomethane was performed prior to GC/IRMS analysis.<sup>35</sup> The CSIA methods were validated following quality assurance recommendations from the US-EPA.<sup>7</sup> The trueness of the isotope measurements was expressed as the deviation of isotope signatures measured by



GC/IRMS and LC/IRMS from reference isotope ratios of the calibrated in-house standards of known carbon and nitrogen isotope ratios, which were previously determined by Elemental Analyzer (EA)/IRMS based on two-point normalization using the international organic reference materials USG 40 (L-glutamic acid), USG 41 (L-glutamic acid) and IAEA 600 (caffeine), provided by the International Atomic Agency (Vienna, Austria).<sup>35</sup> Isotope ratios of the in-house standards are listed in Table S3 (ESI†). Carbon and nitrogen isotope values are reported in per mil (‰) using the delta notation relative to the international standards Vienna PeeDee Belemnite (V-PDB) and air, respectively:

$$\delta \text{ (in ‰)} = \left( \frac{R}{R_{\text{std}}} - 1 \right) \quad (1)$$

where  $R$  and  $R_{\text{std}}$  are the isotope ratios of the sample and the standard, respectively. All reported isotope ratios are expressed as arithmetic means of replicate measurements with 1 standard deviation ( $\pm\sigma$ ) in  $\delta^{13}\text{C}$  and  $\delta^{15}\text{N}$  values as a measure for instrumental precision.

#### Limits of precise isotope analysis, amount dependency, and reproducibility

The GC/IRMS and LC/IRMS instrumental limit of precise isotope analysis ( $\text{Limit}_{\text{instrument}}$ ) was determined for each target compound according to the moving mean method,<sup>61,62</sup> using standard solutions of known isotope composition and uncertainty intervals of  $\pm 0.5\text{‰}$  for  $\delta^{13}\text{C}$  and  $\pm 1\text{‰}$  for  $\delta^{15}\text{N}$ . The linearity range (*i.e.* the range between the smallest and the largest concentration for which the standard deviation of the mean isotope ratio value is within the projected uncertainty intervals) was determined for each compound for both  $\delta^{13}\text{C}$  and  $\delta^{15}\text{N}$ . The reproducibility and long-term stability of the GC/IRMS and LC/IRMS systems were established for different concentrations within the linear range over a period of time ranging between 1 and 3 months.

The limit of precise isotope analysis of the whole SPE-CSIA method ( $\text{Limit}_{\text{method}}$ ) (*i.e.* the minimum concentration in water needed to reach the  $\text{Limit}_{\text{instrument}}$ ), for both  $\delta^{13}\text{C}$  and  $\delta^{15}\text{N}$ , was estimated for each target compound according to eqn (2):

$$\text{Limit}_{\text{SPE-CSIA method}} = \frac{\text{Limit}_{\text{instrument}}}{\text{Conc. factor}} \times \frac{1}{\text{Recov.}} \quad (2)$$

where  $\text{Recov.}$  and  $\text{Conc. factor}$  are the extraction recoveries and pre-concentration factors achieved with the optimized large-volume SPE method, respectively. The validation tests with spiked drainage water samples were also used for experimental validation of the estimated  $\text{Limits}_{\text{method}}$ .

## Results and discussion

### Optimization of the extraction methods

**Sorbent screening.** An initial screening study was performed to select the most promising sorbents in terms of extraction

efficiency for the mixture of selected herbicides and metabolites. For all the selected sorbents, 0.2 g bulk phase was used, except in the case of the sorbents with the lowest specific surface area (ENVI-Carb and Strata SDB-L), for which 0.5 g of sorbent was utilized. Extraction efficiencies for each sorbent were evaluated in replicate trials from a mixture of the target compounds at the same mass load (0.25  $\mu\text{g}$  of each compound, except DPC, for which 0.5  $\mu\text{g}$  was added) and sample volume (20 mL) and using the same eluent solvent (EtAc) and the same eluent volume (3 mL).

Results of this sorbent screening are shown in Table 1. The two sorbents with the lowest surface area (ENVI-Carb and Strata SDB-L) were not able to retain neither CLZ nor DPC. M-DPC was not retained by ENVI-Carb, whereas partial recovery (54%) was achieved with Strata SDB-L. Recoveries for the rest of the target compounds were lower than 70%, except for the chloroacetanilides with ENVI-Carb (84–94%). Regarding the hydrophilic (*i.e.* with presence of polar moieties in their structures, and thus polar functionalities) PS-DVB sorbents, better performance was achieved with Septra ZT than with Oasis HLB. Except for DPC (less than 10% recovery with both sorbents), recoveries for all compounds were satisfactory with Septra ZT, ranging from 89 to 106%, with RSD values lower than 18% in all cases. Complete recovery of DPC (90–99%) was only achieved with the two hydrophobic hypercrosslinked HC-PS-DVB sorbents with ultra-high surface area (SDB-1 and LiChrolut EN), in accordance with the results of Schatz.<sup>53</sup> M-DPC was partially retained by SDB-1 (77%) and not tested with LiChrolut EN. For the rest of the analytes, high recoveries were also achieved using the HC-PS-DVB sorbents, ranging between 84 and 105% (RSDs up to 16%) with SDB-1 and between 83 and 103% (RSDs up to 16%) with LiChrolut EN.

Optimization at small scale (20–500 mL). Given the results of the sorbent screening, Septra ZT, LiChrolut EN and SDB-1 were selected for further optimization of the extraction method. Extraction efficiency from a mixture of the target compounds at different concentration levels (from 1 to 25  $\mu\text{g L}^{-1}$ ) and for different water volumes (from 20 to 500 mL) was investigated by varying the following key parameters, one at a time: pH of water sample, and type and volume of elution solvent. Similar results in terms of extraction efficiency of Septra ZT and SDB-1 were obtained with the three tested elution procedures: 3 mL EtAc, 3 mL MeOH and elution with a sequence of the two solvents (3 mL EtAc followed by 3 mL MeOH) (Fig. 1). Elution with 3 mL EtAc was finally selected due to higher recovery for DPC. Mass load effect was assessed for 0.2 g-cartridges of Septra ZT. Increasing the mass by a factor 25 (from loading 0.02  $\mu\text{g}$  to 0.5  $\mu\text{g}$ ) did not cause important changes in the extraction efficiency, except for M-DPC, BAM and ACETO (Fig. 2).

With the hydrophobic HC-PS-DVB sorbents, two strategies for increasing DPC recovery were tested: modifying the pH of the sample and increasing sorbent mass.<sup>53</sup> First, triplicate extractions using 0.2 g-cartridges of SDB-1 and LiChrolut EN were performed with 20 mL of distilled water containing 25  $\mu\text{g L}^{-1}$  DPC with unmodified pH and with pH adjusted to

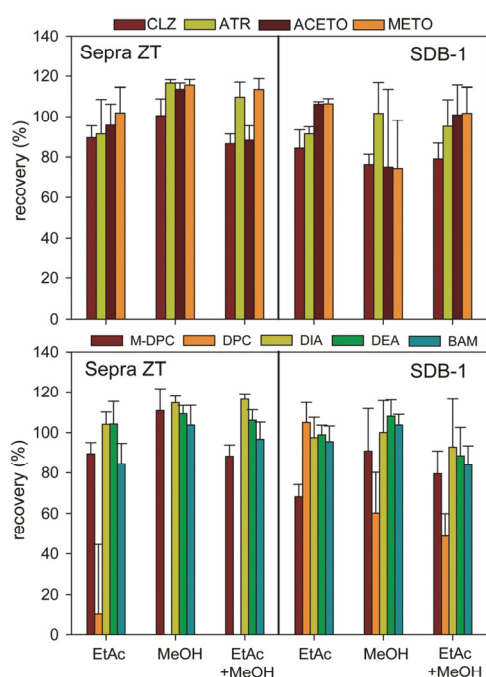


Fig. 1 Elution procedure optimization. Extraction efficiencies (mean recoveries, %) for the three different elution procedures using Septra ZT and Bakerbond SDB-1 0.2 g-cartridges for 20 mL distilled water samples spiked to  $12.5 \mu\text{g L}^{-1}$  each analyte ( $25 \mu\text{g L}^{-1}$  for DPC). Error bars show RSDs ( $n = 3$ ). Herbicides are shown in the upper panel and metabolites, in the lower panel.

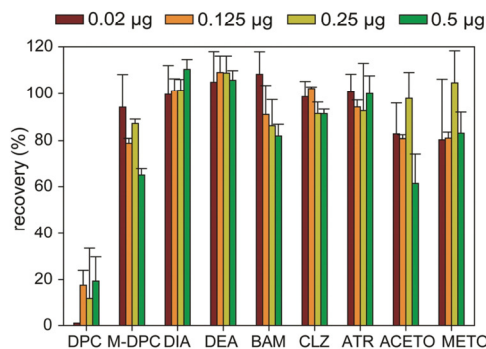


Fig. 2 Mass load effect. Extraction efficiencies (mean recoveries, %) of Septra ZT 0.2 g-cartridges for 20 mL distilled water samples spiked with 0.02 to 0.5  $\mu\text{g}$  each analyte. Cartridges were eluted with 3 mL EtAc. Error bars show RSDs ( $n = 3$ ).

3 with HCl. For both sorbents, higher DPC recovery has been reported at pH 3 than at pH 7.<sup>53</sup> In the present experiments, however, no significant changes were observed for SDB-1 ( $113 \pm 5$  and  $109 \pm 8$ , respectively) and DPC recovery using LiChrolut EN was only marginally enhanced at pH 3 ( $104 \pm 3$  vs.  $92 \pm 3$  with unmodified pH). Similar results were also obtained for the rest of the metabolites (Fig. S1, ESI<sup>†</sup>). Second, to determine if an increase in sorbent mass would result in an increase in DPC recovery, two SDB-1 sorbent masses (0.2 and 1 g) were tested for extracting samples spiked with 0.005 to 0.5  $\mu\text{g}$  DPC. The mass of 0.2 g resulted in complete recoveries of DPC for mass load of 0.25 and 0.5 g. For DPC mass load lower than 0.25  $\mu\text{g}$ , however, 1 g of sorbent was required (90–100% recovery), rather than 0.2 g (40–60% recovery) (Fig. S2, ESI<sup>†</sup>).

Finally, the breakthrough effect related to sample volume was assessed. The hydrophilic sorbent Septra ZT and the hydrophobic hypercrosslinked sorbents with ultra-high surface area SDB-1 and LiChrolut EN were tested. For developing an efficient method that allows extracting all the analytes in one run in order to decrease workload, time and costs, layered cartridges containing one hydrophilic and one hydrophobic hypercrosslinked sorbent were also tested. Distilled water samples (20, 100 and 500 mL) spiked at 0.5  $\mu\text{g}$  of each analyte (1  $\mu\text{g}$  for DPC) were loaded onto the cartridges. For the commercial cartridges, elution was performed with 3 mL EtAc, whereas 6 mL EtAc were used for the homemade-layered cartridges due to the doubled sorbent mass. With Septra ZT, all metabolites except BAM showed breakthrough (Table 2), most pronounced for M-DPC and DPC. Regarding the parent compounds, the breakthrough effect was also significant for ATR and METO. The HC-PS-DVB sorbents with ultra-high surface area (SDB-1 and LiChrolut EN) reduced, as expected, breakthrough volume for the most polar compounds, but, surprisingly, performed poorly for the chloroacetanilides. In contrast, using the layered column with Septra ZT and SDB-1, breakthrough volumes higher than 100 mL were obtained for all analytes, except for DPC (between 20 and 100 mL). Therefore, the combination of the hydrophilic sorbent Septra ZT and the hydrophobic hypercrosslinked sorbent SDB-1 provided the best performance to deal with the broad range of polarity of the selected analytes.

**Scale-up to large volumes.** Sorbent mass and breakthrough effects were assessed for cartridges containing Septra ZT and SDB-1 alone and combined. Tap water samples (5 and 10 L) spiked with 0.1  $\mu\text{g L}^{-1}$  of each analyte were loaded onto cartridges containing different sorbent masses (5 and 10 g of single sorbents and 8 g each for the combined approach) (Table 3). For 5 L samples, cartridges with 5 g of Septra ZT, as expected, failed to recover DPC. Furthermore, recoveries for the rest of the compounds were low for M-DPC, ACETO and METO (19–36%) and acceptable for DIA, DEA, BAM, CLZ and ATR, but in all cases with high RSDs (up to 49%). Increasing the sorbent mass to 10 g resulted in excellent recoveries (92–108%) and RSDs (4–19%) for all the compounds, except DPC. Using 10 g of SDB-1, DPC was more strongly retained

**Table 2** Breakthrough effect. Mean recoveries (%) and relative standard deviation (RSDs) are shown, obtained on loading different sample volumes of distilled water spiked with 0.5 µg with each analyte (1 µg for DPC) on 0.2 g-cartridges of Septra ZT, SDB-1 or LiChrolut EN, and on layered columns containing 0.2 g Septra ZT and 0.2 g SDB-1. Tests were performed in duplicate ( $n = 2$ ), except for 100 mL with LiChrolut EN, for which only one test was done. na = for some of the tests, M-DPC was not added because the standard was not available when the tests were performed

log $K_{ow}$	Septra ZT			Bakerbond SDB-1		LiChrolut EN		Septra ZT + SDB-1	
	20 mL ( $n = 2$ )	100 mL ( $n = 2$ )	500 mL ( $n = 2$ )	20 mL ( $n = 2$ )	100 mL ( $n = 2$ )	20 mL ( $n = 2$ )	100 mL ( $n = 1$ )	20 mL ( $n = 2$ )	100 mL ( $n = 2$ )
	Recovery [%] (RSD)			Recovery [%] (RSD)		Recovery [%] (RSD)		Recovery [%] (RSD)	
DPC	−0.40	19 (10)	0	110 (3)	110 (5)	111 (2)	102	91 (1)	62 (18)
M-DPC	−0.30	65 (3)	56 (8)	65 (3)	na	na	na	93 (5)	80 (12)
DIA	1.15	111 (4)	69 (7)	77 (6)	92 (13)	101 (12)	100 (3)	85 (3)	82 (3)
DEA	1.51	106 (4)	70 (7)	72 (16)	96 (6)	94 (16)	92 (6)	98 (1)	96 (14)
BAM	0.77	82 (5)	92 (9)	87 (9)	87 (1)	80 (4)	100 (4)	100 (1)	96 (5)
CLZ	1.14	91 (2)	90 (10)	89 (12)	75 (2)	76 (4)	81 (7)	94 (1)	88 (15)
ATR	2.61	100 (8)	60 (12)	65 (17)	90 (1)	92 (1)	96 (2)	81	89 (7)
ACETO	3.03	61 (13)	44 (6)	36 (9)	38 (15)	18 (3)	99 (9)	34	89 (8)
METO	3.13	83 (9)	51 (6)	45 (6)	56 (3)	39 (6)	82 (14)	81	83 (3)

**Table 3** Scale-up of SPE procedure to large sample volumes. Mean recoveries (%) and RSDs (in parenthesis) obtained on loading 5 or 10 L of tap or agricultural drainage water spiked with 0.5 to 500 µg of each analyte on cartridges containing 5 or 10 g of Septra ZT, 5 or 10 g of SDB-1 or two layers of 8 g each sorbent. Replicated tests were performed ( $n = 2$  to 9), except for 10 L drainage water at 5 µg L<sup>−1</sup> with the layered cartridge, for which unfortunately only one sample was available. na = for some of the tests, M-DPC was not added because the standard was not available when the tests were performed

Extraction material	Septra ZT (5 g)		Septra ZT (10 g)		Bakerbond SDB-1 (10 g)		Septra ZT (8 g) + SDB-1 (8 g)					
	Tap water		Tap water		Tap water		Tap water		Drainage water		Drainage water	
	5 L 0.1 ( $n = 9$ )	0.1 ( $n = 7$ )	5 L 0.1 ( $n = 7$ )	10 L 0.1 ( $n = 2$ )	5 L 0.1 ( $n = 2$ )	10 L 0.1 ( $n = 2$ )	5 L 0.1 ( $n = 2$ )	10 L 0.1 ( $n = 2$ )	10 L 0.1 ( $n = 2$ )	10 L 1.0 ( $n = 2$ )	10 L 5.0 ( $n = 1$ )	10 L 50 ( $n = 2$ )
Conc. (µg L <sup>−1</sup> )	Recovery [%] (RSD)											
DPC	0	3 (126)	0	46 (28)	33 (20)	76 (17)	53 (12)	24 (30)	46 (15)	23	24 (25)	
M-DPC	35 (10)	92 (19)	95 (25)	100 (10)	92 (2)	90 (3)	100 (4)	na	na	na	na	
DIA	96 (15)	96 (13)	89 (4)	68 (7)	79 (3)	104 (9)	97 (10)	35 (14)	30 (13)	28	108 (2)	
DEA	81 (37)	99 (11)	104 (6)	71 (8)	93 (21)	92 (9)	109 (16)	105 (7)	98 (17)	97	108 (3)	
BAM	81 (49)	107 (9)	100 (5)	83 (9)	89 (5)	107 (14)	90 (22)	111 (3)	104 (10)	114	90 (12)	
CLZ	101 (28)	102 (13)	113 (3)	101 (2)	97 (7)	91 (10)	97 (19)	92 (11)	74 (29)	80	109 (6)	
ATR	103 (3)	108 (5)	112 (5)	94 (4)	101 (5)	109 (16)	93 (21)	95 (10)	100 (10)	109	113 (4)	
ACETO	19 (20)	96 (12)	101 (14)	96 (9)	91 (25)	95 (8)	75 (14)	110 (4)	110 (17)	113	104 (4)	
METO	36 (14)	95 (4)	92 (1)	87 (8)	94 (12)	100 (17)	97 (17)	99 (14)	112 (5)	113	110 (1)	

(46%) and similar results as those with Septra ZT were achieved for the rest of the compounds, except in the case of DIA, DEA and BAM, for which recoveries were slightly lower (70–80%). The best results were obtained with the combination of 8 g of each sorbent in a layered cartridge. Excellent recoveries (90–109%, RSD < 17%) were achieved for all the compounds, even for DPC (76 ± 17%). The breakthrough effect was assessed increasing the sample volume to 10 L for the three cartridges (10 g Septra ZT, 10 g SDB-1 and 8 g each) (Table 3). No compound displayed important breakthrough, except DPC, for which recovery slightly decreased (from 76% to 53%).

Finally, for the layered cartridges containing 8 g of SDB-1 and 8 g of Septra ZT, matrix spikes were extracted to assess the influence of matrix components of real samples. To this end, known amounts of the target analytes (0.1 to 5 µg) were added to 10 L filtered (0.7 µm glass fibre filters) samples of agricul-

tural drainage water<sup>59</sup> (Table 3). At 0.1 µg L<sup>−1</sup>, similar recoveries were obtained for drainage water and tap water, except for DPC (24 ± 30%) and DIA (35 ± 14%). Increasing the load by a factor of 50 (from 0.1 µg to 5 µg) did not result in changes in the extraction efficiency, except for a significant improvement for DIA. Loading 50 µg led to excellent retention of all compounds, except DPC, for which similar results were obtained independently of the mass load (approx. 25%).

The optimal SPE procedure for large-volume samples is detailed in the ESI (section 3).†

#### CSIA methods

We determined the trueness, precision, reproducibility and amount-dependency of the CSIA methods for each target compound using EtAc solutions of standard of known isotope composition determined by EA/IRMS. Results are shown in the ESI



(Table S4, Fig. S3†). Briefly,  $\delta^{13}\text{C}$  and  $\delta^{15}\text{N}$  values of the ATR, DEA, ACETO, METO and BAM working standards measured by GC/IRMS were reproducible over the whole period of analysis. Good precision (expressed as  $\pm\sigma$ ) of  $\pm 0.3$ – $0.5\text{‰}$  ( $n = 52$ – $94$ ) for  $\delta^{13}\text{C}$  and  $\pm 0.1$ – $0.8\text{‰}$  for  $\delta^{15}\text{N}$  analysis were achieved ( $n = 71$ – $84$  for ATR, DEA, ACETO and METO, and  $n = 11$  for BAM). For ATR, ACETO and METO measurements, the trueness was within  $\leq \pm 0.5\text{‰}$  for  $\delta^{13}\text{C}$  and  $\leq \pm 0.9\text{‰}$  for  $\delta^{15}\text{N}$  and was thus within typical uncertainties of  $\pm 0.5\text{‰}$  and  $\pm 1\text{‰}$ , respectively. DEA, on contrast, showed very reproducible offsets of  $+2.0 \pm 0.3\text{‰}$  for  $\delta^{13}\text{C}$  and  $+1.1 \pm 0.1\text{‰}$  for  $\delta^{15}\text{N}$  analysis compared to the reference EA/IRMS values. BAM isotope analysis also showed a reproducible offset for  $\delta^{13}\text{C}$  ( $-1.6 \pm 0.5\text{‰}$ ), whereas consistent  $\delta^{15}\text{N}$  values were obtained ( $\Delta\delta^{15}\text{N} = +0.3 \pm 0.8\text{‰}$ ). The occurrence of these offsets in GC/IRMS usually result from incomplete combustion of the target analytes. Since these deviations are reproducible, true analysis can be nevertheless be achieved by bracketing samples with external compound-specific standards and subsequent offset correction. The LC/IRMS method for  $\delta^{13}\text{C}$  analysis of DPC showed excellent reproducibility over the whole period of analysis ( $\pm 0.4\text{‰}$ ,  $n = 74$ ),

but with an offset of  $+3.2\text{‰}$  compared to the reference EA/IRMS value. This offset is likely related to incomplete wet oxidation of DPC.<sup>35</sup> Offset correction is therefore also required for true analyses. Regarding the derivatization-GC/IRMS method for determining  $\delta^{15}\text{N}$  values of DPC, good precision was achieved ( $\pm 0.4\text{‰}$ ,  $n = 12$ ), with an offset of  $-1.6\text{‰}$  compared to the reference EA/IRMS value.<sup>35</sup> For direct injection of M-DPC, good precision was also achieved ( $\pm 0.4\text{‰}$ ,  $n = 46$ ), with the offset of  $-1.6\text{‰}$  compared to the reference EA/IRMS value.

The performance of  $\delta^{13}\text{C}$  and  $\delta^{15}\text{N}$  measurements was also assessed as a function of injected concentration (Fig. S4 and Fig. S5, ESI†) and limits of precise isotope analysis ( $\text{Limits}_{\text{instrument}}$ ) were then derived according to the moving mean procedure.<sup>61</sup> For  $\delta^{13}\text{C}$  analysis by GC/IRMS for ATR, ACETO, METO and DEA, instrumental limits of 0.15 to 0.20 mM (corresponding to 1.2–2.8 nmol C) were obtained. For BAM, a higher  $\text{Limit}_{\text{instrument}}$  of 1.0 mM (7.1 nmol C) was obtained. Similarly,  $\text{Limits}_{\text{instrument}}$  for  $\delta^{15}\text{N}$  ranged between 0.10 and 0.25 mM (0.7–6.3 nmol N) for ATR, ACETO, METO and DEA, whereas for BAM the limit amounted to 0.50 mM (2.5 nmol N). No amount dependency of the precision was

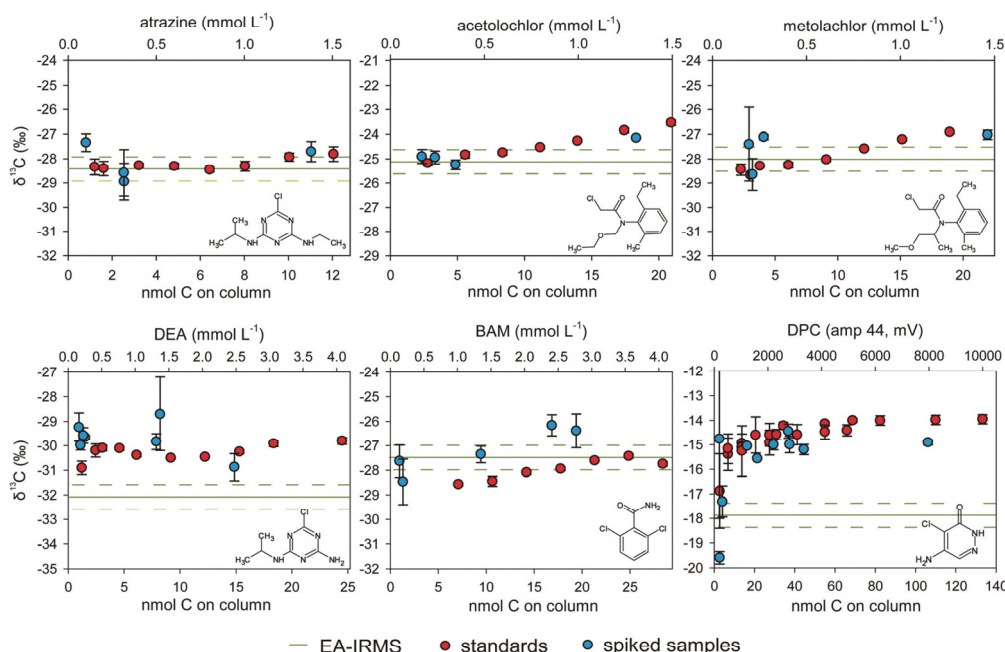


Fig. 3 Validation of the SPE-CSIA procedure for the determination of carbon isotope ratios of the target compounds in 10 L drainage water samples (blue circles) spiked with  $0.5$  to  $5 \mu\text{g L}^{-1}$  for ATR, ACETO and METO,  $0.5$  to  $10 \mu\text{g L}^{-1}$  for DEA and BAM, and  $0.5$  to  $50 \mu\text{g L}^{-1}$  for DPC. Results of the amount-dependence tests (red circles) and EA/IRMS analysis of the standards (green lines) are also shown. The error bars indicate the standard deviations of quadruplicate measurements. The dashed lines represent the interval of  $\delta^{13}\text{C}$  measured by EA/IRMS  $\pm 0.5\text{‰}$ . The molecular structure of the target analytes is also shown. For DPC, amplitude and not analyte concentration is shown because different injection volumes (10 to 100  $\mu\text{L}$ ) were used and thus there is not a straightforward correlation between injected C mass and DPC concentration.

observed between 0.15 and 4.1 mM for  $\delta^{13}\text{C}$  and from 0.10 to 7.5 mM for  $\delta^{15}\text{N}$  for ATR, ACETO, METO and DEA. The linearity ranges for BAM were 1.0–4.1 mM and 0.5–4.0 mM, respectively. The determined  $\text{Limit}_{\text{instrument}}$  for LC/IRMS analysis of DPC was 0.14 mM (27.5 nmol C for an injection volume of 50  $\mu\text{L}$ ), and the linearity range was 27.5–133 nmol C. For  $\delta^{15}\text{N}$  of DPC,  $\text{Limit}_{\text{instrument}}$  was 0.69 mM (corresponding to 2.1 nmol N), and the linearity range was 0.69–6.9 mM.<sup>35</sup> Obtained values are summarized in the ESI (Table S5†).

#### Validation of the SPE-CSIA procedure for the determination of $\delta^{13}\text{C}$ and $\delta^{15}\text{N}$ values of the target compounds in water samples

For evaluating the effect of the SPE extraction procedure on  $\delta^{13}\text{C}$  and  $\delta^{15}\text{N}$  values, standards of the target compounds of known isotope ratios were spiked into 10 L agricultural drainage water samples to give concentrations in the range of 0.5–50  $\mu\text{g L}^{-1}$ . Extraction was performed using the cartridges containing 8 g of SDB-1 and 8 g of Septra ZT. Results are shown in Fig. 3 and 4 and listed in the ESI (Table S6†). In most cases, both trueness and precision were comparable between SPE

extracts and freshly prepared standards. The SPE-CSIA method therefore induced negligible isotope fractionation, which was within the uncertainty of analysis. The deviation from the EA/IRMS values of the  $\delta^{13}\text{C}$  values for DEA and DPC and  $\delta^{15}\text{N}$  values for DPC was almost identical to the offset from the reference value measured without SPE, indicating that this deviation did not originate from the enrichment procedure. It is worth noting that precise  $\delta^{13}\text{C}$  values for DPC were obtained despite relatively low extraction efficiencies. In general, for GC/IRMS measurements of the spiked samples, proper chromatographic separation of the target compounds was achieved. Contrary to GC/IRMS, LC/IRMS measurements are more susceptible to interferences that could compromise the accuracy of isotope analysis produced by the concomitant enrichment of organic matrix. The chromatographic resolution was lower and thus there was a higher probability that analytes overlap with matrix compounds. The agricultural drainage water used in this work comes from lysimeters filled with 2.5 m arable soils, containing up to 2% organic matter, mostly in the first 70 cm.<sup>59</sup> Dissolved organic carbon (DOC) content in the water samples, measured by organic-matter combustion, ranged between 1.1 and 2.4  $\text{mg C L}^{-1}$ . Although no attempts were

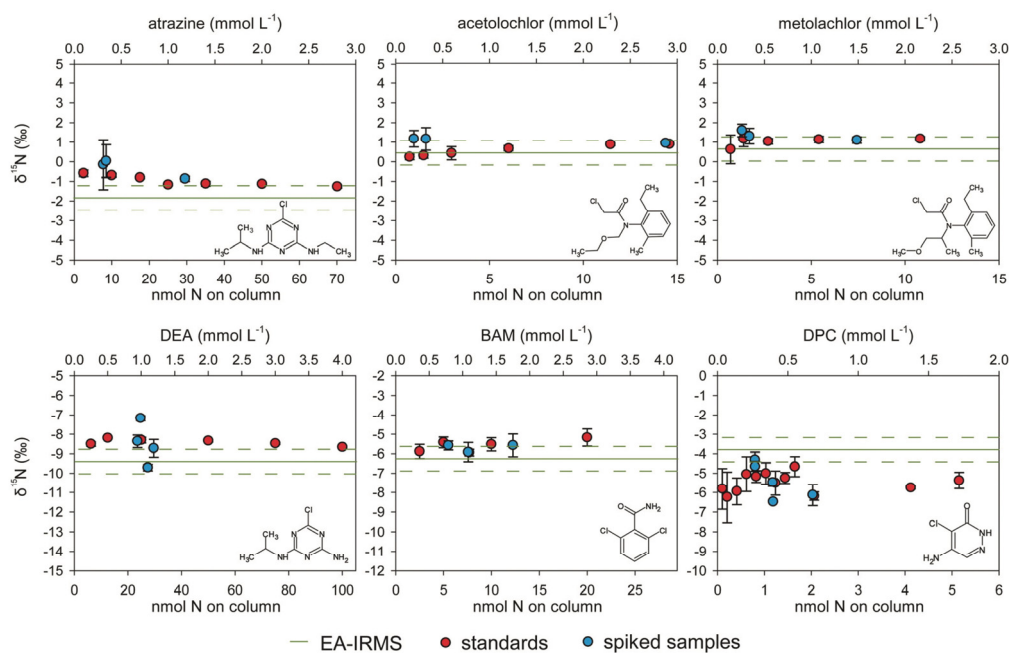


Fig. 4 Validation of the SPE-CSIA procedure for the determination of nitrogen isotope ratios of the target compounds in 10 L drainage water samples (blue circles) spiked with 0.5 to 5  $\mu\text{g L}^{-1}$  for ATR, ACETO and METO, 1.0 to 10  $\mu\text{g L}^{-1}$  for DEA and BAM, and 1.0 to 20  $\mu\text{g L}^{-1}$  for DPC. Results of the amount-dependence tests (red circles) and EA/IRMS analysis of the standards (green lines) are also shown. The error bars indicate the standard deviations of quadruplicate measurements (triplicate for DPC). The dashed lines represent the interval of  $\delta^{15}\text{N}$  measured by EA/IRMS  $\pm 1.0\%$ . The molecular structure of the target analytes is also shown.

made to characterize organic compounds of the drainage water, a high content of fulvic acids is expected.<sup>63</sup> A previous study using the same hydrophobic HC-PS-DVB sorbent with ultra-high surface area (Bakerbond SDB-1 cartridges, with a surface area of  $1060 \text{ m}^2 \text{ g}^{-1}$ ) demonstrated that fulvic acids are not retained at neutral pH and thus no co-retention/co-elution with the target pesticides occurred.<sup>52</sup> Similarly, in our study, the DOC did not interfere with CSIA analysis. Precise  $\delta^{13}\text{C}$ -DPC values were obtained even at concentrations below the instrumental limit of  $27.5 \text{ nmol C on-column}$ . Examples of resulting GC/IRMS and LC/IRMS chromatograms for both standards and spiked drainage water samples are shown in the ESI (Fig. S6†).

#### SPE-CSIA method limits for precise isotope analyses in water samples

The minimum concentrations of the target analytes in water samples necessary for precise and true isotope analysis ( $\text{Limits}_{\text{method}}$ ) were calculated following eqn (2). For calculations, extraction recoveries of 25% for DPC and 95% for the other compounds (Table 3) were applied. A reconstitution volume of  $80 \mu\text{L}$  was assumed, except for LC/IRMS analysis, for which  $150 \mu\text{L}$  was used. The obtained  $\text{Limit}_{\text{method}}$  for ATR, ACETO, METO and DEA ranged from  $0.3$  to  $0.5 \mu\text{g L}^{-1}$  for  $\delta^{13}\text{C}$  and from  $0.2$  to  $0.4 \mu\text{g L}^{-1}$  for  $\delta^{15}\text{N}$  values (Table S5, ESI†). Higher limits were obtained for BAM ( $1.6$  and  $0.8 \mu\text{g L}^{-1}$ , respectively) and DPC ( $1.2$  and  $3.2 \mu\text{g L}^{-1}$ , respectively). Consistent with these calculations, in the validation tests, accurate  $\delta^{13}\text{C}$  and  $\delta^{15}\text{N}$  values (*i.e.* deviation from bracketing standards and precision within typical uncertainties of  $\pm 0.5\%$  and  $\pm 1\%$ , respectively) were obtained for ATR, ACETO and METO at concentrations as low as  $0.5 \mu\text{g L}^{-1}$ . For DEA, the SPE-CSIA method was also validated for water samples at concentrations as low as  $0.5 \mu\text{g L}^{-1}$  for  $\delta^{13}\text{C}$ , whereas higher concentrations ( $2.5 \mu\text{g L}^{-1}$ ) were required for accurate measurements of  $\delta^{15}\text{N}$ . True results (meaning that the deviation from bracketing standards was within  $\pm 1.0\%$ ) were obtained for  $\delta^{15}\text{N}$  of BAM, although the method was only tested with environmental water samples at concentrations much above the  $\text{Limit}_{\text{method}}$  ( $4$  to  $10 \mu\text{g L}^{-1}$ ). For  $\delta^{13}\text{C}$ , however, deviation from bracketing standards (up to  $+2.2\%$ ) was higher than the typical uncertainty of  $\pm 0.5\%$ . Nevertheless, the two samples investigated at  $0.5$  and  $1 \mu\text{g L}^{-1}$ , at concentrations below  $\text{Limit}_{\text{method}}$ , resulted still in true results (deviation from bracketing standards within  $\pm 0.7\%$ ).

The accuracy of  $\delta^{15}\text{N}$  analysis of DPC was also validated at concentrations as low as  $1.0 \mu\text{g L}^{-1}$ . For  $\delta^{13}\text{C}$ -DPC for few spiked samples at concentrations close to the calculated method limit, the accuracy of LC/IRMS measurements was compromised since lower signal ( $m/z$  44) sizes than expected were obtained and/or the concomitant enrichment of organic matrix led to interferences. Nevertheless, as stated above, when amplitudes were higher than those corresponding to the  $\text{Limit}_{\text{instrument}}$ , accurate  $\delta^{13}\text{C}$ -DPC values were achieved.

## Conclusions

With this study, we validate a SPE-CSIA method for analyzing carbon and nitrogen isotope ratios of mixtures of herbicides and metabolites that commonly occur together in environmental water samples. Isotope ratios at analyte concentrations in the sub- $\mu\text{g L}^{-1}$ -range can be measured accurately with substantial pre-concentration of up to  $200\,000$ -fold. For the optimized SPE method, a hydrophobic hypercrosslinked sorbent with ultra-high surface area (SDB-1) and a polymeric sorbent chemically modified introducing polar functional groups (Septra ZT) were used to obtain an appropriate balance between selectivity and the ability to retain as many analytes as possible, covering a broad polarity range. SPE followed by CSIA enables carbon and nitrogen isotope measurements of a mixture of herbicides and metabolites with a wide range of polarity ( $K_{ow}$  from  $-0.4$  to  $3.1$ ) in agricultural drainage water.<sup>59</sup> We developed the SPE-CSIA method for compounds that frequently occur in groundwater. For common unconsolidated sand and/or gravel aquifer, the DOC concentration in groundwater tends to decrease rapidly as function of depth to the water table,<sup>64</sup> thus limiting matrix effect. Our lysimeter study<sup>59</sup> with a rather shallow layer ( $1.5 \text{ m}$ ) between the organic carbon-rich top soil and the water sampling point represents a rather unfavorable case. Thus, we expect that our method is widely applicable for groundwater. For water samples containing higher DOC contents than in our study (*e.g.* river water, groundwater from aquifers with organic deposits, waste water treatment plant influent or effluent), additional clean-up steps may be required to reduce the effect of the organic matrix and thus obtain reliable isotope measurements. Further extracts clean-up can for example be performed with preparative HPLC, a technique previously used for various pesticides.<sup>30,65,66</sup> Selective clean-up by molecularly-imprinted polymers has also recently been proposed for CSIA of enriched organic micropollutants.<sup>67</sup> The described SPE-CSIA method can also be extended to other elements, such as hydrogen, given that analytical methods have recently been validated for  $^2\text{H}/^1\text{H}$  analysis of some pesticides.<sup>18,68,69</sup> Nevertheless, a higher limit for precise isotope analysis is expected for hydrogen than for carbon, since larger amounts of hydrogen usually need to be injected.<sup>37</sup>

The method proposed in this study is an important step towards analyzing isotope ratios of pesticide mixtures in aquatic systems. Isotope fractionation during pesticide degradation has been proven at lab scale,<sup>16</sup> demonstrating the potential of CSIA for tracing transformation of these contaminants in the environment. Our study demonstrates that, despite the analytical challenges, multi-element CSIA of wide-polarity mixtures of pesticides at environmentally relevant concentrations is viable. This method will thus enable the application of CSIA to field sites for tracking pesticide sources and transformation processes.

## Conflicts of interest

There are no conflicts to declare.



## Acknowledgements

This study was supported by the project CRSII2\_141805/1 from the Swiss National Science Foundation (SNSF). The authors would like to thank the NPAC (UNiNE) and Jakov Bolotin (Eawag) for their help in the laboratory. We thank the editor and two anonymous reviewers for comments that improved the quality of the manuscript.

## References

- M. Leistra and J. J. T. I. Boesten, *Agric., Ecosyst. Environ.*, 1989, **26**, 369.
- D. W. Kolpin, E. M. Thurman and S. M. Linhart, *Arch. Environ. Contam. Toxicol.*, 1998, **35**, 385.
- D. W. Kolpin, E. M. Thurman and S. M. Linhart, *Sci. Total Environ.*, 2000, **248**, 115.
- J. E. Barbash, G. P. D. Thelin, W. Kolpin and R. J. Gilliom, *J. Environ. Qual.*, 2001, **30**, 831.
- R. Loos, G. Locoro, S. Comero, S. Contini, D. Schwesig, F. Werres, P. Balsaa, O. Gans, S. Weiss, L. Blaha, M. Bolchi and B. M. Gawlik, *Water Res.*, 2010, **44**, 4115.
- K. Fenner, S. Canonica, L. P. Wackett and M. Elsner, *Science*, 2013, **341**, 752.
- D. Hunkeler, R. U. Meckenstock, B. Sherwood Lollar, T. Schmidt, J. Wilson, T. Schmidt and J. Wilson, A guide for assessing biodegradation and source identification of organic ground water contaminants using compound specific isotope analysis (CSIA), PA 600/R-08/148, US EPA, Oklahoma, USA, 2008.
- T. B. Hofstetter, R. P. Schwarzenbach and S. M. Bernasconi, *Environ. Sci. Technol.*, 2008, **42**, 7737.
- M. Elsner, A. Jochmann, T. B. Hofstetter, D. Hunkeler, A. Bernstein, T. C. Schmidt and A. Schimmelmann, *Anal. Bioanal. Chem.*, 2012, **403**, 2471.
- M. Braeckvelt, A. Fischer and M. Kästner, *Appl. Microbiol. Biotechnol.*, 2012, **94**, 1401.
- M. Elsner, *J. Environ. Monit.*, 2010, **12**, 2005.
- T. B. Hofstetter and M. Berg, *TrAC, Trends Anal. Chem.*, 2011, **30**, 618.
- C. Vogt, C. Dorer, F. Musat and H.-H. Richnow, *Curr. Opin. Biotechnol.*, 2016, **41**, 90.
- I. Nijenhuis, J. Renpenning, S. Kümmel, H.-H. Richnow and M. Gehre, *Trends Environ. Anal. Chem.*, 2016, **11**, 1.
- J. Masbou, G. Drouin, S. Payraudeau and G. Imfeld, *Chemosphere*, 2018, **213**, 368.
- M. Elsner and G. Imfeld, *Curr. Opin. Biotechnol.*, 2016, **41**, 60.
- H. Penning and M. Elsner, *Anal. Chem.*, 2007, **79**, 8399.
- A. E. Hartenbach, T. B. Hofstetter, P. R. Tentscher, S. Canonica, M. Berg and R. P. Schwarzenbach, *Environ. Sci. Technol.*, 2008, **42**, 7751.
- A. H. Meyer, H. Penning, H. Lowag and M. Elsner, *Environ. Sci. Technol.*, 2008, **42**, 7757.
- S.-L. Badea, C. Vogt, S. Weber, A.-F. Danet and H.-H. Richnow, *Environ. Sci. Technol.*, 2009, **43**, 3155.
- S. Reinnicke, A. Bernstein and M. Elsner, *Anal. Chem.*, 2010, **82**, 2013.
- S.-L. Badea, C. Vogt, M. Gehre, A. Fischer, A.-F. Danet and H.-H. Richnow, *Rapid Commun. Mass Spectrom.*, 2011, **25**, 363.
- S. Reinnicke, A. Simonsen, S. R. Sørensen, J. Aamand and M. Elsner, *Environ. Sci. Technol.*, 2012, **46**, 1447.
- N. Milosevic, S. Qiu, M. Elsner, F. Einsiedl, M. P. Maier, H. K. V. Bensch, H. J. Albrechtsen and P. L. Bjerg, *Water Res.*, 2013, **47**, 637.
- O. F. Elsayed, E. Maillard, S. Vuilleumier, I. Nijenhuis, H. H. Richnow and G. Imfeld, *Chemosphere*, 2014, **99**, 89.
- N. Ivdrá, S. Herrero-Martín and A. Fischer, *J. Chromatogr. A*, 2014, **1355**, 36.
- L. Wu, J. Yao, P. Trebse, N. Zhang and H.-H. Richnow, *Chemosphere*, 2014, **111**, 458.
- E. O. Mogusu, J. B. Wolbert, D. M. Kujawinski, M. A. Jochmann and M. Elsner, *Anal. Bioanal. Chem.*, 2015, **407**, 5249.
- X. Tang, Y. Yang, W. Huang, M. B. McBride, J. Guo, R. Tao and Y. Dai, *Bioresour. Technol.*, 2017, **233**, 264.
- K. Schreglmann, M. Hoeche, S. Steinbeiss, S. Reinnicke and M. Elsner, *Anal. Bioanal. Chem.*, 2013, **405**, 2857.
- S. Bashir, K. L. Hitzfeld, M. Gehre, H. H. Richnow and A. Fischer, *Water Res.*, 2015, **71**, 187.
- S. R. Lutz, Y. V. D. Velde, O. F. Elsayed, G. Imfeld, M. Lefrancq, S. Payraudeau and B. M. van Breukelen, *Hydrol. Earth Syst. Sci.*, 2017, **21**, 5243.
- Y. Liu, S. Bashir, R. Stollberg, R. Trabitzzsch, H. Weiß, H. Paschke, I. Nijenhuis and H.-H. Richnow, *Environ. Sci. Technol.*, 2017, **51**, 8909.
- P. Alvarez-Zaldívar, S. Payraudeau, F. Meite, J. Masbou and G. Imfeld, *Water Res.*, 2018, **139**, 198.
- A. Melsbach, V. Ponsin, C. Torrentó, C. Lihl, T. B. Hofstetter, D. Hunkeler and M. Elsner, *Anal. Chem.*, 2019, **91**, 3412.
- ISO 5. 5725-1. Accuracy [Trueness and Precision] of Measurement Methods and Results, Part 1: General Principles and Definitions, International Standard Organization, Geneva, 1994.
- T. C. Schmidt and M. A. Jochmann, *Annu. Rev. Anal. Chem.*, 2012, **5**, 133.
- M. Blessing, M. A. Jochmann and T. C. Schmidt, *Anal. Bioanal. Chem.*, 2008, **390**, 591.
- N. Masqué, R. M. Marcé and F. Borrull, *TrAC, Trends Anal. Chem.*, 1998, **17**, 384.
- H. Sabik, R. Jeannot and B. Rondeau, *J. Chromatogr. A*, 2000, **885**, 217.
- N. Fontanals, R. M. Marcé and F. Borrull, *J. Chromatogr. A*, 2007, **1152**, 14.
- B. Buszewski and M. Szultka, *Crit. Rev. Anal. Chem.*, 2012, **42**, 198.
- H. Sabik and R. Jeannot, *J. Chromatogr. A*, 1998, **818**, 197.
- S. Weigel, K. Bester and H. Hühnerfuss, *J. Chromatogr. A*, 2001, **912**, 151.
- A. Hildebrandt, S. Lacorte and D. Barceló, *Anal. Bioanal. Chem.*, 2007, **387**, 1459.

- 46 V. Matamoros, E. Jover and J. M. Bayona, *Anal. Chem.*, 2010, **82**, 699.
- 47 T. B. Huff and G. D. Foster, *J. Environ. Sci. Health, Part B*, 2011, **46**, 723.
- 48 C. Valls-Cantenys, M. Scheurer, M. Iglesias, F. Sacher, H.-J. Brauch and V. Salvadó, *Anal. Bioanal. Chem.*, 2016, **408**, 6189.
- 49 L. T. D. Cappelini, D. Cordeiro, S. H. G. Brondi, H. R. Prieto and E. M. Vieira, *Environ. Technol.*, 2012, **33**(20), 2299.
- 50 S. Y. Panshin, D. S. Carter and E. R. Bayless, *Environ. Sci. Technol.*, 2000, **34**, 2131.
- 51 A. Junker-Buchheit and M. Witznabacher, *J. Chromatogr. A*, 1996, **737**, 67.
- 52 V. Pichon, C. Cau-Dit-Coumes, L. Chen, S. Guenu and M. C. Hennion, *J. Chromatogr. A*, 1996, **737**, 25.
- 53 N. J. Schatz, *PhD Thesis*, Karlsruhe Institute of Technology, Karlsruhe, 2012.
- 54 G. Buttiglieri, M. Peschka, T. Frömel, J. Müller, F. Malpei, P. Seel and T. P. Knepper, *Water Res.*, 2009, **43**, 2865.
- 55 R. A. Yokley, L. C. Mayer, S.-B. Huang and J. D. Vargo, *Anal. Chem.*, 2002, **74**, 3754.
- 56 E. Porazzi, M. P. Martinez and F. E. Benfenati, *Talanta*, 2005, **68**, 146.
- 57 G. G. Jensen, E. Björklund, A. Simonsen and B. Halling-Sørensen, *J. Chromatogr. A*, 2009, **1216**, 5199.
- 58 S.-L. McManus, M. Moloney, K. G. Richards, C. E. Coxon and M. Danaher, *Molecules*, 2014, **19**, 20627.
- 59 C. Torrentó, V. Prasuhn, E. Spiess, V. Ponsin, A. Melsbach, C. Lihl, G. Glauser, T. B. Hofstetter, M. Elsner and D. Hunkeler, *Vadose Zone J.*, 2018, **17**, 170033.
- 60 S. Spahr, S. Huntscha, J. Bolotin, M. P. Maier, M. Elsner, J. Hollender and T. B. Hofstetter, *Anal. Bioanal. Chem.*, 2013, **405**, 2843.
- 61 M. A. Jochmann, M. Blessing, S. B. Haderlein and T. C. Schmidt, *Rapid Commun. Mass Spectrom.*, 2006, **20**, 3639.
- 62 A. L. Sessions, *J. Sep. Sci.*, 2006, **29**, 1946.
- 63 R. Artinger, G. Buckau, S. Geyer, P. Fritz, M. Wolf and J. I. Kim, *Appl. Geochem.*, 2000, **15**, 97.
- 64 W. J. Pabich, I. Valiela and H. F. Hemond, *Biogeochemistry*, 2001, **55**, 247.
- 65 H. Penning, S. R. Sørensen, A. H. Meyer, J. Aamand and M. Elsner, *Environ. Sci. Technol.*, 2010, **44**, 2372.
- 66 H. K. V. Schürner, M. P. Maier, D. Eckert, R. Brejcha, C.-C. Neumann, C. Stumpp, O. A. Cirpka and M. Elsner, *Environ. Sci. Technol.*, 2016, **50**, 5729.
- 67 R. Bakkour, J. Bolotin, B. Sellergren and T. B. Hofstetter, *Anal. Chem.*, 2018, **90**, 7292.
- 68 L. Wu, S. Kümmel and H. H. Richnow, *Anal. Bioanal. Chem.*, 2017, **409**, 2581.
- 69 J. Renpenning, S. Kümmel, K. L. Hitzfeld, A. Schimmelmann and M. Gehre, *Anal. Chem.*, 2015, **87**, 9443.

## C. Supporting Information of Chapter 3

## C.1. Formation and Transformation of Desphenylchloridazon

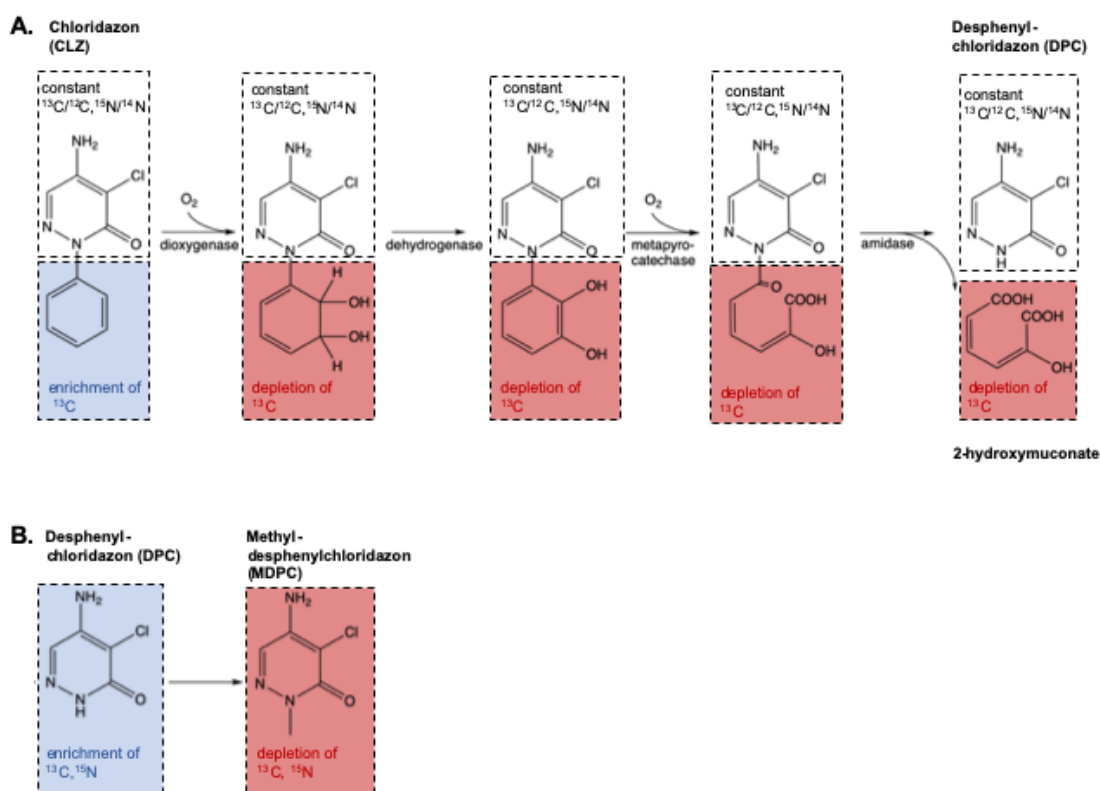


Figure C1: A. Formation of DPC, where the newly formed DPC is expected to contain equally or lower  $^{13}\text{C}/^{12}\text{C}$  isotope ratio than its precursor CLZ; B. Transformation of DPC, where carbon and nitrogen isotope effects are expected (primary isotope effect); Reactive groups in CLZ and DPC for which isotope enrichment is expected compared to their initial isotope value are indicated in blue, while isotope depletion (which is expected for the formed MDPC and for 2-hydroxymuconate formed from the phenyl ring of CLZ) is indicated by red boxes; adapted from Lingens et al.<sup>86</sup> and Roberts et al.<sup>88</sup>

## C.2. Materials and Methods

## C.2.1. Chemicals

For experiments and isotope analysis, CLZ (5-Amino-4-chloro-2-phenylpyridazin-3(2H)-one, CAS no. 1698-60-8) was purchased from Cfm Oskar Tropitzsch GmbH (purity n.a., Marktredwitz, Germany), DPC (5-Amino-4-chloro-3-pyridazinone, CAS no.: 6339-19-1) was kindly provided from BASF (99.8%, Limburgerhof, Germany) and MDPC (5-amino-4-chloro-2-methyl-3(2H)-pyridazinone, CAS no.: 17254-80-7) was supplied by LGC Standards GmbH (Wesel, Germany). (Trimethylsilyl)diazomethane, 2.0 M dissolved in diethyl ether (CAS no.:

### C. Supporting Information of Chapter 3

---

18107-18-1, acute toxicity and health hazardous), sodium persulfate ( $\geq 99.9\%$ , CAS no.: 7775-27-1) and phosphoric acid ( $\geq 85\%$ , CAS no.: 7664-38-2) were obtained from Sigma Aldrich (Merck KGaA, Darmstadt, Germany), while methanol ( $\geq 99.9\%$ , CAS no.: 67-56-1) and acetone ( $\geq 99.9\%$ , CAS no.: 67-64-1) were received from Roth (Karlsruhe, Germany). Ethyl acetate ( $\geq 99.9\%$ , CAS no.: 141-78-6) was supplied by Honeywell (Burdick & Jackson, Muskegon, USA). Ultrapure water was derived from a Millipore DirectQ apparatus (Millipore, Bedford, MA, USA). Empty polyethylene cartridges (6 mL and 60 mL) and matching polyethylene frits (20- $\mu\text{m}$  pore size) were obtained from Grace (Columbia, SC, USA). Bakerbond SDB-1 sorbent was supplied by J.T. Baker (Phillipsburg, NJ, USA), whereas the Septra ZT sorbent was received from Phenomenex (Torrance, CA, USA). For concentration analysis, Pestanal-quality CLZ and terbuthylazine (CAS no.: 5915-41-3) standards were purchased from Sigma-Aldrich (Seelze, Germany). Certified standards of DPC, M-DPC and chloridazon- $\text{d}_5$  (CAS no.: 1346818-99-4) were purchased from Dr. Ehrenstorfer GmbH (Wesel, Germany).

C.2.2. Lysimeter Facility Set-Up

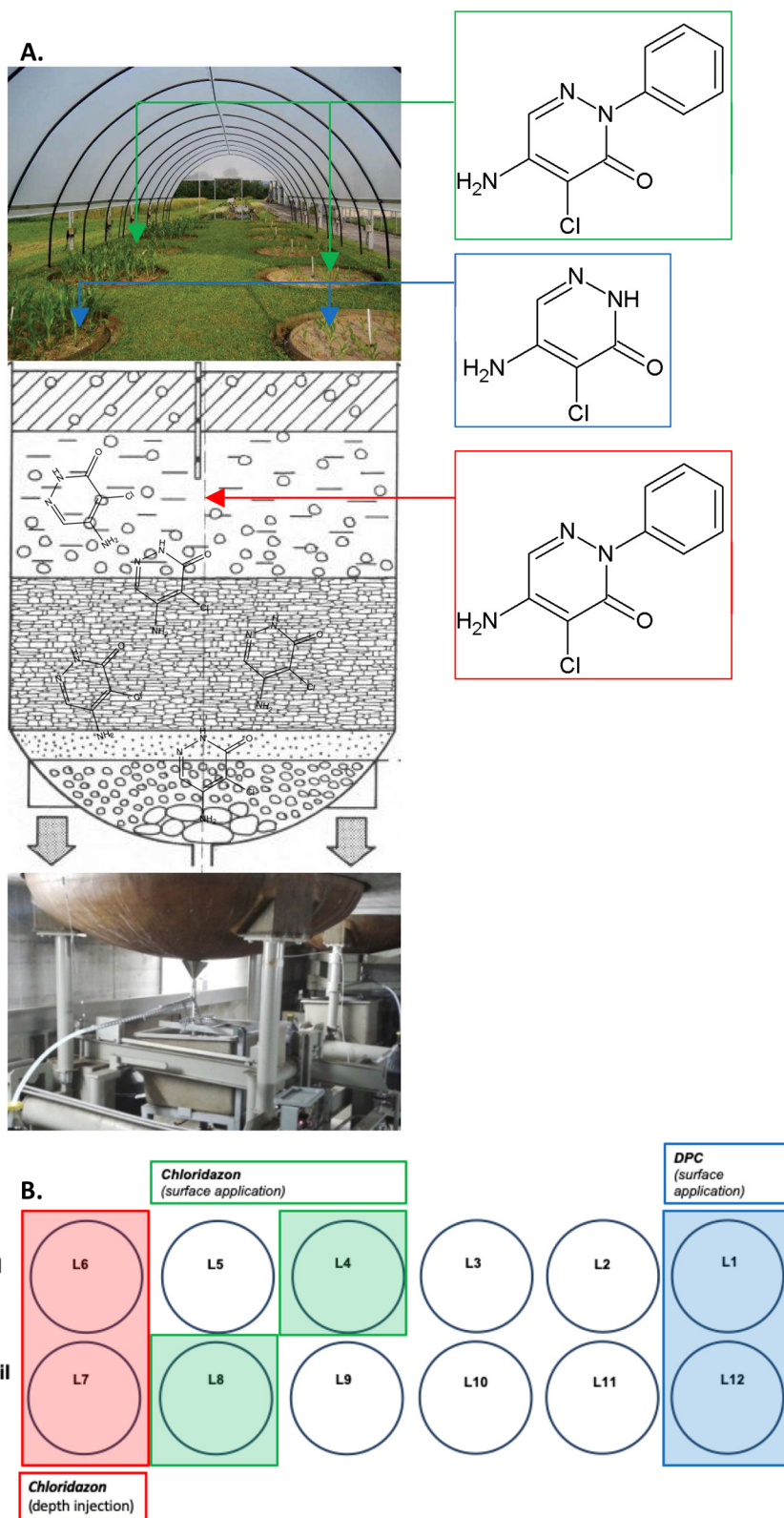


Figure C2: A. Facility and B. lysimeter set-up used for the lysimeter field study provided by Agroscope, pictures adapted from Reckenholtz<sup>186, 187</sup>

### C. Supporting Information of Chapter 3

Table C1: Main properties of the two lysimeter soils as described by Torrentó et al.<sup>103</sup>

Soil Horizon	Depth [cm]	Organic Matter [%]	Size Distribution of Mineral Particles [%]		
			Clay	Silt	Sand
<b>Gravel Soil</b>					
<b>A<sub>p</sub></b>	0 - 50	1.7	20	23	57
<b>B<sub>1</sub></b>	50 - 60	0.9	27	20	64
<b>B<sub>2</sub></b>	60 - 70	1.1	19	24	57
<b>B<sub>3</sub></b>	70 - 100		20	24	57
<b>B<sub>4</sub></b>	110 - 120		19	21	60
<b>C</b>	120 - 135		17	18	65
<b>C</b>	Sandy alluvial deposits				
<b>Moraine Soil</b>					
<b>A<sub>p</sub></b>	0 - 50	2.1	22	34	44
<b>B<sub>1</sub></b>	50 - 70	1.5	23	35	43
<b>B<sub>2</sub></b>	70 - 90	0.4	22	38	40
<b>B<sub>3</sub></b>	90 - 110		20	40	40
<b>B<sub>4</sub></b>	110 - 140		21	42	37
<b>C</b>	140 - 160		20	41	38
<b>C</b>	Loamy moraine deposits				

**C.2.3. Application Details of Chloridazon and Desphenylchloridazon**

Table C2: DPC and CLZ and tracer application to the lysimeters (L) and heavy irrigation events (30-50 mm at 1 mm/min) during the period of monitoring. Although not shown here, regular low-intensity irrigation events (5-20 mm once a week at 0.2 mm/min) were also applied. Sowing and harvest dates are also shown. The following winter covers were used: stubbles (2014), bare fallow (2015) and stubbles (2016 and 2017)

Date	DPC / CLZ Application	Heavy Irrigation [mm]
<b><i>12-05-2014 Corn sowing</i></b>		
14-05-2014	-	30 mm
12-06-2014	CLZ depth injection (L6, L7): 2.0 g per lysimeter + uranine (0.41 g per lysimeter)	40-55 mm
28-07-2014	-	40 mm
31-07-2014	-	30-35 mm
<b><i>10-09-2014 Corn harvesting</i></b>		
10-09-2014	-	40 mm
15-09-2014	-	40 mm
24-02-2015	-	30 mm
<b><i>25-03-2015 Sugar beet sowing</i></b>		
06-05-2015	CLZ surface application (L4, L8): 3.0 kg/ha + uranine (1.3 kg/ha) DPC surface application (L1, L12): 3.2 kg/ha + uranine (1.3 kg/ha) and NaBr (500 kg/ha)	50 mm
21-05-2015	-	55 mm
03-08-2015	-	30 mm
10-08-2015	-	45 mm
07-10-2015	-	40 mm
12-10-2015	-	40 mm
<b><i>13-11-2015 Sugar beet harvesting</i></b>		
<b><i>12-05-2016 Corn sowing</i></b>		
28-06-2016	-	50 mm
04-07-2016	-	50 mm
<b><i>14-09-2016 Corn harvesting</i></b>		
31-10-2016	-	50 mm
07-11-2016	-	50 mm
07-03-2017	-	30 mm

C. Supporting Information of Chapter 3

<b>Date</b>	<b>DPC / CLZ Application</b>	<b>Heavy Irrigation [mm]</b>
09-03-2017	-	40 mm
<i>18-04-2017 Broccoli (L1,L4,L6) and Chinese cabbage (L12,L8,L7) planting</i>	-	-
<i>20-06-2017 Broccoli and Chinese cabbage harvesting</i>	-	-
10-07-2017	-	40 mm
<i>11-07-2017 Lettuce (L1,L4,L6) and leek Allium (L12,L8,L7) planting</i>	-	-
<i>22-08-2017 Lettuce harvesting</i>	-	-
<i>23-08-2017 Lettuce (L1,L4,L6) planting</i>	-	-
02-09-2017	-	40 mm
<i>30-10-2017 Lettuce harvesting</i>	-	-
<i>09-11-2017 Leek harvesting</i>	-	-



**C.2.4. UHPLC-MS/MS Parameters****Table C3: Optimized compound dependent MS/MS parameters. Other source and collision cell parameters were set as follows: ion spray (IS) voltage +5.5 kV, gas temperature (TEM) 500 °C, nebulizing gas (GS1) 60 psi, drying gas (GS2) 40 psi, curtain gas (CUR) 15 psi**

Compound	Retention time [min]	Precursor [m/z]	Fragment [m/z]	DP [V]	EP [V]	CE [V]	CXP [V]	Dwell time [ms]
CLZ (Q)	5.99	222.1	104.0	96	10	33	6	75
CLZ (q)	5.99	222.1	77.0	96	10	53	4	75
DPC (Q)	1.12	146.0	117.0	76	10	37	8	75
DPC (q)	1.12	146.0	66.0	81	10	55	4	75
M-DPC (Q)	1.96	160.0	117.0	81	10	33	8	75
M-DPC (q)	1.96	160.0	88.0	86	10	45	6	75
CLZ-d <sub>5</sub> (Q)	5.97	227.0	108.0	96	10	39	6	75
CLZ-d <sub>5</sub> (q)	5.97	227.0	81.0	91	10	55	4	75

Q: quantification ion; q: qualification ion; DP: declustering potential; EP: entrance potential; CE: collision energy; CXP: collision cell exit potential

**C.2.5. UHPLC-QTOF-MS method**

An Acquity UPLC™ system was coupled with a Synapt G2 QTOF-MS (Waters). A guard column (5 mm × 2.1 mm, 1.7 μm) and Acquity UPLC BEH C18 column (50 mm × 2.1 mm, 1.7 μm, Waters) were used at a flow rate of 0.4 mL/min in gradient mode. The mobile phase consisted of water (incl. formic acid 0.05 %) and acetonitrile (ACN) containing 0.05 % formic acid. The gradient method started at 2 % ACN/formic acid and was increased linearly to 65 % within 4.5 min. Subsequently, the gradient was increased to 100 % within 1 min, held for 1 min and re-set to 2 % for re-equilibration. The analytes were quantified based on peak area ratios using terbuthylazine as an internal standard. The quantifier ions for CLZ, DPC and MDPC were 222.039, 146.012 and 160.028, respectively.

**C.2.6. Large Volume Solid-Phase Extraction According to Torrentó et al.<sup>62</sup>**

For isotope analysis, all lysimeter samples were filtered through 0.7 μm glass fiber filters and were concentrated by SPE using the method described in Torrentó et al.<sup>62</sup>, Shortly, hand-filled 60 mL polyethylene cartridges packed with 8 g of Bakerbond SDB-1 sorbent and 8 g of Septra ZT sorbent were rinsed with 60 mL ethyl acetate (EtAc), conditioned with 60 mL methanol and 60 mL ultrapure water. Subsequently, sample volumes between 1 and 11 L were extracted

### C. Supporting Information of Chapter 3

---

at a flow rate of 5 mL/min. Each cartridge was then washed with 60 mL ultrapure water. To remove residual water, all cartridges were dried under vacuum overnight. The analytes were then eluted with 120 mL EtAc and the extracts were finally evaporated until dryness using a CentriVap Benchtop vacuum concentrator (Labconco, Kansas City, MO, USA). Each dry extract was reconstituted in several steps. The final reconstitution volume and solvent varied depending on the isotope analysis method. For carbon isotope analysis, samples were reconstituted in 0.1 mL to 2.5 mL ultrapure water, while in preparation for nitrogen isotope analysis, each sample was reconstituted in 1 mL methanol.

#### C.2.7. Preparative HPLC

As already described by Melsbach et al.<sup>118</sup>, SPE extracts were reconstituted in 800  $\mu$ L ultrapure water/ACN (90/10 v/v) and manually injected into a Shimadzu UHPLC-DAD (Nexera XR, LC-20AD XR) equipped with a Synergi 4  $\mu$ m Hydro-RP 80 Å (100 mm x 4.6  $\mu$ m; Phenomenex, Aschaffenburg, Deutschland). The oven was set to a temperature of 35 °C. A 0.5 mM KH<sub>2</sub>PO<sub>4</sub> buffer at pH 7 and ACN were used as mobile phases. At a flow rate of 1.0 mL/min, a gradient method was used for peak separation. The proportion of ACN was 1 % for 2 min, was linearly increased to 10 % within 4 min (held for 0 minutes) was again linearly increased to 50 % within 3 minutes (held for 2 min) before a finally linear increase to 75 % within 9 min (held for 2 min). At the end of the run, the proportion of ACN was decreased to 1 % again (held for 5 min). The absorbance of the detector was set to 210 nm. DPC-containing fractions were collected from 1.8 min to 7.0 min and MDPC-containing fractions from 7.0 min to 11.0 min. Subsequently, the fractions were evaporated until dryness by freeze-drying. Afterwards, the fraction containing MDPC was reconstituted in 50  $\mu$ L acetone, while the DPC fraction was prepared for derivatization by reconstituting the sample in 1 mL methanol.

#### C.2.8. Elemental-Analyzer Isotope Ratios used for Correction Procedure

Table C4: Isotope ratios of <sup>13</sup>C and <sup>15</sup>N of selected compounds used for isotope correction determined by EA-IRMS; measurement uncertainty is shown as standard deviation (SD) of n=5 measurements

Standard	$\delta^{13}\text{C} \pm \text{SD} [\text{‰}]$	$\delta^{15}\text{N} \pm \text{SD} [\text{‰}]$
Desphenylchloridazon	$-17.84 \pm 0.05$	$-3.81 \pm 0.04$
Methyl-desphenylchloridazon	$-21.17 \pm 0.06$	$+0.99 \pm 0.12$

**C.2.9. Calculation of Analyte Recovery from the Lysimeter Drainage Water**

The balance between the applied/injected mass and the total recovered mass  $\%Re_{total}$  (i.e. sum of the recovered masses of the applied/injected compound and its metabolite(s)) is based on the cumulative recovery  $\%Re_{Compound}$  of CLZ, DPC and DPC from the drainage water according to equations C1 and C2:

$$\%Re_{Compound} = \frac{\sum_0^n c_{detected} \times V_{drainage\ water}}{m_{analyte\ applied}} \times 100 \quad (C1)$$

$$\%Re_{total} = \sum \%Re_{CLZ} + \%Re_{DPC} + \%Re_{MDPC} \quad (C2)$$

where  $n$  is the time of monitoring (days),  $c_{detected}$  is the analyte concentration measured in the drainage water of the particular date,  $V_{drainage\ water}$  is the corresponding volume of the drainage water eluting from the lysimeter and  $m_{analyte\ applied}$  is the mass of the analyte (DPC or CLZ) applied/injected on the lysimeter. The mass balance was considered incomplete when  $\%Re_{total}$  differs from 100%. When possible, analyte mass retained in the first layer of the soil was also considered for the mass balance. To this end, the percentage of retained analyte was calculated from concentration measurements in soil samples assuming (i) homogenous areal distribution of the analytes, and (ii) that the first 10 cm soil layer corresponds to 408 kg of soil (using a bulk density of approximately 1.3 g/cm<sup>3</sup> for the topsoil).

**C.3. Results**









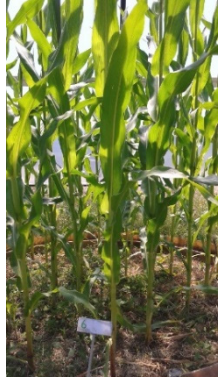



**C.3.1. Water balance**

**Table C5: Average monthly sums (in mm) of the water-balance components from the two soil types during 2014, 2015, 2016 and 2017: irrigation (I), drainage (D), change in soil water storage ( $\Delta$ SW<sub>S</sub>), and evapotranspiration (ET).**













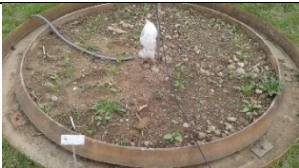

















	2014								2016							
	Gravel				Moraine				Gravel				Moraine			
	I	D	$\Delta$ SW <sub>S</sub>	ET	I	D	$\Delta$ SW <sub>S</sub>	ET	I	D	$\Delta$ SW <sub>S</sub>	ET	I	D	$\Delta$ SW <sub>S</sub>	ET
<b>Jan</b>	60	70	-1	0	60	68	-4	0	33	20	2	10	32	12	7	13
<b>Feb</b>	74	62	12	1	74	60	15	4	26	9	0	17	27	6	3	17
<b>Mar</b>	7	39	-60	29	8	37	-66	36	50	14	6	30	50	9	6	35
<b>Apr</b>	86	12	10	65	89	12	5	72	54	22	-7	39	53	17	-9	45
<b>May</b>	111	13	14	84	97	2	23	72	18	12	-19	26	18	10	-19	27
<b>Jun</b>	167	117	-51	102	187	126	-40	101	88	15	18	56	88	7	22	59
<b>Jul</b>	86	11	-3	78	89	9	0	80	115	41	-92	166	112	36	-103	178
<b>Aug</b>	91	19	-34	106	94	15	-27	105	60	4	-73	128	59	1	-83	141
<b>Sep</b>	123	14	49	60	126	18	51	58	27	1	-8	34	28	0	-16	43
<b>Oct</b>	32	8	9	16	32	11	7	15	73	0	56	16	73	0	53	19
<b>Nov</b>	30	4	13	13	30	7	7	15	160	21	125	13	158	5	134	18
<b>Dec</b>	68	39	4	24	65	45	1	19	0	15	-23	8	0	2	-14	12
<b>Total</b>	936	407	-38	577	950	409	-27	578	704	175	-15	544	697	108	-18	607
	2015								2017							
	Gravel				Moraine				Gravel				Moraine			
	I	D	$\Delta$ SW <sub>S</sub>	ET	I	D	$\Delta$ SW <sub>S</sub>	ET	I	D	$\Delta$ SW <sub>S</sub>	ET	I	D	$\Delta$ SW <sub>S</sub>	ET
<b>Jan</b>	27	14	-2	16	29	11	1	17	0	4	-5	3	0	2	-3	3
<b>Feb</b>	60	23	18	19	63	28	16	20	16	2	5	9	16	1	3	12
<b>Mar</b>	49	30	-12	31	52	30	-10	32	60	36	1	24	64	24	15	26
<b>Apr</b>	52	12	-3	43	52	9	-3	46	26	7	6	12	22	8	5	10
<b>May</b>	172	109	-8	71	164	104	-6	66	31	15	-34	50	31	12	-39	58
<b>Jun</b>	28	13	-80	95	27	10	-88	104	56	7	-40	88	62	3	-1	59
<b>Jul</b>	74	5	-38	108	73	2	-45	116	95	5	73	18	95	15	60	20
<b>Aug</b>	107	12	7	88	111	12	6	92	50	14	-17	53	42	36	-44	51
<b>Sep</b>	114	16	42	57	112	12	33	67	87	64	26	2	87	31	20	36
<b>Oct</b>	112	24	58	30	112	9	59	45	19	15	-3	7	16	5	-30	41
<b>Nov</b>	29	10	2	17	26	4	6	15	69	51	31	0	73	6	66	1
<b>Dec</b>	36	20	6	11	35	8	15	12	71	107	6	0	80	122	10	0
<b>Total</b>	861	287	-11	585	855	240	-18	633	581	327	48	266	588	266	61	315

**C.3.2. Vegetation cover**

No attempts were made to estimate the percentage of each lysimeter area covered by vegetation since no significant differences in the evolution with time of the plants development between the two soil types or between the two pesticide application methods were observed. In the lysimeters with DPC application (L1 and L12), most of the sugar beet plants died and thus the vegetation cover was much lower in these two lysimeters compared to the lysimeters with CLZ application. Figure S3 shows pictures of the evolution of the vegetation cover on selected lysimeters and dates. The effect of vegetation cover on DPC leaching and isotope fractionation was thus not assessed.

Lysimeters with CLZ application		Lysimeters with CLZ injection		Lysimeters with DPC application	
Gravel soil (L4)	Moraine soil (L8)	Gravel soil (L6)	Moraine soil (L7)	Gravel soil (L1)	Moraine soil (L12)
					
327 days before CLZ application (13.06.2014)	327 days before CLZ application (13.06.2014)	1 day after CLZ injection (13.06.2014)	1 day after CLZ injection (13.06.2014)	327 days before DPC application (13.06.2014)	327 days before DPC application (13.06.2014)
					
292 days before CLZ application (18.07.2014)	292 days before CLZ application (18.07.2014)	36 days after CLZ injection (18.07.2014)	36 days after CLZ injection (18.07.2014)	292 days before DPC application (18.07.2014)	292 days before DPC application (18.07.2014)



					
238 days before CLZ application <b>(10.09.2014)</b>	238 days before CLZ application <b>(10.09.2014)</b>	90 days after CLZ injection <b>(10.09.2014)</b>	90 days after CLZ injection <b>(10.09.2014)</b>	238 days before DPC application <b>(10.09.2014)</b>	238 days before DPC application <b>(10.09.2014)</b>
					
Corn harvesting, 238 days before CLZ application <b>(10.09.2014)</b>	Corn harvesting, 238 days before CLZ application <b>(10.09.2014)</b>	Corn harvesting, 90 days after CLZ injection <b>(10.09.2014)</b>	Corn harvesting, 90 days after CLZ injection <b>(10.09.2014)</b>	Corn harvesting, 238 days before DPC application <b>(10.09.2014)</b>	Corn harvesting, 238 days before DPC application <b>(10.09.2014)</b>
					
6 days before CLZ application <b>(30.04.2015)</b>	6 days before CLZ application <b>(30.04.2015)</b>	322 days after CLZ injection <b>(30.04.2015)</b>	322 days after CLZ injection <b>(30.04.2015)</b>	6 days before DPC application <b>(30.04.2015)</b>	6 days before DPC application <b>(30.04.2015)</b>
					
9 days after CLZ application <b>(15.05.2015)</b>	9 days after CLZ application <b>(15.05.2015)</b>	337 days after CLZ injection <b>(15.05.2015)</b>	337 days after CLZ injection <b>(15.05.2015)</b>	9 days after DPC application <b>(15.05.2015)</b>	9 days after DPC application <b>(15.05.2015)</b>
					
14 days after CLZ application <b>(20.05.2015)</b>	14 days after CLZ application <b>(20.05.2015)</b>	342 days after CLZ injection <b>(20.05.2015)</b>	342 days after CLZ injection <b>(20.05.2015)</b>	14 days after DPC application <b>(20.05.2015)</b>	14 days after DPC application <b>(20.05.2015)</b>



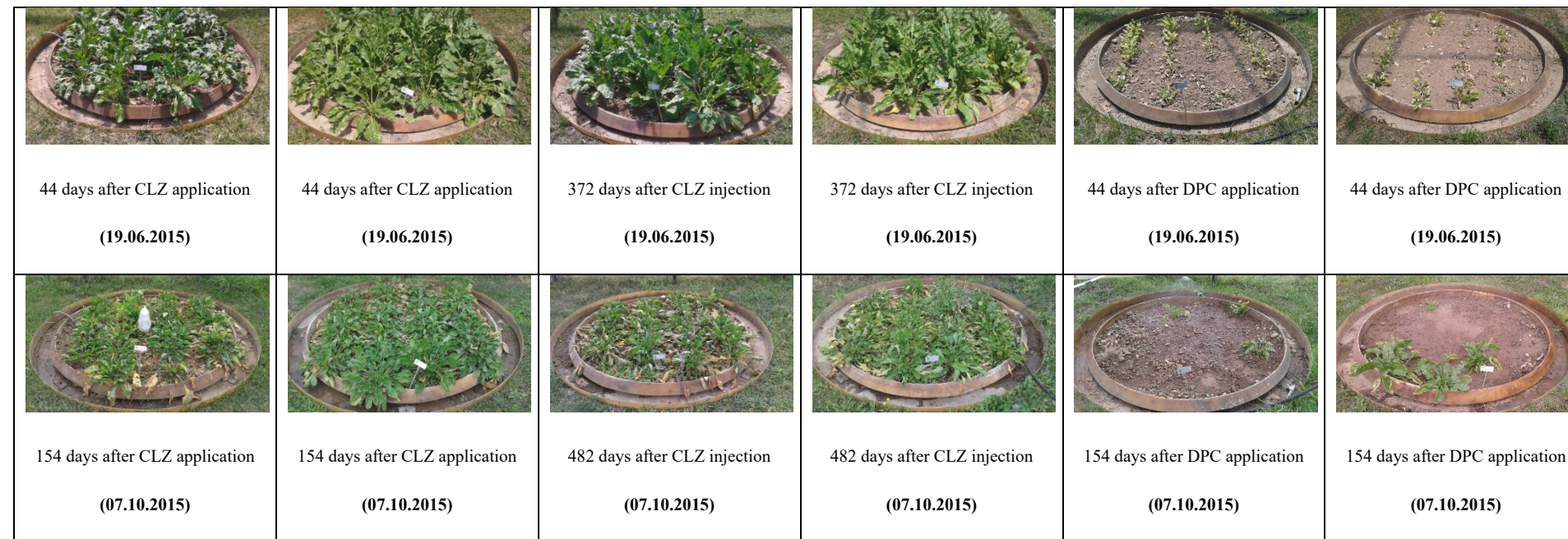


Figure C3: Changes with time in the vegetation cover of the lysimeters with CLZ application (left panels), the lysimeters with CLZ injection (middle panels) and the lysimeters with DPC application (right panels)





### C.3.3. Analytes breakthrough and recovery

Table C6: Observed breakthrough parameters and recoveries for chloridazon (CLZ), desphenylchloridazon (DPC), bromide (BR), and uranine (UR) in the six lysimeters used in this study. Time and cumulative drainage values correspond to days passed and millimeters accumulated since application or injection, respectively. Maximum concentrations are shown as the absolute and normalized by the applied or injected mass ( $C/M_{\text{applied}}$ ) values. Details about the calculation of analyte recovery can be found on section II.9. Note that bromide was only applied in lysimeters with DPC application. DPC data are also shown for lysimeters with CLZ application or injection for comparison (in grey). \*: incomplete series, bql: below quantification limit ( $0.05 \mu\text{g/L}$  for UR and  $10 \mu\text{g/L}$  for BR). Details about analytical methods for determining tracer concentrations can be found in Torrentó et al.<sup>62</sup>

DPC surface application	gravel soil (L1)			moraine soil (L12)		
	DPC	BR	UR	DPC	BR	UR
time of first arrival [d]	137	0.2	bql	15	0.4	0.4
time of peak concentration [d]	566	180	bql	425	354	0.4
maximum concentration [ $\mu\text{g/L}$ ]	97	118020	bql	8.3	57400	bql
maximum concentration, $C/M_{\text{applied}}$	9.7E-05	9.7E-01	-	8.2E-06	4.7E-01	-
cumulative drainage at peak concentration [mm]	458	260	-	303	269	-
time of total recovery [d]	930	352*	566	939	354*	425
total recovery [%]	5.9	47.3*	0.001	0.3	10.5*	0.002
	No early breakthrough			No early breakthrough		

CLZ surface application	gravel soil (L4)			moraine soil (L8)		
	CLZ	DPC	UR	CLZ	DPC	UR
time of first arrival [d]	595	427	bql	425	425	0.1
time of peak concentration [d]	595	847	bql	425	889	0.1
maximum concentration [ $\mu\text{g/L}$ ]	0.09	17.2	bql	0.23	5.64	3.55
maximum concentration, $C/M_{\text{applied}}$	9.6E-08	-	-	2.4E-07	-	8.7E-06
cumulative drainage at peak concentration [mm]	327	414	-	169	331	4
time of total recovery [d]	931	931	568	940	940	440
total recovery [%]	0.001	0.5	0.000	0.004	0.1	0.121
	No early breakthrough			Early breakthrough: UR		

C. Supporting Information of Chapter 3

CLZ depth injection	gravel soil (L6)			moraine soil (L7)		
	CLZ	DPC	UR	CLZ	DPC	UR
time of first arrival [d]	0.2	1.1	0.2	0.2	6.1	0.2
time of peak concentration [d]	270	495	11	266	756	0.2
maximum concentration [ $\mu\text{g/L}$ ]	232.9	469.7	22.07	97.0	485.1	39.88
maximum concentration, $C/M_{\text{applied}}$	1.2E-04	-	5.4E-05	4.8E-05	-	9.8E-05
cumulative drainage at peak concentration [mm]	166	325	53	183	474	8
time of total recovery [d]	1259	1259	320*	1217	1217	320*
total recovery [%]	3.4	19.8	0.8*	2.0	21.2	1.2*
	Early breakthrough: CLZ, DPC, UR			Early breakthrough: CLZ, UR		

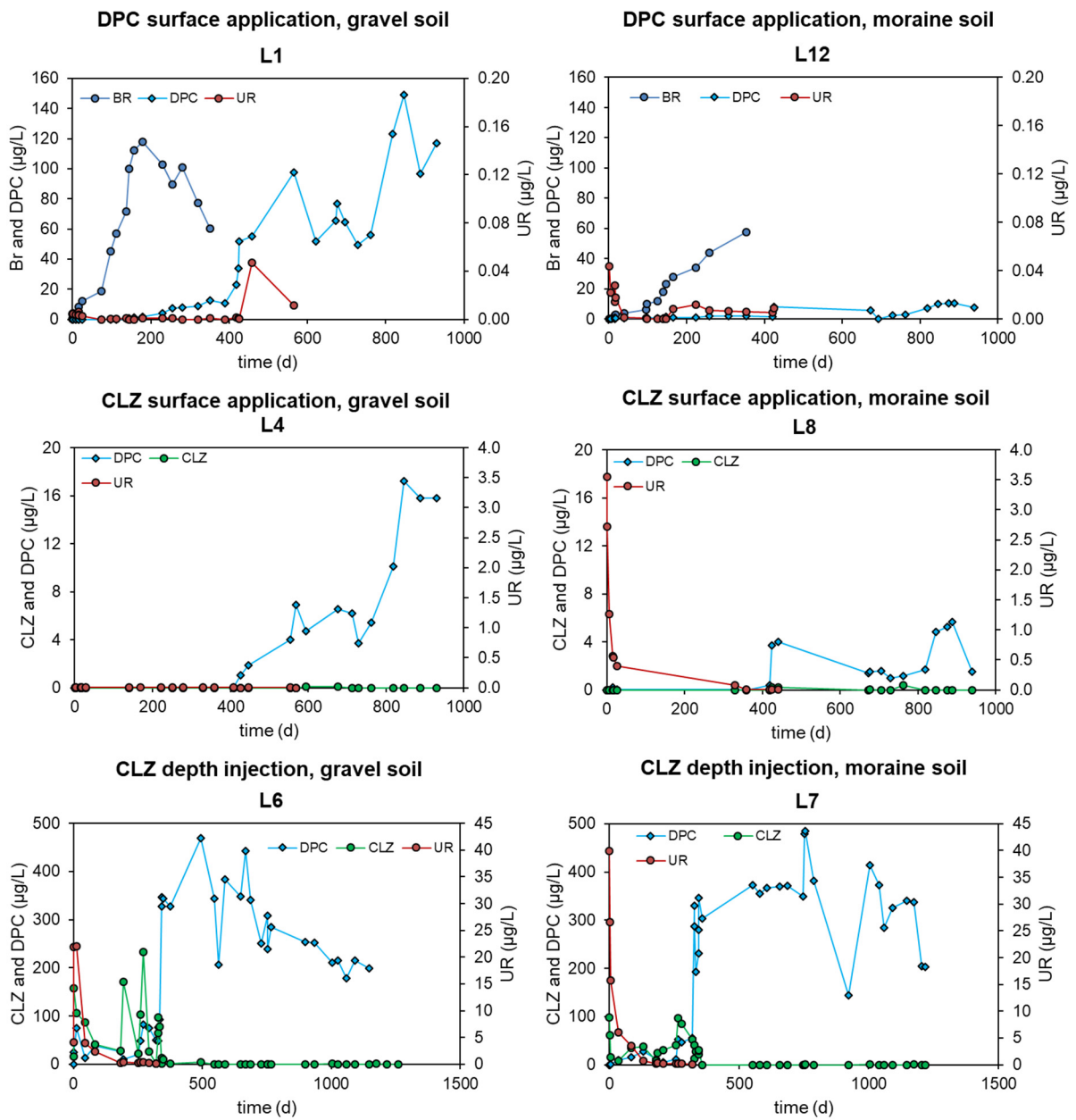


Figure C4: Breakthrough curves for chloridazon (CLZ), desphenylchloridazon (DPC), bromide (BR) and uranine (UR) in the six lysimeters used in this study.



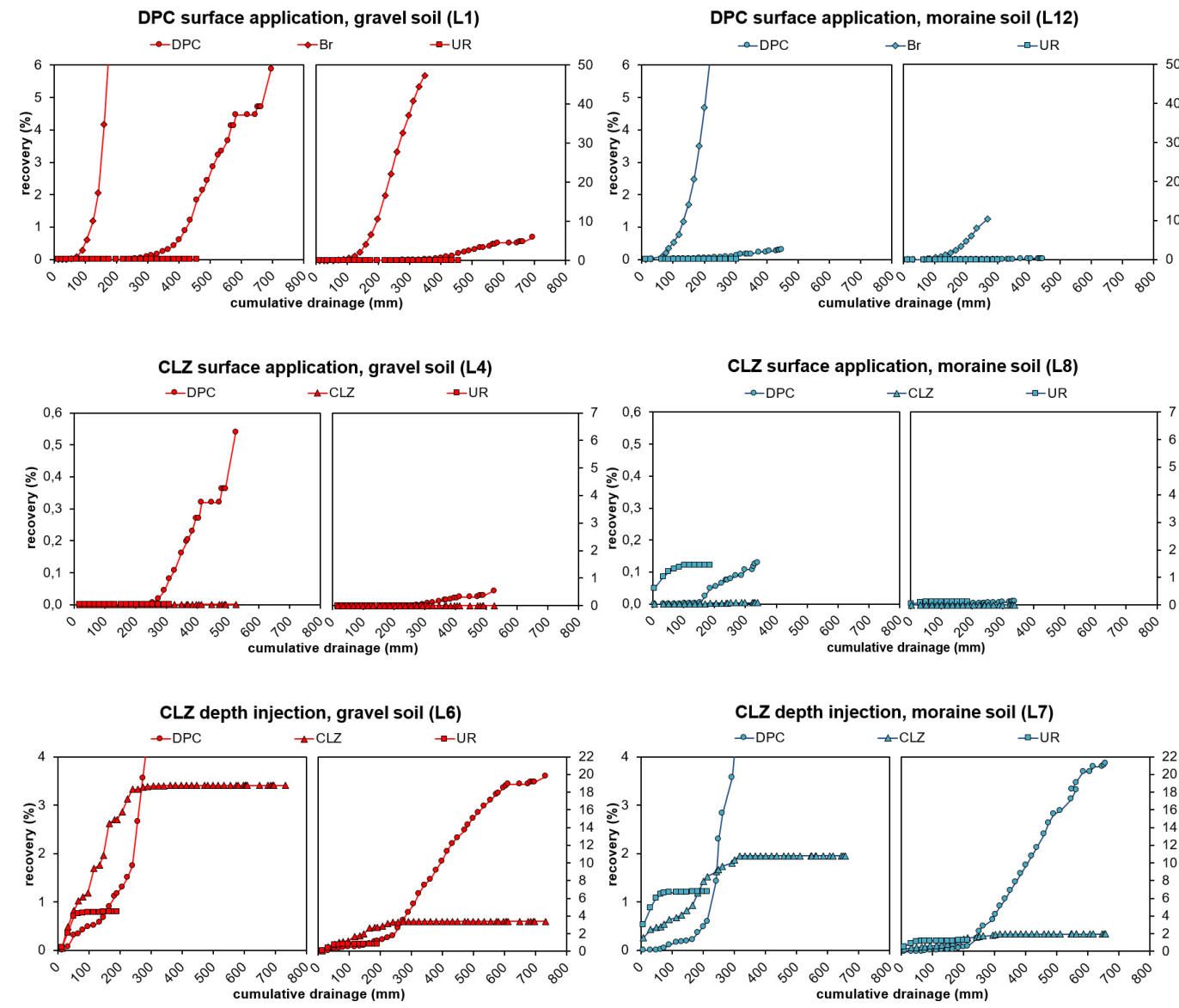


Figure C5. DPC, CLZ, bromide (Br), uranine (UR) recoveries against cumulative drainage for the six combinations of application method and soil type. Note that each lysimeter is shown in two different plots with different scales, as recoveries were in general much higher for bromide than for DPC, CLZ and uranine



**C.3.4. Soil Analysis****Table C7: Concentration measurements of chloridazon and desphenylchloridazon residues within the first soil layers; the limit of quantification (LOQ) was 0.05 mg/kg for CLZ and DPC; measurement uncertainty is shown as 95 % confidence interval (95 % CI)**

<b>Lysimeter</b>	<b>CLZ [mg/kg ± 95 % CI]</b>	<b>DPC [mg/kg ± 95 % CI]</b>
L1	n.a.	0.082 ± 0.041
L12	n.a.	0.18 ± 0.09
L6	<LOQ	<LOQ
L7	<LOQ	<LOQ
L4	<LOQ	0.081 ± 0.041
L8	<LOQ	0.12 ± 0.06

**C.3.5. Elemental-Analyzer Isotope Ratios****Table C8: Isotope ratios of <sup>13</sup>C and <sup>15</sup>N of chloridazon and desphenylchloridazon applied to the lysimeters determined by EA-IRMS; measurement uncertainty is shown as standard deviation (SD) of n=5 measurements**

<b>Compound</b>	<b>δ<sup>13</sup>C ± SD [‰]</b>	<b>δ<sup>15</sup>N ± SD [‰]</b>
Desphenylchloridazon	-17.84 ± 0.05	-3.81 ± 0.04
Chloridazon	-27.43 ± 0.02	-5.70 ± 0.03

C.3.6. Chloridazon Depth Injection

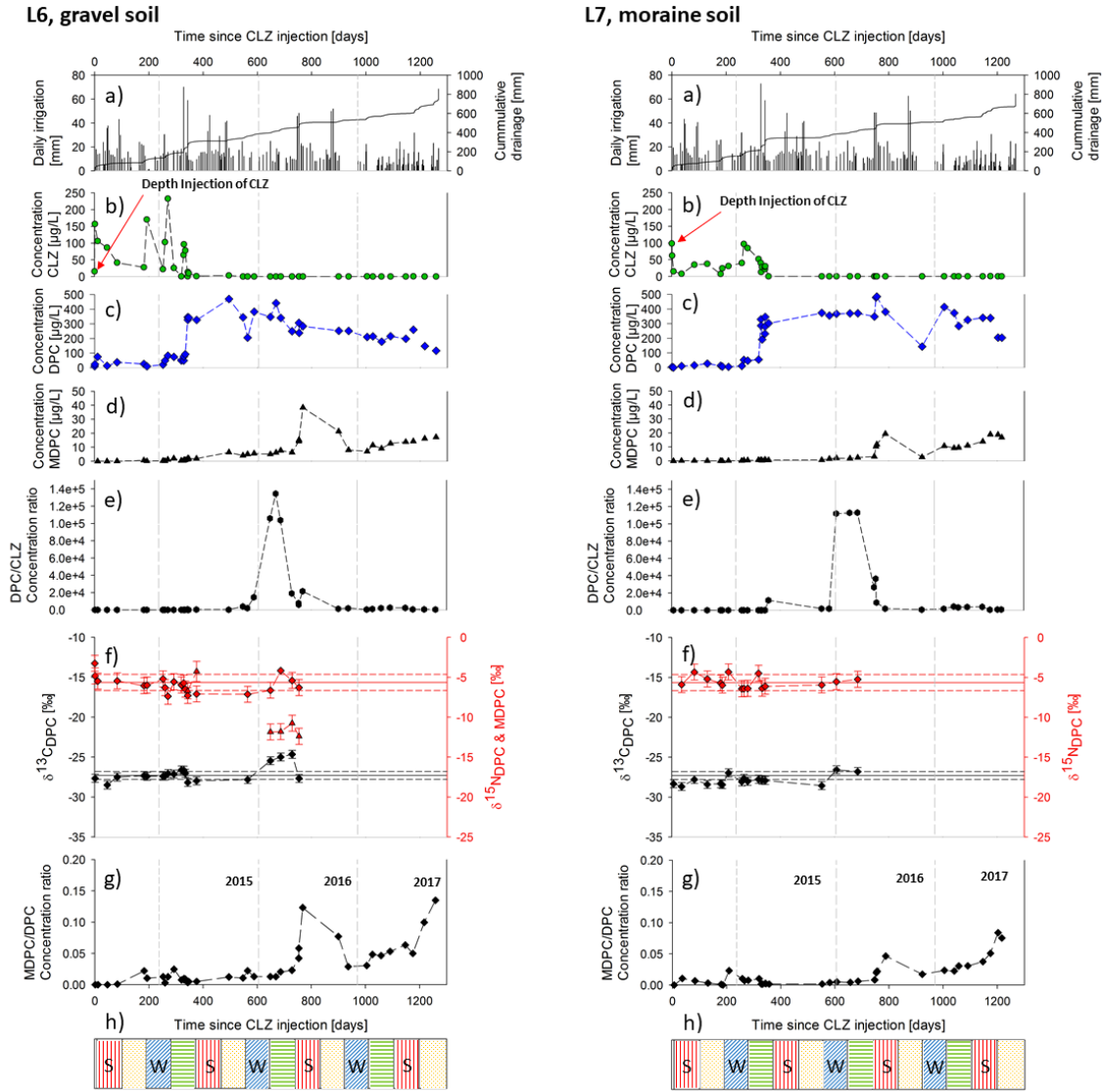


Figure C6: Lysimeters with CLZ injection in depth (a single injection in June 2014 at a depth of 40 cm): L6 in gravel soil (left panels) and L7 in moraine soil (right panels). a) Daily irrigation (black bars) and cumulative drainage (grey line), b-d) Concentration of CLZ (green circles), DPC (blue diamonds) and MDPC (black triangles), e) metabolite-to-parent compound molar ratio of DPC/CLZ (black hexagon), f) Carbon (black diamonds) and nitrogen (red diamonds) isotope ratios of DPC, and nitrogen isotope values of MDPC (red triangles), error bars show the associated uncertainties ( $\pm 0.5\text{‰}$  for carbon,  $\pm 1.0\text{‰}$  for nitrogen isotope analysis; or when exceeding this uncertainty, standard deviations of triplicate measurements are given, EA isotope values of the injected CLZ is shown as a line within the accepted standard deviation  $\pm \sigma$  shown as a dashed line in the corresponding color; g) metabolite-to-parent compound molar ratio of MDPC/DPC (black diamonds), h) season corresponding to the time since injection – spring (green horizontal lines), summer (red vertical lines), autumn (yellow dots), winter (blue diagonal lines); the grey dashed lines repeated in each sub-figure represent the start of a new year.



**C.3.7. Nitrogen Isotope Ratios of DPC and MDPC**

**Table C9: Nitrogen isotope ratio of DPC and their corresponding MDPC isotope values of lysimeter L1; measurement uncertainty is shown as standard deviation (SD) of triplicate measurements**

<b>Sample Date</b>	<b><math>\delta^{15}\text{N}</math> DPC <math>\pm</math> SD [‰]</b>	<b><math>\delta^{15}\text{N}</math> MDPC <math>\pm</math> SD [‰]</b>	<b><math>\Delta\delta^{15}\text{N}</math> [‰]</b>
23/11/16	-0.9 $\pm$ 0.5	-5.3 $\pm$ 0.3	-4.4
09/03/17	-1.2 $\pm$ 0.2	-4.9 $\pm$ 1.0	-3.7
05/05/17	-1.0 $\pm$ 0.1	-5.2 $\pm$ 0.9	-4.2

**Table C10: Nitrogen isotope ratio of DPC and their corresponding MDPC isotope values of lysimeter L12; measurement uncertainty is shown as standard deviation (SD) of triplicate measurements**

<b>Sample Date</b>	<b><math>\delta^{15}\text{N}</math> DPC <math>\pm</math> SD [‰]</b>	<b><math>\delta^{15}\text{N}</math> MDPC <math>\pm</math> SD [‰]</b>	<b><math>\Delta\delta^{15}\text{N}</math> [‰]</b>
05/07/2016	-1.2 $\pm$ 0.3	-8.5 $\pm$ 0.7	-7.3
09/03/2017	-2.7 $\pm$ 0.1	-8.0 $\pm$ 1.4	-5.3

**Table C11: Nitrogen isotope ratio of DPC and their corresponding MDPC isotope values of lysimeter L6; measurement uncertainty is shown as standard deviation (SD) of triplicate measurements; for one sample only a single measurement was possible, indicated by a missing standard deviation**

<b>Sample Date</b>	<b><math>\delta^{15}\text{N}</math> DPC <math>\pm</math> SD [‰]</b>	<b><math>\delta^{15}\text{N}</math> MDPC <math>\pm</math> SD [‰]</b>	<b><math>\Delta\delta^{15}\text{N}</math> [‰]</b>
21/05/15	-7.3 $\pm$ 0.4	-6.7 $\pm$ 0.8	-1.1
23/06/15	-7.1 $\pm$ 0.4	-4.3 $\pm$ 1.3	-1.0
21/03/16	-6.6 $\pm$ 0.5	-11.9 $\pm$ 0.5	-5.8
28/04/16	-4.2	-11.8 $\pm$ 0.1	-6.6
09/06/16	-5.4 $\pm$ 0.8	-10.8 $\pm$ 0.4	-4.5
05/07/16	-6.3 $\pm$ 0.4	-12.4 $\pm$ 0.3	-6.8

## D. Adsorbing vs. Nonadsorbing Tracers for Assessing Pesticide Transport in Arable Soils

Published September 14, 2017

Special Section: Lysimeters in Vadose Zone Research



### Core Ideas

- Atrazine preferential flow shortly after application was governed by soil type.
- Injection of atrazine at depth enhanced preferential flow.
- Uranine realistically illustrated the rapid and significant atrazine breakthrough.
- In reserve, bromide mimicked early atrazine breakthrough only with moraine soil.
- Using dye tracers as pesticide surrogates might assist in making sustainable decisions.

C. Torrentó, V. Ponsin, and D. Hunkeler, Centre for Hydrogeology and Geothermics (CHYN), Univ. of Neuchâtel, 2000 Neuchâtel, Switzerland; V. Prasuhn and E. Spiess, Agroscope, Research Division, Agroecology and Environment, 8046 Zürich, Switzerland; A. Melsbach, C. Lihl, and M. Elsner, Institute of Groundwater Ecology, Helmholtz Zentrum München, 85764 Neuherberg, Germany; M. Elsner, Analytical Chemistry and Water Chemistry, Technical Univ. of Munich, D-81377 Munich, Germany; G. Gläuser, Neuchâtel Platform of Analytical Chemistry, Univ. of Neuchâtel, 2000 Neuchâtel, Switzerland; T.B. Hofstetter, Eawag, Swiss Federal Institute of Aquatic Science and Technology, 8600 Dübendorf, Switzerland. \*Corresponding author (clara.torrento@unine.ch).

Received 31 Jan. 2017.

Accepted 18 May 2017.

Supplemental material online.

Citation: Torrentó, C., V. Prasuhn, E. Spiess, V. Ponsin, A. Melsbach, C. Lihl, G. Gläuser, T.B. Hofstetter, M. Elsner, and D. Hunkeler. 2018. Adsorbing vs. nonadsorbing tracers for assessing pesticide transport in arable soils. *Vadose Zone J.* 17:170033. doi:10.2136/vzj2017.01.0033

© Soil Science Society of America. This is an open access article distributed under the CC BY-NC-ND license (<http://creativecommons.org/licenses/by-nc-nd/4.0/>).

## Adsorbing vs. Nonadsorbing Tracers for Assessing Pesticide Transport in Arable Soils

Clara Torrentó,\* Volker Prasuhn, Ernst Spiess, Violaine Ponsin, Aileen Melsbach, Christina Lihl, Gaëtan Gläuser, Thomas B. Hofstetter, Martin Elsner, and Daniel Hunkeler

The suitability of two different tracers to mimic the behavior of pesticides in agricultural soils and to evidence the potential for preferential flow was evaluated in outdoor lysimeter experiments. The herbicide atrazine [6-chloro-N-ethyl-N'-(1-methylethyl)-1,3,5-triazine-2,4-diamine] was used as a model compound. Two tracers were used: a nonadsorbing tracer (bromide) and a weakly adsorbing dye tracer (uranine). Two soils that are expected to show a different extent of macropore preferential flow were used: a well-drained sandy-loamy Cambisol (gravel soil) and a poorly drained loamy Cambisol (moraine soil). Conditions for preferential flow were promoted by applying heavy simulated rainfall shortly after pesticide application. In some of the experiments, preferential flow was also artificially simulated by injecting the solutes through a narrow tube below the root zone. With depth injection, preferential leaching of atrazine occurred shortly after application in both soil types, whereas with surface application, it occurred only in the moraine soil. Thereafter, atrazine transport was mainly through the porous soil matrix, although contributions of preferential flow were also observed. For all the application approaches and soil types, after 900 d, <3% of the applied amount of atrazine was recovered in the drainage water. Only uranine realistically illustrated the early atrazine breakthrough by transport through preferential flow. Uranine broke through during the first intense irrigation at the same time as atrazine. Bromide, however, appeared earlier than atrazine in some cases. The use of dye tracers as pesticide surrogates might assist in making sustainable decisions with respect to pesticide application timing relative to rainfall or soil potential for preferential flow.

Abbreviations: DAR, desethylatrazine/atrazine molar ratio; DEA, desethylatrazine; DIA, desisopropylatrazine; ET, evapotranspiration.

Herbicides are extensively used in agriculture for the protection of plants against weeds. Subsequently, the potential exists for leaching of these active substances and their metabolites to groundwater. Indeed, pesticides and their degradation products are frequently detected in groundwater (Leistra and Boesten, 1989; Kolpin et al., 1998, 2000; Loos et al., 2010; Lopez et al., 2015).

After application, the dissolved part of the herbicide that is neither taken up by plants nor carried with runoff to surface water moves downward and percolates through the soil profile into groundwater. The flow of water and solutes through soil is largely determined by the size and connectivity of the water-filled pores (Jarvis, 2007). In addition to transport through the porous matrix, pesticides may be rapidly leached below the root zone by advective transport through macropores (e.g., cracks, earthworm channels, root holes, fissures, and interaggregate packing voids), largely bypassing the soil matrix (Bouma and Dekker, 1978; Beven and Germann, 1982; Jarvis, 2007), reducing the potential for pollutant adsorption and degradation and thus increasing the threat of groundwater contamination (Kördel et al., 2008). This preferential flow is recognized as prevalent under a wide range of conditions in soils with unstable, poor structure as well as those containing cracks

and channels (Flury et al., 1994). The potential for preferential flow is generally large for structured loamy and clayey soils containing large interaggregate pores. Pesticide losses resulting from macropore flow are typically <1% of the applied dose, but losses of between 1 and 5% may also occur (Jarvis, 2007). Leaching of as little as 0.1% of an applied pesticide may result in contaminant concentrations in shallow groundwater that already exceed the EU drinking water standard ( $<0.1 \mu\text{g L}^{-1}$ ) (Jarvis, 2007).

Degradation processes and sorption of solutes to soil particles can mitigate pesticide migration through the soil matrix. Degradation is governed by both abiotic and biotic factors, and degradation rates depend on many microbiological, physical, and chemical properties of the soil as well as the properties of the pesticide (Fenner et al., 2013). Once in the body of the soil, pesticide molecules partition between the aqueous and solid phases of the soil. The level of sorption is a function of the pesticide and the organic matter content of the soil (Wauchope et al., 2002). Physical entrapment within the soil solid phase and covalent bonding to soil organic matter or the clay mineral fraction of the soil might give rise to the so-called bound pesticide residues (Gevao et al., 2000). With longer residence times in the soil, these residues tend to lose their biological activity and become even more resistant to degradation (Calderbank, 1989). Bound residues of the herbicide atrazine corresponding to 9 and 25% of the applied amount have been found 9 and 22 yr after application, respectively (Capriel et al., 1985; Jablonowski et al., 2008). Jablonowski et al. (2009) and Vonberg et al. (2014) found up to 1.0 and  $0.2 \mu\text{g kg}^{-1}$  atrazine, respectively, in the topsoil >20 yr after the last application. A number of studies have observed a soil-bound residue fraction of other pesticides such as ethidimuron (*N*-[5-(ethylsulfonyl)-1,3,4-thiadiazol-2-yl]-*N,N'*-dimethylurea), methabenzthiazuron (*N*-2-benzothiazolyl-*N,N'*-dimethylurea), anilazine [4,6-dichloro-*N*-(2-chlorophenyl)-1,3,5-triazin-2-amine] (Jablonowski et al., 2012), and chloridazon [5-amino-4-chloro-2-phenyl-3(2*H*)-pyridazinone] (Schuhmann et al., 2016). However, even long-term immobilized compounds may be accessible to degradation by microorganisms (Jablonowski et al., 2008) and may also be released back to the soil solution. Long-term leaching of both extractable and bound pesticide residues, as well as metabolites, might occur as a result of changing environmental conditions in the soil (Gevao et al., 2000). Although the environmental risk posed by bound pesticide residues is considered to be low (Barraclough et al., 2005), leaching of extractable pesticide residues and microbial transformation of bound residues to mobile metabolites may represent a potential risk for groundwater contamination.

Strongly sorbing dye tracers have been used for identifying active flow paths and transport mechanisms in the vadose zone (Flury and Wai, 2003, and references therein). For marking preferential flow paths, many studies have applied a sorbing dye at the soil surface, excavated the soil profile after a specific infiltration time, and analyzed the dye distribution visually or using a computer

software for photo interpretation (e.g., Flury and Wai, 2003, and references therein; Kasteel et al., 2005; Wang and Zhang, 2011; Kodešová et al., 2012). Brilliant Blue FCF is the most prominent dye tracer in vadose zone hydrology (Flury and Wai, 2003, and references therein).

Detection of preferential flow in soils has also been achieved by applying a tracer to the soil surface and measuring its outflow concentration with time to produce a breakthrough curve. Bromide has been mainly used for this purpose (Everts and Kanwar, 1990; Lennartz et al., 1999; Haws et al., 2004; Brown et al., 2000; Jaynes et al., 2001) but also the dye rhodamine WT (Everts et al., 1989; Kung et al., 2000). Sorption or reactivity of bromide is reported to be negligible. In the case of pesticides, however, reactive transport is expected, and therefore conservative tracers might not realistically illustrate pesticide breakthrough to the groundwater. Furthermore, high bromide concentrations commonly used in tracer tests have been shown under certain conditions to inhibit pesticide degradation by reducing soil bacterial presence and activity and by altering pesticide sorption (Bech et al., 2017). Therefore, alternative tracers for illustrating pesticide breakthrough to groundwater are required.

The reactive nature of some fluorescent dye tracers has been exploited by using them as sorbing tracers as a surrogate to simulate pesticide leaching. At the laboratory scale, several studies have compared sorption and transport of atrazine and the dye rhodamine WT in column experiments (Sabatini and Austin, 1991; Everts and Kanwar, 1994; Kanwar et al., 1997). At the field scale, fluorescent dye tracers, such as uranine, sulforhodamine B, or rhodamine WT, have mainly been used for mimicking the transport of pesticides in wetlands (Passeport et al., 2010; Lange et al., 2011; Maillard et al., 2016). For evaluating pesticide transport by preferential flow in arable soils, dye tracers have been applied in tile-drainage plots (Czapar et al., 1994). These researchers compared the behavior of alachlor [2-chloro-*N*-(2,6-diethylphenyl)-*N*-(methoxymethyl)acetamide] and rhodamine WT during the first 10 h after application in field drainage tiles with silty clay loam soil. Even though both compounds differ in their chemical properties (molecular size, charge, octanol–water partition coefficient [ $K_{OW}$ ], etc.), they found that rapid breakthrough of the herbicide correlated reasonably well with that of the dye, although different recovery rates were measured. Tile-drainage plots, however, show limitations in controlling total water, and therefore solutes, percolating through the soil profile (Bergström, 1990; Jacobsen and Kjær, 2007). Lysimeters offer a greater degree of control over environmental factors and solute mass balances can be properly established. Pesticide environmental behavior and fate in soils have been studied in numerous lysimeters studies (Bowman, 1990; Dousset et al., 1995; Vink et al., 1997; Francaviglia and Capri, 2000; Renaud et al., 2004; Kasteel et al., 2010; Schuhmann et al., 2016). Outdoor lysimeters are subject to climatic conditions similar to those of the surrounding field and provide information regarding the



transport, plant uptake, and degradation of solutes under relevant soil water content regimes and crop production practices. To the best of our knowledge, comparison of pesticide and dye tracer transport through arable soils in large outdoor lysimeters has not been reported so far.

The main goal of this work was, therefore, to evaluate the suitability of different tracers as proxy for pesticide transport in arable soils by comparing their behavior with a model pesticide in outdoor lysimeters during a 2.5-yr period. The herbicide atrazine was chosen as a model compound because its behavior in soil has been extensively studied. Uranine was used as a surrogate of atrazine leaching because similar sorption has been reported for uranine and atrazine (Sabatini and Austin, 1991). Furthermore, uranine is the most widely used fluorescent tracer in hydrological and hydrogeological applications. Thus, it is of considerable interest to know how it behaves relative to pesticides. Bromide, probably the most widely used tracer in soil sciences, was also included for comparison. Because we were mainly interested in the ability of tracers to track preferential transport, we performed the test in two soil types that were expected to show a different extent of preferential flow: a well-drained sandy-loamy Cambisol and a poorly drained loamy Cambisol. Conditions for preferential flow were promoted by applying heavy simulated rainfall shortly after atrazine application. Preferential flow was also artificially simulated by injecting the solutes below the root zone through a narrow tube.

## Materials and Methods

### Compounds and Their Properties

Atrazine is highly persistent in the environment and moderately mobile, with a low aqueous solubility ( $30 \text{ mg L}^{-1}$  at  $20^\circ\text{C}$ ). It sorbs to clay minerals and organic matter (Mudhoo and Garg, 2011), showing a relatively low adsorption coefficient ( $K_{OC}$ ), with values ranging from 40 to  $394 \text{ mL g}^{-1}$  (Burnett et al., 2000). Atrazine is degraded in the soil by both abiotic and biotic processes through hydrolysis and dealkylation (Mudhoo and Garg, 2011), with a half-life in aerobic soil ranging from 20 to 146 d (Burnett et al., 2000). Desethylatrazine (DEA) is the atrazine metabolite most frequently detected in groundwater (Kolpin et al., 2000; Loos et al., 2010). Desethylatrazine has a  $K_{OC}$  of  $110 \text{ mL g}^{-1}$  (Steinheimer and Scoggin, 2001), an aqueous solubility of  $2700 \text{ mg L}^{-1}$  at  $20^\circ\text{C}$ , and a typical half-life in aerobic soil of 45 d (Lewis et al., 2016). It is classified as moderately persistent and moderately mobile (Lewis et al., 2016). The presence of DEA in concentrations greater than atrazine in groundwater has been documented in Europe (Loos et al., 2010).

In laboratory experiments with alluvial sandy aquifer material, Sabatini and Austin (1991) measured similar  $K_{OC}$  values of  $120 \text{ cm}^3 \text{ g}^{-1}$  for uranine and  $148 \text{ cm}^3 \text{ g}^{-1}$  for atrazine, even though both compounds differ in their chemical and physical

properties: molecular weight ( $376$  and  $216 \text{ g mol}^{-1}$ ), aqueous solubility ( $25,000$  and  $30 \text{ mg L}^{-1}$ ), acid dissociation constant  $pK_a$  ( $5.1$  and  $1.68$ ), and  $\log K_{OW}$  ( $-0.39$  and  $2.34$ ) for uranine and atrazine, respectively (Sabatini and Austin, 1991; Kasnavia et al., 1999; Lewis et al., 2016).

### Experimental Site

This study was performed in a lysimeter facility from Agroscope at Zurich-Reckenholz, Switzerland ( $47.26^\circ \text{ N}$ ,  $8.31^\circ \text{ E}$ ,  $443 \text{ m asl}$ ). The facility consists of 12 weighing backfilled gravitation lysimeters ( $3.14\text{-m}^2$  surface area,  $2.5\text{-m}$  depth,  $\sim 14,000 \text{ kg}$  soil in each). The large outdoor lysimeters were constructed in 1979, and a sequence of arable crops has been grown since 1980 (Albisser and Prasuhn, 2013). Six of the lysimeters (L1–L6) were filled with a well-drained sandy-loamy Cambisol developed from a stony alluvium (gravel soil), and the other six (L7–L12) were filled with a poorly drained loamy Cambisol developed from moraine deposits (moraine soil) (Troxler et al., 1998). The two soil types are widely used for farming in Swiss lowlands and mainly differ in the texture of the B horizon and the draining properties of the parent material (Table 1). The moraine soil displayed lower water permeability and was slightly pseudogleyic (i.e., periodic water saturation of the soil leading to reducing conditions) (Troxler et al., 1998). Nievergelt (1997) calculated the available water capacity from the difference between the lysimeter weight at field capacity and the lowest lysimeter weight during a 16-yr study period and assessed it to be at least  $260 \text{ mm}$  for the moraine soil and  $190 \text{ mm}$  for the gravel soil. In the present study, all lysimeters were sown to corn (*Zea mays* L.) in 2014, to sugarbeet (*Beta vulgaris* ssp. *vulgaris* var. *altissima* Doel) in 2015, and to corn again in 2016 (Table 2). Only

Table 1. Main properties of the two soils

Soil horizon	Depth	Organic matter	Size distribution of mineral particles		
			Clay	Silt	Sand
	cm		%		
			Gravel soil		
A <sub>p</sub>	0–50	1.7	20	23	57
B <sub>1</sub>	50–60	0.9	17	20	64
B <sub>2</sub>	60–70	1.1	19	24	57
B <sub>3</sub>	70–100		20	24	57
B <sub>4</sub>	110–120		19	21	60
C	120–135		17	18	65
C	sandy alluvial deposits				
			Moraine soil		
A <sub>p</sub>	0–50	2.1	22	34	44
B <sub>1</sub>	50–70	1.5	23	35	43
B <sub>2</sub>	70–90	0.4	22	38	40
B <sub>3</sub>	90–110		20	40	40
B <sub>4</sub>	110–140		21	42	37
C	140–160		20	41	38
C	loamy moraine deposits				

## D. Adsorbing vs. Nonadsorbing Tracers for Assessing Pesticide Transport

Table 2. Crops grown in the study period with sowing and harvest dates and winter cover

Year	Crop	Sowing date	Harvest date	Winter cover
2014	corn	12 May 2014	10 Sept. 2014	stubble
2015	sugarbeet	25 Mar. 2015	13 Nov. 2015	bare fallow
2016	corn	12 May 2016	14 Sept. 2016	stubble

eight out of the 12 lysimeters (L3–L10) were used in this study. The last four lysimeters (L1, L2, L11, and L12) were used for an additional experiment involving pesticide metabolites application (not included in this work). The lysimeter facility was covered with a plastic tunnel, and an irrigation system was used to ensure full control of irrigation rates.

### Irrigation

Regular low-intensity irrigation events (5–20 mm once a week at 0.2 mm min<sup>-1</sup>) were applied in addition to occasional intense irrigation events (30–50 mm at 1 mm min<sup>-1</sup>). The low-intensity irrigation events were performed using a fixed spray-irrigation system, whereas for the intense irrigation events, a mobile sprinkler system was used. Figure 1 shows daily and cumulative irrigation during the study period, and Table 3 details the heavy irrigation events. For enhancing atrazine leaching, high water content in the soil was maintained before application and an intense irrigation event was performed just after herbicide application.

During the study period (January 2014–December 2016), the total amount of water applied in each lysimeter by sprinkler irrigation was ~2500 mm. Approximately 950 mm was applied during 2014, 870 mm during 2015, and 690 mm during 2016. In a Federal Office of Meteorology and Climatology (MeteoSwiss) station located close to the lysimeter facility (Zurich-Affoltern, 47.43° N, 8.52° E, 444 m asl), the wettest months are from May to September. For the Ebnet-Kappel station (47.27° N, 9.11° E, 623 m asl), irrigation data from

Table 3. Atrazine (and tracers) application to the lysimeters (L) and intense irrigation events during the study period

Date	Atrazine (and tracers) application	Intense irrigation (mm)
14 May 2014	–	30
30 May 2014	atrazine surface application (L4, L5, L8, L9): 2.1 kg ha <sup>-1</sup>	–
31 May 2014	–	40–55
3 June 2014	–	20–35
5 June 2014	tracer application on surface (L4, L5, L8, L9)	40–55
12 June 2014	atrazine depth injection (L3, L6, L7, L10): 0.66 g per lysimeter; tracers were injected at the same time	40–55
28 July 2014	–	40
31 July 2014	–	30–35
10 Sept. 2014	–	40
15 Sept. 2014	–	40
24 Feb. 2015	–	30
6 May 2015	–	50
21 May 2015	–	55
3 Aug. 2015	–	30
10 Aug. 2015	–	45
7 Oct. 2015	–	40
12 Oct. 2015	–	40
28 June 2016	–	50
4 July 2016	–	50
31 Oct. 2016	–	50
7 Nov. 2016	–	50

2010 to 2014 shows that >20 mm per 24-h precipitation events are more frequent in December and between June and September. One-hour precipitation events of >20 mm occur mainly in May and July. Accordingly, in these experiments, the heavy irrigation events were

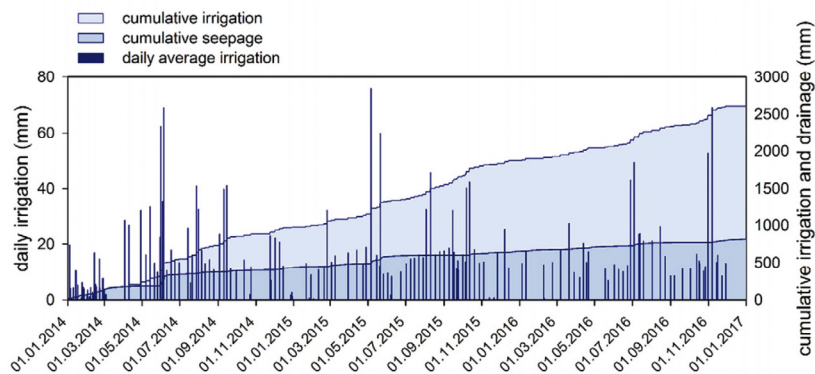


Fig. 1. Daily irrigation, cumulative irrigation, and cumulative drainage during the studied period for the gravel soil (Lysimeter L4).

mostly performed in June through September and in November through December (Fig. 1).

### Pesticide and Tracer Application

In four lysimeters (two replicates per soil type; L4, L5, L8, and L9), atrazine was applied at the surface as an early post-emergence herbicide at the two- to three-leaf stage, simulating the common scenario of herbicide application; whereas in the other four lysimeters (L3, L6, L7, and L10), atrazine was injected through a 40-cm narrow tube below the root zone, simulating high preferential transport of the solutes through the topsoil.

For surface application, a sprinkler system was used, ensuring a uniform distribution of the pesticide on the soil surface of the lysimeter. On 30 May 2014, 22 L (7 mm) of a 30 mg L<sup>-1</sup> atrazine stock solution was applied at each lysimeter at 1 mm min<sup>-1</sup>, which corresponds to 659 mg per lysimeter. This dose is equivalent to 2.1 kg ha<sup>-1</sup>, just below the maximum recommended application rate of 2.2 kg ha<sup>-1</sup> (Syngenta, 2005). For depth injection, 11 injection points were uniformly distributed on the surface of each lysimeter. On 12 June 2014, 2 L of the atrazine stock solution were injected in each point at 1 L min<sup>-1</sup> by using a 6-mm-diameter metal rod with 1-mm-diameter holes around the bottom connected to a gear pump through a 3-mm i.d. Teflon tube. Thereafter, 1 L of water was poured in to rinse the injection apparatus. A similar pesticide injection procedure has been previously used for assessing the risk of groundwater contamination in relation to the depth of pesticide penetration (Delphin and Chapot, 2006). Given the surface area of each lysimeter, the injection rate corresponded to 0.46 m d<sup>-1</sup>, which is within the range of reported rates of preferential flow. Nimmo (2007) reviewed the infiltration velocity of preferential flow in 64 field test studies. The maximum flow rate in macropores for loamy sand, sandy soil, and silty clay loam ranged from 0.05 to 1.40 m d<sup>-1</sup>. Cey and Rudolph (2009) measured dye tracer infiltration rates for preferential flow in slightly stony silt loam ranging from 40.06 to 2.69 m d<sup>-1</sup>. Nevertheless, velocities up to 115 m d<sup>-1</sup> for tracer transport along preferential pathways were measured by Jaynes et al. (2001) in fine-loamy soil. There was no atrazine application in 2015 and 2016 in any of the lysimeters.

In addition to atrazine, NaBr (500 kg ha<sup>-1</sup>) and uranine (1.3 kg ha<sup>-1</sup>) were applied as tracers. Whereas the tracers were injected at the same time as atrazine in the lysimeters with depth injection, they were applied 6 d after atrazine in the lysimeters with surface application (5 June 2014) followed by a heavy irrigation event.

Previous tracer experiments (500 kg NaBr ha<sup>-1</sup>) were performed between October 2010 and April 2014 on the same lysimeters cropped with corn in 2010, potato (*Solanum tuberosum* L.) in 2011, broccoli (*Brassica oleracea* L. var. *italica* Plenck) in 2012, and a grass-clover mixture (standard mixture 330, Suter et al., 2012) in 2013 (Prasuhn et al., 2015). Low residual bromide content was detected in the soil and the drainage water before starting

the present experiments. Decreased contents of bromide with depth were measured in the soil profile from 60 to 135 cm for the gravel soil (L4) and from 15 to 160 cm for the moraine soil (L9). The maximum measured content was 0.8 mg kg<sup>-1</sup>. The total bromide soil content corresponded to <2% of the applied amount. Bromide concentration in the drainage water before the start of the experiments ranged from 0.1 to 0.5 mg L<sup>-1</sup> for the gravel soil and between 0.3 and 0.9 mg L<sup>-1</sup> for the moraine soil.

### Management Practices

Crop management followed the good agricultural practices of the region. Because farm machinery cannot be used on lysimeters of this type, tillage practices were performed by hand to a depth of 20 cm before sowing the crops. After harvest, no tillage occurred until next spring.

Under corn, N fertilizer was applied as NH<sub>4</sub>NO<sub>3</sub> and split into two applications (30 and 60 kg N ha<sup>-1</sup>), whereas P and K were supplied before sowing (35 kg P ha<sup>-1</sup> as superphosphate and 183 kg K ha<sup>-1</sup> as potassium magnesia, respectively). Sugarbeet received applications of 110 kg N ha<sup>-1</sup>, 39 kg P ha<sup>-1</sup>, and 309 kg K ha<sup>-1</sup>, using the same fertilizers as for corn.

At harvest, the aboveground corn parts were cut off because the corn was grown for silage. Sugarbeet roots were removed from the lysimeters, whereas beet tops were left. Crop samples were taken for further analysis of bromide residues.

### Monitoring

Pictures of the aboveground and belowground parts of the lysimeter facility can be found in Supplemental Fig. S1. Each lysimeter is set on a weigh bridge measuring the lysimeter weight at 5-min intervals. The balances have an accuracy of 500 g (0.16-mm water equivalent). The changes in the obtained values, which represent changes in the nominal mass, were divided by the lysimeter surface area and the density of water to obtain the changes in water content expressed as equivalent water column.

In two of the lysimeters (one for each type of soil), capacitive, multilevel probes EasyAG (Sentek) equipped with four frequency capacitance sensors (at 16, 36, 56, 76, and 96 cm for L9 and at 11, 51, and 71 cm for L4) were installed, and changes in volumetric soil water content were monitored at 15-min intervals. A meteorological station was installed for measuring air temperature and relative humidity, wind speed and direction, and solar radiation. Data from all the sensors were collected with a DS3 datalogger (Sensorscope). All data were taken at 1-min intervals and were accessible in real time on the internet.

Drainage water was collected at the bottom of the lysimeters via stainless steel funnels and Teflon tubes in 54-L glass bottles placed on balances (PCE-SD 60 SST-C, PCE Instruments) to continuously record the outflow. The balances have a resolution of 20 g



(0.066-mm water equivalent), and the data were monitored at 1-h intervals. Outflow data were divided by the lysimeter surface to obtain the cumulative drainage water expressed as equivalent water column. The leachate was subsampled for tracers and pesticide analysis every 50 L. All leachate samples were stored at 4°C until analysis.

In May 2016, soil samples from the 0- to 10-cm depth were taken from the eight lysimeters for analysis of pesticide residues. Soil samples were stored at 4°C until analysis.

Evapotranspiration was estimated by the water balance computation during a specific period:

$$ET = I - D - \Delta SWS \quad [1]$$

where ET is evapotranspiration (mm),  $I$  is irrigation (mm),  $D$  is drainage (mm), and  $\Delta SWS$  is the change in soil water storage (mm) determined from lysimeter weight changes. Runoff can be excluded for the given lysimeters' construction. The 5-min-based time series of lysimeter weight changes was used for precisely determining daily irrigation and  $\Delta SWS$  values. The processing of weight balance data consisted of five steps. In Step 1, the 5-min raw data were manually filtered, and all data during revision or control services were removed. In Step 2, a threshold filter was applied for removing outliers. In Step 3, if the resulting gaps did not exceed a period of 3 h, values were estimated by linear interpolation. In Step 4, an adaptive window and adaptive threshold filter (Peters et al., 2014; Hannes et al., 2015) was applied for correction of external forces such as management practices and wind. In Step 5, inconsistencies of the filter output were corrected manually on a daily basis.

### Chemicals and Reagents

A 30 mg L<sup>-1</sup> atrazine (Oskar Tropitzsch) solution was prepared in distilled water with 0.2% methanol. Sodium bromide and uranine (Fluorescein sodium salt, C<sub>20</sub>H<sub>10</sub>O<sub>5</sub>Na<sub>2</sub>) were purchased from VWR Chemicals and FluorTechnik, respectively.

Atrazine, desisopropylatrazine (DIA), and DEA (Pestanal quality), the single isotopically labeled surrogate (atrazine-D5, Pestanal quality), and the internal standard (terbuthylazine [6-chloro-*N*-(1,1-dimethylethyl)-*N'*-ethyl-1,3,5-triazine-2,4-diamine], Pestanal quality) were purchased from Sigma Aldrich. Standard stock solutions (1 mg mL<sup>-1</sup>) were prepared in ethanol and stored in darkness at -18°C for 6 mo. Working solutions (10 µg mL<sup>-1</sup>) were prepared by dilution of the stock solution in ethanol. These solutions were renewed every 2 mo. Atrazine, DIA, and DEA calibration solutions were prepared in a methanol/MilliQ (70:30 v/v) mixture with concentrations ranging from 10 to 1000 µg L<sup>-1</sup>. Methanol, ethyl acetate, and ethanol of analytical grade were used. Ultrapure water was prepared by ultrafiltration with a Millipore DirectQ apparatus (Millipore).

### Extraction of Pesticides from Water Samples

Leachate samples were filtered through 0.7-µm glass fiber filters before extraction. For the pre-concentration and extraction of the pesticides, a combination of hydrophilic (Septra ZT, Phenomenex) and hydrophobic (Bakerbond SDB-1, J.T. Baker) polymer-based sorbents with high specific surface area was used. Both sorbents show high adsorption capacity for highly polar micropollutants (Pichon et al., 1996; Mendaš, et al., 2001; Weigel et al., 2001; D'Archivio et al., 2007). Empty 6-mL solid-phase extraction (SPE) polyethylene cartridges (Grace) were packed with 0.2 g of each of the selected sorbents, with the Septra ZT as the first material in the enrichment flow direction and the SDB-1 as the second one, separated by polyethylene frits (Grace). The SPE cartridges were placed on a Phenomenex 12-position vacuum manifold. They were first rinsed with 3 mL of ethyl acetate, conditioned with 2 × 3 mL of methanol, and finally washed with 2 × 3 mL of MilliQ water. A 20-mL sample was loaded on each cartridge using a 5 mL min<sup>-1</sup> flow. Atrazine-d5 was added to the samples at 1.25 µg L<sup>-1</sup> for use as a surrogate standard. After the loading step, the sorbent was rinsed with 3 mL of MilliQ water and dried under vacuum for 15 min. The target compounds were then eluted from the cartridges in 75-mL Pyrex glass tubes (VWR Scientific) with two portions of 1.5 mL of ethyl acetate at a flow rate of 3 mL min<sup>-1</sup>. The extracts were evaporated until dryness using a CentriVap benchtop vacuum concentrator (Labconco). The evaporated samples were reconstituted to obtain a volume of 500 mL of methanol/MilliQ (70:30 v/v) mixture. At this stage, the internal standard terbuthylazine was added at 50 µg L<sup>-1</sup>. The SPE recoveries at concentrations between 0.5 and 25 µg L<sup>-1</sup> ranged from 84 to 100% for atrazine and from 97 to 113% for DEA.

### Analytical Methods

The bromide concentration in the drainage water was measured by ion chromatography using a Dionex LC20 chromatograph with ED40 electrochemical detector (Dionex Corp.). The detection limit was 0.014 mg L<sup>-1</sup>. Bromide in the crop samples was extracted with water. An additive of trichloroacetic acid was used for precipitation of proteins. Bromide concentrations were then measured as explained above.

Uranine concentrations were measured by fluorescence spectrometry using a PerkinElmer LS-50B luminescence spectrometer. The excitation wavelength was set to 488 nm, and emission was measured at 516 nm, with excitation and emission slits of 28 nm. To transform relative fluorescence units into uranine concentrations, a six-point standard curve was established using increasing concentrations of uranine from 0.1 to 5 µg L<sup>-1</sup>. The quantification limit was 0.05 µg L<sup>-1</sup>.

Atrazine, DIA, and DEA concentrations in the SPE eluates were determined by ultra-high-pressure liquid chromatography quadrupole time-of-flight mass spectrometry. A Synapt G2 Q-TOF mass spectrometer (Waters) equipped with an electrospray probe was used. Quantification of atrazine, DIA, and DEA was performed

by the internal standard method based on peak areas using terbuthylazine as the internal standard. The estimated instrument method quantification limit was 3, 11.4, and  $6 \mu\text{g L}^{-1}$  for atrazine, DIA, and DEA, respectively. The corresponding method quantification limits, corrected for the SPE concentration factor, were 0.075, 0.28, and  $0.15 \mu\text{g L}^{-1}$ , respectively.

There was no difference in detection sensitivity to the mass applied between bromide and the other two solutes. The quantification limit for atrazine was 187 times lower than for bromide, and 185 times more bromide mass was applied. In the case of uranine, the quantification limit was 280 times lower than for bromide, and 299 times more bromide mass was applied. Therefore, breakthrough results for the three solutes can be compared without applying any correction.

Soils samples were sent to an external, DIN-certified laboratory (Eurofins Sofia GmbH) for pesticide extraction and analysis by liquid chromatography coupled with tandem mass spectrometry. The quantification limit was  $0.05 \text{ mg kg}^{-1}$ .

## Results and Discussion

### Water Dynamics

Daily irrigation and soil water content variations at two different depths for the moraine (L9) and gravel soil (L4) are shown in

Fig. 2 and 3, respectively. In the moraine soil (L9), rapid soil water content increases were observed at the 16-cm depth after any irrigation event, whereas at the 56-cm depth, only intense irrigation events led to rapid and significant soil water content rises (Fig. 2). For example, following 20- and 13-mm irrigation events on 28 Apr. and 15 May 2015, respectively, rapid (within 3 h) soil water content increases occurred at the 16-cm depth but not at the 56-cm depth. Following the 6 May 2015 intense irrigation event (54 mm), however, a significant increase in soil water content was recorded at both the 16- (within 1 h) and 56-cm depths, although the latter was not recorded until 3 h later. Fluctuations in the soil water content were smaller for the gravel soil (L4; Fig. 3), especially at greater depths. Because the occurrence of sidewall flow (i.e., potential artificial water and solute flow along the inside of the lysimeter wall) can be disregarded because of the dimensions of the present lysimeters (Bergström, 2000; Fank, 2009), this rapid rise of deep soil water content could only be related to preferential paths of water flow as a result of the presence of macropores or because of spatial variability in soil properties. The presence of conductive zones through which matrix flow may have been unexpectedly fast could have delivered water to greater depths. Nevertheless, preferential flow through macropores, which are likely to occur in the moraine but not in the gravel soil, seems to be the most likely explanation of the results. Breakthrough of the applied solutes will allow further discussion of this hypothesis.

Daily irrigation, cumulative irrigation, and cumulative drainage for one of the lysimeters are shown in Fig. 1. Drainage volumes

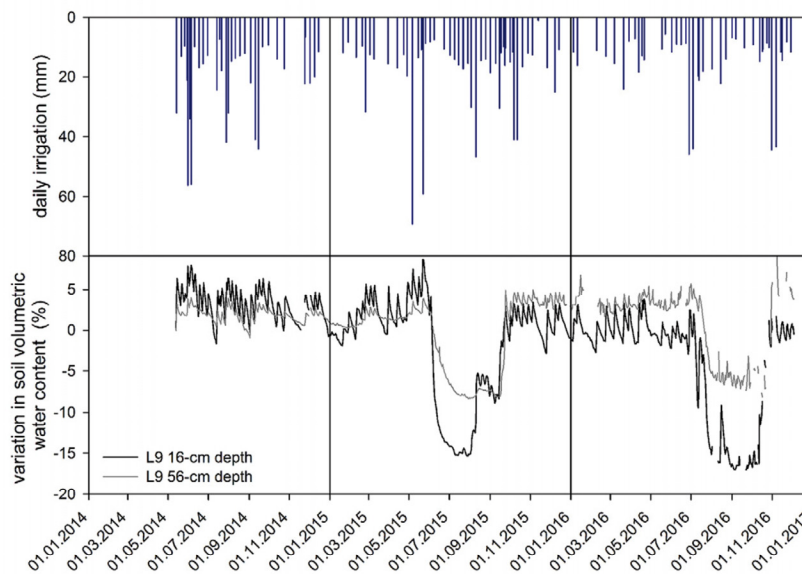


Fig. 2. Daily irrigation and variations in soil water content (with respect to the soil water content on 13 May 2014) at two different depths during the studied period for the moraine soil (Lysimeter L9).



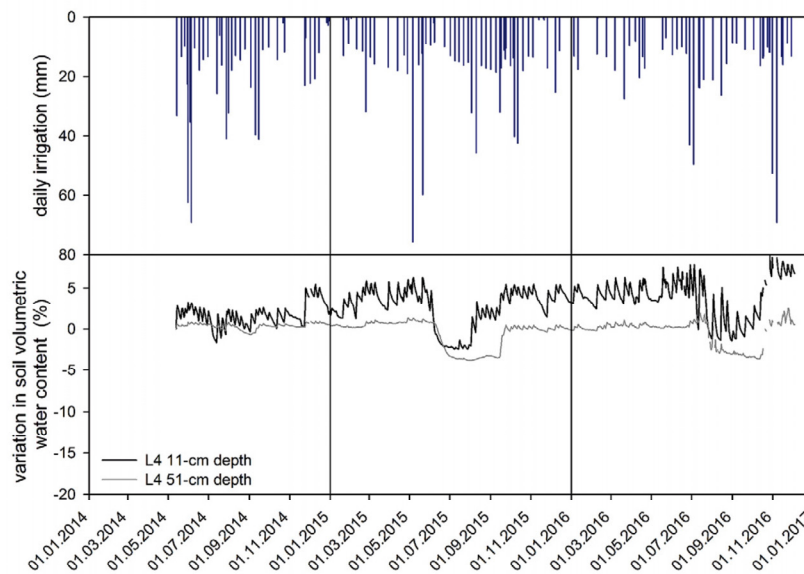


Fig. 3. Daily irrigation and variations in soil water content (with respect to the soil water content on 13 May 2014) at two different depths during the studied period for the gravel soil (Lysimeter L4).

during the study period were between 700 and 900 mm. In relation to water input, drainage volume represented 45% of the total irrigation in 2014, 25% in 2015, and 20% in 2016. Increased drainage coincided with periods of high irrigation volume and high soil water content. The two most significant increases in the drainage rate occurred after the intense irrigation following solute application (31 May 2014) and after the intense irrigations on 6 and 22 May 2015. For both soil types, these two intense irrigation events promoted a rapid and significant response in the drainage at the bottom of the lysimeter, as shown for L4 in Fig. 1. Monthly, the highest drainage volumes were obtained in May through June and in December through March (Fig. 4). Similar drainage volumes were observed for the two soil types, although in 6 of 36 mo, drainage amounts were 5 mm mo<sup>-1</sup> higher in the gravel than the moraine soil (Fig. 4; Supplemental Table S1).

A water balance approach was adopted to compute the estimated monthly ET for each lysimeter and year following Eq. [1]. The accumulated values of  $I$ ,  $D$ , and ET for one of the lysimeters are illustrated in Supplemental Fig. S2. The average monthly and total sums of all components are shown in Fig. 4 and listed in Supplemental Table S1 as the average across the four lysimeters for each soil type. The ET for all the lysimeters averaged 541 mm yr<sup>-1</sup> in 2014, 664 mm yr<sup>-1</sup> in 2015, and 598 mm yr<sup>-1</sup> in 2016. Evapotranspiration was similar in the gravel (544–642 mm yr<sup>-1</sup>) and moraine soils (537–683 mm yr<sup>-1</sup>). On a monthly basis, the ET was higher from May to September (Fig.

4) when average air temperature and plant growth were high (Supplemental Fig. S3).

#### Bromide, Uranine, and Atrazine Breakthrough after Surface Application

With surface application, in the moraine soil, the maximum concentration of bromide (82 mg L<sup>-1</sup> for L9 and 115 mg L<sup>-1</sup> for L8) occurred within 360 d, after ~400 to 450 mm of cumulative drainage, followed by a steady decrease (Fig. 5). Table 4 summarizes the observed tracers and atrazine breakthrough parameters for each lysimeter. In the gravel soil, a similar pattern was observed, although high bromide peaks (maximum concentration of 184 and 124 mg L<sup>-1</sup> for L4 and L5, respectively) were more rapidly reached after 290 to 330 d and 300 to 350 mm of cumulative drainage, respectively (Fig. 5; Table 4). This is consistent with the higher water retention capacity of the moraine soil than the gravel soil.

The leaching patterns of uranine and atrazine were different from that of bromide (Fig. 5). Under the moraine soil, both solutes were detected in the first leachate collected after the intense irrigation that followed application—within a few hours—and the maximum concentration occurred after only 100 mm of accumulated drainage (Table 4). Thereafter, the uranine concentration decreased to below the detection limit between 50 and 100 d after application, after which it was not detected anymore. In the case of atrazine, after the initial peak, continuous low concentrations in the drainage water (below 4 μg L<sup>-1</sup>) were observed during several months (until 280

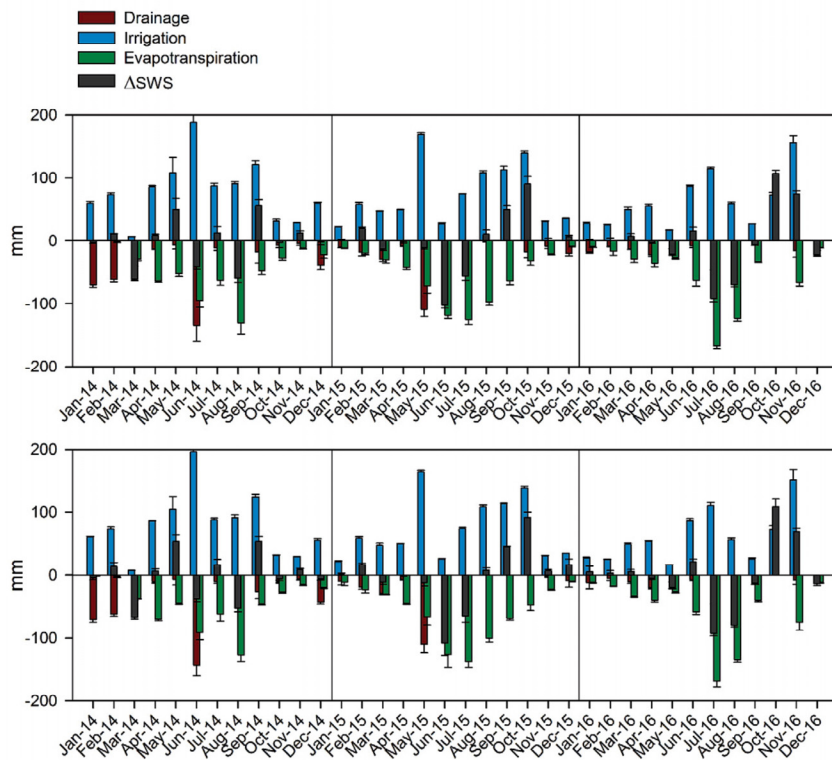


Fig. 4. Average monthly irrigation, drainage, evapotranspiration, and the change in water storage ( $\Delta$ SWS) for the gravel (upper panel) and moraine soils (lower panel) during the three monitoring years.

d after application). In the gravel soil, neither uranine nor atrazine rapid breakthrough was observed. Concentrations of both solutes remained below the detection limit during the first 200 to 300 d.

The heavy irrigation on 24 Feb. 2015 (Fig. 1; Table 3) caused a small atrazine breakthrough peak  $\sim$ 280 d after application in both soil types, more significant for the moraine than the gravel soil. For the moraine soil, the occurrence of this peak coincided with a sharp increase in the bromide concentration. The heavy irrigation events on 6 and 22 May 2015 (340 and 356 d after application, respectively) caused a significant increase in the drainage volume and promoted greater atrazine leaching. As a result, another atrazine pulse occurred 340 d after application in both soil types (the first peak in the case of the gravel soil) once the cumulative drainage volume was higher than 300 to 350 mm (Fig. 5). This peak lasted for 1 to 2 mo (cumulative drainage to  $\sim$ 400–500 mm) followed by a long period with small and slow arrivals coincident with a very low drainage rate and soil water content. For the moraine soil, this atrazine peak occurred at the same time as the maximum concentration of bromide was reached, whereas for the gravel soil there was a delay of 7 d.

Atrazine degradation was confirmed by the detection of metabolites (mostly DEA). For the moraine soil, low DEA contents ( $<0.2 \mu\text{g L}^{-1}$ ) were measured during the initial atrazine breakthrough followed by a period with a gradual increase of DEA concentration with time, although some fluctuations occurred (Fig. 6). A significant increase in the concentration of DEA in the drainage water was observed after 340 d, coinciding with the atrazine peak of May 2015. A similar DEA pattern was observed for the gravel soil, even though atrazine contents remained close to the detection limit during the first 250 d. Desethylatrazine is considered less persistent (lower half-life) and more mobile (higher solubility) than atrazine, showing a high leaching potential to groundwater. Accordingly, significant leaching of DEA to the drainage water was observed.

### Bromide, Uranine, and Atrazine Breakthrough after Depth Injection

In the experiments with depth injection, similar bromide breakthrough curves as those for surface application were observed except that measured concentrations were higher and the peaks

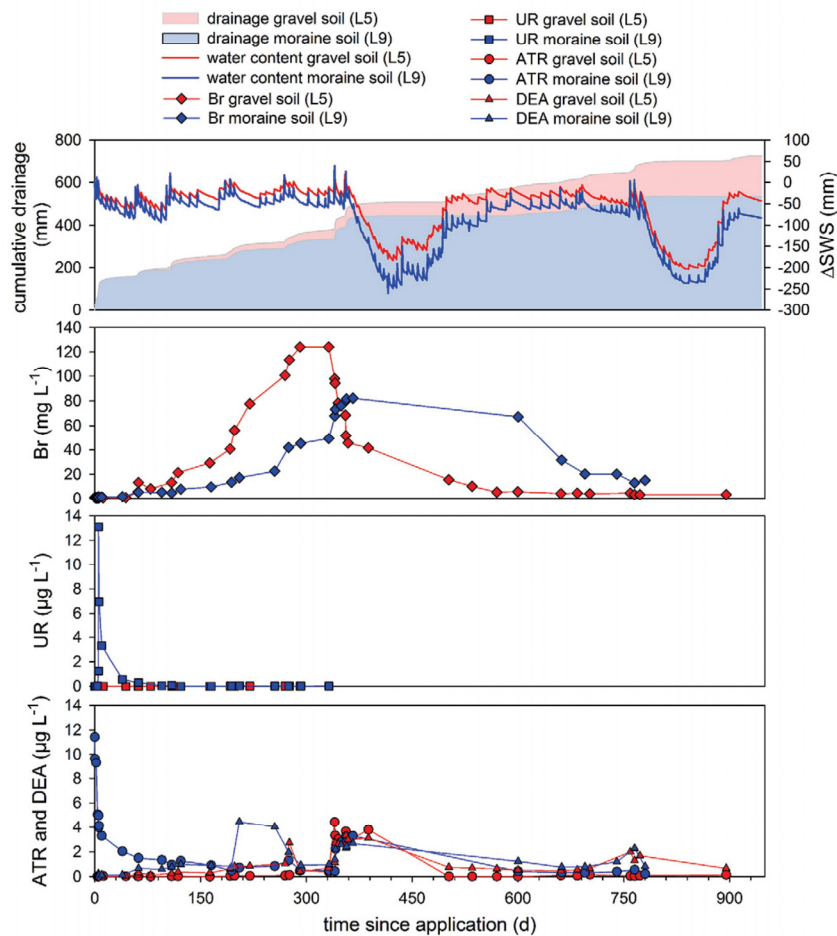


Fig. 5. Bromide (Br), uranine (UR), atrazine (ATR), and desethylatrazine (DEA) breakthrough curves after surface application in the gravel (Lysimeter L5) and moraine soils (Lysimeter L9). Cumulative drainage and changes in the soil water storage ( $\Delta$ SWS) for each lysimeter are also shown.

were reached earlier after only 180 to 220 mm of accumulated drainage (Fig. 6). Interestingly, maximum bromide concentrations were achieved at the same time in both soils, in contrast to observations for surface application (Table 4).

For the moraine soil, both uranine and atrazine early breakthrough peaks were reached after a small amount of accumulated drainage (<55 mm for both L6 and L7; Table 4), in line with observations for surface application. Maximum concentrations were higher and were achieved faster than with surface application in <24 h (up to 40  $\mu\text{g L}^{-1}$  uranine and up to 110  $\mu\text{g L}^{-1}$  atrazine; Fig. 6). For the gravel soil (L3 and L6), uranine and atrazine were also detected in the first leachates collected after injection, in contrast

to observations for surface application. A peak of up to 22  $\mu\text{g L}^{-1}$  uranine was achieved within 3 d (L6, much lower for L3), whereas the atrazine peak (up to 46  $\mu\text{g L}^{-1}$ ) was reached in 10 to 50 d (Table 4).

As in surface application, another atrazine peak was observed 330 to 340 d after injection ( $\sim$ 210–250 mm of accumulated drainage) in both soil types subsequent to intense irrigation (Fig. 6). Measured atrazine peak concentrations were higher than with surface application and higher for the gravel than the moraine soil. Interestingly, for both soil types, before the occurrence of this May 2015 peak, additional atrazine pulses were observed after intense irrigation events. The response to heavy irrigation was therefore

Table 4. Observed breakthrough parameters for atrazine (ATR), bromide (BR), and uranine (UR) in the lysimeters (L). Time and cumulative drainage values correspond to days passed and millimeters accumulated since application, respectively. Maximum concentrations are shown as the absolute and normalized by the applied mass ( $C/M_{\text{applied}}$ ) values.

Parameter	Gravel soil (L3)			Gravel soil (L4)			Gravel soil (L4)			Gravel soil (L4)		
	ATR	BR	UR	ATR	BR	UR	ATR	BR	UR	ATR	BR	UR
Time of first arrival, d	5.2	5.2	bd†	5.4	5.1	bd†	0.1	0.1	0.1	0.1	0.1	0.2
Time of peak conc., d	35.6	33.2	bd†	34.0	29.1	bd†	5.2	35.7	5.2	5.4	36.6	5.4
Max. conc., $\mu\text{g L}^{-1}$	2.8	$1.84 \times 10^5$	bd†	4.4	$1.24 \times 10^5$	bd†	30	$1.15 \times 10^5$	3.3	11	$8.21 \times 10^4$	13.1
Max. conc., $C/M_{\text{applied}}$	$4.2 \times 10^{-6}$	$1.5 \times 10^{-3}$	bd†	$6.7 \times 10^{-6}$	$1.0 \times 10^0$	bd†	$4.6 \times 10^{-5}$	$9.4 \times 10^{-1}$	$8.1 \times 10^{-6}$	$1.7 \times 10^{-5}$	$6.7 \times 10^{-1}$	$3.2 \times 10^{-5}$
Cumulative drainage at peak conc., mm	368	300	bd†	396	361	bd†	102	436	102	104	436	104
Time of final recovery, d	908	908	327	895	895	327	780	780	327	780	780	327
Final recovery, %	0.16	62.7	0.0003	0.22	57.8	0.0001	1.79	62.3	0.13	0.66	34.7	0.33
							Depth injection					
Time of first arrival, d	0.3	0.3	0.3	0.2	-	0.2	0.2	-	0.2	0.8	0.8	0.8
Time of peak conc., d	49	291	2.8	11	-	11	1.0	-	0.2	0.8	285	0.8
Max. conc., $\mu\text{g L}^{-1}$	33	$1.84 \times 10^5$	0.9	47	-	22	45	-	40	110	$1.18 \times 10^5$	27
Max. conc., $C/M_{\text{applied}}$	$5.0 \times 10^{-5}$	$1.5 \times 10^0$	$2.1 \times 10^{-6}$	$7.1 \times 10^{-5}$	-	$5.4 \times 10^{-5}$	$6.8 \times 10^{-5}$	-	$9.8 \times 10^{-5}$	$1.7 \times 10^{-4}$	$9.7 \times 10^{-1}$	$6.6 \times 10^{-5}$
Cumulative drainage at peak conc., mm	48	183	23	53	-	53	31	-	8	34	225	34
Time of total recovery, d	902	902	319	900	-	320	788	-	320	895	895	320
Total recovery, %	2.08	88.8	0.03	2.60	-	0.80	1.91	-	1.21	2.93	77.4	0.86

† bdl, below detection limit.

more significant than with surface application. During and right after application, a higher mass of atrazine was probably transported deeper in the lysimeters with depth than in the lysimeter with surface application, and therefore the increases in water and solute mass flux after these intense irrigation events triggered atrazine leaching. These additional pulses were more intense in the gravel than the moraine soil. Peak concentrations were considerably lower in these additional pulses than the initial breakthrough probably because of degradation and longer contact times, allowing the herbicides to diffuse into the less-mobile pore water. As in the surface application, slight pesticide breakthrough took place during the period with a very low drainage rate and soil water content (Fig. 6).

As observed with surface application, a continuous breakthrough of DEA was detected except for the first days after injection (Fig. 6). Some fluctuations in the DEA concentration were observed, coinciding with the atrazine peaks. The DEA concentrations were, in general, higher for the moraine than the gravel soil. Although biological activity and organic matter content decrease with depth (Table 1), the detection of DEA in the drainage water of the lysimeters in which atrazine was injected at 40 cm suggests that atrazine degradation occurred even at depths greater than 40 cm, albeit probably to a lesser extent than in surface application.

Therefore, atrazine (and DEA) leaching was driven by large drainage events for both application methods. Several intense irrigation events were performed during the monitoring period (Fig. 1; Table 3), which led to increases in the drainage volume consistent with the change in the soil water content. The event following atrazine application (May–June 2014) and the one performed in May 2015 (340 d after application) resulted in the two main atrazine leaching events (Fig. 5 and 6). Between 30 May and 5 June 2014 for lysimeters with surface application and between 30 May and 13 June 2014 for lysimeters with depth injection, ~175 mm of irrigation was applied. Between 6 and 21 May 2015, 160 mm was irrigated. These amounts are significantly higher than the water applied during other heavy irrigation events (Fig. 1; Table 3). These findings



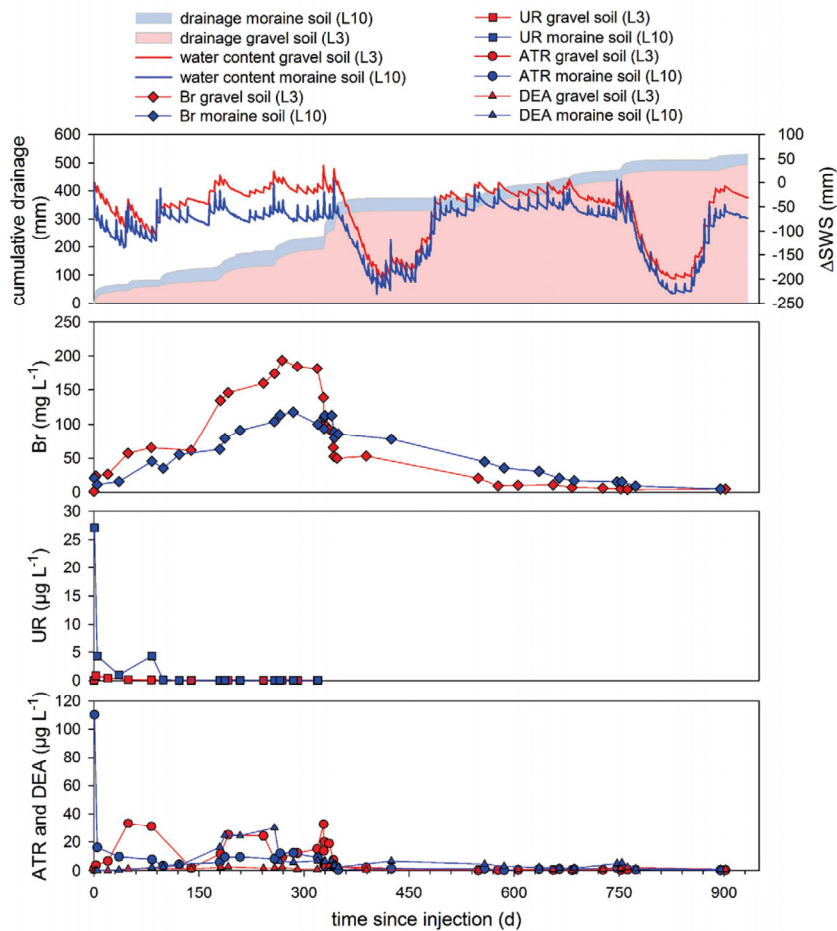


Fig. 6. Bromide (Br), uranine (UR), atrazine (ATR), and desethylatrazine (DEA) breakthrough curves after depth injection in the gravel (Lysimeter L3) and moraine soils (Lysimeter L10). Cumulative drainage and changes in the soil water storage ( $\Delta SWS$ ) for each lysimeter are also shown.

are consistent with previous studies that have shown that pesticide preferential flow increases with irrigation intensity (Edwards et al., 1992; McGrath et al., 2010). Nevertheless, the occurrence of macropore flow seems to depend also on the soil water content. Some studies have found that wetter soils tend to generate more macropore flow than drier soils as a result of reduced lateral losses into the soil matrix (Beven and Germann, 1982; Greve et al., 2010; Jarvis, 2007) and that higher antecedent soil water content increases the depth to which macropore flow penetrates (Greve et al., 2010). Other field studies have shown, however, that antecedent wetness does not necessarily govern preferential flow occurrence (Flury et al., 1994; Hardie et al., 2011). This is also consistent with the nonequilibrium flow theory (Jarvis, 2007), which indirectly implies that water flow

through macropores occurs independently of antecedent wetness conditions (Beven and Germann, 2013). In the present experiments, the relationship between soil water content before irrigation and the occurrence of preferential flow was not straightforward (Supplemental Fig. S4). It seems that the occurrence of preferential flow is mainly governed by the intensity of the irrigation. The effect of the previous soil water content cannot be evaluated because, for the two heavy irrigation events that promoted significant preferential flow, antecedent wetness conditions were similar.

### Solute Mass Balances

At the end of the monitoring period (900 d after application), an average of 0.7% of the surface-applied atrazine mass was recovered

## D. Adsorbing vs. Nonadsorbing Tracers for Assessing Pesticide Transport

in the drainage water (0.2% for the gravel and 1.2% for the moraine soil), similar to what was observed for uranine (up to 0.3%) (Table 4). Similar low recoveries of atrazine in drainage water (0.01–0.5%) have been previously reported in subsurface-drained fields and in lysimeters (Hall et al., 1991; Kladvik et al., 1991; Masse et al., 1996; Douset et al., 2004; Fortin et al., 2002). Higher recoveries were obtained with depth injection: 2.3% for the gravel and 2.4% for the moraine soil, which are on the same order of magnitude than the uranine recovery (up to 1.2%) (Table 4). In both soil types, recovery of DEA in the drainage water 900 d after atrazine application corresponded to only 0.4 and 1.8% of the atrazine applied mass for surface and depth application, respectively.

Pesticide residues in the crops were not measured, but Roeth and Lavy (1971) reported 12 to 23% uptake of  $^{14}\text{C}$ -atrazine by corn after 4 wk of growth in sandy-loamy soil in laboratory experiments. Furthermore, no residues of atrazine were detected in the 0- to 10-cm soil layer 2 yr after application.

Assuming similar atrazine uptake by the crop as that found by Roeth and Lavy (1971), in the present experiments at least 73% of the applied atrazine was therefore degraded or sorbed to the soil particles. Based only on the concentration of atrazine and DEA, quantification of atrazine (and DEA) degradation is not possible

because of several issues such as further transformation of DEA, production of other metabolites in addition to DEA (e.g., DIA and atrazine-2-hydroxy), selective sorption, or new recharge of atrazine into the system. Here, compound-specific isotope analysis may serve as a complementary tool to identify and quantify pesticide degradation (Fenner et al., 2013; Meyer and Elsner, 2013).

The present experiments were performed using free-drainage lysimeters, where water is allowed to drain freely through the soil under gravity. The lower boundary of the lysimeter is exposed to atmospheric pressure, and therefore, because of the disruption of the hydraulic gradient, a water-saturated zone must form at the bottom of the lysimeter before water can drain. In general, such a local saturation does not occur in the field. However, in the case of soils with tube drainage, free-draining lysimeters might be an accurate representation of field conditions. Modeling and experimental studies comparing solute transport in free-drainage lysimeters and under field conditions have reported differences in relation to soil texture, water fluxes, pore-water velocity, soil heterogeneity, sorption, and solute leaching (Flury et al., 1999; Abdou and Flury, 2004; Kasteel et al., 2007, 2010; Boesten, 2007). Therefore, the results of the present experiments need to be used with caution when transferring to field conditions, especially in the case of the moraine soil, where significant preferential flow occurred and

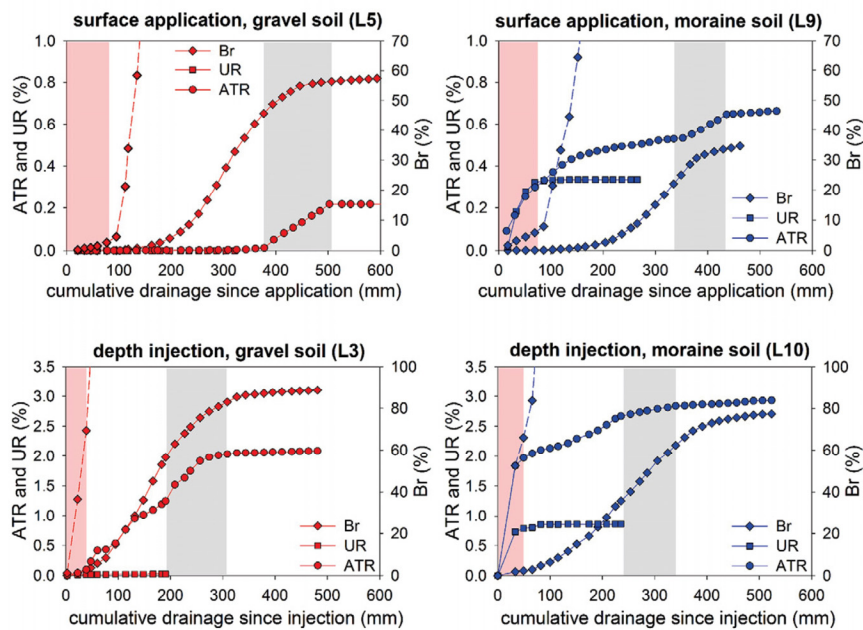


Fig. 7. Atrazine (ATR), bromide (Br), and uranine (UR) breakthrough curves against cumulative drainage for the four combinations of application method and soil type. Note that the scale for bromide recovery (solid lines) is different than for the other two solutes. For comparison during the first 150 mm, bromide curves are also shown using the same scale as for atrazine and uranine (dashed lines). The shaded areas show the two main irrigation and drainage events.

therefore the amount of atrazine leached might be underestimated (Vercecken and Dust, 1998; Abdou and Flury, 2004).

Total bromide recovery was between 35 and 63% of the applied mass for surface application and between 77 and 89% for depth injection (Table 4). Higher recoveries were achieved in the gravel than the moraine soil. Therefore, total recoveries of bromide 900 d after application were  $\sim 40$  and 100 times higher than for atrazine and uranine, respectively. The removal of bromide by harvested plant products was low. With surface application, 10 to 13% of the applied bromide was found in corn plants harvested 3 mo after application, and between 0.1 and 1% was removed by sugarbeet harvested 17 mo after application. As expected, because of the deeper injection, the removal of bromide by plant uptake and harvesting was lower with depth injection than with surface application (5–7% for corn and 0.1–0.3% for sugarbeet). Similarly, in a previous experiment on the same lysimeters, 3.5 to 3.9% of the applied bromide was found in corn harvested 3 mo after application (Prasuhn et al., 2015). On other lysimeters at the same site, Prasuhn et al. (2015) measured 3.0 to 4.2% of the applied bromide in sugarbeet harvested 5 mo after application.

### Comparison of the Behavior of Pesticides and Adsorbing and Nonadsorbing Tracers

For evaluating the use of adsorbing fluorescent dye tracers (uranine) and conservative nonadsorbing tracers (bromide) as a proxy to assess pesticide (atrazine) transport processes in agricultural soils, the behavior of the three solutes was compared. Because pesticide leaching is governed by drainage, this comparison was performed in terms of breakthrough against accumulated drainage (Fig. 7) for the four combinations of soil type and application method. Most of the discussion is focused on the ability of the tracers to indicate the potential for pesticide leaching by preferential flow. The periods with the most intense irrigation and drainage are highlighted.

With surface application, rapid breakthrough of the three solutes was observed a few hours or days after application within 100 mm of accumulated drainage in the moraine soil but not in the gravel soil (Fig. 7). Recoveries in the drainage water of the moraine soil lysimeters (L8 and L9) during this early preferential transport ranged from 0.4 to 1.0% for atrazine, from 0.3 to 0.6% for bromide, and between 0.1 and 0.4% for uranine (Fig. 7). The small amount of accumulated drainage needed for uranine and atrazine peaks to occur (Fig. 5) suggests that both solutes were mainly transported through preferential flow, bypassing large fractions of the soil matrix. The pronounced peak tailing for both solutes (Fig. 5) is also typical of preferential flow (Brusseau and Rao, 1990). It is commonly accepted that high precipitation or irrigation shortly after application increases the losses through macropores (Kördel et al., 2008), as was observed in the present experiments. Accordingly, detection of pesticides and non-conservative tracers in leachate within a few hours or days after irrigation has been

previously observed at the laboratory and field scales and attributed to preferential flow (Kladivko et al., 1991; Kanwar et al., 1997; Kung et al., 2000; Haws et al., 2004). In the present experiments, the effect was more significant for the moraine than the gravel soil. Probably several dead-end macropores in the moraine soil were formed because the lysimeters were filled up and these macropores were well preserved, at least below 20 cm, where they are not destroyed by tillage practices.

With depth injection, more intense early preferential breakthrough than for surface application was detected for the three solutes within a few days and after  $< 50$  mm of accumulated drainage (Fig. 7). Early preferential breakthrough occurred in both soil types, although it was more significant for the moraine soil. Recoveries were higher than for surface application: up to 1.0 and 1.8% for atrazine, up to 1.3 and 1.8% for bromide, and up to 0.7 and 0.9% for uranine in the gravel (L3 and L6) and moraine soils (L7 and L10), respectively.

During the early breakthrough, although for the three solutes similar recoveries were measured, uranine was a better marker than bromide for illustrating this preferential transport. In the moraine soil, independent of the application method, both atrazine and uranine broke through during the first intense irrigation; in the gravel soil, both of them were below or close to the detection limit. Uranine always showed the same trend as atrazine when preferential flow occurred (Fig. 7). Furthermore, when atrazine was not detected in the drainage water, uranine was not detected either. Bromide mimicked early preferential atrazine leaching for the moraine soil with depth application but failed for the other combinations of soil type and application method (Fig. 7). In some cases, bromide appeared early but neither atrazine nor uranine was present, suggesting that rapid transport occurred along flow paths with a substantial sorption capacity. Only between 0.1 and 2.5% of the total mass of bromide accumulating in the drainage water was recovered during the early preferential breakthrough, whereas for uranine and atrazine this fraction ranged from 11 to 88%.

After the early breakthrough, the two tracers—uranine and bromine—continued to show a contrasting behavior. Bromide breakthrough curves showed a characteristic asymmetric sigmoidal shape for transport through a porous matrix irrespective of surface or depth injection (Fig. 7). For both application methods, bromide breakthrough in the gravel soil was higher and was achieved more rapidly than in the moraine soil in accordance with the lower water retention capacity of the former (Fig. 7). In stark contrast, the uranine recovery did not increase any more. In contrast to bromide, the smoother breakthrough curves of atrazine suggest that atrazine transport through the soil matrix was retarded by sorption and attenuated by degradation. A steady increment in accumulated mass recovery was observed for atrazine and bromide but not for uranine (Fig. 7). Retardation was, therefore, more significant for uranine than for atrazine, especially for surface



application. Sabatini and Austin (1991) compared the sorption of atrazine and uranine in an alluvial sand with a low organic matter content in laboratory experiments and found similar sorption coefficient values ( $K_{oc}$  of  $120 \text{ cm}^3 \text{ g}^{-1}$  for uranine and  $148 \text{ cm}^3 \text{ g}^{-1}$  for atrazine), although different sorption mechanisms were proposed. Sorption of uranine, because of its high polarity and ionizable nature, is dominated by electrostatic rather than hydrophobic interactions and thus is more dependent on mineralogy than organic content. Uranine shows higher sorption to positively charged surfaces such as limestones or carbonates at neutral pH (Kasnavia et al., 1999). This different sorption mechanism might be the cause of the different atrazine and uranine retardation observed in the present experiments.

The DEA/atrazine molar ratio (DAR) is often used as a proxy for atrazine degradation in the environment (Adams and Thurmann, 1991). With surface application, higher DAR values were measured for the gravel (up to 49) than the moraine soil (up to 7) during the first 340 d (Supplemental Fig. S5), suggesting that the extent of atrazine degradation was higher for the gravel soil or that DEA moved more rapidly through the soil matrix because of higher permeability. This difference in DAR values is consistent with the greater contribution of preferential flow in the moraine soil, which bypasses the top layer where degradation mostly takes place. During the first 340 d, lower DAR values were measured for depth injection than for surface application (up to 1 for the gravel and up to 4 for the moraine soil). Because by depth injection the atrazine molecules were emplaced deeper, they persisted longer in the soil matrix and slower degradation occurred. Similarly, Kruger et al. (1997) found that atrazine application in subsurface soils (90–120 cm) compared with surface soils (0–30 cm) resulted in greater persistence and more mobility during the subsequent drainage periods. Similar results were obtained by Delphin and Chapot (2006) for atrazine injection at different depths (30 and 80 cm). The maximum depth of macropores might therefore have a significant effect on the persistence and mobility of the applied pesticides. Deeper macropores would result in high pesticide mass fluxes to shallow groundwater. The results of the present experiments show that degradation of atrazine occurred not only in the microbiologically active topsoil but also deeper in the soil profile because DEA was also detected in the drainage water of the lysimeters in which atrazine was injected at 40 cm.

The heavy irrigation performed 340 d after solute application promoted leaching of atrazine and DEA molecules that were retained in the soil matrix for both surface (Fig. 5) and depth applications (Fig. 6). Between 0.1 and 0.8% of the atrazine applied mass was recovered during this May 2015 breakthrough, whereas this fraction corresponded to 20 to 30% of the applied bromide. Whereas no changes were observed in the sigmoidal shape of the bromide curves, sharp recovery increases were detected for atrazine at this time (Fig. 7). Atrazine leaching during this breakthrough appeared

to be of slightly higher significance in the gravel than the moraine soil (Fig. 7). For bromide, transport occurred mainly through the matrix in the two soils, whereas atrazine leaching was dominated by large drainage events when a greater contribution of preferential flow probably occurred.

Uranine concentration in the drainage water was monitored only during the first 330 d after application. A second uranine application was performed at this time. Although not included here, the results suggest rapid uranine arrival after application, coinciding in time with the May 2015 atrazine peak. Although most of the leached mass is expected to be related to the second application, the contribution of the uranine applied in 2014 cannot be excluded. The suitability of uranine for mimicking the second atrazine breakthrough was therefore not evaluated.

### Conclusions

Evaluation of pesticide transport through arable soils using dye tracers has been done so far at the laboratory scale (e.g., Sabatini and Austin, 1991) or with tile-drainage plots (e.g., Czapar et al., 1994) but not with large lysimeters. Large lysimeters are more likely to mimic natural soils than laboratory column experiments. Furthermore, greater control over environmental factors and more precise solute mass balances are achieved with lysimeters than with drainage plots. Using large lysimeters, we demonstrated that uranine is a more realistic marker than bromide for early atrazine preferential breakthrough shortly after pesticide application. Uranine broke through during the first intense irrigation event at the same time as atrazine. Bromide, however, appeared in some cases earlier than atrazine.

The rapid preferential atrazine breakthrough was more significant for the moraine than the gravel soil and, as expected, more evident after depth injection. In the moraine soil, more macropores were probably formed with time and were better preserved because of the clayey matrix. The high soil water content present before atrazine application, the heavy irrigation applied just after, and the low ET promoted preferential flow. This movement bypassed large fractions of the soil matrix, reducing the degradation and sorption potential, and therefore high atrazine and low DEA contents were detected in the drainage water. During the slow atrazine transport by matrix flow, the concentration in the drainage water was higher for the lysimeters with depth injection, as expected for the deeper starting point of migration. Atrazine and uranine concentrations during leaching via matrix flow were greatly reduced by sorption and degradation. The detection of DEA in the drainage water confirmed herbicide degradation, although sorption to the soil particles was probably the main retardation factor in atrazine transport. Atrazine leaching was driven by large drainage events, when a greater contribution of preferential flow probably occurred. As a consequence, another atrazine breakthrough peak occurred 10 mo after application.



For both surface and depth application approaches, bromide was transported by both matrix and preferential flow. However, because preferential flow accounts for only a small fraction of water flow, the bromide breakthrough curve was dominated by the matrix flow component. In contrast, atrazine and uranine are retained or degraded in the matrix, and leaching was dominated by large drainage events when preferential flow occurs.

In the present experiments, uranine was a reliable marker for atrazine breakthrough shortly after atrazine application. Atrazine represents a realistic worst case of pesticide leaching because of its moderate mobility and relatively low adsorption coefficient. For extending the use of sorbing dye tracers as a surrogate of other pesticides, tracers with similar mobility as the target compound should be chosen.

Overall, these results point to the potential use of uranine as a surrogate of atrazine for preferential leaching shortly after application. Uranine also may be a valuable tool for evaluating the potential of preferential flow in different soil types. Uranine application may therefore be used for rapid screening of the possibility of inducing preferential flow in a given soil. Application of uranine might also help to delimit the threshold range of soil water content, rain amount, and intensity that induces a given degree of early preferential flow. The application of dye tracers at the same time as the pesticides may also be used as a low-cost approach in pesticide risk studies and thus applying measures to limit irrigation and potential threats to groundwater—however, only for assessing rapid pesticide leaching by preferential flow. The use of dye tracers as pesticide surrogates might assist in making sustainable decisions with respect to pesticide application timing relative to rainfall, application method, or rainfall or irrigation regime.

### Supplemental Material

The supplemental material includes pictures of the Agroscope lysimeters facility, water balance components for Lysimeter L4, evapotranspiration and air temperature data, DAR trends, results for the first 375 d after application or injection, and average monthly sums of the water-balance components from the two soil types.

### Acknowledgments

This study was supported by the project CRSII2\_141805/1 from the Swiss National Science Foundation (SNSF). We are grateful to Clay Humphrys and Karin Meier Zimmermann (Agroscope) for technical assistance with field work on the lysimeter facility. We also want to thank the Plateforme neuchâtoise de chimie analytique (NPAC) for their services and Vincent Gruber, Roberto Costa, and Laurent Marguet (University of Neuchâtel) for their help during the setting up and monitoring of the lysimeter experiments. We thank the associate editor (Dr. Markus Flury) and three anonymous reviewers for comments that improved the quality of the manuscript.

### References

- Abdou, H.M., and M. Flury. 2004. Simulation of water flow and solute transport in free-drainage lysimeters and field soils with heterogeneous structures. *Eur. J. Soil Sci.* 55:229–241. doi:10.1046/j.1365-2389.2004.00592.x
- Adams, C.D., and E.M. Thurmann. 1991. Formation and transport of deethylatrazine in the soil and vadose zone. *J. Environ. Qual.* 20:540–547. doi:10.2134/jeq1991.00472425002000030007x
- Albisser, C., and V. Prasuhn. 2013. Auswirkungen des Klimawandels auf die Schadstoffverfrachtung ins Grundwasser: Projekt-Schlussbericht, Studie im Auftrag des BAFU. Publ. Forschungsanstalt Agroscope Reckenholz-Tänikon ART, Zürich.
- Barracough, D., T. Kearney, and A. Croxford. 2005. Bound residues: Environmental solution or future problem? *Environ. Pollut.* 133:85–90. doi:10.1016/j.envpol.2004.04.016
- Bech, T.B., A.E. Rosenbom, S.R. Sørensen, and C.S. Jacobsen. 2017. Conservative tracer bromide inhibits pesticide mineralisation in soil. *Environ. Pollut.* 222:404–411. doi:10.1016/j.envpol.2016.12.016
- Bergström, L. 1990. Use of lysimeters to estimate leaching of pesticides in agricultural soils. *Environ. Pollut.* 67:325–347. doi:10.1016/0269-7491(90)90070-5
- Bergström, L. 2000. Leaching of agrochemicals in field lysimeters: A method to test mobility of chemicals in soil. In: J. Cornejo et al., editors, *Pesticide/soil interactions: Some current research methods*. INRA, Paris.
- Beven, K., and P. Germann. 1982. Macropores and water flow in soils. *Water Resour. Res.* 18:1311–1325. doi:10.1029/WR018i005p01311
- Beven, K., and P. Germann. 2013. Macropores and water flow in soils revisited. *Water Resour. Res.* 49:3071–3092. doi:10.1002/wrcr.20156
- Boesten, J.J.T.I. 2007. Simulation of pesticide leaching in the field and in zero-tension lysimeters. *Vadose Zone J.* 6:793–804. doi:10.2136/vzj2007.0067
- Bouma, J., and L.W. Dekker. 1978. A case study on infiltration into dry clay soil: I. Morphological observations. *Geoderma* 20:27–40. doi:10.1016/0016-7061(78)90047-2
- Bowman, B.T. 1990. Mobility and persistence of alachlor, atrazine and metolachlor in Plainfield sand, and atrazine and isozofos in Honeywood silt loam using field lysimeters. *Environ. Toxicol. Chem.* 9:453–461. doi:10.1002/etc.5620090406
- Brown, C.D., J.M. Hollis, R.J. Bettinson, and A. Walker. 2000. Leaching of pesticides and a bromide tracer through lysimeters from five contrasting soils. *Pest Manage. Sci.* 56:83–93. doi:10.1002/(SICI)1526-4998(200001)56:1<83::AID-P598>3.0.CO;2-8
- Brusseau, M.L., and P.S.C. Rao. 1990. Modeling solute transport in structured soils: A review. *Geoderma* 46:169–192. doi:10.1016/0016-7061(90)90014-7
- Burnett, G., K. Balu, H. Barton, W. Chen, B. Gold, P. Herli, et al. 2000. Summary of environmental fate of atrazine. Study No. 1213-99. Novartis Crop Protection, Greensboro, NC.
- Calderbank, A. 1989. The occurrence and significance of bound pesticide residues in soil. *Rev. Environ. Contam. Toxicol.* 108:71–103. doi:10.1007/978-1-4613-8850-0\_2
- Capriel, P., A. Haisch, and S.U. Khan. 1985. Distribution and nature of bound (nonextractable) residues of atrazine in a mineral soil nine years after the herbicide application. *J. Agric. Food Chem.* 33:567–569. doi:10.1021/jf00064a004
- Cey, E.E., and D.L. Rudolph. 2009. Field study of macropore flow processes using tension infiltration of a dye tracer in partially saturated soils. *Hydrol. Processes* 23:1768–1779. doi:10.1002/hyp.7302
- Czapar, G.F., R.S. Kanwar, and R.S. Fawcett. 1994. Herbicide and tracer movement to field drainage tiles under simulated rainfall conditions. *Soil Tillage Res.* 30:19–32. doi:10.1016/0167-1987(94)90148-1
- D'Archivio, A.A., M. Fanelli, P. Mazzeo, and F. Ruggieri. 2007. Comparison of different sorbents for multiresidue solid-phase extraction of 16 pesticides from groundwater coupled with high-performance liquid chromatography. *Talanta* 71:25–30. doi:10.1016/j.talanta.2006.03.016
- Delphin, J.E., and J.Y. Chapot. 2006. Leaching of atrazine, metolachlor and diuron in the field in relation to their injection depth into a silt loam soil. *Chemosphere* 64:1862–1869. doi:10.1016/j.chemosphere.2006.01.049
- Doussel, S., M. Babut, F. Andreux, and M. Schiavon. 2004. Alachlor and bentazone losses from subsurface drainage of two soils. *J. Environ. Qual.* 33:294–301. doi:10.2134/jeq2004.2940
- Doussel, S., C. Mouvet, and M. Schiavon. 1995. Leaching of atrazine and some of its metabolites in undisturbed field lysimeters of three soil types. *Chemosphere* 30:511–524. doi:10.1016/0045-6535(94)00414-P
- Edwards, W.M., M.J. Shipitalo, W.A. Dick, and L.B. Owens. 1992. Rainfall intensity affects transport of water and chemicals through macropores in no-till soil. *Soil Sci. Soc. Am. J.* 56:52–58. doi:10.2136/sssaj1992.03615995005600010008x
- Everts, C.J., and R.S. Kanwar. 1990. Estimating preferential flow to a subsurface drain with tracers. *Trans. ASAE* 33:451–457. doi:10.13031/2013.31350
- Everts, C.J., and R.S. Kanwar. 1994. Evaluation of Rhodamine WT as an adsorbed tracer in an agricultural soil. *J. Hydrol.* 153:53–70. doi:10.1016/0022-1694(94)90186-4
- Everts, C.J., R.S. Kanwar, E.C. Alexander, and S.C. Alexander. 1989.

## D. Adsorbing vs. Nonadsorbing Tracers for Assessing Pesticide Transport

- Comparison of tracer mobilities under laboratory and field conditions. *J. Environ. Qual.* 18:491–498. doi:10.2134/jeq1989.00472425001800040018x
- Fank, J. 2009. Tracerhydrologie in der Lysimetrie. In: 13th Gumpenstein Lysimeterlagung zum Thema Lysimeter: Perspektiven in Forschung und Anwendung, Raumberg. 21–22 Apr. 2009. Höhere Bundeslehr- und Forschungsanstalt für Landwirtschaft, Raumberg, Austria. p. 63–68.
- Fenner, K., S. Canonica, L.P. Wackelt, and M. Elsner. 2013. Evaluating pesticide degradation in the environment: Blind spots and emerging opportunities. *Science* 341:752–758. doi:10.1126/science.1236281
- Flury, M., H. Flüher, W.A. Jury, and J. Leuenberger. 1994. Susceptibility of soils to preferential flow of water: A field study. *Water Resour. Res.* 30:1945–1954. doi:10.1029/1994WR00871
- Flury, M., and N.N. Wai. 2003. Dyes as tracers for vadose zone hydrology. *Rev. Geophys.* 41:1002. doi:10.1029/2001RG000109
- Flury, M., M.V. Yates, and W.A. Jury. 1999. Numerical analysis of the effect of the lower boundary condition on solute transport in lysimeters. *Soil Sci. Soc. Am. J.* 63:1493–1499. doi:10.2136/sssaj1999.6361493x
- Fortin, J., E. Gagnon-Bertrand, L. Vézina, and M. Rompré. 2002. Preferential bromide and pesticide movement to tile drains under different cropping practices. *J. Environ. Qual.* 31:1940–1952. doi:10.2134/jeq2002.1940
- Francoaviglia, R., and E. Capri. 2000. Lysimeter experiments with metolachlor in Tor Mancina (Italy). *Agric. Water Manage.* 44:63–74. doi:10.1016/S0378-3774(99)00084-0
- Gevao, B., K.T. Semple, and K.C. Jones. 2000. Bound pesticide residues in soils: A review. *Environ. Pollut.* 108:3–14. doi:10.1016/S0269-7491(99)00197-9
- Greve, A., M.S. Andersen, and R.I. Acworth. 2010. Investigations of soil cracking and preferential flow in a weighing lysimeter filled with cracking clay soil. *J. Hydrol.* 393:105–113. doi:10.1016/j.jhydrol.2010.03.007
- Hall, J.K., R.O. Mumma, and D.W. Walls. 1991. Leaching and runoff losses of herbicides in a filled and unfilled field. *Agric. Ecosyst. Environ.* 37:303–314. doi:10.1016/0167-8809(91)90158-T
- Hannes, M., U. Wollschläger, F. Schrader, W. Durner, S. Gebler, T. Pütz, et al. 2015. A comprehensive filtering scheme for high-resolution estimation of the water balance components from high-precision lysimeters. *Hydrol. Earth Syst. Sci.* 19:3405–3418. doi:10.5194/hess-19-3405-2015
- Hardie, M., W.E. Cotching, R.B. Doyle, G. Holz, S. Lisson, and K. Mattern. 2011. Effect of antecedent soil moisture on preferential flow in a texture-contrast soil. *J. Hydrol.* 398:191–201. doi:10.1016/j.jhydrol.2010.12.008
- Haws, N.W., B.S. Das, and P.S.C. Rao. 2004. Dual-domain solute transfer and transport processes: Evaluation in batch and transport experiments. *J. Contam. Hydrol.* 75:257–280. doi:10.1016/j.jconhyd.2004.07.001
- Jablonski, N.D., S. Köppchen, D. Hofmann, A. Schäffer, and P. Burauel. 2009. Persistence of <sup>14</sup>C-labeled atrazine and its residues in a field lysimeter soil after 22 years. *Environ. Pollut.* 157:2126–2131. doi:10.1016/j.envpol.2009.02.004
- Jablonski, N.D., A. Linden, S. Köppchen, B. Thiele, D. Hofmann, W. Mittelstaedt, et al. 2012. Long-term persistence of various <sup>14</sup>C-labeled pesticides in soils. *Environ. Pollut.* 168:29–36. doi:10.1016/j.envpol.2012.04.022
- Jablonski, N.D., J. Modler, A. Schaeffer, and P. Burauel. 2008. Bioaccessibility of environmentally aged <sup>14</sup>C-atrazine residues in an agriculturally used soil and its particle-size aggregates. *Environ. Sci. Technol.* 42:5904–5910. doi:10.1021/es800196z
- Jacobsen, O.H., and J. Kjær. 2007. Is tile drainage water representative of root zone leaching of pesticides? *Pest Manage. Sci.* 63:417–428. doi:10.1002/ps.1372
- Jarvis, N.J. 2007. A review of non-equilibrium water flow and solute transport in soil macropores: Principles, controlling factors and consequences for water quality. *Eur. J. Soil Sci.* 58:523–546. doi:10.1111/j.1365-2389.2007.00915.x
- Jaynes, D.B., S.I. Ahmed, and K.-J.S. Kung. 2001. Temporal dynamics of preferential flow to a subsurface drain. *Soil Sci. Soc. Am. J.* 65:1368–1376. doi:10.2136/sssaj2001.6551368x
- Kanwar, R.S., J.L. Baker, and P. Singh. 1997. Use of chloride and fluorescent dye as tracers in measuring nitrate and atrazine transport through soil profile under laboratory conditions. *J. Environ. Sci. Health A* 32:1907–1919. doi:10.1080/10934529709376654
- Kasnavia, T., D. Vu, and D.A. Sabatini. 1999. Fluorescent dye and media properties affecting sorption and tracer selection. *Ground Water* 37:376–381. doi:10.1111/j.1745-6584.1999.tb01114.x
- Kasteel, R., M. Burkhardt, S. Giesa, and H. Vereecken. 2005. Characterization of field tracer transport using high-resolution images. *Vadose Zone J.* 4:101–111. doi:10.2113/4.1.101
- Kasteel, R., T. Pütz, J. Vanderborght, and H. Vereecken. 2010. Fate of two herbicides in zero-tension lysimeters and in field soil. *J. Environ. Qual.* 39:1451–1466. doi:10.2134/jeq2009.0236
- Kasteel, R., T. Pütz, and H. Vereecken. 2007. An experimental and numerical study on flow and transport in a field soil using zero-tension lysimeters and suction plates. *Eur. J. Soil Sci.* 58:632–645. doi:10.1111/j.1365-2389.2006.00850.x
- Kladivko, E.J., G.E. Van Scoyoc, E.J. Monke, K.M. Oates, and W. Pask. 1991. Pesticide and nutrient movement into subsurface tile drains on a silt loam soil in Indiana. *J. Environ. Qual.* 20:264–270. doi:10.2134/jeq1991.00472425002000010043x
- Kodešová, R., K. Němeček, V. Kodeš, and A. Žigová. 2012. Using dye tracer for visualization of preferential flow at macro- and microscales. *Vadose Zone J.* 11(1). doi:10.2136/vzj2011.0088
- Kolpin, D.W., E.M. Thurman, and S.M. Linhart. 1998. The environmental occurrence of herbicides: The importance of degradates in ground water. *Arch. Environ. Contam. Toxicol.* 35:385–390. doi:10.1007/s002449900392
- Kolpin, D.W., E.M. Thurman, and S.M. Linhart. 2000. Finding minimal herbicide concentrations in ground water? Try looking for their degradates. *Sci. Total Environ.* 248:115–122. doi:10.1016/S0048-9697(99)00535-5
- Kördel, W., H. Egli, and M. Klein. 2008. Transport of pesticides via macropores (IUPAC Technical Report). *Pure Appl. Chem.* 80:105–160. doi:10.1351/pac20080010105
- Kung, K.-J.S., T.S. Steenhuis, E.J. Kladivko, T.J. Gish, G. Bubenzer, and C.S. Helling. 2000. Impact of preferential flow on the transport of adsorbing and non-adsorbing tracers. *Soil Sci. Soc. Am. J.* 64:1290–1296. doi:10.2136/sssaj2000.6441290x
- Kruger, E.L., P.J. Rice, J.C. Anhalt, T.A. Anderson, and J.R. Coats. 1997. Comparative fates of atrazine and deethylatrazine in sterile and nonsterile soils. *J. Environ. Qual.* 26:95–101. doi:10.2134/jeq1997.00472425002600010015x
- Lange, J., T. Schuetz, C. Gregoire, D. Elsässer, R. Schulz, E. Passeport, and J. Tournebise. 2011. Multi-tracer experiments to characterize contaminant mitigation capacities for different types of artificial wetlands. *Int. J. Environ. Anal. Chem.* 91:768–785. doi:10.1080/03067319.2010.525635
- Leistra, M., and J.J.T.I. Boesten. 1989. Pesticide contamination of groundwater in Western Europe. *Agric. Ecosyst. Environ.* 26:369–389. doi:10.1016/0167-8809(89)90018-2
- Lennartz, B., J. Michaelsen, P. Widmoser, and W. Wichtmann. 1999. Time variance analysis of preferential solute movement at a tile-drained field site. *Soil Sci. Soc. Am. J.* 63:39–47. doi:10.2136/sssaj1999.03615995006300010007x
- Lewis, K.A., J. Trilivakis, D. Warner, and A. Green. 2016. An international database for pesticide risk assessments and management. *Hum. Ecol. Risk Assess.* 22:1050–1064. doi:10.1080/10807039.2015.1133242
- Loos, R., G. Locoro, S. Comero, S. Contini, D. Schwesig, F. Werres, et al. 2010. Pan-European survey on the occurrence of selected polar organic persistent pollutants in ground water. *Water Res.* 44:4115–4126. doi:10.1016/j.watres.2010.05.032
- Lopez, B., P. Ollivier, A. Togola, N. Baran, and J.P. Ghestem. 2015. Screening of French groundwater for regulated and emerging contaminants. *Sci. Total Environ.* 518-519:562–573. doi:10.1016/j.scitotenv.2015.01.110
- Maillard, E., J. Lange, S. Schreiber, J. Dollinger, B. Herbstreit, M. Millet, and G. Imfeld. 2016. Dissipation of hydrological tracers and the herbicide 5-metolachlor in batch and continuous-flow wetlands. *Chemosphere* 144:2489–2496. doi:10.1016/j.chemosphere.2015.11.027
- Masse, L., N.K. Patni, P.Y. Jui, and B.S. Clegg. 1996. Tile effluent quality and chemical losses under conventional and no tillage: 2. Atrazine and metolachlor. *Trans. ASAE* 39:1673–1679. doi:10.13031/2013.27684
- McGrath, G.S., C. Hinz, M. Sivapalan, J. Dressel, T. Pütz, and H. Vereecken. 2010. Identifying a rainfall event threshold triggering herbicide leaching by preferential flow. *Water Resour. Res.* 46:W02513. doi:10.1029/2008WR007506
- Mendaš, G., V. Drevenkar, and L. Zupancic-Kralj. 2001. Solid-phase extraction with styrene-divinylbenzene sorbent for high-performance liquid or gas chromatographic determination of urinary chloro- and methylthio-triazines. *J. Chromatogr. A* 918:351–359. doi:10.1016/S0021-9673(01)00768-3
- Meyer, A.H., and M. Elsner. 2013. <sup>13</sup>C/<sup>12</sup>C and <sup>15</sup>N/<sup>14</sup>N isotope analysis to characterize degradation of atrazine: Evidence from parent and daughter compound values. *Environ. Sci. Technol.* 47:6884–6891. doi:10.1021/es305242q
- Mudhoo, A., and V.K. Garg. 2011. Sorption, transport and transformation of atrazine in soils, minerals and composts: A review. *Pedosphere* 21:1–25. doi:10.1016/S1002-0160(10)60074-4
- Nievergelt, J. 1997. Lysimeterversuch 1981 bis 1996: N-Auswaschung in Fruchfolgen. *Agrarforschung* 4:209–212.

- Nimmo, J.R. 2007. Simple predictions of maximum transport rate in unsaturated soil and rock. *Water Resour. Res.* 43:W05426. doi:10.1029/2006WR005372
- Passeport, E., J. Tournebise, S. Jankowsky, B. Prömse, C. Chaumont, Y. Coquet, and J. Lange. 2010. Artificial wetland and forest buffer zone: Hydraulic and tracer characterization. *Vadose Zone J.* 9:73–84. doi:10.2136/vzj2008.0164
- Peters, A., T. Nehls, H. Schonsky, and G. Wessolek. 2014. Separating precipitation and evapotranspiration from noise: A new filter routine for high-resolution lysimeter data. *Hydrol. Earth Syst. Sci.* 18:1189–1198. doi:10.5194/hess-18-1189-2014
- Pichon, V., C.C.D. Coumes, L. Chen, S. Guenu, and M.C. Hennion. 1996. Simple removal of humic and fulvic acid interferences using polymeric sorbents for the simultaneous solid-phase extraction of polar acidic, neutral and basic pesticides. *J. Chromatogr. A* 737:25–33. doi:10.1016/0021-9673(95)01339-3
- Prasuhn, V., E. Spiess, and C. Humphrys. 2015. Tracerversuche mit Bromid auf verschiedenen Lysimetern in der Schweiz. In: 16th Gumpensteiner Lysimetertagung zum Thema Lysimeter: Forschung im System Boden–Pflanze–Atmosphäre, Raumberg, Austria. 21–22. Apr. 2015. Höhere Bundeslehr- und Forschungsanstalt, Irdning-Steinach, Austria. p. 21–28.
- Renaud, F.G., C.D. Brown, C.J. Fryer, and A. Walker. 2004. A lysimeter experiment to investigate temporal changes in the availability of pesticide residues for leaching. *Environ. Pollut.* 131:81–91. doi:10.1016/j.envpol.2004.02.028
- Roeth, F.W., and T.L. Lavy. 1971. Atrazine uptake by sudangrass, sorghum, and corn. *Weed Sci.* 19:93–97. doi:10.1017/S0043174500048372
- Sabatini, D.A., and T. Austin. 1991. Characteristics of rhodamine WT and fluorescein as adsorbing ground-water tracers. *Ground Water* 29:341–349. doi:10.1111/j.1745-6584.1991.tb00524.x
- Schuhmann, A., O. Gans, S. Weiss, J. Fank, G. Klammler, G. Haberhauer, and M.H. Gerzabek. 2016. A long-term lysimeter experiment to investigate the environmental dispersion of the herbicide chloridazon and its metabolites: Comparison of lysimeter types. *J. Soils Sediments* 16:1032–1045. doi:10.1007/s11368-015-1311-3
- Steinheimer, T.R., and K.D. Scoggin. 2001. Fate and movement of atrazine, cyanazine, metolachlor and selected degradation products in water resources of the deep loess hills of southwestern Iowa, USA. *J. Environ. Monit.* 3:126–132. doi:10.1039/B006871N
- Suter, D., E. Rosenberg, E. Mosimann, and R. Frick. 2012. Standardmischungen für den Futterbau. Revision 2013–2016. *Agrarforsch. Schweiz* 3:1–12.
- Syngenta. 2005. Using atrazine and protecting water quality: A guide for corn/sorghum producers and sugarcane growers. GS 405.00001. Syngenta Crop Protection, Greensboro, NC.
- Troxler, J., M. Zala, A. Natsch, J. Nievergelt, C. Keel, and G. Défago. 1998. Transport of a biocontrol *Pseudomonas fluorescens* through 2.5-m deep outdoor lysimeters and survival in the effluent water. *Soil Biol. Biochem.* 30:621–631. doi:10.1016/S0038-0717(97)00158-2
- Vereecken, H., and M. Dust. 1998. Modelling water flow and pesticide transport at lysimeter and field scale. *ACS Symp. Ser.* 699:189–202. doi:10.1021/bk-1998-0699.ch014
- Vink, J.P.M., B. Golljesbüren, B. Diekkrüger, and S. Van der Zee. 1997. Simulation and model comparison of unsaturated movement of pesticides from a large clay lysimeter. *Ecol. Modell.* 105:113–127. doi:10.1016/S0304-3800(97)00147-6
- Vonberg, D., D. Hofmann, J. Vanderborcht, A. Leickens, S. Köppchen, T. Pütz, P. Burauel, and H. Vereecken. 2014. Atrazine soil core residue analysis from an agricultural field 21 years after its ban. *J. Environ. Qual.* 50:294–306. doi:10.2134/jeq2013.12.0497
- Wang, K., and R. Zhang. 2011. Heterogeneous soil water flow and macropores described with combined tracers of dye and iodine. *J. Hydrol.* 397:105–117. doi:10.1016/j.jhydrol.2010.11.037
- Wauchope, R.D., S. Yeh, J.B.J.H. Linders, R.R. Kloskowski, K. Tanaka, B. Rubin, et al. 2002. Pesticide soil sorption parameters: Theory, measurement, uses, limitations and reliability. *Pest Manage. Sci.* 58:419–445. doi:10.1002/ps.489
- Weigel, S., K. Bester, and H. Hühnerfuss. 2001. New method for rapid solid-phase extraction of large-volume water samples and its application to non-target screening of North Sea water for organic contaminants by gas chromatography-mass spectrometry. *J. Chromatogr. A* 912:151–161. doi:10.1016/S0021-9673(01)00529-5

## E. Supporting Information of Chapter 4

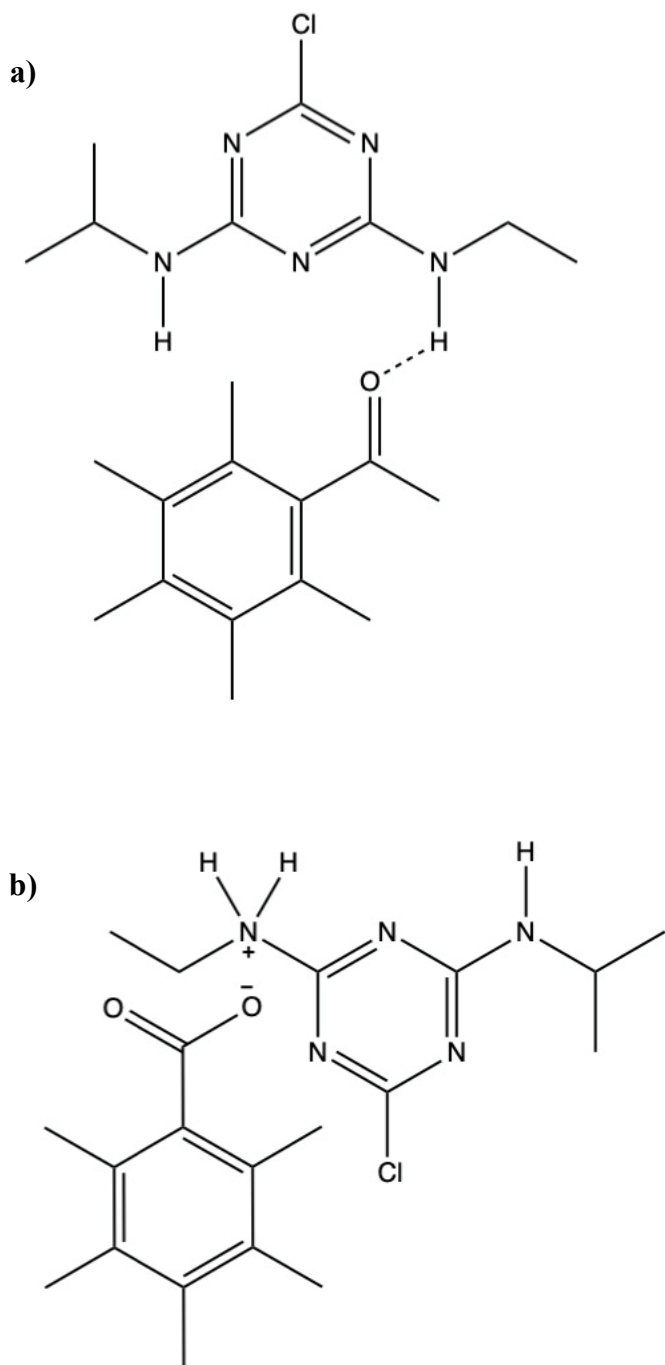
### E.1. Volumes and Concentrations of Groundwater used for this Study

Table E1: Concentration of ATZ, DEA and BAM spiked in relation to the volume extracted

Volume [L]	Concentration of spiked pesticide [ng/L]
1	2000
5	400
10	200
20	100
50	50
100	25



## E.2. Hypothesized ATZ-Humic Substance-Complex



Scheme E1: Hypothesized ATZ-Humic substance-complex by a) hydrogen-bonding and b) proton transfer as suggested by Sposito et al.<sup>188</sup>



## E. Supporting Information of Chapter 4

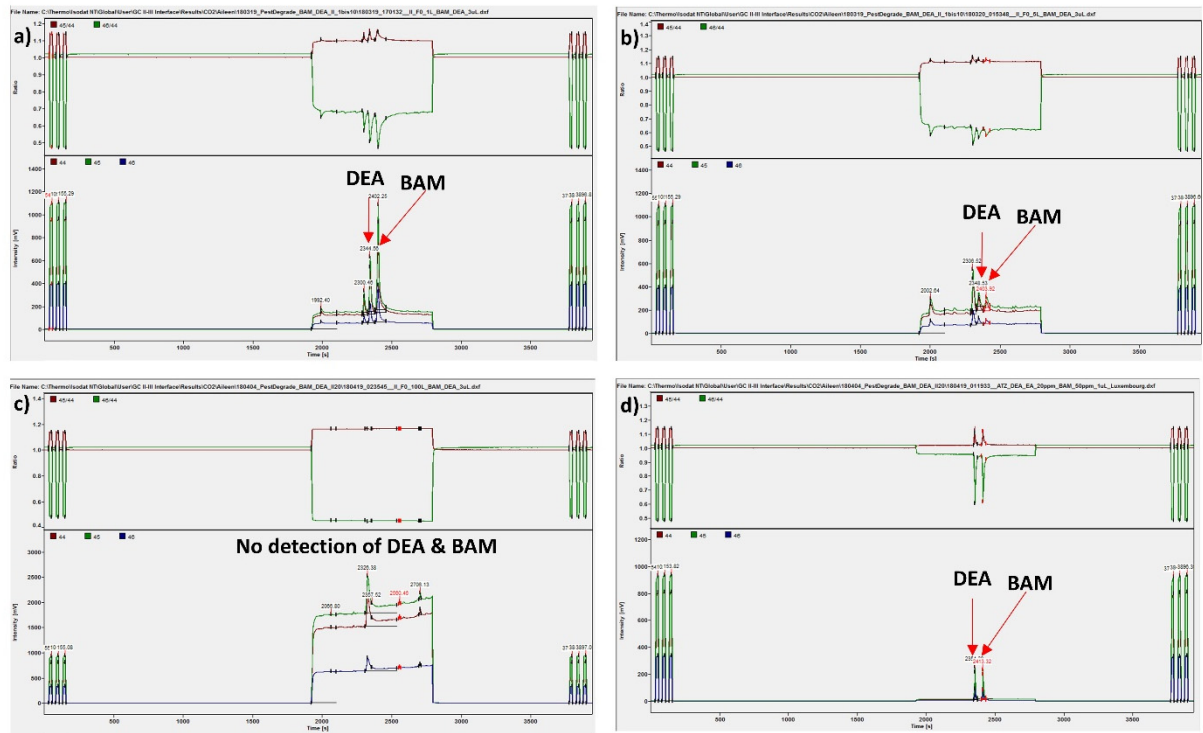


Figure E2: Chromatograms of DEA and BAM after HPLC-cleanup and on-column injection of a) 1 L b) 10 L and c) 100 L of water extraction; d) measurement of a 20 mg/L DEA and BAM standard prior to the analysis of the extracted 100 L sample

## Abbreviations

%	per centum (Latin) – percent; parts per hundred
µg	microgram; $1 \mu\text{g} = 1 \cdot 10^{-6} \text{ g}$
µL	microliter; $1 \mu\text{L} = 1 \cdot 10^{-6} \text{ L}$
µmol	micromole; $1 \mu\text{mol} = 1 \cdot 10^{-6} \text{ mol}$
‰	pro mille (Latin) – per mil; parts per thousand
2D	two dimensional
ACETO	acetochlor
ACN	acetonitrile
ATZ	atrazine
BAM	2,6-dichlorobenzamid
CAS	chemical abstracts service
CI	control interval
CLZ	chloridazon
cm	centimeter; $10 \cdot 10^{-2} \text{ m}$
CSIA	compound-specific stable isotope analysis
d	day
DAD	diodearray detector
DCB	dichlobenil
DEA	desethylatrazine
DIA	desisopropylatrazine
DOI	digital object finder



## Abbreviations

---

DPC	desphenylchloridazon
Dr.	Doktor (German) - Doctor, equivalent to PhD
e.g.	exempli gratia (Latin) - for example
EA	elemental analysis
ESI	electrospray ionization
et al.	et alii (Latin) – and others
g	gram; $1\text{ g} = 1 \cdot 10^{-3}\text{ kg}$
GC	gas chromatography
GC-qMS	gas chromatography – quadrupole mass spectrometer
h	hour; $1\text{ h} = 60\text{ min}$
HAT	2-hydroxyatrazine
HMGU	Helmholtz Zentrum München GmbH
HPLC	high performance liquid chromatography
HS	humic substances
IAEA	International Atomic Energy Agency
IRMS	isotope ratio mass spectrometry
kg	kilogram
KIE	kinetic isotope effect
L	lysimeter
L	liter
LC	liquid chromatography
m/z	ratio of molecular (or atomic) mass to the charge number if the ion
M	molar; $1\text{ mol} \cdot \text{L}^{-1}$

## Abbreviations

---

MDPC	methyldesphenylchloridazon
METO	metolachlor
mg	milligram; $1 \text{ mg} = 1 \cdot 10^{-6} \text{ kg}$
min	minute; $1 \text{ min} = 60 \text{ s}$
mL	milliliter; $1 \text{ mL} = 1 \cdot 10^{-3} \text{ L}$
mM	millimolar; $1 \text{ mM} = 1 \cdot 10^{-3} \text{ M}$
mmol	millimol; $1 \text{ mmol} = 1 \cdot 10^{-3} \text{ mol}$
MS	mass spectrometry
n.a.	not applicable
ng	nanogram; $1 \text{ ng} = 1 \cdot 10^{-9} \text{ g}$
nmol	nanomol; $1 \text{ nmol} = 1 \cdot 10^{-9} \text{ mol}$
pg	picogram; $1 \text{ pg} = 1 \cdot 10^{-12} \text{ g}$
pH	potential Hydrogenii (Latin) – decimal logarithm of the reciprocal of the hydrogen activity in water
pK <sub>a</sub>	logarithmic form of the acid dissociation constant $K_a$ ; $\text{p}K_a = -\log_{10} K_a$
pmol	picomol; $1 \text{ pmol} = 1 \cdot 10^{-12} \text{ mol}$
ppm	parts per million; $1 \text{ ppm} = 1 \cdot 10^{-6}$
ref	reference
s	second
SD	standard deviation
SPE	solid-phase extraction
TMSD	trimethylsilyldiazomethane
TOC	total organic carbon

## Abbreviations

---

UHPLC-QTOF-MS	ultra-high performance liquid chromatography- quadrupole time-of-flight mass spectrometry
USGS 40	L-glutamic acid; $\delta^{13}\text{C} = -26.389 \text{‰} \pm 0.042 \text{‰}$ , $\delta^{15}\text{N}$ $= -4.5 \text{‰} \pm 0.1 \text{‰}$
USGS 41	L-glutamic acid; $\delta^{13}\text{C} = 37.626 \text{‰} \pm 0.049 \text{‰}$ , $\delta^{15}\text{N}$ $= 47.6 \text{‰} \pm 0.2 \text{‰}$
UV	ultraviolet
V-PDB	Vienna PeeDee Belemnite
vs.	versus (Latin) – compared to; against



## References

1. European Commission, Groundwater Protection in Europe The new Groundwater Directive: consolidating the EU regulatory framework In *European Commission-Directorate-General for Environment*, EU Publications: Brussels, 2008.
2. Schwarzenbach, R. P.; Egli, T.; Hofstetter, T. B.; von Gunten, U.; Wehrli, B., Global Water Pollution and Human Health. *Annual Review of Environment and Resources* **2010**, *35* (1), 109-136.
3. Völker, J.; Borchardt, D., Drinking Water Quality at Risk: A European Perspective. In *Atlas of Ecosystem Services: Drivers, Risks, and Societal Responses*, Schröter, M.; Bonn, A.; Klotz, S.; Seppelt, R.; Baessler, C., Eds. Springer International Publishing: Cham, 2019; pp 205-210.
4. Loos, R.; Locoro, G.; Comero, S.; Contini, S.; Schwesig, D.; Werres, F.; Balsaa, P.; Gans, O.; Weiss, S.; Blaha, L.; Bolchi, M.; Gawlik, B. M., Pan-European survey on the occurrence of selected polar organic persistent pollutants in ground water. *Water Res.* **2010**, *44* (14), 4115-4126.
5. Postigo, C.; Barceló, D., Synthetic organic compounds and their transformation products in groundwater: Occurrence, fate and mitigation. *Sci. Total Environ.* **2015**, *503-504*, 32-47.
6. Murray, K. E.; Thomas, S. M.; Bodour, A. A., Prioritizing research for trace pollutants and emerging contaminants in the freshwater environment. *Environ. Pollut.* **2010**, *158* (12), 3462-3471.
7. Richardson, S. D.; Ternes, T. A., Water Analysis: Emerging Contaminants and Current Issues. *Anal. Chem.* **2018**, *90* (1), 398-428.
8. Kilchmann, S. R., Miriam; Schürch, Marc; Traber, Daniel *Ergebnisse der Grundwasserbeobachtung Schweiz (NAQUA)*; Bundesamt für Umwelt BAFU: Bern, 2009; p 144.
9. Fent, K.; Weston, A. A.; Caminada, D., Ecotoxicology of human pharmaceuticals. *Aquat. Toxicol.* **2006**, *76* (2), 122-159.
10. Schwarzenbach, R. P.; Escher, B. I.; Fenner, K.; Hofstetter, T. B.; Johnson, C. A.; von Gunten, U.; Wehrli, B., The Challenge of Micropollutants in Aquatic Systems. *Science* **2006**, *313* (5790), 1072-1077.
11. Tappe, W.; Groeneweg, J.; Jantsch, B., Diffuse atrazine pollution in German aquifers. *Biodegradation* **2002**, *13* (1), 3-10.
12. Graymore, M.; Stagnitti, F.; Allinson, G., Impacts of atrazine in aquatic ecosystems. *Environ. Int.* **2001**, *26* (7-8), 483-495.
13. Vonberg, D.; Vanderborght, J.; Cremer, N.; Pütz, T.; Herbst, M.; Vereecken, H., 20 years of long-term atrazine monitoring in a shallow aquifer in western Germany. *Water Res.* **2014**, *50*, 294-306.
14. Byrne, D., COMMISSION DECISION of 10 March 2004 concerning the non-inclusion of atrazine in Annex I to Council Directive 91/414/EEC and the withdrawal of authorisations for plant protection products containing this active substance. In *2004/248/EC*, Commission, E., Ed. Official Journal of the European Union: 2004.
15. Reemtsma, T.; Berger, U.; Arp, H. P. H.; Gallard, H.; Knepper, T. P.; Neumann, M.; Quintana, J. B.; Voogt, P. d., Mind the Gap: Persistent and Mobile Organic

- Compounds—Water Contaminants That Slip Through. *Environ. Sci. Technol.* **2016**, *50* (19), 10308-10315.
16. Kolpin, D. W.; Thurman, E. M.; Linhart, S. M., Occurrence of Cyanazine Compounds in Groundwater: Degradates More Prevalent Than the Parent Compound. *Environ. Sci. Technol.* **2001**, *35* (6), 1217-1222.
17. Clausen, L.; Larsen, F.; Albrechtsen, H. J., Sorption of the Herbicide Dichlobenil and the Metabolite 2,6-Dichlorobenzamide on Soils and Aquifer Sediments. *Environ. Sci. Technol.* **2004**, *38* (17), 4510-4518.
18. Björklund, E.; Anskjær, G. G.; Hansen, M.; Styrihave, B.; Halling-Sørensen, B., Analysis and environmental concentrations of the herbicide dichlobenil and its main metabolite 2,6-dichlorobenzamide (BAM): A review. *Sci. Total Environ.* **2011**, *409* (12), 2343-2356.
19. Schuhmann, A.; Gans, O.; Weiss, S.; Fank, J.; Klammler, G.; Haberhauer, G.; Gerzabek, M., A long-term lysimeter experiment to investigate the environmental dispersion of the herbicide chloridazon and its metabolites—comparison of lysimeter types. *J. Soils Sediments* **2016**, *16* (3), 1032-1045.
20. Farlin, J.; Gallé, T.; Bayerle, M.; Pittois, D.; Köppchen, S.; Krause, M.; Hofmann, D., Breakthrough dynamics of s-metolachlor metabolites in drinking water wells: Transport pathways and time to trend reversal. *Journal of Contaminant Hydrology* **2018**, *213*, 62-72.
21. Farlin, J.; Drouet, L.; Gallé, T.; Pittois, D.; Bayerle, M.; Braun, C.; Maloszewski, P.; Vanderborght, J.; Elsner, M.; Kies, A., Delineating spring recharge areas in a fractured sandstone aquifer (Luxembourg) based on pesticide mass balance. *Hydrogeol. J.* **2013**, *21* (4), 799-812.
22. Farlin, J.; Gallé, T.; Bayerle, M.; Pittois, D.; Braun, C.; El Khabbaz, H.; Lallement, C.; Leopold, U.; Vanderborght, J.; Weihermueller, L., Using the long-term memory effect of pesticide and metabolite soil residues to estimate field degradation half-life and test leaching predictions. *Geoderma* **2013**, *207–208*, 15-24.
23. Meyer, A. H.; Elsner, M., <sup>13</sup>C/<sup>12</sup>C and <sup>15</sup>N/<sup>14</sup>N Isotope Analysis To Characterize Degradation of Atrazine: Evidence from Parent and Daughter Compound Values. *Environ. Sci. Technol.* **2013**, *47* (13), 6884-6891.
24. Elsner, M., Stable isotope fractionation to investigate natural transformation mechanisms of organic contaminants: principles, prospects and limitations. *J. Environ. Monit.* **2010**, *12* (11), 2005-2031.
25. Meier-Augenstein, W., GC and IRMS technology for <sup>13</sup>C and <sup>15</sup>N analysis on organic compounds and related gases. *Handbook of Stable Isotope Analytical Techniques* **2004**, *1*, 153-176.
26. Werner, R. A.; Brand, W. A., Referencing strategies and techniques in stable isotope ratio analysis. *Rapid Commun. Mass Spectrom.* **2001**, *15*, 501-519.
27. Brand, W. A.; Coplen, T. B., Stable isotope deltas: tiny, yet robust signatures in nature. *Isotopes Environ Health Stud* **2012**, *48* (3), 393-409.
28. Meier-Augenstein, W., Applied gas chromatography coupled to isotope ratio mass spectrometry. *J. Chromatogr. A* **1999**, *842*, 351–371.
29. Alvarez-Zaldívar, P.; Payraudeau, S.; Meite, F.; Masbou, J.; Imfeld, G., Pesticide degradation and export losses at the catchment scale: Insights from compound-specific isotope analysis (CSIA). *Water Res.* **2018**, *139*, 198-207.
30. Maier, M. P.; Prasse, C.; Pati, S. G.; Nitsche, S.; Li, Z.; Radke, M.; Meyer, A. H.; Hofstetter, T. B.; Ternes, T. A.; Elsner, M., Exploring Trends of C and N Isotope Fractionation to Trace Transformation Reactions of Diclofenac in Natural and Engineered Systems. *Environ. Sci. Technol.* **2016**.

31. Abe, Y.; Aravena, R.; Zopfi, J.; Parker, B.; Hunkeler, D., Evaluating the fate of chlorinated ethenes in streambed sediments by combining stable isotope, geochemical and microbial methods. *Journal of Contaminant Hydrology* **2009**, *107* (1-2), 10-21.
32. Kujawinski, D. M.; Wolbert, J. B.; Zhang, L.; Jochmann, M. A.; Widory, D.; Baran, N.; Schmidt, T. C., Carbon isotope ratio measurements of glyphosate and AMPA by liquid chromatography coupled to isotope ratio mass spectrometry. *Anal. Bioanal. Chem.* **2013**, *405* (9), 2869-2878.
33. Mogusu, E. O.; Wolbert, J. B.; Kujawinski, D. M.; Jochmann, M. A.; Elsner, M., Dual element ( $^{15}\text{N}/^{14}\text{N}$ ,  $^{13}\text{C}/^{12}\text{C}$ ) isotope analysis of glyphosate and AMPA by derivatization-gas chromatography isotope ratio mass spectrometry (GC/IRMS) combined with LC/IRMS. *Anal. Bioanal. Chem.* **2015**, 1-12.
34. Schmidt, T. C.; Zwank, L.; Elsner, M.; Berg, M.; Meckenstock, R. U.; Haderlein, S. B., Compound-specific stable isotope analysis of organic contaminants in natural environments: a critical review of the state of the art, prospects, and future challenges. *Anal. Bioanal. Chem.* **2004**, *378* (2), 283-300.
35. Sherwood Lollar, B.; Slater, G. F.; Ahad, J.; Sleep, B.; Spivack, J.; Brennan, M.; MacKenzie, P., Contrasting carbon isotope fractionation during biodegradation of trichloroethylene and toluene: implications for intrinsic bioremediation. *Org. Geochem.* **1999**, *30* (8), 813-820.
36. Meyer, A. H.; Dybala-Defratyka, A.; Alaimo, P. J.; Geronimo, I.; Sanchez, A. D.; Cramer, C. J.; Elsner, M., Cytochrome P450-catalyzed dealkylation of atrazine by *Rhodococcus* sp. strain NI86/21 involves hydrogen atom transfer rather than single electron transfer. *Dalton Trans.* **2014**, *43* (32), 12111-12432.
37. Aelion, C. M.; Hohener, P.; Hunkeler, D.; Aravena, R., *Environmental Isotopes in Bioremediation and Biodegradation*. CRC Press: 2009.
38. Hofstetter, T. B.; Schwarzenbach, R. P.; Bernasconi, S. M., Assessing transformation processes of organic compounds using stable isotope fractionation. *Environ. Sci. Technol.* **2008**, *42* (21), 7737-7743.
39. Hofstetter, T. B.; Berg, M., Assessing transformation processes of organic contaminants by compound-specific stable isotope analysis. *TrAC, Trends Anal. Chem.* **2011**, *30* (4), 618-627.
40. Abe, Y.; Hunkeler, D., Does the Rayleigh equation apply to evaluate field isotope data in contaminant hydrogeology? *Environ. Sci. Technol.* **2006**, *40* (5), 1588-1596.
41. Aeppli, C.; Hofstetter, T. B.; Amaral, H. I. F.; Kipfer, R.; Schwarzenbach, R. P.; Berg, M., Quantifying In Situ Transformation Rates of Chlorinated Ethenes by Combining Compound-Specific Stable Isotope Analysis, Groundwater Dating, And Carbon Isotope Mass Balances. *Environ. Sci. Technol.* **2010**, *44* (10), 3705-3711.
42. Shouakar-Stash, O.; Drimmie, R. J.; Zhang, M.; Frape, S. K., Compound-specific chlorine isotope ratios of TCE, PCE and DCE isomers by direct injection using CF-IRMS. *Appl. Geochem.* **2006**, *21* (5), 766-781.
43. Cretnik, S.; Thoreson, K. A.; Bernstein, A.; Ebert, K.; Buchner, D.; Laskov, C.; Haderlein, S.; Shouakar-Stash, O.; Kliegman, S.; McNeill, K.; Elsner, M., Reductive Dechlorination of TCE by Chemical Model Systems in Comparison to Dehalogenating Bacteria: Insights from Dual Element Isotope Analysis ( $^{13}\text{C}/^{12}\text{C}$ ,  $^{37}\text{Cl}/^{35}\text{Cl}$ ). *Environ. Sci. Technol.* **2013**, *47* (13), 6855-6863.
44. Hunkeler, D.; Abe, Y.; Broholm, M. M.; Jeannotat, S.; Westergaard, C.; Jacobsen, C. S.; Aravena, R.; Bjerg, P. L., Assessing chlorinated ethene degradation in a large scale contaminant plume by dual carbon-chlorine isotope analysis and quantitative PCR. *Journal of Contaminant Hydrology* **2011**, *119* (1-4), 69-79.
45. Rodríguez-Fernández, D.; Heckel, B.; Torrentó, C.; Meyer, A.; Elsner, M.; Hunkeler, D.; Soler, A.; Rosell, M.; Domènech, C., Dual element ( $\text{CCl}$ ) isotope approach to

- distinguish abiotic reactions of chlorinated methanes by Fe(0) and by Fe(II) on iron minerals at neutral and alkaline pH. *Chemosphere* **2018**, *206*, 447-456.
46. Heckel, B.; McNeill, K.; Elsner, M., Chlorinated Ethene Reactivity with Vitamin B12 Is Governed by Cobalamin Chloroethylcarbanions as Crossroads of Competing Pathways. *ACS Catal.* **2018**, *8* (4), 3054-3066.
47. Lihl, C.; Douglas, L. M.; Franke, S.; Perez-de-Mora, A.; Meyer, A. H.; Daubmeier, M.; Edwards, E. A.; Nijenhuis, I.; Sherwood Lollar, B.; Elsner, M., Mechanistic dichotomy in bacterial trichloroethene dechlorination revealed by carbon and chlorine isotope effects. *Environ. Sci. Technol.* **2019**.
48. Schreglmann, K.; Hoeche, M.; Steinbeiss, S.; Reinnicke, S.; Elsner, M., Carbon and nitrogen isotope analysis of atrazine and desethylatrazine at sub-microgram per liter concentrations in groundwater. *Anal. Bioanal. Chem.* **2013**, *405* (9), 2857-2867.
49. Reinnicke, S.; Simonsen, A.; Sørensen, S. R.; Aamand, J.; Elsner, M., C and N Isotope Fractionation during Biodegradation of the Pesticide Metabolite 2,6-Dichlorobenzamide (BAM): Potential for Environmental Assessments. *Environ. Sci. Technol.* **2012**, *46* (3), 1447-1454.
50. Lihl, C.; Heckel, B.; Ponsin, V.; Hunkeler, D.; Elsner, M., Compound-specific Chlorine Isotope Fractionation in Biodegradation of Atrazine. **in preparation**.
51. Elsner, M.; Jochmann, M. A.; Hofstetter, T. B.; Hunkeler, D.; Bernstein, A.; Schmidt, T. C.; Schimmelmann, A., Current challenges in compound-specific stable isotope analysis of environmental organic contaminants. *Anal. Bioanal. Chem.* **2012**, *403* (9), 2471-2491.
52. Brand, W. A., Mass Spectrometer Hardware for Analyzing Stable Isotope Ratios. In *Handbook of Stable Isotope Analytical Techniques, Volume-I*, Groot, P. A. d., Ed. Elsevier B.V.: 2004; pp 835-857.
53. Teffera, Y.; Kusmierz, J. J.; Abramson, F. P., Continuous-Flow Isotope Ratio Mass Spectrometry Using the Chemical Reaction Interface with Either Gas or Liquid Chromatographic Introduction. *Anal. Chem.* **1996**, *68* (11), 1888-1894.
54. Krummen, M.; Hilkert, A. W.; Juchelka, D.; Duhr, A.; Schluter, H. J.; Pesch, R., A new concept for isotope ratio monitoring liquid chromatography/mass spectrometry. *Rapid Commun. Mass Spectrom.* **2004**, *18* (19), 2260-2266.
55. Godin, J. P.; Hau, J.; Fay, L. B.; Hopfgartner, G., Isotope ratio monitoring of small molecules and macromolecules by liquid chromatography coupled to isotope ratio mass spectrometry. *Rapid Commun. Mass Spectrom.* **2005**, *19* (18), 2689-2698.
56. Godin, J. P.; McCullagh, J. S. O., Review: Current applications and challenges for liquid chromatography coupled to isotope ratio mass spectrometry (LC/IRMS). *Rapid Commun. Mass Spectrom.* **2011**, *25* (20), 3019-3028.
57. Godin, J.-P.; Fay, L.-B.; Hopfgartner, G., Liquid chromatography combined with mass spectrometry for <sup>13</sup>C isotopic analysis in life science research. *Mass Spectrom. Rev.* **2007**, *26* (6), 751-774.
58. Reinnicke, S.; Bernstein, A.; Elsner, M., Small and Reproducible Isotope Effects during Methylation with Trimethylsulfonium Hydroxide (TMSH): A Convenient Derivatization Method for Isotope Analysis of Negatively Charged Molecules. *Anal. Chem.* **2010**, *82* (5), 2013-2019.
59. Sessions, A. L., Isotope-ratio detection for gas chromatography. *J. Sep. Sci.* **2006**, *29*, 1946-1961.
60. Fourel, F.; Martineau, F.; Seris, M.; Lécuyer, C., Measurement of <sup>34</sup>S/<sup>32</sup>S Ratios of NBS 120c and BCR 32 Phosphorites Using Purge and Trap EA-IRMS Technology. *Geostand. Geoanal. Res.* **2015**, *39* (1), 47-53.



61. Elsner, M.; Imfeld, G., Compound-specific isotope analysis (CSIA) of micropollutants in the environment — current developments and future challenges. *Curr. Opin. Biotechnol.* **2016**, *41*, 60-72.
62. Torrentó, C.; Bakkour, R.; Gaétan, G.; Melsbach, A.; Ponsin, V.; Hofstetter, T. B.; Elsner, M.; Hunkeler, D., Solid-phase extraction method for stable isotope analysis of pesticides from large volume environmental water samples. *Analyst* **2019**, *144* (9), 2898-2908
63. Bakkour, R.; Bolotin, J.; Sellergren, B.; Hofstetter, T. B., Molecularly Imprinted Polymers for Compound-Specific Isotope Analysis of Polar Organic Micropollutants in Aquatic Environments. *Anal. Chem.* **2018**, *90* (12), 7292-7301.
64. Sacks, G. L.; Zhang, Y.; Brenna, J. T., Fast Gas Chromatography Combustion Isotope Ratio Mass Spectrometry. *Anal. Chem.* **2007**, *79* (16), 6348-6358.
65. Flenker, U.; Hebestreit, M.; Piper, T.; Hulsemann, F.; Schanzer, W., Improved Performance and Maintenance in Gas Chromatography/Isotope Ratio Mass Spectrometry by Precolumn Solvent Removal. *Anal. Chem.* **2007**, *79* (11), 4162-4168.
66. Baczynski, A. A.; Polissar, P. J.; Juchelka, D.; Schwieters, J.; Hilker, A.; Summons, R. E.; Freeman, K. H., Picomolar-scale compound-specific isotope analyses. *Rapid Commun. Mass Spectrom.* **2018**, *32* (9), 730-738.
67. Tobias, H.; Brenna, J., Microfabrication of high temperature micro-reactors for continuous flow isotope ratio mass spectrometry. *Microfluid. Nanofluid.* **2010**, *9* (2), 461-470.
68. Marriott, P.; Shellie, R., Principles and applications of comprehensive two-dimensional gas chromatography. *TrAC, Trends Anal. Chem.* **2002**, *21* (9), 573-583.
69. Pani, O.; Górecki, T., Comprehensive two-dimensional gas chromatography (GC×GC) in environmental analysis and monitoring. *Anal. Bioanal. Chem.* **2006**, *386* (4), 1013-1023.
70. Llewellyn, G. T.; Dorman, F.; Westland, J. L.; Yoxtheimer, D.; Grieve, P.; Sowers, T.; Humston-Fulmer, E.; Brantley, S. L., Evaluating a groundwater supply contamination incident attributed to Marcellus Shale gas development. *PNAS* **2015**, 6325-6330
71. Gauchotte-Lindsay, C.; Richards, P.; McGregor, L. A.; Thomas, R.; Kalin, R. M., A one-step method for priority compounds of concern in tar from former industrial sites: Trimethylsilyl derivatisation with comprehensive two-dimensional gas chromatography. *J. Chromatogr. A* **2012**, *1253*, 154-163.
72. Tobias, H. J.; Sacks, G. L.; Zhang, Y.; Brenna, J. T., Comprehensive Two-Dimensional Gas Chromatography Combustion Isotope Ratio Mass Spectrometry. *Anal. Chem.* **2008**, *80* (22), 8613-8621.
73. Tobias, H. J.; Zhang, Y.; Auchus, R. J.; Brenna, J. T., Detection of Synthetic Testosterone Use by Novel Comprehensive Two-Dimensional Gas Chromatography Combustion–Isotope Ratio Mass Spectrometry. *Anal. Chem.* **2011**, *83* (18), 7158-7165.
74. Tobias, H. J.; Brenna, J. T., Cryofocus fast gas chromatography combustion isotope ratio mass spectrometry for rapid detection of synthetic steroid use in sport doping. *Analyst* **2018**, *143* (5), 1124-1132.
75. Ponsin, V.; Buscheck, T. E.; Hunkeler, D., Heart-cutting two-dimensional gas chromatography–isotope ratio mass spectrometry analysis of monoaromatic hydrocarbons in complex groundwater and gas-phase samples. *J. Chromatogr. A* **2017**, *1492*, 117-128.
76. Meyer, A. H.; Penning, H.; Lowag, H.; Elsner, M., Precise and accurate compound specific carbon and nitrogen isotope analysis of atrazine: critical role of combustion oven conditions. *Environ. Sci. Technol.* **2008**, *42* (21), 7757-7763.
77. Richardson, S. D.; Ternes, T. A., Water Analysis: Emerging Contaminants and Current Issues. *Anal. Chem.* **2011**, *83* (12), 4614-4648.

78. Fenner, K.; Canonica, S.; Wackett, L. P.; Elsner, M., Evaluating Pesticide Degradation in the Environment: Blind Spots and Emerging Opportunities. *Science* **2013**, *341* (6147), 752-758.
79. Weber, W. H.; Seitz, W.; Schulz, W.; Wagener, H.-A., Nachweis der Metaboliten Desphenyl-chloridazon und Methyl-desphenyl-chloridazon in Oberflächen, Grund- und Trinkwasser. *Vom Wasser* **2007**, *105* (1), 7-14.
80. Reinhardt, M. K., Ronald; Hofacker, Anke; Leu, Christian Monitoring von PSM-Rückständen im Grundwasser. *Aqua Gas* **2017**, *6*, 78-89.
81. Sturm, S.; Kiefer, J.; Kollotzek, D.; Rogg, J.-m., Aktuelle Befunde der Metaboliten von Tolyfluanid und Chloridazon in den zur Trinkwasserversorgung genutzten Grundwasservorkommen Baden-Württembergs. *gwf Wasser | Abwasser* **2013**, (10), 950-959%V 151.
82. Grummt, T. P., Rudolf, Gesundheitliche Orientierungswerte (GOW) für nicht relevante Metaboliten (nrM) von Wirkstoffen aus Pflanzenschutzmitteln (PSM). Risikobewertung, U. a. B. f., Ed. Umweltbundesamt and Bundesinstitut für Risikobewertung: <https://www.umweltbundesamt.de/dokument/gesundheitsliche-orientierungswerte-gow-fuer-nicht>, 2017; p 12.
83. UBA, Pflanzenschutzmittelfunde im Grundwasser. Umweltbundesamt: 2004.
84. BAFU, B. f. U., Pflanzenschutzmittel PSM und PSM-Abbauprodukte im Grundwasser. NAQUA, N. G., Ed. Switzerland, 2013.
85. Buttiglieri, G.; Peschka, M.; Frömel, T.; Müller, J.; Malpei, F.; Seel, P.; Knepper, T. P., Environmental occurrence and degradation of the herbicide n-chloridazon. *Water Res.* **2009**, *43* (11), 2865-2873.
86. Lingens, F.; Blecher, R.; Blecher, H.; Blobel, F.; Eberspächer, J.; Fröhner, C.; Görisch, H.; Görisch, H.; Layh, G., Phenylobacterium immobile gen. nov., sp. nov., a Gram-Negative Bacterium That Degrades the Herbicide Chloridazon. *Int. J. Syst. Evol. Microbiol.* **1985**, *35* (1), 26-39.
87. Thier, H.-P.; Zeumer, H., *Manual of Pesticide Residue Analysis Volume I*. VCH Verlagsgesellschaft: 1987; p 443.
88. Roberts, M. C.; Croucher, L.; Roberts, T. R.; Hutson, D. H.; Lee, P. W.; Nicholls, P. H.; Plimmer, J. R., *Metabolic Pathways of Agrochemicals: Part 1: Herbicides and Plant Growth Regulators*. Royal Society of Chemistry: 2007.
89. PPDB, The Pesticide Properties Database (PPDB) developed by the Agriculture & Environment Research Unit (AERU). In *funded by the EU-funded FOOTPRINT project (FP6-SSP-022704)*, University of Hertfordshire: 2009.
90. Elsayed, O. F.; Maillard, E.; Vuilleumier, S.; Nijenhuis, I.; Richnow, H. H.; Imfeld, G., Using compound-specific isotope analysis to assess the degradation of chloroacetanilide herbicides in lab-scale wetlands. *Chemosphere* **2014**, *99* (0), 89-95.
91. Schürner, H. K. V.; Seffernick, J. L.; Grzybkowska, A.; Dybala-Defratyka, A.; Wackett, L. P.; Elsner, M., Characteristic Isotope Fractionation Patterns in s-Triazine Degradation Have Their Origin in Multiple Protonation Options in the s-Triazine Hydrolase TrzN. *Environ. Sci. Technol.* **2015**, *49* (6), 3490-3498.
92. Wu, L.; Yao, J.; Trebse, P.; Zhang, N.; Richnow, H. H., Compound specific isotope analysis of organophosphorus pesticides. *Chemosphere* **2014**, *111* (0), 458-463.
93. Maier, M. P.; De Corte, S.; Nitsche, S.; Spaett, T.; Boon, N.; Elsner, M., C & N Isotope Analysis of Diclofenac to Distinguish Oxidative and Reductive Transformation and to Track Commercial Products. *Environ. Sci. Technol.* **2014**, *48* (4), 2312-2320.
94. Maier, M. P.; Qiu, S.; Elsner, M., Enantioselective stable isotope analysis (ESIA) of polar herbicides. *Anal. Bioanal. Chem.* **2013**, *405* (9), 2825-2831.
95. Silber, J. A.; Engel, M. H.; Macko, S. A.; Jumeau, E. J., Stable carbon isotope analysis of amino acid enantiomers by conventional isotope ratio mass spectrometry and

- combined gas chromatography/isotope ratio mass spectrometry. *Anal. Chem.* **1991**, *63* (4), 370-374.
96. Kowal, S.; Balsaa, P.; Werres, F.; Schmidt, T. C., Reduction of matrix effects and improvement of sensitivity during determination of two chloridazon degradation products in aqueous matrices by using UPLC-ESI-MS/MS. *Anal. Bioanal. Chem.* **2012**, *403* (6), 1707-1717.
97. Reemtsma, T.; Alder, L.; Banasiak, U., A multimethod for the determination of 150 pesticide metabolites in surface water and groundwater using direct injection liquid chromatography–mass spectrometry. *J. Chromatogr. A* **2013**, *1271* (1), 95-104.
98. Fuhrmann, A.; Gans, O.; Weiss, S.; Haberhauer, G.; Gerzabek, M. H., Determination of Bentazone, Chloridazon and Terbutylazine and Some of Their Metabolites in Complex Environmental Matrices by Liquid Chromatography–Electrospray Ionization–Tandem Mass Spectrometry Using a Modified QuEChERS Method: an Optimization and Validation Study. *Water, Air, Soil Pollut.* **2014**, *225* (5), 1944.
99. Kuhlmann, F., Rückstandsbestimmung von Pyrazon und seinen Metaboliten in Zuckerrüben. *Zeitschrift für Lebensmittel-Untersuchung und Forschung* **1981**, *173* (1), 35-39.
100. Presser, A.; Hüfner, A., Trimethylsilyldiazomethane – A Mild and Efficient Reagent for the Methylation of Carboxylic Acids and Alcohols in Natural Products. *Monatshefte für Chemie / Chemical Monthly* **2004**, *135* (8), 1015-1022.
101. Ranz, A.; Korpecka, J.; Lankmayr, E., Optimized derivatization of acidic herbicides with trimethylsilyldiazomethane for GC analysis. *J. Sep. Sci.* **2008**, *31* (4), 746-752.
102. International-Standardization-Organization, Accuracy (trueness and precision) of measurement methods and results — Part 1: General principles and definitions. In *ISO 5. 5725-1*, Geneva, 1994; Vol. ISO 5. 57251.
103. Torrentó, C.; Prasuhn, V.; Spiess, E.; Ponsin, V.; Melsbach, A.; Lihl, C.; Glauser, G.; Hofstetter, T. B.; Elsner, M.; Hunkeler, D., Adsorbing vs. Nonadsorbing Tracers for Assessing Pesticide Transport in Arable Soils. *Vadose Zone J.* **2018**, *17* (1).
104. Jochmann, M. A.; Blessing, M.; Haderlein, S. B.; Schmidt, T. C., A new approach to determine method detection limits for compound-specific isotope analysis of volatile organic compounds. *Rapid Commun. Mass Spectrom.* **2006**, *20* (24), 3639-3648.
105. Smith, C. I.; Fuller, B. T.; Choy, K.; Richards, M. P., A three-phase liquid chromatographic method for  $\delta^{13}\text{C}$  analysis of amino acids from biological protein hydrolysates using liquid chromatography–isotope ratio mass spectrometry. *Anal. Biochem.* **2009**, *390* (2), 165-172.
106. McCullagh, J. S. O., Mixed-mode chromatography/isotope ratio mass spectrometry. *Rapid Commun. Mass Spectrom.* **2010**, *24* (5), 483-494.
107. Zhang, L.; Kujawinski, D. M.; Jochmann, M. A.; Schmidt, T. C., High-temperature reversed-phase liquid chromatography coupled to isotope ratio mass spectrometry. *Rapid Commun. Mass Spectrom.* **2011**, *25* (20), 2971-2980.
108. Kujawinski, D. M.; Zhang, L.; Schmidt, T. C.; Jochmann, M. A., When other separation techniques fail: compound-specific carbon isotope ratio analysis of sulfonamide containing pharmaceuticals by high-temperature-liquid chromatography-isotope ratio mass spectrometry. *Anal. Chem.* **2012**, *84* (18), 7656-63.
109. Loos, R.; Gawlik, B. M.; Locoro, G.; Rimaviciute, E.; Contini, S.; Bidoglio, G., EU-wide survey of polar organic persistent pollutants in European river waters. *Environ. Pollut.* **2009**, *157* (2), 561-568.
110. Drescher, N.; Otto, S., Über den Abbau von 1-Phenyl-4-amino-5-chlor-pyridazon-6 (Pyrazon) im Boden *Zeitschrift für Pflanzenkrankheiten (Pflanzenpathologie) und Pflanzenschutz* **1969**, *76* (1), 27-33.

111. Hertfordshire, U. o., PPDB: Pesticide Properties DataBase. University of Hertfordshire: <http://sitem.herts.ac.uk/aeru/ppdb/en/Reports/141.htm>, 2018.
112. Deutsche-Forschungsgemeinschaft, *Rückstandsanalytik von Pflanzenschutzmitteln*“, *Mitteilung VI der Senatskommission für Pflanzenschutz-, Pflanzenbehandlungs- und Vorratsschutzmittel, Methodensammlung der Arbeitsgruppe Analytik, 11*. Wiley VCH: 1990.
113. Gustafson, D. I., Groundwater ubiquity score: A simple method for assessing pesticide leachability. *Environmental Toxicology and Chemistry* **1989**, 8 (4), 339-357.
114. Farlin, J.; Bayerle, M.; Pittois, D.; Gallé, T., Estimating Pesticide Attenuation From Water Dating and the Ratio of Metabolite to Parent Compound. *Groundwater* **2017**, 55 (4), 550-557.
115. Hunkeler, D.; Meckenstock, R. U.; Sherwood Lollar, B.; Schmidt, T.; Wilson, J.; Schmidt, T.; Wilson, J. *A Guide for Assessing Biodegradation and Source Identification of Organic Ground Water Contaminants using Compound Specific Isotope Analysis (CSIA)*; PA 600/R-08/148 | December 2008 | [www.epa.gov/ada](http://www.epa.gov/ada); US EPA: Oklahoma, USA, 2008.
116. Thullner, M.; Richnow, H.-H.; Fischer, A., Characterization and quantification of *in situ* biodegradation of groundwater contaminants using stable isotope fractionation analysis: advantages and limitations. In *Environmental and Regional Air Pollution*, Gallo, D.; Mancini, R., Eds. Nova Science Publishers: 2009.
117. Meckenstock, R. U.; Morasch, B.; Griebler, C.; Richnow, H. H., Stable isotope fractionation analysis as a tool to monitor biodegradation in contaminated aquifers. *Journal of Contaminant Hydrology* **2004**, 75 (3-4), 215-255.
118. Melsbach, A.; Ponsin, V.; Torrentó, C.; Lihl, C.; Hofstetter, T. B.; Hunkeler, D.; Elsner, M., <sup>13</sup>C and <sup>15</sup>N isotope analysis of desphenylchloridazon by liquid chromatography isotope ratio mass spectrometry (LC-IRMS) and derivatization-gas chromatography isotope ratio mass spectrometry (GC-IRMS). *Anal. Chem.* **2019**, 91 (5), 3412-3420.
119. Muller, R.; Schmitt, S.; Lingens, F., A novel non-heme iron-containing dioxygenase. Chloridazon-catechol dioxygenase from *Phenylobacterium immobilis* DSM 1986. *European journal of biochemistry / FEBS* **1982**, 125 (3), 579-84.
120. Braeckevelt, M.; Fischer, A.; Kästner, M., Field applicability of Compound-Specific Isotope Analysis (CSIA) for characterization and quantification of *in situ* contaminant degradation in aquifers. *Appl. Microbiol. Biotechnol.* **2012**, 94 (6), 1401-1421.
121. Kopinke, F. D.; Georgi, A.; Voskamp, M.; Richnow, H. H., Carbon isotope fractionation of organic contaminants due to retardation on humic substances: Implications for natural attenuation studies in aquifers. *Environ. Sci. Technol.* **2005**, 39 (16), 6052-6062.
122. Fischer, A.; Theuerkorn, K.; Stelzer, N.; Gehre, M.; Thullner, M.; Richnow, H. H., Applicability of Stable Isotope Fractionation Analysis for the Characterization of Benzene Biodegradation in a BTEX-contaminated Aquifer. *Environ. Sci. Technol.* **2007**, 41 (10), 3689-3696.
123. Morrill, P. L.; Sleep, B. E.; Seepersad, D. J.; McMaster, M. L.; Hood, E. D.; LeBron, C.; Major, D. W.; Edwards, E. A.; Sherwood Lollar, B., Variations in expression of carbon isotope fractionation of chlorinated ethenes during biologically enhanced PCE dissolution close to a source zone. *Journal of Contaminant Hydrology* **2009**, 110 (1-2), 60-71.
124. Stehmeier, L. G.; Francis, M. M.; Jack, T. R.; Diegor, E.; Winsor, L.; Abrajano, T. A., Field and *in vitro* evidence for *in-situ* bioremediation using compound-specific <sup>13</sup>C/<sup>12</sup>C ratio monitoring. *Org. Geochem.* **1999**, 30 (8, Part 1), 821-833.
125. Hunkeler, D.; Aravena, R.; Parker, B. L.; Cherry, J. A.; Diao, X., Monitoring oxidation of chlorinated ethenes by permanganate in groundwater using stable isotopes: laboratory and field studies. *Environ. Sci. Technol.* **2003**, 37, 798-804.

126. Elsner, M.; Lacrampe Couloume, G.; Mancini, S. A.; Burns, L.; Sherwood Lollar, B., Carbon Isotope Analysis to Evaluate Nanoscale Fe(0) Treatment at a Chlorohydrocarbon Contaminated Site. *Groundwater Monitoring and Remediation* **2010**, *30*, 79-95.
127. IUSS\_Working\_Group\_WRB, *World Reference Base for Soil Resources 2014, update 2015 - International soil classification system for naming soils and creating legends for soil maps*. . Food and Agriculture Organization of the United Nations: Rome, 2015; Vol. 106.
128. Stephenson, G. R.; Ries, S. K., Metabolism of Pyrazon in Sugar Beets and Soil. *Weed Science* **1969**, *17* (3), 327-331.
129. Gatzweiler, E., Das Langzeitverhalten der Herbizidwirkstoffe Chloridazon und 2, 4-DP-P nach Praxisanwendung in zwei verschiedenen Boden der Bundesrepublik. **1993**.
130. PESTEMER, W.; MALKOMES, H.-P., Einfluss von Pflanzenschutzmitteln einer Zuckerrüben-Spritzfolge auf biologische Aktivitäten und auf den Abbau von Chloridazon im Boden. I. Freilandversuche. *Weed Res.* **1983**, *23* (5), 283-291.
131. Barra, R.; Vighi, M.; Di Guardo, A., Prediction of surface water input of chloridazon and chlorpyrifos from an agricultural watershed in Chile. *Chemosphere* **1995**, *30* (3), 485-500.
132. Capri, E.; Ghebbioni, C.; Trevisan, M., Metamitron and Chloridazon Dissipation in a Silty Clay Loam Soil. *J. Agric. Food Chem.* **1995**, *43* (1), 247-253.
133. Elsner, M.; Zwank, L.; Hunkeler, D.; Schwarzenbach, R. P., A new concept linking observable stable isotope fractionation to transformation pathways of organic pollutants. *Environ. Sci. Technol.* **2005**, *39* (18), 6896-6916.
134. DE FANG, F.; PESTEMER, W.; MALKOMES, H.-P., Einfluss von Pflanzenschutzmitteln einer Zuckerrüben-Spritzfolge auf biologische Aktivitäten und auf den Abbau von Chloridazon im Boden. II. Gefäß- und Laborversuche. *Weed Res.* **1983**, *23* (5), 293-304.
135. Bohn, T.; Cocco, E.; Gourdol, L.; Guignard, C.; Hoffmann, L., Determination of atrazine and degradation products in Luxembourgish drinking water: origin and fate of potential endocrine-disrupting pesticides. *Food Additives and Contaminants Part a-Chemistry Analysis Control Exposure & Risk Assessment* **2011**, *28* (8), 1041-1054.
136. Baran, N.; Mouvet, C.; Negrel, P., Hydrodynamic and geochemical constraints on pesticide concentrations in the groundwater of an agricultural catchment (Brevilles, France). *Environ. Pollut.* **2007**, *148* (3), 729-738.
137. Barbash, J. E.; Resek, E. A., *Pesticides in ground water: distribution, trends, and governing factors*. Ann Arbor Press: Chelsea, MI, 1996; p xxvii + 588 pp.
138. Meyer, A. H.; Penning, H.; Elsner, M., C and N isotope fractionation suggests similar mechanisms of microbial atrazine transformation despite involvement of different Enzymes (AtzA and TrzN). *Environ. Sci. Technol.* **2009**, *43* (21), 8079-8085.
139. Tomlin, C. S. D., *The Pesticide Manual: A World Compendium of Pesticides*. 13th ed.; British Crop Protection Council: Hampshire, UK, 2003.
140. Johnson, A. C.; Hughes, C. D.; Williams, R. J.; John Chilton, P., Potential for aerobic isoproturon biodegradation and sorption in the unsaturated and saturated zones of a chalk aquifer. *Journal of Contaminant Hydrology* **1998**, *30* (3), 281-297.
141. Tuxen, N.; Tuchsén, P. L.; Rugge, K.; Albrechtsen, H.-J.; Bjerg, P. L., Fate of seven pesticides in an aerobic aquifer studied in column experiments. *Chemosphere* **2000**, *41* (9), 1485-1494.
142. van der Pas, L. J. T.; Leistra, M.; Boesten, J., Rate of transformation of atrazine and bentazone in water-saturated sandy subsoils. *J. Pestic. Sci.* **1998**, *53* (3), 223-232.
143. Adams, C. D.; Thurmann, E. M., Formation and transport of deethylatrazine in the soil and vadose zone. *J. Environ. Qual.* **1991**, *20*, 540-547.

144. Auersperger, P.; Lah, K.; Kus, J.; Marsel, J., High precision procedure for determination of selected herbicides and their degradation products in drinking water by solid-phase extraction and gas chromatography-mass spectrometry. *J. Chromatogr. A* **2005**, *1088* (1-2), 234-241.
145. Törnquist, M.; Kreuger, J.; Adielsson, S., Occuring of pesticides in Swedish water resources against a background of national risk-reduction programmes - results from 20 years of monitoring. In *XIII Symposium Pesticide Chemistry - Environmental Fate and Human Health*, Piacenza, Italy, 2007.
146. Porazzi, E.; Pardo Martinez, M.; Fanelli, R.; Benfenati, E., GC-MS analysis of dichlobenil and its metabolites in groundwater. *Talanta* **2005**, *68* (1), 146-154.
147. Schipper, P. N. M.; Vissers, M. J. M.; van der Linden, A. M. A., Pesticides in groundwater and drinking water wells: overview of the situation in the Netherlands. *Water Sci. Technol.* **2008**, *57* (8), 1277-1286.
148. Vassiliou, A., COMMISSION DECISION of 18 September 2008 concerning the non-inclusion of dichlobenil in Annex I to Council Directive 91/414/EEC and the withdrawal of authorisations for plant protection products containing that substance. In *2008/754/EG*, European Commission, Ed. Official Journal of the European Union: 2008.
149. Dörfler, U.; Feicht, E. A.; Scheunert, I., S-triazine residues in groundwater. *Chemosphere* **1997**, *35* (1), 99-106.
150. Olness, A.; Basta, N. T.; Rinke, J., Redox effects on resin extraction of herbicides from soil. *Talanta* **2002**, *57* (2), 383-391.
151. Carabias-Martinez, R.; Rodriguez-Gonzalo, E.; Herrero-Hernandez, E.; Sanchez-San Roman, F. J.; Prado Flores, M. G., Determination of herbicides and metabolites by solid-phase extraction and liquid chromatography Evaluation of pollution due to herbicides in surface and groundwaters. *J. Chromatogr. A* **2002**, *950*, 157-166.
152. Turiel, E.; Fernández, P.; Pérez-Conde, C.; Cámara, C., Trace-level determination of triazines and several degradation products in environmental waters by disk solid-phase extraction and micellar electrokinetic chromatography. *J. Chromatogr. A* **2000**, *872* (1), 299-307.
153. Hogendoorn, E.; van Zoonen, P., Recent and future developments of liquid chromatography in pesticide trace analysis. *J. Chromatogr. A* **2000**, *892* (1-2), 435-453.
154. Prosen, H.; Zupančič-Kralj, L., The interaction of triazine herbicides with humic acids. *Chromatographia Supplement* **2000**, *51*, 155-164.
155. Wang, Z.; Gamble, D. S.; Langford, C. H., Interaction of atrazine with Laurentian humic acid. *Anal. Chim. Acta* **1991**, *244*, 135-143.
156. Wang, X.; Guo, X.; Yang, Y.; Tao, S.; Xing, B., Sorption Mechanisms of Phenanthrene, Lindane, and Atrazine with Various Humic Acid Fractions from a Single Soil Sample. *Environ. Sci. Technol.* **2011**, *45* (6), 2124-2130.
157. Sposito, G.; Martin-Neto, L.; Yang, A., Atrazine complexation by soil humic acids. *J. Environ. Qual.* **1996**, *25*, 1203-1209.
158. Tosheva, Z.; Kies, A.; Hofmann, H., *Radon in potable waters in Luxembourg*. Nukleonika: 2010; Vol. 55, p 583-588.
159. Umsetzung der europäischen Wasserrahmenrichtlinie (2000/60/EG) - Bericht zur Bestandsaufnahme für Luxemburg. Infrastructures, M. d. D. d. e. d., Ed. Le Gouvernement Du Grand-Duché de Luxembourg: Esch-sur-Alzette, 2014; p 193.
160. Subramanian, G., *Quality assurance in environmental monitoring: Instrumental methods*. VCH: 1995.
161. Annable, W. K.; Frape, S. K.; Shouakar-Stash, O.; Shanoff, T.; Drimmie, R. J.; Harvey, F. E., <sup>37</sup>Cl, <sup>15</sup>N, <sup>13</sup>C isotopic analysis of common agro-chemicals for identifying non-point source agricultural contaminants. *Appl. Geochem.* **2007**, *22* (7), 1530-1536.

162. Hartenbach, A. E.; Hofstetter, T. B.; Tentscher, P. R.; Canonica, S.; Berg, M.; Schwarzenbach, R. P., Carbon, hydrogen, and nitrogen isotope fractionation during light-Induced transformations of atrazine. *Environ. Sci. Technol.* **2008**, *42* (21), 7751-7756.
163. Grundwasserökologie, H. Z. M.-I. f., Carbon and nitrogen isotope analysis of commercially available atrazine in-house standards over the last two decades. in-house database, unpublished.
164. Kueseng, P.; Noir, M. L.; Mattiasson, B.; Thavarungkul, P.; Kanatharana, P., Molecularly imprinted polymer for analysis of trace atrazine herbicide in water. *J. Environ. Sci. Health, Part B* **2009**, *44* (8), 772-780.
165. Turiel, E.; Martín-Esteban, A.; Fernández, P.; Pérez-Conde, C.; Cámara, C., Molecular Recognition in a Propazine-imprinted Polymer and Its Application to the Determination of Triazines in Environmental Samples. *Anal. Chem.* **2001**, *73* (21), 5133-5141.
166. Torrento, C.; Bakkour, R.; Melsbach, A.; Ponsin, V.; Lihl, C.; Prasuhn, V.; Hofstetter, T. B.; Elsner, M.; Hunkeler, D. *Assessing pesticide dynamics in soil and vadose zone using compound-specific isotope analysis (CSIA): A lysimeter study*; Höhere Bundeslehr- und Forschungsanstalt für Landwirtschaft Raumberg-Gumpenstein 2017; pp 39 – 42.
167. Ehrl, B. N.; Gharasoo, M.; Elsner, M., Isotope Fractionation Pinpoints Membrane Permeability as a Barrier to Atrazine Biodegradation in Gram-negative Polaromonas sp. Nea-C. *Environ. Sci. Technol.* **2018**, *52* (7), 4137-4144.
168. Melsbach, A. P., Denis; Farlin, Julien; Bayerle, Michael; Daubmeier, Martina; Hölzer, Kathrin; Meyer, Armin; Gallé, Tom; Elsner, Martin, Isotope fractionation of micropollutants during large-volume extraction: a critical method evaluation for atrazine at low ng/L concentrations in groundwater **in preparation**.
169. Goodman, K. J.; Brenna, J. T., Curve Fitting for Restoration of Accuracy for Overlapping Peaks in Gas Chromatography/Combustion Isotope Ratio Mass Spectrometry. *Anal. Chem.* **1994**, *66* (8), 1294-1301.
170. Merritt, D. A.; Freeman, K. H.; Ricci, M. P.; Studley, S. A.; Hayes, J. M., Performance and Optimization of a Combustion Interface for Isotope Ratio Monitoring Gas-Chromatography Mass-Spectrometry. *Anal. Chem.* **1995**, *67* (14), 2461-2473.
171. Goodman, K. J., Hardware Modifications to an Isotope Ratio Mass Spectrometer Continuous-Flow Interface Yielding Improved Signal, Resolution, and Maintenance. *Anal. Chem.* **1998**, *70* (5), 833-837.
172. Reinnicke, S.; Juchelka, D.; Steinbeiss, S.; Meyer, A. H.; Hilker, A.; Elsner, M., Gas chromatography-isotope ratio mass spectrometry (GC-IRMS) of recalcitrant target compounds: performance of different combustion reactors and strategies for standardization. *Rapid. Commun. Mass. Sp.* **2012**, *26* (9), 1053-1060.
173. Zhang, Y.; Tobias, H. J.; Sacks, G. L.; Brenna, J. T., Calibration and Data Processing in Gas Chromatography Combustion Isotope Ratio Mass Spectrometry. *Drug Test. Anal.* **2012**, *4* (12), 912-922.
174. van Roij, L.; Sluijs, A.; Laks, J. J.; Reichart, G. J., Stable carbon isotope analyses of nanogram quantities of particulate organic carbon (pollen) with laser ablation nano combustion gas chromatography/isotope ratio mass spectrometry. *Rapid Commun. Mass Spectrom.* **2017**, *31* (1), 47-58.
175. Juchelka, D.; Beck, T.; Hener, U.; Dettmar, F.; Mosandl, A., Multidimensional Gas Chromatography Coupled On-Line with Isotope Ratio Mass Spectrometry (MDGC-IRMS): Progress in the Analytical Authentication of Genuine Flavor Components. *J. High Resolut. Chromatogr.* **1998**, *21* (3), 145-151.

176. Nitz, S.; Weinreich, B.; Drawert, F., Multidimensional gas chromatography – isotope ratio mass spectrometry (MDGC-IRMS). Part A: System description and technical requirements. *J. High Resolut. Chromatogr.* **1992**, *15* (6), 387-391.
177. Shellie, R.; Marriott, P., Opportunities for ultra-high resolution analysis of essential oils using comprehensive two-dimensional gas chromatography: a review. *Flavour Fragrance J.* **2003**, *18* (3), 179-191.
178. Edwards, M.; Mostafa, A.; Górecki, T., Modulation in comprehensive two-dimensional gas chromatography: 20 years of innovation. *Anal. Bioanal. Chem.* **2011**, *401* (8), 2335-2349.
179. Górecki, T.; Harynuk, J.; Panić, O., The evolution of comprehensive two-dimensional gas chromatography (GC×GC). *J. Sep. Sci.* **2004**, *27* (5-6), 359-379.
180. Kinghorn, R. M.; Marriott, P. J., High Speed Cryogenic Modulation – A Technology Enabling Comprehensive Multidimensional Gas Chromatography. *J. High Resolut. Chromatogr.* **1999**, *22* (4), 235-238.
181. Ricci, M. P.; Merritt, D. A.; Freeman, K. H.; Hayes, J. M., Acquisition and processing of data for isotope-ratio-monitoring mass spectrometry. *Org. Geochem.* **1994**, *21* (6-7), 561-571.
182. Dunn, P.; Carter, J. F., *Good Practice Guide for Isotope Ratio Mass Spectrometry Second Edition 2018*. 2018.
183. Blumberg, L. M., Comprehensive two-dimensional gas chromatography: metrics, potentials, limits. *J. Chromatogr. A* **2003**, *985* (1-2), 29-38.
184. Blumberg, L. M.; David, F.; Klee, M. S.; Sandra, P., Comparison of one-dimensional and comprehensive two-dimensional separations by gas chromatography. *J. Chromatogr. A* **2008**, *1188* (1), 2-16.
185. Thier H.P, K. J., Individual Pesticide Residue Analytical Methods (contd.). In *Manual of Pesticide Residue Analysis Volume II*, Deutsche, F., Ed. 2006; pp 177-238.
186. Vögeli Albisser, C.; Prasuhn, V., *Auswirkungen des Klimawandels auf die Schadstoffverfrachtung ins Grundwasser*. 2013.
187. Lysimeteranlage Zuerich-Reckenholz mit 12 Gefaessen.  
<https://www.agroscope.admin.ch/agroscope/de/home/themen/umwelt-ressourcen/boden-gewaesser-naehrstoffe/landwirtschaftlicher-gewaesserschutz/auswaschung-lysimeter.html>  
(accessed 25.03.2019).
188. Sposito, G.; Martin-Neto, L., Atrazine complexation by soil humic acids. *Journal of Environmental Quality* **Yang, A.**, *25*, 1203-1209.



# Curriculum Vitae

**Aileen Melsbach**

---

## **Ausbildung**

- 2009 - 2012      Studium der Angewandten Naturwissenschaft an der Technischen Universität Bergakademie Freiberg (Bachelor of Science);  
Bachelorarbeit: „Die Analyse von Heteroatomverbindungen in Pyrolyseölen mittels GC-AED“.  
Betreuer: Dr. Philipp Rathsack und Prof. Dr. Matthias Otto
- 2013 - 2014      Studium der Forensischen Toxikologie („Forensic Toxicology“) an der University of Glasgow (Master of Science);  
Masterarbeit: "Evaluation of tamoxifen abuse in post-mortem cases with GC-MS".  
Betreuer: Dr Hazel Torrance
- 2015 - 2019      Promotion am Helmholtz Zentrum München -German Research Center for Environmental Health, Institut für Grundwasserökologie und der Eberhard Karls Universität Tübingen unter der Betreuung von Prof. Dr. Martin Elsner, Prof. Dr. Christian Zwiener und Prof Dr Robert Kalin.